Author:
Holt, Amy K

Title:
Investigating the effects of aspirin on colorectal cancer cell metabolism

Investigating the effects of aspirin on colorectal cancer cell metabolism

Ms Amy Katherine Holt

A dissertation submitted to the University of Bristol in accordance with the requirements for award of the degree of Doctor of Philosophy in the Faculty of Life Sciences, School of Cellular and Molecular Medicine

October 2021

Word count: 38,846

Abstract

Colorectal cancer (CRC) is the second highest cause of cancer-related mortality in the UK and incidence is increasing, particularly in younger patients. 5-year survival rates in CRC cases diagnosed at later stage are particularly low, highlighting a need for effective preventative interventions and improved therapies.

Aspirin has been found in multiple large studies to be effective in reducing CRC risk, particularly when taken for a long period of time. However, potential side-effects and complications such as the increased risk of bleeding limit its clinical utility as a prophylactic agent. Further understanding of the mechanisms underlying aspirin's anti-cancer effects will help optimise benefits from its use, such as improving patient stratification, dosage, timing of treatment and identifying synergistic therapies.

In order to identify novel mechanisms of long-term aspirin exposure, CRC cell lines were previously treated with aspirin long-term (52 weeks). Proteomic analysis of these cells highlighted a potential role for aspirin in regulating cellular metabolism. Metabolic reprogramming is a key aspect of cancer cell biology and work is ongoing to identify methods of targeting cellular metabolism for cancer therapy. Therefore, the focus of this thesis is the role of aspirin in regulating cancer cell metabolism and investigating metabolic vulnerabilities that could be exploited to increase the efficacy of existing therapies.

This project describes the effect of long-term aspirin on regulation of a number of key metabolic enzymes, as well as causing a shift in nutrient utilisation and TCA cycle carbon sources. It was found that aspirin inhibits glutaminolysis and increases utilisation of glucose. Based on these findings, aspirin was subsequently found to increase sensitivity of CRC cell lines to metabolic inhibitors, most notably CB-839, which is currently in clinical trials for a number of different cancer types. This effect was maintained in physiological cell culture medium, suggesting it is likely to be applicable to *in vivo* conditions.

Findings from this project have highlighted in detail a novel mechanism of action of aspirin on CRC cells, potentially contributing to its function in cancer prevention. Results also suggest that combining aspirin with CB-839 may be an effective clinical approach for treatment of advanced CRC, supporting future clinical trials in patients who currently have limited effective therapeutic options.

Acknowledgements

First and foremost, I would like to thank my two supervisors, Ann Williams and Emma Vincent. You conceived a great project that I have tremendously enjoyed working on, and your guidance and supervision throughout it have been second to none. I've learnt so much from every one of our discussions and you've always inspired me to produce the best science that I could. I've enjoyed working with you both immensely and thank you both so much for the opportunity to complete this PhD, and for your continued encouragement and support.

My sincere thanks go to the James Tudor Foundation and John Maynard for the generous funding for this project. It's been a pleasure to update you on our progress with this work.

I would also like to thank all the members of the lab that I have had the privilege of working with over the last 3 years. Tracey, your impeccable organisation and stellar lab skills have made completing this project an infinitely easier task, I really appreciate all of the support you've given me. I look forward to hearing you on Radio 2 one day, taking your rightful place as PopMaster champion. Penny, Danny, Elle, Chris P, Adam, Steve, Mark, Ashley, Lucy and Chris S, I couldn't have asked for a better bunch of people to share an office (and the struggle of writing up a thesis) with. I will sorely miss playing Word of the Day, eating cake and drinking well-brewed tea with all of you.

To my parents, Susan and Richard. I truly would not have been able to complete this thesis without all of the support you have given me for the last 25 years. For repeatedly ferrying me all over the country, for many, many of hours of phone calls that have got me through the toughest days and a million other things, I wouldn't ever know how to thank you enough. I hope you can display this thesis proudly (even if it understandably goes unopened).

Mike, I couldn't have asked for a better person to be unexpectedly shut in a house with for several months. The last year or two have not been what we expected, but I can't imagine what it would have been like without you. Thank you so much for supporting me (and putting up with me) while I wrote this thesis. I'm so looking forward to the future with you.

Finally, I would like to dedicate this thesis to Ian Manchett, who I wish I could call to tell him it was finally submitted, and how much he inspired me to keep on going.

Author’s Declaration

I declare that the work in this dissertation was carried out in accordance with the requirements of the University's *Regulations and Code of Practice for Research Degree Programmes* and that it has not been submitted for any other academic award. Except where indicated by specific reference in the text, the work is the candidate's own work. Work done in collaboration with, or with the assistance of, others, is indicated as such. Any views expressed in the dissertation are those of the author.

SIGNED: ..... DATE:.....

Table of Contents

List of Figures

List of Tables

Abbreviations

2-DG	2-Deoxy-D-glucose
5-ASA	5-aminosalicylic acid
5-FU	5-flurouracil
ADP	Adenosine diphosphate
AKT	Protein kinase B
AML	Acute myeloid leukaemia
AMPK	5' adenosine monophosphate-activated protein kinase
AOA	Aminooxyacetic acid
APC	Adenomatous polyposis coli
ASCL1	Acyl-CoA synthetase long chain family member 1
ASCT2	Alanine-serine-cystine transporter 2
ASNS	Asparagine synthetase
ATF4	Activating transcription factor 4
ATP	Adenosine triphosphate
ATCC	American type culture collection
BPTES	Bis-2-(5-phenylacetamido-1,3,4-thiadiazol-2-yl)ethyl sulfide
BSA	Bovine serum albumin
CAC	Colitis associated cancer
CCAT	Colon Cancer Associated Transcript 2
CDK	Cyclin dependent kinase
CIMP	CpG island methylator phenotype
CIN	Chromosomal instability
CMS	Consensus molecular subtype
COX	Cyclooxygenase
CRC	Colorectal cancer

CSC	Cancer stem cell
DCA	Dichloroacetate
DHAP	Dihydroxyacetone phosphate
DHBA	Dihydrobenzoic acid
DHODH	Dihydroorotate dehydrogenase
DMEM	Dulbecco's Modified Eagle Medium
DMSO	Dimethyl sulfoxide
DNA	Deoxyribonucleic acid
DON	6-Diazo-5-oxo-L-norleucine
ECAR	Extracellular acidification rate
EDTA	Ethylenediaminetetraacetic acid
EGFR	Epidermal growth factor receptor
EMT	Epithelial-mesenchymal transition
ETC	Electron transport chain
FAD	Flavin adenine dinucleotide
FADH2	Reduced flavin adenine dinucleotide
FAO	Fatty acid oxidation
FAP	Familial Adenomatous Polyposis
FCCP	Carbonyl cyanide-*p*-trifluoromethoxyphenylhydrazone
FCS	Fetal calf serum
FDG	Fluorodeoxyglucose
FH	Fumarate hydratase
FIT	Faecal immunochemical test
GAC	Glutaminase C
GCMS	Gas chromatography mass spectrometry
GI	Gastrointestinal
GLS	Glutaminase

GLUD	Glutamate dehydrogenase
GLUT1	Glucose transporter 1
GO	Gene ontology
GPCR	G protein-coupled receptor
GPT2	Glutamic--pyruvic transaminase 2
GTP	Guanosine triphosphate
HCC	Hepatocellular carcinoma
HCl	Hydrochloric acid
HIF	Hypoxia-inducible factor
HK	Hexokinase
HNPCC	Hereditary nonpolyposis colorectal cancer
hnRNPA1	Heterogeneous nuclear ribonucleoprotein A1
hnRNPA2	Heterogeneous nuclear ribonucleoprotein A2
HPLM	Human plasma-like medium
HPRT	Hypoxanthine guanine phosphoribosyltransferase
IDH	Isocitrate dehydrogenase
IKK	IκB kinase
IPA	Ingenuity pathway analysis
KEGG	Kyoto encyclopaedia of genes and genomes
KGA	Kidney-type glutaminase
KRAS	Kirsten rat sarcoma virus
LAT1	Large neutral amino acid transporter 1
LDH	Lactate dehydrogenase
LOH	Loss of heterozygosity
LRP	Low-density lipoprotein receptor-related protein
LT	Long-term
MID	Mass isotopomer distribution

MMR	Mismatch repair
MPC	Mitochondrial pyruvate carrier
mRNA	Messenger ribonucleic acid
MSI	Microsatellite instability
mtDNA	Mitochondrial deoxyribonucleic acid
mTOR	Mammalian target of rapamycin
mTORC1	Mammalian target of rapamycin complex 1
NAC	N-acetyl cysteine
NaCl	Sodium chloride
NAD	Nicotinamide adenine dinucleotide
NADH	Reduced nicotinamide adenine dinucleotide
NADP	Nicotinamide adenine dinucleotide phosphate
NADPH	Reduced nicotinamide adenine dinucleotide phosphate
NEAA	Non-essential amino acid
NEMO	NFκB essential modulator
NFκB	Nuclear factor kappa B
ns	non-significant OR non-specific
NSAID	Non-steroidal anti-inflammatory drug
OCR	Oxygen consumption rate
ODC	Ornithine decarboxylase
Oxphos	Oxidative phosphorylation
PAGE	Polyacrylamide gel electrophoresis
PBS	Phosphate buffered saline
PC	Pyruvate carboxylase
PCK2	Phosphoenolpyruvate carboxykinase 2
PCR	Polymerase chain reaction
PDH	Pyruvate dehydrogenase

PDK1	Pyruvate dehydrogenase kinase 1
PEPCK	Phosphoenolpyruvate carboxykinase
PET	Positron emission tomography
PFA	Paraformaldehyde
PFK	Phosphofructokinase
PG	Prostaglandin
PGC1α	PPARG coactivator 1 alpha
Pi	Inorganic phosphate
PK	Pyruvate kinase
PKCε	Protein kinase C epsilon
PPAT	Phosphoribosyl pyrophosphate amidotransferase
PPP	Pentose phosphate pathway
PSAT1	Phosphoserine aminotransferase 1
PTB	Polypyrimidine tract binding protein
PTEN	Phosphatase and tensin homolog
PVDF	Polyvinylidene difluoride
qPCR	Quantitative polymerase chain reaction
RCT	Randomised controlled trial
RNA	Ribonucleic acid
ROS	Reactive oxygen species
RPMI	Roswell Park Memorial Institute Medium
RTK	Receptor tyrosine kinase
SASP	Salazosulfapyridine
SDH	Succinate dehydrogenase
SDS	Sodium-dodecyl-sulphate
SDS-PAGE	Sodium-dodecyl-sulphate polyacrylamide gel electrophoresis

Ser	Serine
siRNA	Small interfering ribonucleic acid
SIRT	Sirtuin
SITA	Stable isotope tracer analysis
SLC	Solute-linked carrier
SNP	Single nucleotide polymorphism
SRCC	Colorectal signet ring cell carcinoma
SSAT	Spermidine/spermine N-acetyltransferase 1
ST	Short-term
TBP	TATA-Box Binding Protein
TBST	Tris-buffered saline - Tween (wash buffer)
TCA	Tricarboxylic acid
TCF	T cell factor
TEMED	Tetramethylethylenediamine
TET	Ten-eleven translocation protein
TGF-β	Transforming growth factor beta
TNM	Tumour Node Metastasis
TxA2	Thromboxane A2
USPSTF	United States Preventative Services Task Force
VDAC	Voltage-dependent anion channel
xCT	Cystine/glutamate antiporter
YAP	Yes-associated protein
α-KG	α-ketoglutarate

Chapter 1 Introduction

1.1 Introduction to colorectal cancer

Colorectal cancer (CRC) is the fourth most common cancer in the UK, and the second most common cause of cancer death after lung cancer (1). 5- and 10-year survival rates for CRC are 59% and 57% respectively, although this is highly dependent on the stage diagnosed; 5 year survival rate is 90% for patients diagnosed with stage 1, however this drops to 10% with stage 4 (1). While overall CRC incidence has been slowly decreasing for several decades, partly due to the introduction of screening programs, the incidence in younger people is increasing. A recent study found that in the US since 1974, incidence of rectal cancer has decreased by 2% every year in patients over 75 years old but increased by 4% annually in patients in their 20s (2). Consistent with this, Chambers et al. recently found that CRC incidence in the UK has rapidly increased in patients aged 20-39, highlighting a need for increased awareness of CRC symptoms in younger patients, and possible future changes to the current screening policies (3). Currently in England, CRC screening is performed by a faecal immunochemical test (FIT) every two years in patients aged 60-74, though shortly expanding to start from the age of 56.

The large majority of CRC cases (90-95%) are sporadic, meaning they occur *de novo* in patients with no specific germline genetic risk factors (4). Risk factors for developing sporadic CRCs include inflammatory bowel disease (Crohn's disease or ulcerative colitis), lifestyle related factors such as obesity and smoking and particularly factors relating to diet such as high amounts of processed meat and lack of fibre (1). Type 2 diabetes is also associated with an increased risk of developing CRC (5).

There are also inherited conditions caused by germline mutations which dramatically increase the risk of developing CRC. Familial adenomatous polyposis (FAP) is caused by a germline mutation in the adenomatous polyposis coli (*APC*) gene (6). Patients with FAP develop hundreds of polyps (adenomas) on their intestinal wall by early adulthood, which can eventually develop into invasive carcinomas. Therefore, these patients have a very high risk of developing CRC. Another familial condition that predisposes patients to CRC is Lynch syndrome, also known as hereditary non-polyposis colorectal cancer (HNPCC). This is an autosomal dominant condition caused most frequently by mutations in DNA mismatch repair proteins such as MSH2 and MLH1, leading to development of CRC at an average age of 45 (7).

1.1.1 **The colonic epithelium**

CRCs are adenocarcinomas, arising from the glandular epithelium that lines the colon and rectum. In the normal colonic epithelium (Figure 1.1), the cells are organised into crypts, which increase the surface area of the colon for absorption. The cell population is maintained by stem cells known as crypt-based columnar cells (CBCCs), which self-renew and produce transit amplifying cells, also known as progenitor cells, which move progressively up the crypts and become more differentiated epithelial cells such as enterocyte absorptive cells, goblet cells (for mucous production), neuroendocrine cells (for neural and hormonal signalling in the gut), and tuft cells (for immune surveillance, and possibly stem cell functions). Deep secretory cells are important for maintaining the stem cell niche at the base of the crypt. Wnt signalling (further discussed in section 1.1.3) is also important for the maintenance of the stem cell population, and there is a gradient in levels of Wnt signalling from the base to the top of the crypt.

Colonic stem cells express a number of markers that distinguish them from differentiated cells, such as CD44 (8), LGR5 and ASCL2 (9). In a similar way to the normal cell population, CRCs are thought to be initiated and maintained by a subset of the population of tumour cells known as cancer stem cells (CSCs) (10). Expression of stem cell markers has been shown to be a predictor of relapse in CRC patients who have undergone curative treatment (11). Therefore, targeting CSCs is a priority for research into cancer therapies.

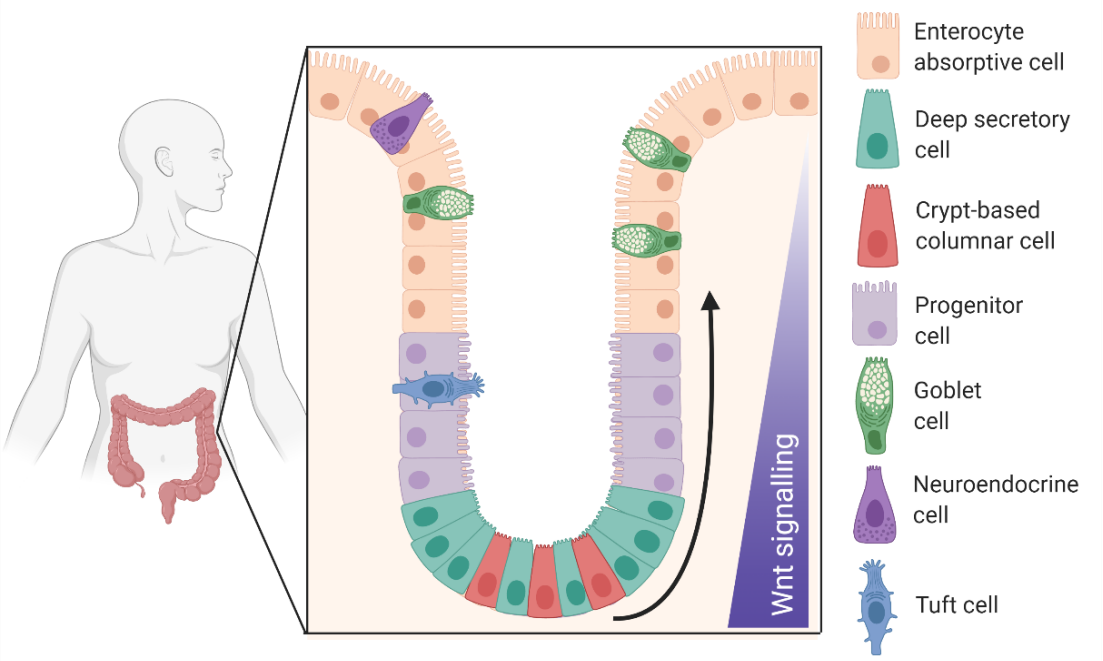

Figure 1.1 The colonic crypt

The epithelium of the colon is organised into crypts. The cell population is maintained by crypt-based columnar cells (stem cells), which divide to self-renew and form progenitor cells. Progenitor cells move progressively up the crypt as they form more differentiated cell types such as enterocyte absorptive cells, goblet cells, neuroendocrine cells and tuft cells. Deep secretory cells are important for maintaining the stem cell niche. Wnt signalling is also important for the maintenance of stem cells; there is a gradient in the amount of Wnt signalling from the top to the bottom of the crypt. Adapted from (10). Created with BioRender.com.

1.1.2 Stepwise carcinogenesis

CRCs develop in a stepwise manner, developing from normal crypts of the epithelium to benign polyps (adenomas), and eventually into an invasive carcinoma which can also metastasise to distant sites such as the liver (6). This progression is underpinned by a well-defined series of genetic mutations (12, 13); while the precise order in which the mutations occur in CRCs varies, the genes and pathways that are impacted tend to be similar. For example, the majority of CRCs are initiated by upregulated Wnt/β-catenin signalling, with 80% of CRCs containing a mutation in the *APC* gene (6). As well as sequence mutations, there are also epigenetic alterations such as hypomethylation that contribute to tumour progression (6). A summary of the process is shown in Figure 1.2, along with detail about the underlying molecular processes, which will be discussed in the next section.

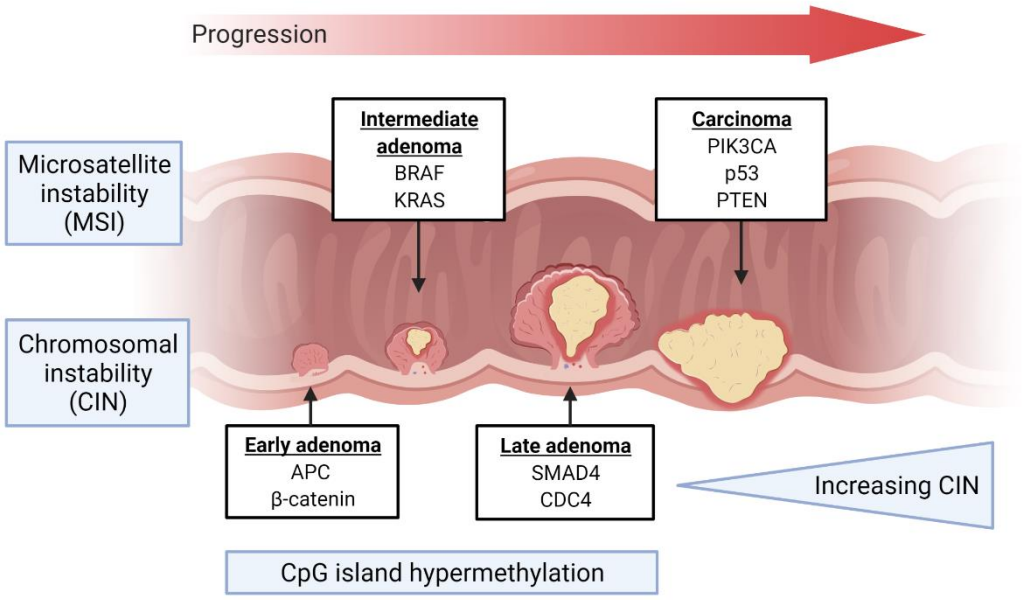

Figure 1.2 Adenoma to carcinoma sequence

Colorectal cancers develop in a stepwise manner from benign adenomas, also known as polyps, to carcinomas that invade surrounding tissues. This progression is underpinned by well characterised molecular changes. Genes that are commonly mutated at each stage of the progression pathway are shown in white boxes. *APC* is a common initiating mutation. Blue boxes show the common underlying molecular processes that facilitate the accumulation of mutations, including microsatellite instability (MSI), chromosomal instability (CIN) and CpG island hypermethylation. Adapted from (13). Created with BioRender.com.

1.1.3 Molecular basis of colorectal cancer

APC mutations, which are the most common initiating mutation in CRC (Figure 1.2), lead to dysregulation of Wnt signalling. The Wnt signalling pathway and the role of APC is illustrated in Figure 1.3. Briefly, loss of APC function leads to constitutive expression of Wnt target genes due to β-catenin accumulation, including c-myc, cyclin D and PPARδ which promote cell cycle progression and proliferation (14). As mentioned previously, germline *APC* mutations lead to a dramatically increased risk of CRC. The vast majority of sporadic CRCs have an *APC* mutation, but in the few that do have wild type *APC*, other mutations in the same pathway are often found, such as in phosphorylation sites of β-catenin that prevent its degradation (6).

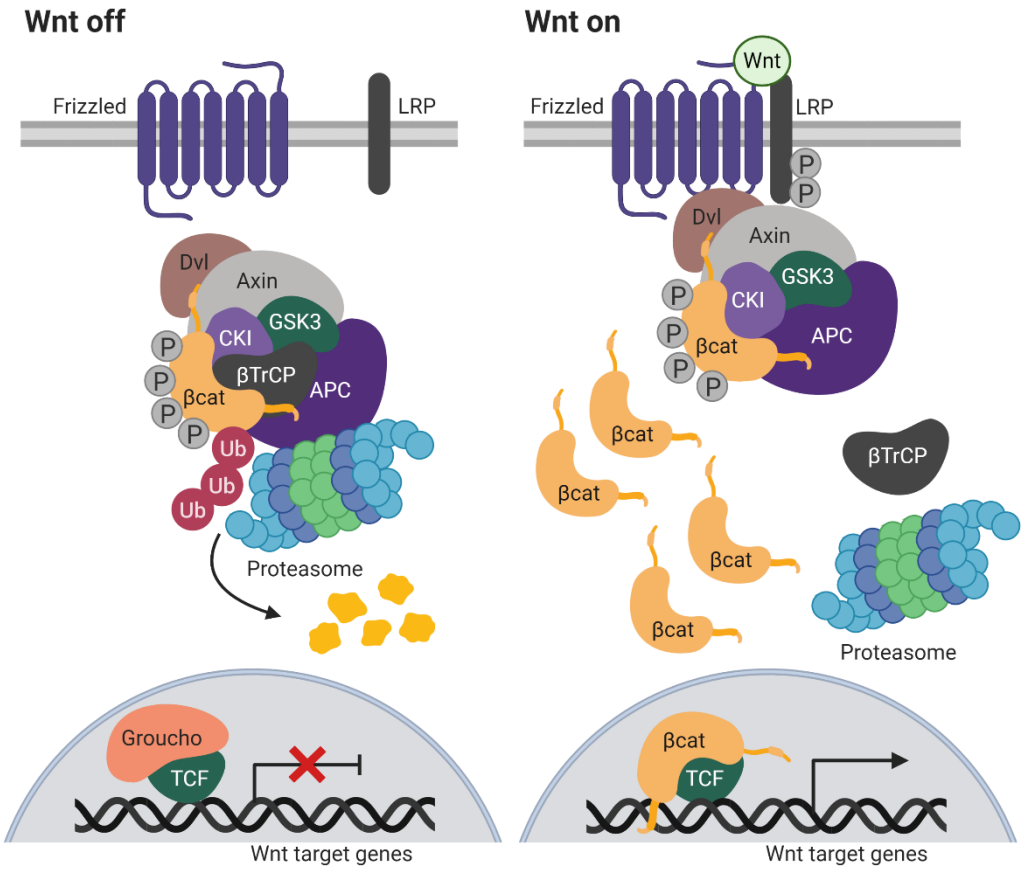

Figure 1.3 The role of APC in Wnt signalling

APC forms part of the destruction complex along with Axin, GSK3 and CK1. In the absence of Wnt ligands, the destruction complex phosphorylates β-catenin (β-cat). This leads to recognition by β-TrCP and ubiquitination and degradation of β-catenin by the proteasome, preventing the activation of the TCF transcription factor. Groucho remains bound to TCF to prevent its activation. When Wnt ligands bind the Frizzled and LRP receptors, the destruction complex is recruited to the cell membrane by Dishevelled (Dvl) and ubiquitination of β-catenin is prevented, which causes accumulation of newly synthesised β-catenin. When APC is mutated and its function lost, this prevents the function of the destruction complex, leading to the accumulation of β-catenin, even in the absence of Wnt ligands. β-catenin is then translocated into the nucleus where it interacts with transcriptions factor TCF and initiates gene transcription. Adapted from (14). Created with BioRender.com.

Another pathway that is commonly constitutively activated in CRC is the Ras/Raf/Mek/Erk pathway (Figure 1.4). This is normally activated by ligands binding to receptor tyrosine kinases (RTKs) such as epidermal growth factor receptor (EGFR), which leads to activation of the small GTPase Ras via the GRB2/SOS complex, causing Ras to bind GTP. Activated Ras triggers a kinase activation cascade beginning with Raf followed by Mek and Erk, which has many downstream effects including regulating survival (15). This pathway is affected by two commonly mutated genes in CRC, *KRAS* and *BRAF* (Figure 1.2), which occur in approximately 32-40% and 15% of CRCs respectively, leading to receptor independent activation of the pathway (16).

Another pathway activated by RTKs is the phosphoinositide 3-kinase (PI3K) pathway (see Figure 1.4). Binding of a ligand to the RTK causes activation of PI3K, which converts the phospholipid phosphatidylinositol (4,5)-bisphosphate (PIP_2) into phosphatidylinositol (3,4,5)-trisphosphate (PIP_3). This leads to recruitment and activation of AKT which has many downstream effects including activation of mammalian target of rapamycin (mTOR) signalling, a kinase that regulates many cellular functions including proliferation and survival. The *PIK3CA* gene, which encodes the p110α subunit of PI3K, is mutated in around 18% of CRCs (Figure 1.2) (17), leading to upregulation of PI3K signalling. Loss of function of the phosphatase and tensin homolog (PTEN) protein is also associated with carcinogenesis, as PTEN converts PIP_3 back to PIP_2, therefore inhibiting PI3K signalling. PTEN function may be lost by multiple mechanisms, including gene deletion and hypermethylation of the promoter region (18).

One study found that over half of sporadic CRCs had a mutation in at least one of the *KRAS*, *BRAF*, or *PIK3CA* genes, and this was associated with significantly lower 3-year survival rate (17). This highlights the importance of these pathways in CRC development. Targeted therapies aimed at these pathways such as the EGFR inhibitors cetuximab and panitumumab have proven effective in patients with advanced CRC (19), however mutations in the downstream effectors in these pathways can facilitate resistance to these therapies (16).

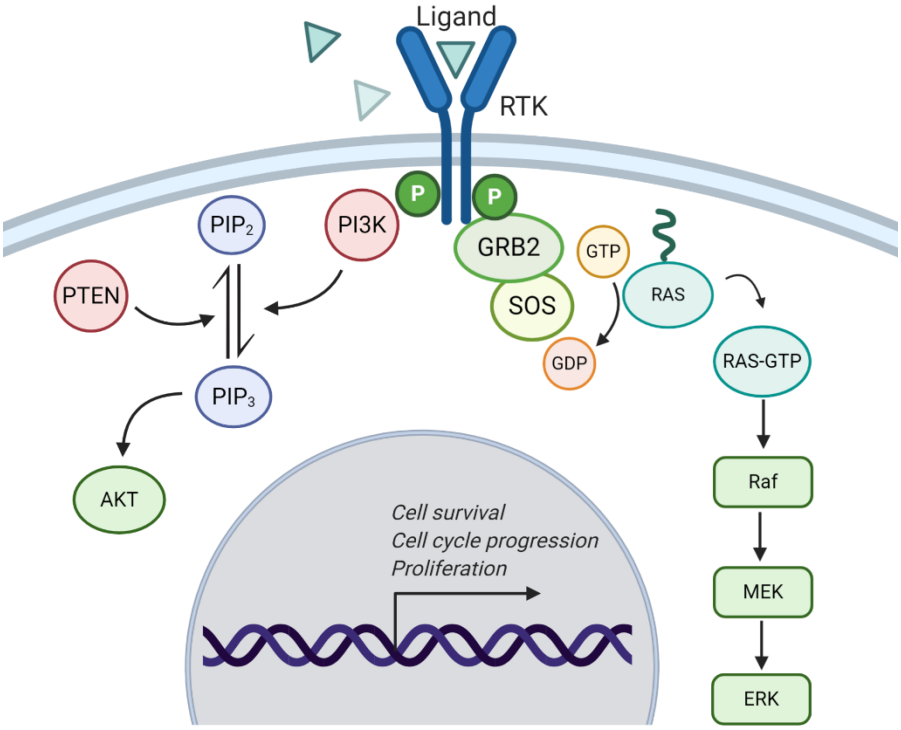

Figure 1.4 Ras-Raf-Mek-Erk and PI3K pathways

Binding of a ligand to a receptor tyrosine kinase (RTK) such as epidermal growth factor receptor (EGFR) triggers the kinase activation cascade consisting of Ras, Raf, Mek and Erk. Activated RTKs also activate PI3K which converts PIP_2 to PIP_3, leading to AKT activation which has many downstream effects. Adapted from (16). Created with BioRender.com.

Mutational progression of colorectal epithelial cells is thought to occur by three main pathways (20). The microsatellite instability (MSI) pathway occurs in around 15-20% of CRCs, and is caused by mutations in mismatch repair (MMR) proteins, leading to high error rates in DNA replication and an increased rate of further tumorigenic mutations occurring. In around 70% of CRC cases, development occurs due to chromosomal instability (CIN), which leads to large chromosomal alterations such as gains and losses of whole or large portions of chromosomes, and loss of heterozygosity (LOH). The final pathway is the CpG island methylator phenotype (CIMP), which is characterised by hypermethylation of CpG islands within the genome, which are epigenetic alterations which can lead to silencing of genes including tumour suppressors (20).

1.1.4 **CMS subtypes**

While the classic signalling pathways and mutations implicated in CRC are well-established, more recently work has been done to further subcategorise CRC based on gene expression profiles into consensus molecular subtypes (CMS), in order to better predict disease progression and therapeutic response. In 2015, four subtypes of CRC were categorised in this way, which are summarised in Table 1.1 (21, 22).

The four subtypes vary in their pathways of mutational progression as well as the mutations present and the subsequent phenotypes. CMS1 is characterised by CIMP and MSI pathways of genetic alterations, with high frequency of *BRAF* mutations and large involvement of immune cells within the tumours (21). CMS2-4 progress by the CIN pathway, and are distinguished based on their gene expression (shown in Table 1.1) (21). CMS2 is referred to as the 'canonical' subtype, and contains a high frequency of Wnt and Myc activating mutations. CMS3 is the 'metabolic' subtype, with a high frequency of mutations that lead to dysregulated metabolism, such as *KRAS*. And finally, CMS4 is the 'mesenchymal' subtype, which has upregulations of pathways involved with the epithelial-mesenchymal transition (EMT), which gives the cells a more highly metastatic phenotype (21). Because of this, CMS4 has the worst prognosis of the four subtypes, with the worst relapse-free survival as well as overall survival (22).

Table 1.1 Consensus molecular subtypes for colorectal cancer

Abbreviations: consensus molecular subtype (CMS), microsatellite instability (MSI), CpG island methylator phenotype (CIMP). Adapted from (21, 22).

Subtype name	**CMS1** **MSI Immune**	**CMS2** **Canonical**	**CMS3** **Metabolic**	**CMS4** **Mesenchymal**
Molecular features	MSI, CIMP high, hypermutation	Somatic copy number alteration - high	Mixed MSI status Somatic copy number alteration - low CIMP low	Somatic copy number alteration - high
Common mutations	*BRAF* mutations		*KRAS* mutations	
Tumour features	Immune infiltration and activation	Wnt and Myc activation	Metabolic deregulation	Stromal infiltration, TGF-β1 activation, angiogenesis
Prognosis	Worse survival after relapse			Worse relapse-free and overall survival

1.2 Colorectal cancer metabolism

1.2.1 Introduction to cellular metabolism

Metabolism can be defined as the sum of biochemical reactions within cells which involve the transfer of energy (23). Metabolism is a key aspect of cancer cell biology, and is fundamental to meeting the energetic and biosynthetic demands of chronic proliferation, as well as adapting to the changing and often metabolically stressful microenvironment. The importance of metabolism for cancer growth and development is increasingly being recognised; there is a rapidly growing body of research leading to its incorporation by Hanahan and Weinberg as an emerging hallmark of cancer in their more recent review (24). The apparent specificity of certain metabolic characteristics in cancer cells makes them attractive targets for cancer therapies. There are existing therapies that exploit these changes, such as asparaginase for acute lymphoblastic leukaemia which has been in use for many years (25) and there is a large amount research into new ways of targeting cancer metabolism.

Cellular metabolism consists of an enormous and complex network of pathways, however the key pathways for producing energy (in the form of adenosine triphosphate, ATP) from nutrients in cells are glycolysis, the tricarboxylic acid (TCA) cycle and oxidative phosphorylation (oxphos), otherwise known as central carbon metabolism.

Glycolysis involves the breakdown of glucose into pyruvate. A small amount of ATP is also produced from glycolysis without the need for oxygen (anaerobic respiration). To maintain this process, lactate is produced from pyruvate, in order to regenerate the NAD+ that is required for the pathway. Pyruvate can also be converted into acetyl-coA, before entering the TCA cycle. The TCA cycle occurs in the mitochondria and involves the stepwise oxidation of acetyl-coA, and production of ATP. As well as producing ATP, intermediate metabolites of both glycolysis and the TCA cycle feed into biosynthetic pathways, in order to produce the necessary macromolecules for cell proliferation. The steps of glycolysis and the TCA cycle, with the branch points for biosynthesis and key enzymes for cancer metabolism which will be discussed in subsequent sections, are shown in Figure 1.5 and Figure 1.6.

Key biosynthetic pathways branching from glycolysis and the TCA cycle include lipid synthesis, amino acid synthesis such as the serine biosynthesis pathway (26),

the pentose phosphate pathway (PPP) and one carbon metabolism. The PPP is important for the production of NADPH required for anabolic pathways, as well as precursors for nucleotide biosynthesis. One carbon metabolism is also important for nucleotide biosynthesis and it produces one-carbon units that contribute to methylation reactions such as histone and DNA methylation (27).

As TCA cycle intermediates can exit the cycle to fuel anabolic pathways, carbon entry into the cycle occurs by multiple entry points in order to maintain flow through the cycle. There are several entry points that are alternate to the conversion of pyruvate to acetyl-CoA, and these are known as anaplerotic pathways, or anaplerosis (see Figure 1.6). Pyruvate anaplerosis can occur by the direct conversion of pyruvate to oxaloacetate by pyruvate carboxylase (PC). As well as glucose, glutamine is also a key carbon source for the TCA cycle. Glutamine anaplerosis occurs via conversion of glutamine to α-ketoglutarate.

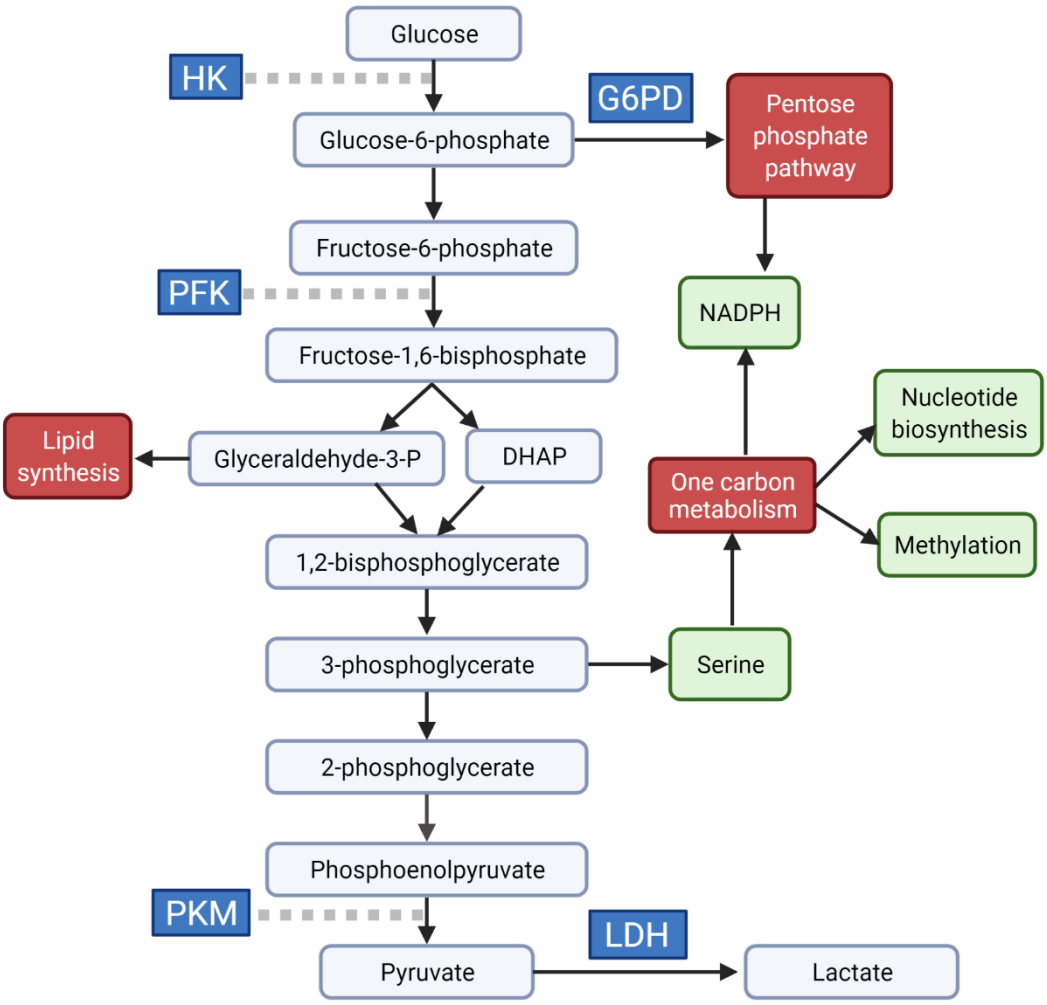

Figure 1.5 Overview of glycolysis and branch points for cancer metabolic reprogramming

Steps in the conversion of glucose to pyruvate (glycolysis). Dark blue shows enzymes that are key for cancer metabolic reprogramming. Red and green show key branch points for biosynthesis. Acronyms: dihydroxyacetone phosphate (DHAP), hexokinase (HK), reduced nicotinamide adenine dinucleotide phosphate (NADPH), phosphofructokinase (PFK), pyruvate kinase (PKM), lactate dehydrogenase (LDH), glucose-6-phosphate dehydrogenase (G6PD). Created with BioRender.com. Adapted from (26).

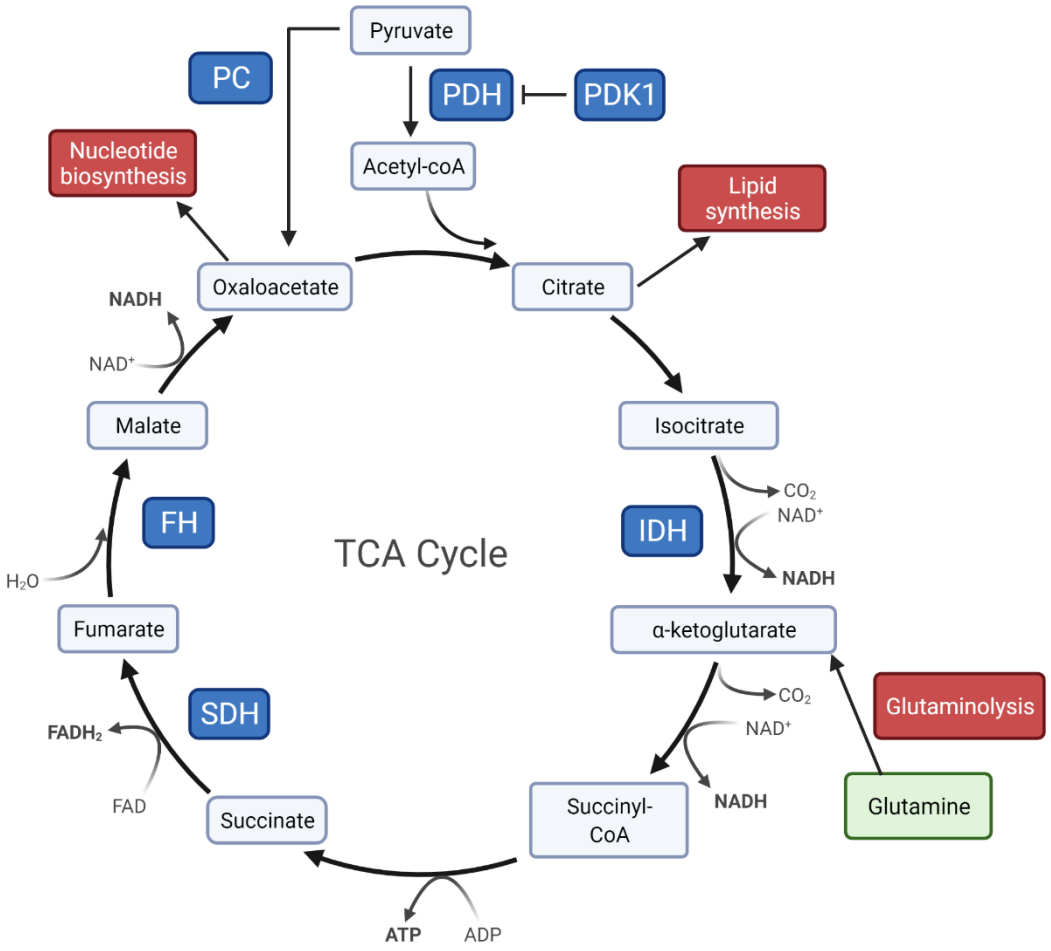

Figure 1.6 Overview of the TCA cycle and key steps for cancer metabolic reprogramming

Steps of the TCA cycle, including intermediate metabolites and production of NADH, $FADH_2$, CO_2 and ATP. Blue shows key enzymes for cancer metabolism, red shows branching pathways for biosynthesis and anaplerosis. Acronyms: adenosine di/triphosphate (ADP/ATP), flavin adenine dinucleotide ($FAD/FADH_2$), fumarate hydratase (FH), isocitrate dehydrogenase (IDH), nicotinamide adenine dinucleotide (NAD+/NADH), pyruvate carboxylase (PC), pyruvate dehydrogenase (PDH), pyruvate dehydrogenase kinase 1 (PDK1), succinate dehydrogenase (SDH). Created with BioRender.com. Adapted from (26).

The TCA cycle also involves reduction of NAD+ and FAD+ to NADH and $FADH_2$ respectively, which carry electrons to the electron transport chain (ETC) on the inner membrane of the mitochondria, shown in Figure 1.7. Transport of electrons along the ETC facilitates the pumping of protons from the mitochondrial matrix into the intermembrane space, creating an electrochemical gradient and consuming oxygen, which is the final electron acceptor and results in conversion to water. The flow of protons back across the inner mitochondrial membrane through the enzyme ATP synthase (complex V) drives the conversion of ADP (adenosine diphosphate) to ATP, which is used as the 'energy currency' of the cell to drive unfavourable reactions. This process is known as oxidative phosphorylation (oxphos), and is the method by which the majority of ATP is produced in the cell.

Although the TCA cycle and the ETC/oxphos are distinct processes, their activities are intimately linked by NADH levels. For example, accumulation of NADH due to decrease in ETC activity leads to allosteric inhibition of TCA cycle enzymes (28). Therefore, TCA cycle activity will closely reflect ETC and oxphos activity, and vice versa.

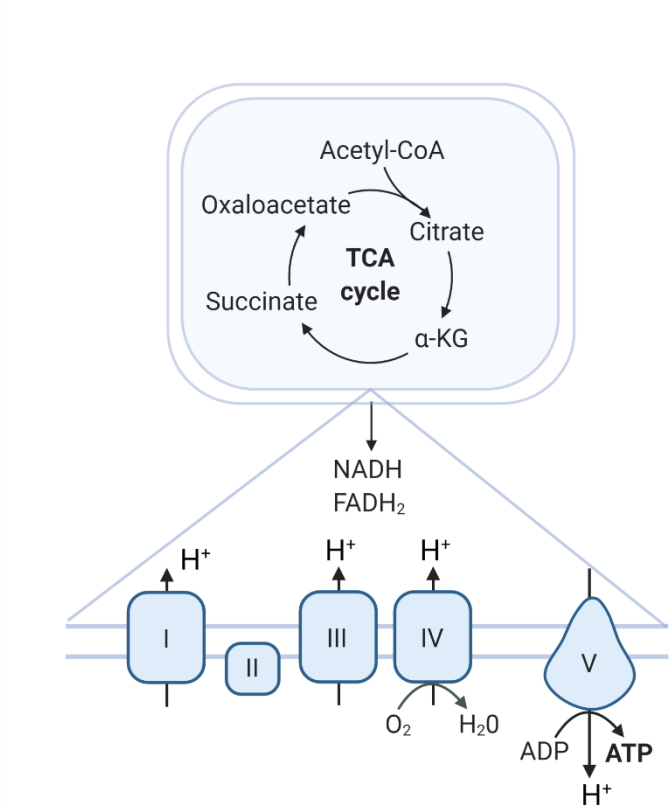

Figure 1.7 Electron transport chain

The TCA cycle in the mitochondria produces NADH and $FADH_2$, which donate electrons to the electron transport chain (ETC). The ETC is on the inner mitochondrial membrane and consists of complexes I-V. Complexes I, III and IV facilitate pumping of protons into the intermembrane space from the mitochondrial matrix. These flow back across the membrane via complex V, leading to production of ATP.

As rapidly proliferating cancer cells have increased requirements for both ATP and biosynthesis, they tend to increase flux through all of the pathways involved in central carbon metabolism. However, there is generally thought to be a tendency of cancer cells to increase glycolysis to a greater extent, resulting in an increase lactate production, even in the presence of sufficient oxygen. This phenomenon is known as aerobic glycolysis or the Warburg effect (further discussed in Section 1.2.4). However, this trend does not apply across all cancers. The specific metabolic program of cancer cells depends on many factors, including their site of origin and mutational status.

1.2.2 **Oncogenic signalling pathways and metabolism**

While metabolic reprogramming has previously been thought not to be a driver but a secondary outcome of tumorigenesis, it is now understood that many of the initiating and driver mutations in cancer directly influence metabolic pathways (29). Some examples that are related to CRC are discussed here. A summary of the effects of these signalling pathways and how they integrate with metabolic pathways is shown in Figure 1.8.

1.2.2.1 **Wnt**

Wnt signalling, the most common deregulated pathway involved in initiation of CRC tumorigenesis (see Figure 1.3), has been recently found to directly promote reprogramming of glycolysis in colorectal cancer (30). It was found that pyruvate dehydrogenase kinase 1 (PDK1, see Figure 1.6) was a novel Wnt target, therefore Wnt signalling regulates the rate of conversion of pyruvate to acetyl co-A.

1.2.2.2 **PI3K**

The PI3K pathway (see Figure 1.4) is another example of a common pathway which is deregulated in CRC which can influence metabolism. Activation of AKT downstream of PI3K signalling can increase glucose metabolism via upregulation of glucose transporters and glycolytic enzymes (31). Oncogenic *PIK3CA* mutations have also been shown to regulate glutamine metabolism in CRC (32).

1.2.2.3 **Myc**

Myc (which is also target of the Wnt and PI3K pathways) has an important role in regulating tumorigenic metabolism (33). A recent study showed that Myc activation reprograms cell metabolism at the adenoma stage of CRC development, including downregulation of genes involved in mitochondrial biogenesis (29, 34). Myc is also an important regulator of glutamine metabolism (35).

1.2.2.4 **mTORC1 and AMPK**

mTORC1 (mammalian target of rapamycin complex 1) is activated downstream of AKT and is another important metabolic regulator. mTORC1 signalling leads to regulation in several metabolic pathways (36), but its key role is integration of growth signals and nutrient abundance, activating anabolic/biosynthesis pathways and cell proliferation when the conditions are favourable. Presence of both essential and non-essential amino acids signal to activate mTORC1 (37). Constitutive mTORC1 signalling can therefore promote tumorigenesis, however,

excessive signalling can lead to cell death if proliferation is promoted when there are insufficient nutrients available. AMPK is an important signalling partner of mTORC1, which acts to inhibit mTORC1 and prevent cell proliferation when nutrients are scarce, therefore promoting cell survival in nutrient deplete environments, which cancer cells often face (38). Therefore, a balance between mTORC1 and AMPK signalling is essential for controlling cancer cell metabolism to promote increased growth and maintain survival.

1.2.2.5 **p53**

p53 is a key tumour suppressor protein involved in regulating cell cycle arrest and apoptosis, and loss of function of p53 occurs in a large proportion of CRC cases (29). p53 is increasingly being recognised as an important regulator of cell metabolism, and loss of p53 has been found to increase glycolytic flux (39).

1.2.2.6 **Ras**

Ras signalling, induced by receptor tyrosine kinases (RTKs) and affected by multiple mutations in CRC such as *KRAS* and *BRAF* (see Figure 1.4), can also influence metabolic pathways. Both *KRAS* and *BRAF* mutations have been found to drive reprogramming of glucose and glutamine metabolism in CRC cells (40). *KRAS* mutations have recently been shown to increase glutamine consumption in mouse models of CRC (41). *BRAF* mutated colorectal tumours have also recently been shown to have increased expression of the glycolytic enzyme enolase 2 (42). Activation of Ras signalling can also activate mTORC1.

1.2.2.7 **HIF**

Hypoxia inducible factor (HIF) signalling, which is important for regulating metabolism in response to low oxygen levels in normal cells, often becomes deregulated in cancer cells and influences metabolic reprogramming, such as promoting glycolysis. This is further discussed in section 1.2.5.

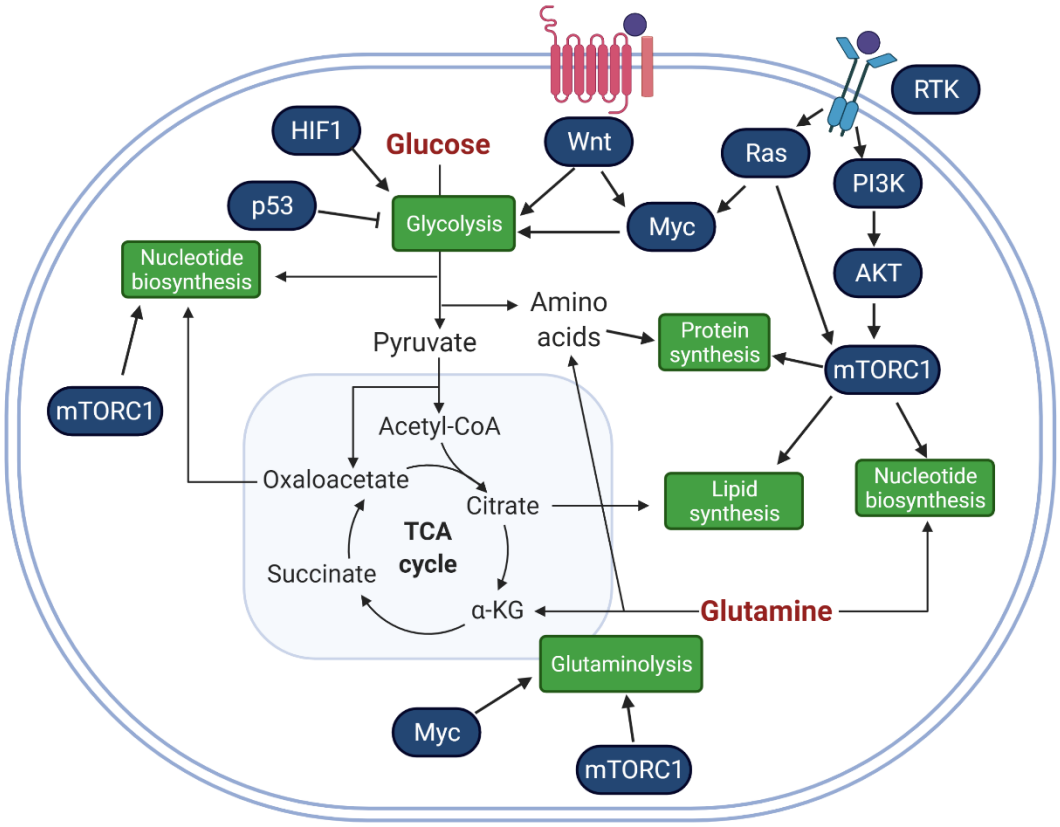

Figure 1.8 Cancer metabolism and signalling pathways

Overview of oncogenic signalling pathways that influence metabolism. mTORC1 signalling promotes anabolic pathways such as protein, nucleotide and lipid synthesis. Glycolysis can be regulated by many pathways including p53, Myc and Wnt signalling. Glutaminolysis can also be regulated by Myc and mTORC1. Abbreviations: receptor tyrosine kinase (RTK). Adapted from (26). Created with BioRender.com.

1.2.3 Role of metabolites in tumorigenesis

As well as oncogenic signalling affecting metabolism, metabolites themselves can influence signalling pathways in cells, affecting their tumorigenicity. The term “oncometabolites” is used to describe metabolites that can directly cause cells to become cancerous when they build up to unusually high levels, due to certain mutations in metabolic enzymes. Examples of oncometabolites include succinate, fumarate and R-2-hydroxyglutarate (R-2HG), the accumulation of which are caused by mutations in succinate dehydrogenase (SDH), fumarate hydratase (FH)

and isocitrate dehydrogenase (IDH) respectively, which occur in certain familial cancer syndromes (43). There are a variety of mechanisms by which these metabolites are thought to induce tumorigenesis, but a key mechanism is by the inhibition of α-ketoglutarate dependent dioxygenases (αKGDDs) (43). This group of enzymes includes prolyl hydroxylases (PHDs), which are involved in the degradation of hypoxia inducible factors (HIFs) in the presence of sufficient oxygen. Therefore, oncometabolites can lead to the constituent activation of HIFs, which promotes tumorigenesis (further described in section 1.2.5). These metabolites also inhibit other classes of αKGDDs that are involved in epigenetic modification, such as ten-eleven translocation proteins (TETs) and histone lysine demethylases (KDMs), leading to CpG island hypermethylation and histone hypermethylation, which can promote tumorigenic phenotypes (43).

Conversely, the TCA cycle metabolite α-ketoglutarate has been found in multiple scenarios to have anti-tumorigenic properties, via activation of αKGDDs. A recent study showed that in CRC organoids that had adapted to low-glutamine conditions, supplementation with α-ketoglutarate was sufficient to reduce Wnt signalling and stemness, which occurred at least in part through the promotion of TET activity and DNA demethylation (44). A similar effect has also been found in epidermal stem cells (45). Oncogenic epidermal stem cells were found to be reliant on extracellular serine, despite the ability to synthesise it. It was shown that activity of the serine synthesis pathway leads to an increase in α-ketoglutarate and activation of αKGDDs, promoting stem cell differentiation, therefore shutting down this pathway and relying on exogenous serine is a mechanism for promoting tumorigenesis (45).

Furthermore, a novel mechanism of epigenetic alteration by metabolites has recently been discovered. Lactate has been shown to modify histones with a novel epigenetic marker ‘lactylation’, which led to stimulation of gene transcription (46). These examples demonstrate how metabolic pathways and metabolites can directly influence cell fate and tumorigenicity.

1.2.4 **The Warburg effect**

Metabolic reprogramming in cancer cells was first recognised in the 1920s when Otto Warburg observed that cancer cells preferentially rely on glycolysis for energy production even in the presence of sufficient oxygen, resulting in a higher glucose consumption and lactate excretion than normal cells (47). This characteristic of cancer cells is known as aerobic glycolysis or the Warburg effect, and has been well established in many cancer types including CRC (29). The Warburg effect is

exploited to detect metastatic tumours using fluorine-18 fluorodeoxyglucose positron emission tomography ([^{18}F]FDG-PET) scanning. Due to increased uptake of glucose, the radioactive tracer FDG has a higher uptake in cancer tissue relative to healthy tissue, which can be visualised in the scan. As glycolysis produces ATP less efficiently than oxphos, it was at first unclear why cancer cells tend to rely more on this pathway. However, upregulation of glycolysis allows the build-up of glycolytic intermediates which can be diverted into anabolic pathways that are required to produce the biomass required for the high level of proliferation in cancer cells, such as the pentose phosphate pathway (PPP) which is required for the production of nucleotides (48). This may be an explanation as to the increased reliance on glycolysis, due to the increased demand for biosynthesis to support proliferation.

As well as providing biosynthetic intermediates, the Warburg effect can also affect the tumour microenvironment. Increased lactate excretion leads to extracellular acidification, which can promote tumour invasiveness, angiogenesis, and immunosuppression (49, 50). Lactate can also provide a fuel source for surrounding cancer cells and stromal cells, and has been shown to directly enter the TCA cycle (51).

1.2.5 **Molecular drivers of the Warburg effect**

The Warburg effect is driven by several known molecular changes and gene expression alterations within metabolic pathways. Several signalling pathways known to be implicated in CRC progression have been found to directly promote the Warburg effect. β-catenin signalling induced by APC loss has been recently shown to induce the Warburg effect (52), as well as p53 signalling (53).

These signalling pathways lead to regulation of key metabolic enzymes and transporters that promote aerobic glycolysis. Several of these have been shown to be important drivers of tumorigenesis and linked to poor patient outcomes in CRC, and some examples are discussed below.

1.2.5.1 **Glucose transporter 1**

As glycolysis produces fewer ATP molecules per molecule of glucose, cells undergoing the Warburg effect must increase their intake of glucose in order to produce a sufficient amount of energy and carbon for biosynthetic pathways. One way in which this is achieved is by the upregulation of glucose transporter 1 (GLUT1), which transports glucose across the plasma membrane into the

cytoplasm. GLUT1 has been shown to be significantly more highly expressed in CRC compared to the adjacent healthy tissue, and increased GLUT1 expression significantly associated with poorer prognosis of CRC (54). GLUT1 expression has also been found to be impacted by *KRAS* mutation; *KRAS* mutant CRC cells have been found to express significantly higher levels of GLUT1 compared to *KRAS* wild-type cells (55).

1.2.5.2 **Hexokinase 2**

Another enzyme involved in promoting the Warburg effect is hexokinase 2 (HK2), which catalyses the first step of glycolysis by conversion of glucose to glucose-6-phosphate. HK2 is one of a family of four HK genes, and expression of this particular isoform is usually limited to skeletal muscle, heart and adipose tissue (56). However, it also plays an important role in the metabolic reprogramming of cancer cells and has been found to be upregulated in several cancer types including breast (57) and stomach (58).

The role of HK2 in CRC is not completely clear. Increased expression of HK2 would be expected to increase the Warburg effect, increase tumour growth and subsequently lead to poorer patient outcomes. One study correlated positive HK2 expression in clinical samples with increased tumour size and higher stage of disease (59). However, another study of HK2 in CRC patients found the reverse relationship, with lower HK2 expression being associated with poorer progression-free and overall survival (60). However, in this study there was an association between increased HK2 expression in the tumour stromal cells and poorer outcomes (60). Therefore this difference in results may be partly explained by the metabolic interaction of tumour cells with the microenvironment including the surrounding stromal cells, known as the reverse Warburg effect (61). In this model, tumour cells induce the surrounding stromal cells to undergo aerobic glycolysis, providing the substrates such as lactate and pyruvate to the tumour cells, which can enter the TCA cycle and allow them to undergo more efficient ATP production via oxphos (61). This model is also supported by the association between tumours with high ratio of stroma-carcinoma composition and poorer prognoses (62). Therefore, the stroma-specific expression of HK2 needs to be studied in more detail to fully understand the importance of HK2 in CRC progression.

1.2.5.3 **Pyruvate kinase**

Expression of pyruvate kinase (PK) isoforms is another key mechanism that promotes the Warburg effect. This is the final rate limiting enzyme in glycolysis, catalysing the conversion of phosphoenolpyruvate to pyruvate (Figure 1.5). This enzyme is expressed from a single gene (*PKM*) but has two main splice variants: PKM1, which is expressed in most normal tissues, and PKM2, which is often expressed in cancer cells (63). PKM1 and PKM2 vary by one exon (Figure 1.9); the *PKM* gene has 12 exons in total, and exons 9 and 10 are unique to PKM1 and PKM2 respectively (64, 65). Splice factors that regulate expression of PKM1/2 include polypyrimidine tract binding protein (PTB), heterogeneous nuclear ribonucleoprotein A1 and A2 (hnRNPA1 and hnRNPA2), which repress production of PKM1 (66), and serine/arginine-rich splicing factor 3 (SRSF3), which promotes production of PKM2 (65, 67) (see Figure 1.9).

High expression of the PKM2 splice variant is known to be an important factor in the promotion of the Warburg effect in cancer cells. PKM2 is less catalytically active than PKM1, which leads to decreased production of pyruvate (65, 68). This reduces the substrate available for the TCA cycle, meaning cells become more reliant on glycolysis for ATP production. It also increases the pool of glycolytic intermediates available for anabolic pathways. By these same mechanisms, PKM2 is also important for the proliferation of normal cells; deletion of PKM2 in primary mouse embryonic fibroblasts prevents proliferation due to the insufficient production of nucleotides (69). PKM2 is often upregulated in CRC, and upregulation of PKM2 has been found to be a significant indicator of poorer prognosis in CRC patients (70, 71). It has also recently been found to be regulated by Wnt/β-catenin signalling (52). Furthermore, the *PKM* splicing proteins PTB, hnRNPA1 and SRSF3 (see Figure 1.9) have all been found to be overexpressed in patient CRC samples compared to adjacent healthy tissue, and silencing these proteins with siRNA has been found to slow cell growth by increasing the reliance on oxphos as well as inducing cell death (72). A recent study suggests that the long non-coding RNA SNHG6, which is a known oncogene in CRC, was found to interact with hnRNPA1 to induce alternative splicing of PKM and increase the PKM2/PKM1 ratio (73).

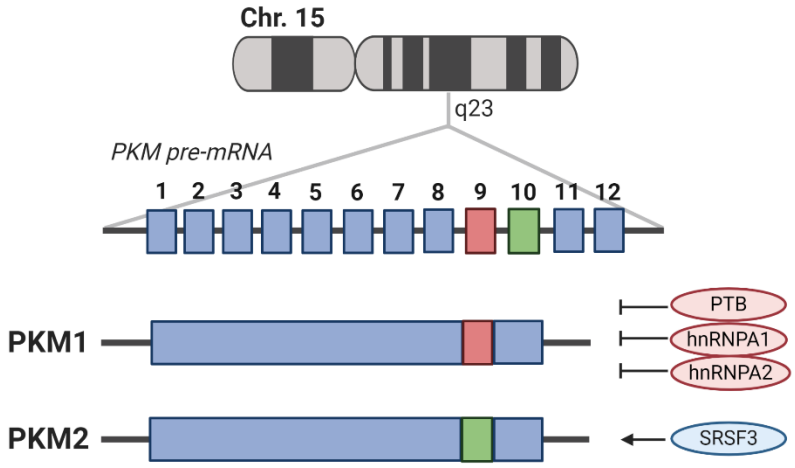

Figure 1.9 Alternative splicing of the *PKM* gene

The gene consists of 12 exons, and exons 9 and 10 are unique to the two main splice variants PKM1 and PKM2 respectively. Splicing of the *PKM* product is controlled by splicing factors PTB, hnRNPA2/1, SRSF3. Adapted from (65). Created with BioRender.com.

1.2.5.4 Pyruvate dehydrogenase kinase 1

Another key enzyme controlling the switch between glycolysis and oxphos in cancer cells is pyruvate dehydrogenase kinase 1 (PDK1). This is an inhibitor of the pyruvate dehydrogenase kinase (PDH) complex, which converts pyruvate to acetyl-CoA so it can enter the TCA cycle (see Figure 1.6). Activation of PDK1 would therefore decrease activity of PDH, decreasing entry of pyruvate into the TCA cycle and promoting the Warburg effect. Regulation of PDK1 by HIF-1 is an important component of regulating the switch from oxidative metabolism to glycolysis in hypoxia (74). It has also been shown to be a direct target of Wnt signalling in the promotion of the Warburg effect in CRC (30). Attempts have been made to inhibit PDK1 for cancer therapy, as this could promote increased reliance on oxphos and decrease the Warburg effect. PDK1 inhibitor dichloroacetate (DCA) has been shown to promote oxidative phosphorylation and reduce glycolysis, leading to cell cycle arrest and apoptosis in CRC cells (75).

1.2.5.5 **Lactate dehydrogenase**

In order to rely on energy production from glycolysis, cells must regenerate the nicotinamide adenine dinucleotide (NAD) required by glycolytic reactions to continually produce pyruvate. This is achieved by converting pyruvate into lactate, which is catalysed by lactate dehydrogenase (LDH) (Figure 1.5) (76). LDHA, a subunit of the LDH tetramer, is upregulated in CRC, and knockdowns of LDHA in CRC cell lines have been shown to reduce cell proliferation (77). LDHA has recently been found to be regulated by Wnt/β-catenin signalling and contribute to the Warburg effect in CRC cells (52).

1.2.5.6 **Hypoxia inducible factor-1α**

Hypoxia inducible factor-1α (HIF-1α) is also key to promoting the Warburg effect in CRC. HIFs are associated with activation of pathways such as glycolysis which allow cells to survive in conditions of low oxygen, and are important for allowing tumour cells to survive in the hypoxic conditions within tumours once they outgrow their blood supply, or where there is poor perfusion from the tumour vasculature (78, 79). However, they are also involved in promoting tumour cells growth in normoxic conditions by promoting aerobic glycolysis and the Warburg effect (79); expression of PKM (80), HK2 (60), GLUT1, LDH (77) and PDK1 (74) are all induced by HIF-1α. HIF-1α is commonly overexpressed in CRC and has been found to be associated with poorer prognosis (81).

1.2.6 **Role of oxidative metabolism in cancer**

When Otto Warburg originally observed the trend for increased aerobic glycolysis in cancer cells, he deduced that cancer was therefore caused by defective mitochondrial metabolism, and that impaired oxphos was a feature of all cancer cells (82). While some cancers are known to have dysfunctional mitochondrial metabolism due to mutations in TCA cycle enzymes such as FH, SDH and IDH as previously mentioned (43), the majority of cancer cells do still utilise mitochondrial metabolism; oxphos is actually increased compared to healthy tissue in several cancer types (26). Furthermore, increased lactate production does not necessarily indicate a defect in mitochondrial metabolism, as lactate has recently been shown to directly enter the TCA cycle therefore fuelling oxphos (51). This phenomenon has also been demonstrated specifically in CRC cells, and was found to occur particularly in conditions of nutrient depletion (83).

As well as being an efficient method of ATP production, the TCA cycle is important for fuelling anabolic pathways, such as nucleotide, fatty acid and amino acid synthesis in cancer cells (see Figure 1.6) (26, 84). The ETC itself has also been shown to be essential for biosynthesis as well as ATP production. In 2020, a study by Martínez-Reyes et al. showed that the ETC was important for the synthesis of nucleotides by activation of dihydroorotate dehydrogenase (DHODH), a key enzyme for purine synthesis (85). Complexes I and II of the ETC regenerate NAD and FAD by donating electrons to ubiquinone, converting it to ubiquinol. Complex III oxidises ubiquinol back to ubiquinone, which provides an electron acceptor for DHODH. Martínez-Reyes et al. showed that lack of complex III led to impaired tumour growth. This could be rescued by ectopic expression of alternative oxidase, which could also regenerate ubiquinone, but not an NADH oxidase that allowed regeneration of NAD. This shows that NAD regeneration is not the main function of complex III, and that it is required for activation of DHODH (85).

Recent studies have also shown that ETC function is important for synthesis of aspartate and asparagine; asparagine and aspartate supplementation have been shown to rescue proliferation when the ETC is inhibited, suggesting synthesis of these amino acids is a key function of the ETC (86-91). These findings challenge previous assumptions that the main function of the ETC is ATP production.

There is significant heterogeneity in the utilisation of mitochondrial metabolism for growth in different cancers; one recent study that measured mitochondrial membrane potential *in vivo* found that mitochondrial function significantly differed between multiple sub-types of lung cancer (92). This study demonstrates the importance of mitochondrial metabolism in cancer, and how the original concept of the Warburg effect is an oversimplified view of cancer metabolism.

Recent studies have also highlighted the importance of oxidative metabolism in CRC specifically (31); one study found that in CRC biopsy material, there was an upregulation of oxphos compared to surrounding healthy tissue (93). Oxphos has also been found to be an important feature of drug resistance and stemness in cancer cells (94, 95). A recent study compared mitochondrial function in CRC cell lines with different metastatic capabilities, finding that cells with increased metastatic potential has increased mitochondrial function, particularly increased function of complex I of the ETC, and were sensitive to inhibition of complex I, suggesting ETC and mitochondrial function is important for the metastatic potential of the cells (96).

Copy number of mitochondrial DNA (mtDNA) has been used as a way of investigating mitochondrial function in cancer cells. Increased copy number of mtDNA has been observed to induce oxphos, and enhance cell proliferation and metastatic potential of CRC cells (97), and a correlation between mtDNA copy number and CRC stage in patient samples has also been observed (98). Interestingly, it has been recently found that age-associated mutations in mtDNA that lead to defects in oxphos in the intestinal crypts may promote development of CRC, suggesting that as well as increasing oxphos, oxphos deficiency may also provide a growth advantage for tumour cells in certain contexts (99).

Similarly to the Warburg effect, classic signalling pathways and driver mutations in CRC have been shown to directly influence oxidative metabolism as previously mentioned, including KRAS/BRAF, Myc and p53 (31).

1.2.7 **Metabolism and stem cells**

Metabolism is also recognised as an important regulator in the maintenance of stem cells (100). This has significant implications for research into cancer therapies due to the importance of cancer stem cells (CSCs) in tumour regeneration and disease relapse. Although the metabolism of CSCs has been found to be highly plastic depending on the microenvironment, CSCs are generally thought to have a higher reliance on oxphos for energy production than the main population of cancer cells (101), and this has been found to be the case in CRC cells (102). More detailed understanding of the unique metabolic characteristics of CSCs will provide opportunities to improve CSC targeted therapy.

1.2.8 **Glutamine metabolism in cancer**

As well as relying on increased glucose metabolism, cancer cells also heavily rely on glutamine. Glutamine is a 'conditionally essential' amino acid, as it can be synthesised by cells but is required in larger amounts in metabolic stress, and is an important source of energy and biomass formation in rapidly dividing cells (103). Many cancer cell lines in several cancer types have been found to be 'glutamine addicted', meaning they cannot grow in the absence of glutamine (104).

1.2.8.1 **Roles of glutamine**

Glutamine is imported into the cell via transporters such as SLC1A5 (ASCT2, alanine-serine-cystine transporter 2) (105). This is one of several glutamine transporters however, it is of particular interest due to its increased expression being associated with CRC (106, 107).

Once imported, glutamine has several important roles in cancer cell metabolism (103, 108). It can be broken down by glutaminolysis to form α-ketoglutarate (α-KG) allowing it to enter the TCA cycle, a process known as anaplerosis (Figure 1.8). Glutamine is converted first to glutamate, this is mainly carried out by glutaminase enzymes 1 and 2 (GLS1 and GLS2), and then to α-ketoglutarate (α-KG) (109). Glutamate can be converted to α-KG by two main pathways, either by glutamate dehydrogenase (GLUD) which releases ammonia, or by transaminases, which transfer the amine group to other metabolites (Figure 1.10).

Glutamine anaplerosis is particularly important in the Warburg effect as there is a decreased proportion of glucose entering the TCA cycle. It has been shown that glutamine can fuel the TCA cycle independently of glucose in hypoxia or glucose depletion in B lymphocytes (110). Though previously thought to be mainly an important source of nitrogen for biosynthesis of amino acids and nucleotides, in 2007 DeBerardinis et al. showed that a large proportion of nitrogen derived from glutamine is excreted, highlighting it's importance as a carbon source for the TCA cycle in cancer (111).

By TCA cycle anaplerosis, glutamine contributes to ATP production, but it can also be used as a carbon and nitrogen for the synthesis of nucleotides and amino acids, as well as uridine diphosphate *N*-acetylglucosamine (UDP-GlcNAc), which supports the processing of proteins (112). Utilisation of glutamine for synthesis of pyrimidines has recently been shown to be increased by *PTEN* mutations (113). Another recent study has shown that an increased expression of phosphoribosyl

pyrophosphate amidotransferase (PPAT) is important for diverting glutamine into nucleotide biosynthesis pathways and supporting proliferation in cancer cells (114).

Once glutamine is converted into glutamate by GLS1/GLS2, this can also be used to regenerate glutathione, which is an electron acceptor that is able to clear excess reactive oxygen species (ROS) (103). This is particularly important for survival of cancer cells as the higher metabolic rate leads to an increase in ROS production, which can lead to cell death if the levels are too high. Glutamate, along with other amino acids, is important for maintaining synthesis of glutathione in cancer (115). Glutamine can also be converted to citrate via α-KG, an anti-clockwise step in the TCA cycle. This is known as reductive carboxylation and supports the diversion of citrate into lipid synthesis pathways (103).

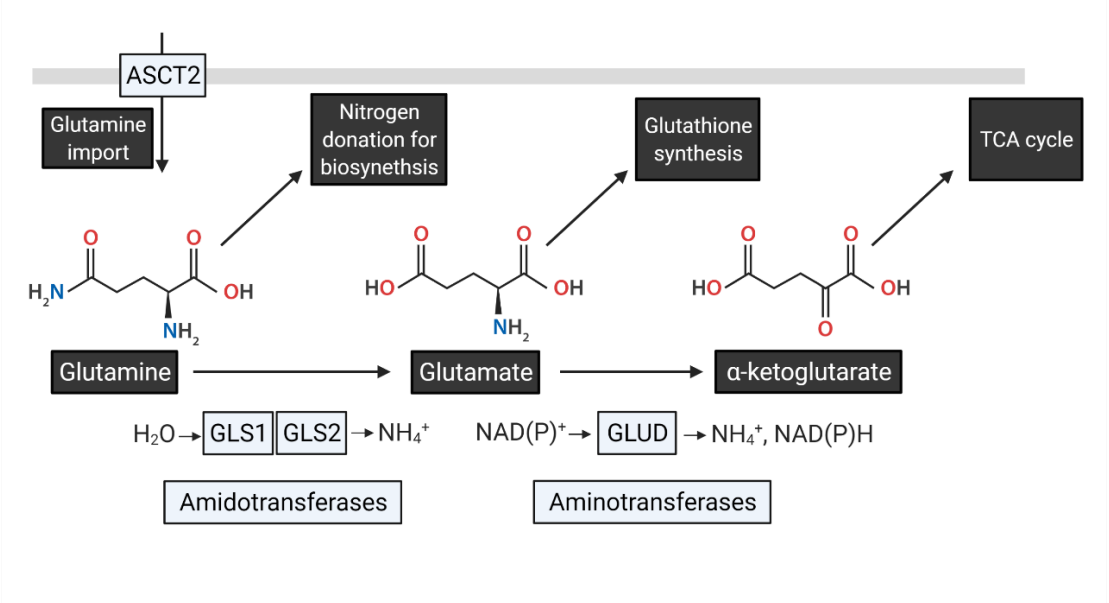

Figure 1.10 Overview of glutamine metabolism in cancer

In cancer cells, glutamine can be transported into the cell by the amino acid transporter SLC1A5/ASCT2 and used as a carbon source for the TCA cycle, as a nitrogen donor for biosynthesis, and for synthesis of glutathione which neutralises ROS. Abbreviations: glutaminase (GLS), glutamate dehydrogenase (GLUD). Adapted from (103). Created with BioRender.com.

On top of TCA cycle anaplerosis and biosynthesis, glutamine can also be used as an amino acid exchange factor, which has recently been shown to have an important role in CRC. A recent study found that *KRAS* mutant CRCs had increased glutamine consumption and increased sensitivity to glutamine withdrawal, however this was not dependent on expression of GLS1, and there

was not increased entry of glutamine into the TCA cycle (41). In this context, it was found that glutamine was being exported in order to allow import of essential amino acids for protein synthesis, via the large neutral amino acid transporter (LAT1), and these tumours showed sensitivity to genetic ablation of *SLC7A5*, which encodes a subunit of LAT1 (41). It had been previously found that the glutamine transporter ASCT2 and LAT1 are functionally coupled in this way to support tumour growth in certain cancer cells (116), but ASCT2 has also been found promote growth in a CRC cell line independently of LAT1 (117). More recently, it has been found that upregulation of LAT1 and ASCT2 in CRC cells overexpressing mutant KRAS is mediated by the pro-proliferative transcriptional regulator YAP1 (yes-associated protein 1), a transcriptional coactivator involved in the hippo tumour suppressor pathway (118).

1.2.8.2 **Importance of glutamine metabolism**

Understanding the role of glutamine metabolism in cancer has been difficult due to the nature of studying cellular metabolism *in vitro*. The metabolite composition of traditional cell culture media such a DMEM and RPMI is known not to be representative of metabolites available to cancer cells in the tumour microenvironment, including supraphysiological levels of glutamine. This can lead to a distinct metabolic program of cells cultured *in vitro* compared to *in vivo* conditions (119). As well as glutamine levels, high cysteine levels in cell culture media have also been shown to increase reliance on glutamine metabolism *in vitro* (120). This has led to difficulty in developing effective cancer therapies targeting glutamine metabolism, as drugs that are effective *in vitro* may not be effective *in vivo*, due to decreased reliance on glutamine.

Despite this, it is now well established that glutamine metabolism is key for certain tumour types *in vivo*. As with all aspects of cellular metabolism, the extent of reliance on glutamine metabolism is greatly heterogeneous between cancer types and sub-types. CRC in particular has been found to be especially reliant on glutamine metabolism. Using *in vivo* metabolic tracing of ^{13}C-glutamine, glutamine has been shown to enter the TCA cycle at a higher rate in tumour compared to normal tissue in CRC (121). Another study found that CRC cells are particularly reliant on glutamine entry into the TCA cycle compared to other cancer cell types, and this was suggested to be due to the nature of glutamine metabolism in the healthy colon (114). Increased reliance on glutamine to fuel the TCA cycle in normal intestinal tissue is thought to decrease glucose consumption and therefore

improve efficiency of glucose absorption into the bloodstream (114). Furthermore, approximately 30% of total glutamine consumption in the body is thought to occur in the intestine, and glutamine has been found to be important for intestinal function, including tissue integrity and regulation of inflammation (122).

Increased expression of genes involved in glutamine metabolism have been significantly associated with CRC. GLS1, which catalyses the first stage of glutaminolysis, has been shown to be upregulated in CRC compared to the surrounding tissue, and knockdown of its expression reduces proliferation and viability of CRC cells (123). GLS1 expression has also been associated with a lower differentiation state of CRC tumours and a higher TNM stage, both of which are indicative of poorer prognosis (123, 124). GLS1 expression has been suggested to be important for the stem-like phenotype of CRC cells, as it has found to be increased in metastatic compared to primary tumours, and correlated with increased mortality and more advanced stage of disease (125).

GLUD, which catalyses the second step of glutaminolysis from glutamate to α-KG, is also upregulated in CRC and a significant marker of poorer prognosis (126). Furthermore, increased GLUD expression has been shown to increase proliferation and migration of CRC cell lines, and vice versa with GLUD knockdown (126). Expression of the glutamine transporter ASCT2 and the glutaminolysis enzyme glutamic-pyruvic transaminase 2 (GPT2) have been found to be increased to support glutamine utilisation in the rare sub-type of CRC known as colorectal signet ring cell carcinoma (SRCC) (127). ASCT2 has also been found to be upregulated in patient CRC samples with *KRAS* mutations (128).GPT2 has been found to be upregulated by oncogenic PI3K signalling via activating transcription factor 4 (ATF4) in CRC, leading to increased glutamine metabolism and anaplerosis, and increased sensitivity to glutamine deprivation (32).

1.2.8.3 **Glutaminases in cancer**

There are two glutaminase genes in the human genome; *GLS*, which is located on chromosome 2, and *GLS2,* which is located on chromosome 12. *GLS* codes for the GLS protein (also known as GLS1). *GLS2* codes for the GLS2 protein, also known liver-type glutaminase (LGA). *GLS* transcripts are alternatively spliced to create two isoforms of the GLS1 protein; kidney-type glutaminase (KGA) and glutaminase C (GAC), which is truncated at the C-terminus compared to KGA (129, 130). Both the KGA and GAC isoforms of GLS1 have been found to be overexpressed in various cancers (131), however GAC is the more active isoform

and has been thought to be the most important isoform in cancer cells, therefore alternative splicing of *GLS* mRNA may be an important mechanism for increasing glutaminolysis in cancer cells (132, 133). Recently, it has been found that the long non-coding RNA (lncRNA) Colon Cancer Associated Transcript 2 (CCAT) interacts with Cleavage Factor I (CFIm) complex to regulate alternative splicing of GLS1 pre-mRNA towards to GAC isoform in CRC (134).

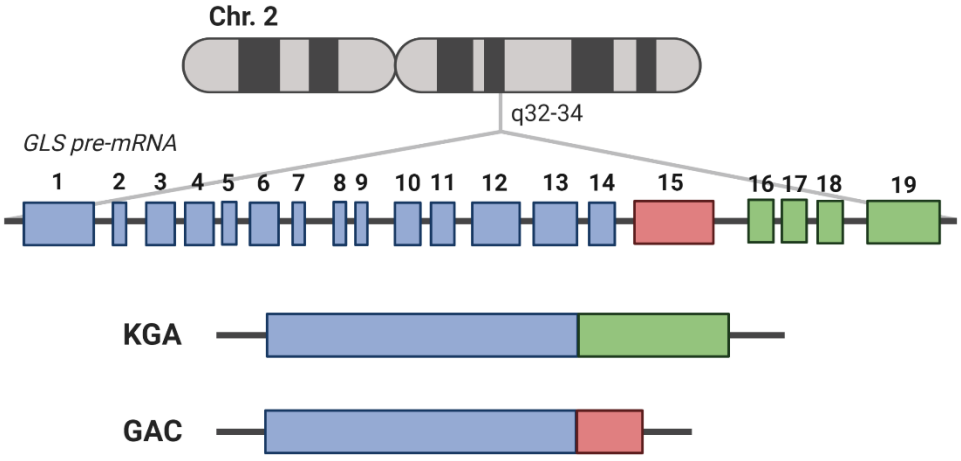

Figure 1.11 Alternative splicing of the *GLS* gene

The *GLS* transcript codes for two splice variants, KGA and GAC. Both variants contain exons 1-14. KGA is the longer isoform containing exons 16-19 at the C-terminus, whereas the GAC isoform only contains exon 15 at the C-terminus. Adapted from (130). Created with BioRender.com.

As well as alternative splicing, GLS1 activity can be modulated both by regulation of transcription and by post-translational modification. Transcription of GLS1 has been shown to be associated with oncogenic pathways, in particular c-Myc, which has been found to promote GLS1 expression via regulation of microRNAs (35, 135). Multiple post-translational modifications have been identified that can affect GLS1 activity, including phosphorylation (136). Presence of inorganic phosphate (Pi) can lead to formation of an active tetramer of the protein being formed from the inactive dimer (132). Phosphorylation of GLS1 has been shown to be vital for its activation; expression levels of GLS1 do not necessarily correlate with its activity levels (137). Cancer cell-derived GAC has higher basal activity than recombinant

GAC, which can be reversed by adding phosphatases, showing that GAC phosphorylation is key to increasing glutaminase activity in cancer cells (137).

GAC has been found to have the largest increase in activity at high levels of inorganic phosphate (Pi) compared to GLS2 and KGA, which could explain its importance in tumours (132). It has been suggested that as Pi levels may increase with hypoxic conditions, which are often found in solid tumours due to poor tumour vasculature, GAC may be an important component in meeting energy demands in response to these conditions (132). Phosphorylation and activation of GLS1 has been shown to be induced by the oncogenic signalling pathway Raf-Mek-Erk (138), as well as NFκB; activation of GLS1 was found to be an important component of cellular transformation downstream of induction of Rho-GTPases, which activate NFκB signalling, though the exact mechanism was not reported (139). However, more recently it has been shown that NFκB signalling leads to phosphorylation of GAC at Ser314 by PKCε, which leads to its activation (136).

Post-translational modification can also affect the stability of the GLS1 protein as well as its activity; for example, one study has shown that SIRT5 can desuccinylate GLS1 protein, which protects it from ubiquitination and subsequent degradation, therefore increasing the stability of the protein (140). Succinylation can also affect GLS1 activity; a recent study found that GLS1 expression is important for pancreatic cancer cell proliferation, and that under oxidative stress, GLS1 has increased succinylation which increases glutaminolysis, increasing production of both NADPH and glutathione, promoting cell growth and survival (141).

Interestingly, GLS2 expression has been found to be activated by p53 and has shown tumour suppressive roles in some studies (142, 143). One study has shown that GLS2 expression is decreased in tumour tissue in hepatocellular carcinoma, in contrast to GLS1 expression which is increased (144). However, GLS2 has also been found to promote tumorigenesis in some cases, so the role of this enzyme is likely to be highly context dependent (145).

1.3 Aspirin and colorectal cancer

Aspirin is a widely used non-steroidal anti-inflammatory drug (NSAID). It is an analgesic and anti-inflammatory agent, as well as a preventative agent in patients at high risk of cardiovascular disease, due to its inhibition of cyclooxygenase 1 (COX1) in platelets and inhibition of blood clotting. It is mainly taken orally and absorbed in the stomach and small intestine (146). Doses vary depending on the intended use from 75mg/day to 1.2g/4 hours, with plasma concentrations reportedly reaching 144μM at the highest doses (147, 148). Concentration of aspirin in the intestine can reach higher levels due to low bioavailability, particularly with enteric coated forms, allowing unabsorbed aspirin to reach the intestine (148, 149). It has been suggested that assuming an intestinal fluid volume of 160-750ml, and 50% absorption rate, a small dose of aspirin (81mg) could reach 1.4mM in the intestinal fluid (148). Other studies have suggested that therapeutic concentrations of aspirin range between 0.1-2mM (150, 151), though concentrations of 4mM and above are frequently used in *in vitro* studies. Aspirin rapidly undergoes hydrolysis in the plasma, intestine and liver to produce salicylic acid (146).

1.3.1 Role of aspirin in CRC prevention and treatment

The link between long-term use of aspirin and a decreased CRC incidence is well established; the association was first reported in a case-control study in 1988 (152, 153), and was found in a 20-year follow up of two large randomised control trials (RCTs) and a review of the observational studies in 2007 (154). This analysis found there to be a 10-year latency before seeing a significant effect of aspirin treatment on CRC incidence. While high-dose aspirin (>500mg) was shown to be effective in reducing CRC risk, this is associated with a significantly increased risk of bleeding. Low-dose aspirin (75-300mg) has also been found to be effective at reducing long-term CRC incidence in a follow up of three low-dose aspirin RCTs (155). Based on an evidence review of the preventative effects of aspirin, the US Preventative Services Task Force (USPSTF) recommended in 2016 that 50-59 year olds with no increased risk of bleeding take daily low-dose aspirin for the prevention of CRC, although it is suggested that this must be continued for at least 10 years to provide a benefit (156). Investigations into the efficacy of aspirin in the prevention of CRC are ongoing; a systematic review and meta-analysis of observational studies published in 2020 estimated that regular aspirin users have between 10-35% reduced risk of CRC; interestingly this study found that a higher dose had a stronger effect on risk reduction (157). Further work is also being done in order to

determine for which individuals the benefits of taking aspirin to prevent CRC outweigh the potential risks (158).

The role of aspirin as an adjuvant treatment for CRC is emerging but less well established than its primary preventative role. While several years of prophylactic aspirin treatment are required in order to see a reduction in CRC risk due to the length of time over which CRCs usually develop, there is evidence that a shorter term effect is seen on CRC mortality, suggesting an effect of aspirin on early CRCs that are already present in patients at the beginning of the aspirin treatment (159). A study of five UK randomised controlled trials (RCTs) of daily aspirin for cardiovascular disease prevention found a reduced risk of diagnosis of metastatic adenocarcinoma after only a few years of treatment, and a reduced risk of subsequent metastasis in those diagnosed with non-metastatic cancer during the trial (159).

Further studies have also identified a significant decreased risk of CRC mortality with aspirin use following a diagnosis of CRC, supporting the effectiveness of aspirin as an adjuvant as well as preventative therapy (160, 161). The role of aspirin as an adjuvant therapy in patients diagnosed with CRC is under ongoing investigation in clinical trials, for example the Add-Aspirin trial, which is a double-blinded randomised trial comparing multiple doses of aspirin to a placebo on survival and disease recurrence in multiple cancer types (162). Most recent reports from this trial show there has been recruitment of 950 patients in the CRC cohort, there has been good adherence to the trial among participants, and that there has been low toxicity to the aspirin treatment in these patients (163).

As with use of aspirin in prevention of CRC, it is not clear which patients are most likely to benefit from aspirin as an adjuvant therapy. Studies have found that in patients who are diagnosed with CRC, long-term use of aspirin prior to diagnosis as a primary preventative does not significantly decrease CRC mortality after a diagnosis (155, 160, 161). Furthermore, use of aspirin after CRC diagnosis has been found to only be effective at increasing survival in patients who were not using aspirin before their diagnosis (161). This suggests that CRCs that arise subsequent to the use of long-term aspirin are resistant to the anti-tumorigenic effects seen with aspirin use post-diagnosis. The protective effects of long-term aspirin use against CRC incidence has been found in one study to be limited to COX2 positive tumours (164), so tumours arising in patients taking long-term aspirin are more likely to be COX2 negative. This may explain the lack of efficacy

of aspirin post-diagnosis in patients previously taking long-term aspirin. Benefit from post-diagnosis use of aspirin has been found to be limited to COX2 positive tumours, and COX2 positive tumours that arose in patients who were using long-term aspirin were still responsive to aspirin after diagnosis (161). Survival benefits of aspirin use after diagnosis have also been reported to be limited to tumours with mutated *PIK3CA* in CRC (165), as well as in breast cancer (166), though an inverse effect has also been found in HER2 positive breast cancer (167). However, this relationship between pre-/post-diagnosis aspirin use and survival is not completely established; other studies have found that both pre- and post-diagnosis use of aspirin is effective at reducing CRC mortality (168). These authors suggest that CRCs arising in long-term users of aspirin tend to be more highly differentiated, which is indicative of a better prognosis than poorly differentiated tumours (168).

1.3.2 **Mechanisms of action of aspirin on CRC**

There are several mechanisms by which aspirin is thought to have these anti-tumour effects both in the prevention and treatment of CRC, however they are difficult to fully elucidate as aspirin and its active metabolite salicylic acid have many cellular targets (169). Further characterisation of the anti-tumour mechanisms of aspirin is an important research priority, as this could lead to the development of more specific drugs that could target the same pathways as aspirin with fewer side effects, leading to decreased incidence of CRC and improved outcomes for patients without the associated risks such as gastrointestinal (GI) bleeding. Further understanding of the effects of aspirin is also required to inform dosing and timing of treatment for optimum effectiveness, and to identify which patients are most likely to benefit from aspirin as either a preventative or therapeutic measure.

1.3.2.1 **COX-dependent**

One of the main mechanisms by which aspirin is thought to impact cancer incidence and outcome is through its acetylation and inhibition of cyclooxygenase (COX) enzymes, which are responsible for producing prostaglandins (PGs) and thromboxanes from arachidonic acid. COX1 is a housekeeping enzyme expressed in many tissues, and the only form that is expressed in platelets. Inhibition of COX1 is thought to be the main mechanism by which aspirin has vascular benefits; COX1 inhibition in platelets is irreversible as they are anuclear and therefore unable to resynthesise COX1 (153). COX1 is important in platelets for the production of thromboxane A2 (TxA2) which is required for platelet aggregation. Platelets have

long been thought to be involved in promoting metastasis of tumour cells (170), therefore inhibition of COX1 may be a mechanism by which aspirin inhibits CRC progression (159, 171).

In contrast to COX1, COX2 is selectively expressed in inflammatory and hypoxic conditions (172), as well as being frequently overexpressed in CRC (173). This leads to increased production of PGs; PGE_2 in particular is thought to have many effects on cell signalling that promote tumorigenesis through its interaction with the G-protein coupled receptors (GPCRs) EP1-4, which influence many pathways relating to cancer hallmarks (174, 175). For example, activation of the EP2 receptor by PGE_2 has been found to activate β-catenin signalling via the PI3K/AKT pathway, as well as by direct interaction with the β-catenin destruction complex (176). The α-subunit of the G protein associated with the EP2 receptor interacts with Axin to promote β-catenin release from the destruction complex (176). The βγ subunits activates phosphoinositide 3-kinase (PI3K), leading to the activation of the protein kinase AKT which inhibits the destruction complex component GSK-3β (176). Both of these pathways lead to increased accumulation and nuclear translocation of β-catenin.

Due to the many roles of PGE_2 in influencing cell signalling pathways related to tumorigenesis, it seems clear that COX2 inhibition is one way which aspirin can exert anti-tumorigenic effects on colorectal epithelial cells. Although it has been suggested that low-dose aspirin is insufficient to inhibit COX2 in epithelial cells (and the effect may therefore be limited to platelets), there is evidence that COX2 inhibition is involved, as the response to aspirin is related to levels of COX2 expression in the tumour (161, 171).

Interestingly, a recent study that sampled metabolites in the aerosols produced from cauterising different breast tumours found that tumours with *PIK3CA* mutations produced higher levels of arachidonic acid (177). As *PIK3CA* mutations has been previously shown to sensitise breast cancer cells to aspirin (166), it was speculated that this could be linked to the arachidonic acid levels, as aspirin inhibits the conversion of arachidonic acid to prostaglandins by COX (177). However, the mechanism has not been fully elucidated, and possibly relies on COX-independent mechanisms of aspirin.

1.3.2.2 **COX-independent**

Despite the clear role of COX inhibition in the anti-cancer effects of aspirin, there is evidence to suggest there are also COX-independent mechanisms. For

example, aspirin also inhibits the growth of the COX2 negative CRC cell line SW480 (178). Furthermore, treatment with prostaglandins is not sufficient to reverse the growth inhibitory effects of the NSAID suldinac sulphide (179, 180). An aspirin derivative that does not inhibit COX has also been found to be more effective against formation of aberrant crypt foci than aspirin in a mouse study (181).

Several COX-independent mechanisms of aspirin's anti-tumour effects have been suggested, including modulation of the NFκB pathway (182) (illustrated in Figure 1.12). NFκB is a family of transcription factors composed of RelA/p65, RelB, c-Rel, p100/p52 and p105/p50, which form dimers (most commonly RelA/p50) that activate transcription of a wide variety of genes involved in processes such as inflammation and proliferation (183). NFκB is classically activated by tumour necrosis factor α (TNFα) and interleukin 1 (IL-1), which lead to degradation of inhibitors of NFκB (IκB), which usually hold NFκB in the cytoplasm and prevent nuclear translocation (183). This occurs via activation of IκB kinase (IKK) complex containing IKKα/β and NFκB essential modulator (NEMO) (183). Upregulation of NFκB is a common occurrence in cancer and can contribute to tumour progression (184). However, the effects of NFκB can be varied and are context dependent, for example in some circumstances it also has pro-apoptotic effects (185).

The initial finding reporting that aspirin regulates NFκB signalling showed that aspirin inhibited IKK and prevented canonical NFκB signalling (182, 186, 187). However, prolonged exposure to aspirin has also been found to activate NFκB by inducing degradation of IκB and therefore promoting translocation of NFκB to the nucleus. While NFκB signalling is most commonly associated with pro-tumorigenic effects, in this context it was found to be pro-apoptotic (188). This mechanism was first identified in vitro in 2001 (188) and has been subsequently verified in *in vivo* models of CRC (189). These roles of aspirin in modulating NFκB signalling are illustrated in Figure 1.12.

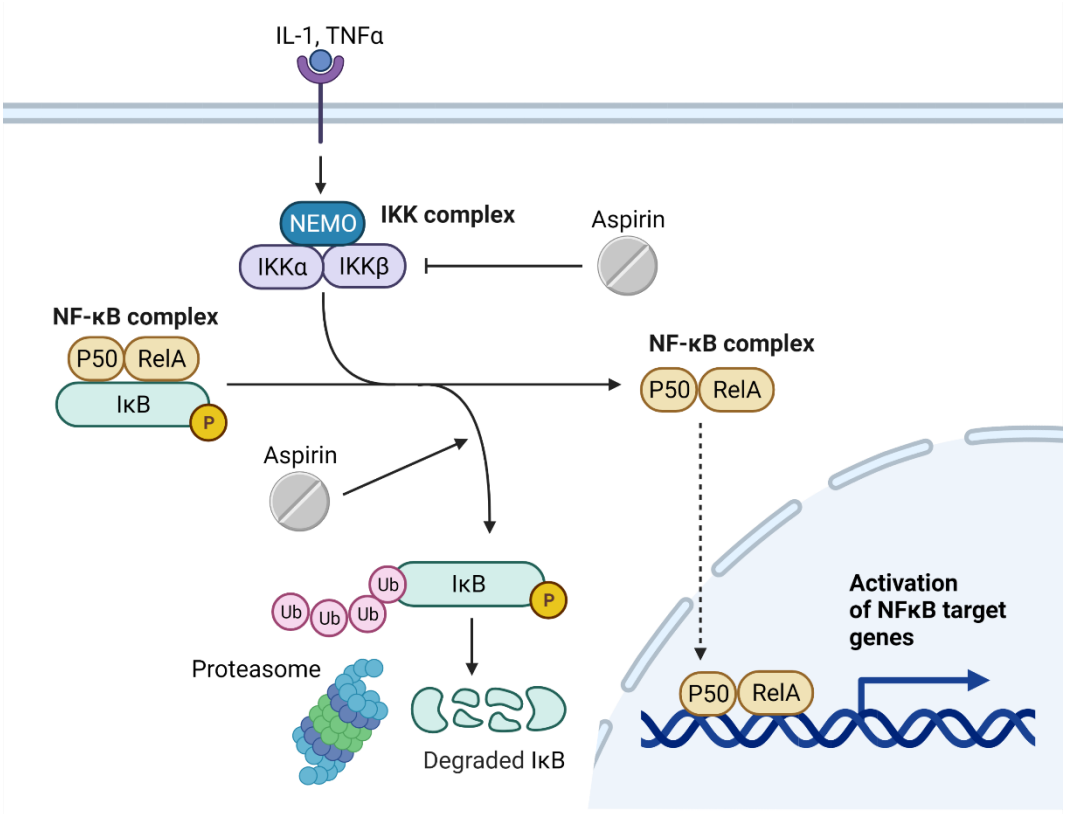

Figure 1.12 NFκB signalling and the roles of aspirin

NFκB complexes are made up of dimers, most commonly p50 and RelA. These are sequestered in the nucleus by inhibitors of NFκB (IκB) until activation by signals such as interleukin 1 (IL1) or tumour necrosis factor α (TNFα). These activate the IKK complex, which is made up of IKKα/β and NFκB essential modulator (NEMO). The IKK complex induces ubiquitination (Ub) of IκB and degradation by the proteasome, therefore allowing translocation of the NFκB complex into the nucleus and activation of NFκB target genes. Aspirin has been shown to inhibit the IKK complex as well as induce the degradation of IκB. Adapted from (182). Created with BioRender.com.

More recently, it has been found that stimulation of NFκB by aspirin occurs via signalling in the nucleolus, the organelle with the primary role in production of ribosomes (190). Aspirin was found to induce degradation of TIF-IA, an important component in the initiation of ribosomal DNA transcription, which leads to disruption of nucleolar function and subsequent activation of NFκB (190, 191).

Interestingly, the effect of aspirin on NFκB signalling has been implicated in overcoming therapeutic resistance in CRC. One study found that incubating CRC cell lines SW620 and SW480 in 5-fluorouracial (5-Fu), a common chemotherapeutic agent in CRC, rendered them resistant to the drug, which

involved upregulation of NFκB signalling (192). Treating with aspirin was found to abolish the induction of NFκB signalling induced by 5-Fu and sensitivity to 5-Fu was increased in both 5-Fu resistant and sensitive cells by aspirin. This effect was also replicated *in vivo* (192). Another known inhibitor of NFκB signalling also increased sensitivity to 5-Fu in resistant cells, but this did not increase the effect of combining aspirin and 5-Fu, further supporting the hypothesis that aspirin was promoting 5-Fu resistance through inhibition of NFκB signalling (192).

Aspirin has also been suggested to affect TGF-β signalling. TGF-β signalling has a complex role in cancer, having been found to have both tumour suppressor and tumorigenic properties. While it has been found to induce growth arrest and apoptosis, it can also promote tumorigenesis by inducing epithelial to mesenchymal transition (EMT), which increases the migratory and metastatic capacity of cancer cells (193). In one recent study, aspirin was found to reduce viability and migration in cells that had been induced to a mesenchymal phenotype with TGF-β1 (194). Aspirin has also been shown to alter expression of genes associated with EMT, including increasing E-cadherin and decreasing N-cadherin, as well as reducing expression of Snail, Slug and Twist (194). Aspirin has also been shown to induce secretion of TGF-β1 in CRC cells, leading to an induction of apoptosis (195). In this study, the effect of aspirin on viability was rescued using an inhibitor of TGF-β1, suggesting aspirin does act via TGF-β1 (195).

The effect of aspirin on migratory capacity of CRC cells has also been found to be mediated by its effect on Wnt signalling. Aspirin has been shown to decrease Wnt signalling, stemness markers and markers of EMT in intestinal organoids (196). Furthermore, the effect of activating Wnt signalling on inducing EMT and stemness was attenuated by aspirin treatment in this study (196).

Some research has also shown that aspirin may have epigenetic effects. Epigenetics involves chromatin modifications that do not alter the sequence of DNA but have effects on gene expression, such as DNA methylation and histone acetylation. Published studies have found aspirin to increase histone acetylation (197, 198). One recent study found that aspirin treatment leads to an increase in histone 3 methylation, which leads to suppressed expression of stemness-associated genes in multiple cancer cell lines, independent of COX inhibition (199). Unpublished work from the Williams lab has shown that long-term treatment (>1 year) of CRC cell lines with aspirin can induce a genome-wide increase in DNA methylation, which is not seen after short-term treatment (48-72 hours). This

included the promoter regions of many genes and is therefore likely to influence transcription. The absence of this effect in short-term treatment suggests that this could explain how cells become resistant to long-term aspirin treatment, as seen in the decreased efficacy of aspirin in treating CRC patients who have previously taken long-term aspirin (see Section 1.3.1).

Recent work has found that the effect of aspirin in the intestine may be in part reliant on metabolites of aspirin produced by gut bacteria (148). 2,3-dihydrobenzoic acid (2,3-DHBA) and 2,5-dihydrobenzoic acid (2,5-DHBA) are thought to be produced as a result of metabolism of aspirin and salicylic acid by gut bacteria and have been found to inhibit cyclin-dependent kinases (CDKs) and colony-forming ability of CRC cells (200).

1.4 Aspirin and cancer metabolism

As described in a review by Zhang et al in 2019 (201), the anti-cancer effects of aspirin are broad and can be related to all of the hallmarks of cancer, including deregulated energy metabolism. A small but increasing number studies have highlighted effects of aspirin on various aspects of metabolism of cancer cells, suggesting this may be a mechanism by which aspirin reduces cancer cell growth. Studies to date that identify metabolic effects of aspirin on cancer cells are summarised in this section.

1.4.1 Glucose metabolism

Aspirin was thought to affect glucose metabolism in platelets as far back as 1969, when it found that incubation with aspirin decreased glycolysis and release of ATP (202). More recently, in breast cancer stem cells (BCSCs), aspirin has been found to suppress glycolysis via inhibition of PDK1 (see Figure 1.6) (203). PDK1 was found to be required for reprogramming BSCSs to a highly glycolytic metabolism in hypoxia, which is important for the maintenance of stemness (203). Furthermore, PDK1 was found to be regulated in these cells via a signalling pathway involving HIF-1α and long non-coding RNA H19, which was also downregulated by aspirin (203).

Aspirin has also been found to have effects on the glycolytic enzyme HK2 in ovarian cancer (204). Loss of function mutation in the tumour suppressor BRCA1 is known to affect DNA damage repair, however this study discovered there is also an effect on metabolism; BRCA1 mutant cells showed increased glycolysis and increased levels of glycolytic enzyme HK2 (204). This effect was found to be reversed by aspirin treatment, suggesting a role for ovarian cancer chemoprevention in carriers of BRCA1 mutations (204).

Two studies have shown effects of aspirin on the glycolytic enzyme phosphofructokinase (PFK). One study showed that both aspirin and its metabolite salicylic acid decreased glycolysis and activity of PFK in the breast cancer cell line MCF-7 (205). In hepatocellular carcinoma (HCC), aspirin was found to increase sensitivity of cells to sorafenib, a kinase inhibitor which is highly effective for treating HCC and to which resistance is common (206). A feature of resistant cells is high glycolytic flux and increased expression of PFK, both of which were countered by aspirin, leading to increased sensitivity to sorafenib (206).

In the CRC cell lines HCT-116 and HT-29, several acetylation targets of aspirin linked to glycolysis have been identified, including PKM2 and LDH, although this was not found to affect the activity of these enzymes (169). One aspirin target in these cells which was found to have altered activity was glucose-6-phosphate dehydrogenase (G6PD), which catalyses the first step of the pentose phosphate pathway (PPP) and was found to have 14 lysine residues that were acetylated by aspirin (207). The PPP involves the synthesis of ribose sugars, a requirement for nucleotide biosynthesis, as well as generation of NADPH which is essential for glycolysis and biosynthesis, and therefore an important pathway for rapidly proliferating cells. G6PD has also been suggested as a promising therapeutic target due to its importance in tumorigenesis (208) and has been found to be overexpressed in CRC cells and correlates with poor prognosis (209). Therefore, acetylation and inhibition of G6PD may be an important mechanism by which aspirin acts on CRC cells.

More recently, a study found that in hepatoma cells, aspirin treatment reduced cell proliferation and glucose consumption via downregulation of the glucose transporter GLUT1 (210). Furthermore, HIF-1α expression was also decreased by aspirin in these cells and induction of HIF-1α partially rescued the decrease in GLUT1 expression caused by aspirin (210). An NFκB binding site has also been found in the GLUT1 promoter (210). As NFκB signalling has previously been shown to be modulated by aspirin (182), this suggests that aspirin may reprogram glucose metabolism in cancer cells via HIF-1α and NFκB signalling and GLUT1 downregulation (210). Aspirin has also been found to decrease expression of GLUT1 and reduce glucose uptake in vascular endothelial cells (211).

1.4.2 **Glutamine metabolism**

A study published in 2020 suggested that the effect of aspirin on glutaminolysis may be an important mechanism of action of aspirin in *PIK3CA* mutated CRC cells. The authors found that in the absence of glutamine, aspirin did not have a growth inhibitory effect on *PIK3CA* mutant CRC cells (212). They also found that aspirin upregulates several genes involved in glutamine metabolism, including ASCT2, LAT1, GLS1 and GPT2, and that aspirin induces activation of ATF4 signalling. They suggest that aspirin treatment promotes glutamine metabolism via induction of ATF4 and mimics the effect of glutamine depletion in *PIK3CA* mutant cells, though glutamine metabolism was not directly measured in this study (212). Interestingly, aspirin has also been found to activate ATF4 signalling in multiple

myeloma cells (213). *PIK3CA* mutations have also been shown to regulate glutamine metabolism via ATF4 in CRC (32), therefore it is interesting to speculate that this may be linked to the increased sensitivity of *PIK3CA* mutant cancers to aspirin treatment (165), though this has yet to be directly investigated.

Aspirin has been shown to affect several signalling pathways that have been linked with glutamine metabolism, though it has not been directly shown that aspirin affects glutamine metabolism through these mechanisms. For example, aspirin is thought to affect NFκB signalling (section 1.3.2.2), which has been found to be important for GLS1 activation (section 1.2.8.3). Furthermore, aspirin is thought to induce TGF-β1 signalling (section 1.3.2.2), which has also recently been shown to upregulate GLS1 (214).

Interestingly, aspirin has been postulated to affect tumour glucose and glutamine metabolism *in vivo*. In this study, a high-fat diet was found to promote obesity as well as tumour growth in a mouse tumour xenograft model (215). Aspirin treatment in the obese tumour-bearing mice was found to slow tumour growth, reduce circulating glucose and glutamine and reduce expression of both glutamine (ASCT2, LAT1 and GLS1) and glucose (GLUT1 and PKM2) metabolism proteins (215).

1.4.3 **Lipid metabolism**

Another metabolic feature of CRC targeted by aspirin is aberrant lipid metabolism. Cancer cells increase their intake of circulating fatty acids (FAs) and increase biosynthesis of lipids and cholesterol due to the increase in production of cell membranes, and to supply the excess energy requirements of the cells by storing lipid droplets, which can be utilised for ATP production by fatty acid oxidation (FAO) (29, 216).

The first step of lipid metabolism after the entry of FAs into the cells is conversion into long-chain acyl CoAs, which is catalysed by acyl-CoA synthetase long chain family member 1 (ASCL1) (217). One study found that in HCC cell lines, aspirin treatment suppresses aberrant lipid metabolism via suppression of ASCL1 expression, which was thought to be via aspirin's interaction with NFκB signalling (217). Expression of ASCL1 along with three other lipid metabolism related proteins have been found to have significant prognostic value in stage II CRC patients (218), suggesting aspirin may also target this pathway in CRC cells.

Aspirin has also been found to affect mitochondrial FAO in cancer cell lines. FAO was increased upon aspirin treatment, but FAO enzyme activity was not affected, the authors suggest that aspirin may have been affecting transport of long-chain fatty acids into the mitochondria (219). Interestingly, a recent study using metabolomic analysis of patient colon tissue after approximately 3 years of aspirin treatment found that both low (81mg/day) and high (325mg/day) doses of aspirin found increased levels of the fatty acid linoleate, which has been previously associated with CRC status and could therefore contribute to the chemopreventive effects of aspirin (220).

1.4.4 **Polyamine metabolism**

Some studies have found an association between aspirin use and polyamine metabolism in CRC. Polyamines, such as putrescine, spermidine and spermine, are small molecules containing two or more amine groups. They are important for many cellular functions such as protein and nucleic acid synthesis and differentiation, and dysregulation of polyamine metabolism is a common feature of tumorigenesis (221). Several oncogenic pathways have effects on polyamine metabolism such as Ras-Raf-Mek-Erk and PTEN-P13K-mTOR and they have been promising candidates for cancer biomarkers and therapeutic targets (221).

Two enzymes involved in polyamine metabolism that have been associated with aspirin are ornithine decarboxylase (ODC), and spermidine/spermine N-acetyltransferase 1 (SSAT) (221). A trial found that patients who were homozygous for a particular SNP in the *ODC* gene which reduced ODC expression were less likely to have recurrence of colorectal adenoma, and this protective effect was dramatically increased with the addition of aspirin use (222). Aspirin was not found to have direct effects on ODC expression or activity but was found to increase both SSAT expression and activity (222). Therefore, aspirin was thought to reduce risk of adenoma recurrence in synergy with the *ODC* genotype, as both increased SSAT activity and decreased ODC activity lead to an overall reduction in polyamine levels (222). Similar findings of an interaction between the *ODC* genotype and aspirin use in adenoma recurrence have been found in subsequent studies (223, 224). One RCT of the ODC inhibitor eflornithine combined with the NSAID suldinac has shown significant effects on the incidence of colorectal adenomas (225). Interestingly, a trial is currently in progress into the effectiveness of eflornithine in combination with aspirin for the prevention of CRC in high risk patients (226).

1.4.5 **mTOR and AMPK**

Aspirin has also been shown to act via mTOR and AMPK in CRC; these signalling partners are crucial for coupling sensing of nutrient availability with cellular metabolism and proliferation, and are key for promoting cancer cell growth as well as survival in nutrient depleted conditions (further described in Section 1.2.2.4) (201). A study from 2013 found that 5mM aspirin inhibits mTOR, activates AMPK and subsequently induces autophagy in CRC cells *in vitro* (227). Aspirin was also found to have this effect *in vivo*; normal rectal mucosal tissue from patients treated with 600mg aspirin for 7 days showed reduced phosphorylation of S6K1 and S6, which are downstream targets of mTOR (227). Aspirin has also been found to inhibit mTOR and induce AMPK and autophagy in PIK3CA mutant breast cancer cells (166).

1.4.6 **Mitochondrial metabolism**

As previously mentioned, R-2HG is an oncometabolite which can accumulate due to mutations in the TCA cycle enzyme IDH. One recent study found that the circulating levels of R-2HG reduced in healthy patients that took 325mg/day aspirin for 60 days, compared to a placebo. Aspirin also reduced levels R-2HG in CRC cell lines, suggesting this may play a role in the cancer preventative effects of aspirin (228).

Aspirin has also been found to promote mitochondrial biogenesis via induction of SIRT1 and PGC1α in HepG2 cells (229). Aspirin was subsequently also shown to induce other regulators of mitochondrial metabolism in these cells including SIRT4, Nrf2, STAT3 and UCP1, suggesting aspirin may significantly affect mitochondrial function, though this was not directly investigated (230).

Multiple studies have also linked the induction of apoptosis by aspirin with its effect on mitochondrial function; in HeLa cells, aspirin has been shown to induce release of cytochrome *c* from the mitochondria (231), and to induce cell death by targeting voltage-dependent anion channel (VDAC1) leading to alteration of mitochondrial membrane potential (232). It has also been found to induce cell death by promoting production of ROS and altering mitochondrial membrane permeability in hepatoma cells (233, 234). Interestingly, studies using yeast cells have also found that aspirin induces apoptosis via induction of ROS (235), and the inhibition of acetyl-CoA transport into the mitochondria (236), leading to mitochondrial dysfunction.

1.5 Aims and hypotheses

There is ample evidence for a role of aspirin in the prevention of CRC. The mechanism of the anti-cancer effect of aspirin is, however, much less understood. Much progress has been made in identifying novel targets of aspirin, and there is emerging evidence that aspirin may affect the deregulated metabolism of cancer cells.

Previous proteomic analysis of long-term (52-week) aspirin treated CRC cells in the Williams lab has highlighted regulation of several metabolic genes, suggesting a potential metabolic effect of long-term aspirin treatment in these cells (unpublished results). This led to the hypothesis that long-term exposure to aspirin causes metabolic reprogramming of CRC cells. Though a number of interesting studies have been carried out to investigate the effect of aspirin on cancer cell metabolism, there is a lack of studies in the literature that employ direct measures of metabolic pathways in cells to demonstrate how these are impacted by aspirin treatment. The majority of studies to date have investigated gene expression or metabolite levels as proxies for investigating the effect of aspirin on metabolism. Metabolic pathway activity is affected by many other factors, including metabolic enzyme activity, substrate and product availability and cell signalling. Therefore, studies to date do not directly show a metabolic reprogramming effect of aspirin.

Therefore, the aim of this project was to directly investigate the role of aspirin in metabolic reprogramming in CRC cells. Specific aims addressed in this project are listed below.

- To validate the protein expression changes highlighted in the proteome data set by western blotting and qPCR (Chapter 3)

- To investigate the impact of aspirin on cellular metabolism by using methods that directly measure metabolic pathways, including stable isotope tracer analysis to study the metabolic fate of glucose and glutamine, as well as extracellular flux analysis to determine the effect of aspirin on glycolysis and oxidative phosphorylation (Chapter 4)

- To investigate the metabolic effects of aspirin to determine whether aspirin may create metabolic vulnerabilities that increase the sensitivity of the cells to further metabolic perturbations (Chapter 5)

Chapter 2 Materials and Methods

2.1 Cell culture

2.1.1 Cell lines

The cell lines SW620, LS174T and HCA7 were used to model colorectal cancer epithelial tissue *in vitro*, from both primary and metastatic locations. These cell lines were purchased form The American Type Culture Collection (ATCC, Maryland, USA). The cell line RG/C2 was used to model colorectal adenoma, the precursor to carcinoma, *in vitro* in order to carry out experiments that may be applicable to prevention of CRC. This cell line was established in this laboratory from a sporadic colorectal adenoma. Further details of all cell lines used are shown in Table 2.1.

These cell lines have also been treated in this laboratory with long-term (LT) (approximately 52 weeks) aspirin (2mM and 4mM) alongside controls that were grown in normal medium for the same time period. They therefore have a higher passage range than the parental cells used to establish them.

All cell lines were routinely assessed for microbial contamination (including mycoplasma), and molecularly characterised using an inhouse panel of cellular and molecular markers to check that cell lines have not been cross contaminated (every 3-6 months; data not shown). Stocks were securely catalogued and stored, and passage numbers were strictly adhered to prevent phenotypic drift.

Table 2.1 Colorectal adenocarcinoma and colorectal adenoma cell line information

LT = long-term

Cell line	Source	Mutation status	Medium	Passage Range
SW620	Metastatic CRC (lymph node) 51-year-old male	Mutant *APC (237), TP53 (238), KRAS (239)* Wild-type *CTNNB1 (240)*	10% DMEM	147 – 152
LT aspirin treated SW620			10% DMEM + 2/4mM aspirin	179 – 205
LS174T	Primary colonic adenocarcinoma 58-year-old female	Mutant *CTNNB1 (241), KRAS (242), PIK3CA (240)* Wild-type *APC (237), TP53 (243)*	10% DMEM	106 – 109
LT aspirin treated LS174T			10% DMEM + 2/4mM aspirin	126 – 138
HCA7	Primary colonic adenocarcinoma 58-year-old female	Mutant *TP53 (244), APC (241)* Wild-type *KRAS (237, 240), CTNNB1 (240)* MMR deficient (245)	10% DMEM	44 – 47
LT aspirin treated HCA7			10% DMEM + 2/4mM aspirin	52 – 72
LT aspirin treated RG/C2	Colonic adenoma 59-year-old female	Mutant *TP53 (246)* Wild-type *APC (247), KRAS (248), PIK3CA (248)*	20% DMEM + 2/4mM aspirin	49– 64

2.1.2 **Cell maintenance**

Carcinoma cell lines were cultured in Dulbecco's Modified Eagle Medium (DMEM), high glucose (Sigma, Merck KGaA, Darmstadt, Germany), supplemented with 2mM L-glutamine, 100 units/ml penicillin (Thermo Fisher Scientific, Paisley, UK), 100µg/ml streptomycin (Thermo Fisher Scientific, Paisley, UK) and 10% v/v fetal calf serum (FCS) (Sigma, Merck KGaA, Darmstadt, Germany). The adenoma cell line RG/C2 was maintained in DMEM with 20% FCS, with the addition of hydrocortisone (1µg/ml) Sigma, Merck KGaA, Darmstadt, Germany) and insulin (0.2 units/ml) (Sigma, Merck KGaA, Darmstadt, Germany), as well as 2mM L-glutamine and 100 units/ml penicillin. Cells were incubated in $25cm^2$ (T25) flasks (Corning Incorporated, Corning, New York, USA) in a non-humidified 5% CO_2 incubator at 37°C. Medium in the flasks was changed twice per week (every 3-4 days).

Long-term aspirin treated cell lines were maintained by culturing in 10% DMEM supplemented with both 2mM and 4mM aspirin, alongside control flasks with normal 10% DMEM. A 20mM stock solution of aspirin (Sigma, Merck KGaA, Darmstadt, Germany) was created by adding 3.6mg/ml aspirin to 10% DMEM, which was rotated for ≥30 minutes to allow the aspirin to dissolve. After filtered sterilisation it was added at the appropriate dilution to the flasks.

2.1.2.1 **HPLM**

For experiments performed in human plasma-like medium (HPLM) (Gibco), HPLM was supplemented with 10% dialysed FCS, and cultured for at least 48 hours in these conditions prior to setting up the experiment.

2.1.3 **Cell passaging**

Media was aspirated from the flask and cells were washed in phosphate buffered saline (PBS, pH 7.4; Severn Biotech Ltd, Kidderminster, UK). The cells were removed by incubation with 0.1% (w/v) trypsin (BD Bioscience, Oxford, UK) and 0.1% (w/v) ethylene-diamine-tetra-acetic acid (EDTA) (Sigma, Merck KGaA, Darmstadt, Germany). Once cells were dissociated from the flask, media was then added to the cell suspension, to neutralise the trypsin, and was spun at 3000rpm for 3 minutes. Trypsin/media was aspirated, and the cell pellet was resuspended in the appropriate volume of media, depending on the passage ratio, which was used to seed new flasks.

In order to seed cells by number, cells are counted using a 0.1mm Neubauer haemocytometer. Once trypsinised and neutralised with media, cells are loaded onto a Neubauer Counting Chamber (VWR International Ltd., Lutterworth, UK) for either manual counting or automated counting using the Corning Cell Counter (CytoSMART, Netherlands). LS174T, HCA7 and RG/C2 cells were syringed prior to loading the haemocytometer through an 18G blunt fill needle (BD Bioscience, Oxford, UK) in order to create a single cell suspension for counting.

2.1.4 **Long-term cell storage and recovery**

Stocks of cell lines were stored at -174°C in liquid nitrogen. To create frozen stocks of cell lines, cells were trypsinised, then resuspended in DMEM with 10% dimethylsulphoxide (DMSO, VWR International Ltd., Lutterworth, UK). 1ml of this suspension was then added to a 1.2ml Cryovial® (Nunc, Fisher Scientific, Loughborough, UK). Cryovials were placed at -80°C for at least four hours in a Mr Frosty™ Freezing Container (Nalgene, Fisher Scientific, Loughborough, UK) to slow the rate of cooling, then transferred to liquid nitrogen. To bring up frozen vials of cells, Cryovials were thawed by incubation at 37°C, then cells spun down and resuspended in fresh medium before being seeded into T25 flasks.

2.1.5 **Treatments**

Aspirin was added to cells by dissolving in DMEM at concentration of 20mM, then adding 0.8ml per 4ml T25 for 4mM treated cells and 0.4ml per 4ml T25 for 2mM treated cells. ABT-737, CB-839, NAC and UK-5099 (purchased from Sigma Merck KGaA, Darmstadt, Germany) were dissolved in DMSO or water to create a stock solution (detailed in Table 2.2). All treatment concentrations maintained the same concentration of DMSO in all conditions.

Non-essential amino acid (NEAA) mix was purchased from Sigma. Stock concentration of 100X was diluted to final concentration of 1X in the medium for experiments investigating NEAA supplementation. 100X NEAA mix contained 890mg/L L-alanine, 1500mg/L L-asparagine monohydrate, 1330mg/L L-aspartic acid, 1470mg/L L-glutamic acid, 750mg/L glycine, 1150mg/L L-proline, and 1050mg/L L-serine.

Table 2.2 Stock solution concentrations for treatments

Treatment	Stock solution concentration
ABT-737	20mM in DMSO
Aspirin	20mM 0.036g/10ml DMEM
CB-839	41.1mM in DMSO
NEAAs (Merck M7145)	100X
NAC	500mM in water
UK-5099	50mM in DMSO

2.1.6 **Seeding densities**

In order to maintain sufficient cell quantity at the end of experiments, the number of cells seeded varied between cell lines It also varied depending on treatment conditions and treatment time. Table 2.3 shows the number of cells seeded in T25 flasks for 72 hours experiments, as a guide.

Table 2.3 Cell seeding densities for different cells in aspirin treatments

Cell line	Cell number seeded per T25
SW620	1 x10^6
SW620 (2mM aspirin)	1.5 x10^6
SW620 (4mM aspirin)	2 x10^6
LS174T	2 x10^6
LS174T (2mM aspirin)	2.5 x10^6
LS174T (4mM aspirin)	2.5 x10^6
HCA7	2 x10^6
HCA7 (2mM aspirin)	3 x10^6
HCA7 (4mM aspirin)	3-4 x10^6

2.2 Proliferation and apoptosis assays

2.2.1 Crystal violet staining

Cells were seeded in 96 well-plates at the appropriate seeding density (20,000 cells per well for all conditions except 4mM aspirin treated HCA7 cells, which were seeded at 40,000 cells per well, as they grew slower under treatment). Cells were treated the following day and cultured for the appropriate length of time (up to 96 hours). Cells were fixed in the plates by aspirating the media, washing with PBS before adding 100µl of chilled 4% paraformaldehyde (PFA) in PBS per well and leaving for 15-20 minutes. PFA was then removed, wells were covered with PBS and refrigerated until staining. Cells were stained with 100µl per well of 0.5% crystal violet solution (Sigma, Merck KGaA, Darmstadt, Germany) diluted in distilled water, and incubated on a rocker at room temperature for 30 minutes. Stain was removed from the wells by pipetting and rinsing in tap water, the plates were left to completely dry before being imaged. Stain was eluted by adding 2% SDS solution (Severn Biotech Ltd, Kidderminster, UK), diluted in distilled water, to the wells and incubating on a rocker for 60 minutes. 75µl of the resulting solution was then transferred to a clean 96 well plate, and the absorbance at 595nm was then read in a 96-well plate using the iMark™ Microplate Absorbance Reader (Bio-Rad, CA, USA). Relative cell number was either expressed as raw absorbance values or calculated relative to the control condition.

2.2.2 Incucyte® Live Cell Imaging

For assays that simultaneously measured cell proliferation and apoptosis Incucyte® Live Cell Imaging system was used. This detects cell confluency over time as a measure of cell proliferation. 20,000 cells per well were seeded in 96 well plates, at least triplicates, and analysed until the control conditions reached a plateau of confluency (~72-96 hours).

For detection of apoptosis, CellEvent™ Caspase-3/7 Green Detection Reagent (Thermo Fisher Scientific, catalogue no. C10423/C10723) was used, according to the manufacturer's protocol. Reagent was added directly to the medium before adding to the cells, at the appropriate concentration (found to be 2µM in SW620 cells after validation). This produced a green fluorescent signal in the presence of active caspases, indicating apoptosis. This was detected by the Incucyte Live Cell Imaging system and quantified by the system as Green Object Count. Green

Object Count was then normalised to confluency in each condition at each time point in order to determine the proportion of apoptotic cells in the wells.

2.3 siRNA transfection

To transiently inhibit protein expression, cells were transfected with double-stranded small-interfering RNAs (siRNAs) for the protein of interest, leading to degradation of the mRNA and therefore silencing of protein expression. siRNAs used are detailed in Table 2.4 (ON-TARGET*plus* SMARTpool. Dharmacon™, Horizon Discovery, Cambridge UK). SMARTpool siRNAs contain 4 sequences covering different sections of the target mRNA, in order to increase success rate of the knockdown.

100µM stocks of siRNAs in nuclease-free water were stored at -20°C. For transfection, sub-confluent flasks of cells were firstly treated with antibiotic free 10% DMEM. Transfection was then performed 24 hours later according to the manufacturer's instructions, using Lipofectamine RNAiMAX transfection reagent (Thermo Fisher Scientific, Paisley, UK). Cells were trypsinised, resuspended and the desired cell number seeded in 1.5ml antibiotic free 10% DMEM into 12.5cm^2 flasks (T12.5, Falcon, Corning, NY, USA) along with 0.5ml of the siRNA-RNAiMAX complexes in OptiMEM Reduced-Serum Medium (Thermo Fisher Scientific, Paisley, UK). siRNA-Lipofectamine RNAiMAX complexes were created by adding 5µl transfection reagent in 250µl OptiMEM to 1µl of stock siRNA, in 250µl OptiMEM, dropwise whilst swirling and leaving for at least 20 minutes, giving a final concentration of 50nM of siRNA per flask. The following day the flasks were changed to normal growth media, lysates were made 72 hours following transfection for western analysis (see section 2.4). Each siRNA transfection was coupled with a negative control siRNA complex.

Table 2.4 Catalogue numbers of Dharmacon™ ON-TARGET*plus* SMARTpool siRNAs used

Target gene	Catalogue number
Activating transcription factor 4 (ATF4)	L-005125-00-0005
Glutaminase (GLS)	L-004548-01-0005
Glutamic pyruvic transaminase 2 (GPT2)	L-004173-01-0005
Pyruvate carboxylase (PC)	L-008950-00-0005
Pyruvate dehydrogenase kinase 1 (PDK1)	L-005019-00-0005
Control Pool	D-001810-10-05

2.4 Western blotting

Cells were seeded in T25 flasks 72 hours prior to sample collection, unless otherwise stated (e.g. for time course experiments). Cell seeding densities for 72-hour assays are shown in Table 2.3. Western analysis of cells treated with siRNA for knockdowns was performed using the same protocol but starting with a T12.5 flasks.

2.4.1 Cell lysis

10X cell lysis buffer (Cell Signaling Technology, Danvers, MA, USA), containing 20mM Tris-HCl pH 7.5, 150mM NaCl, 1mM EDTA, 1% v/v Triton-X100, 2.5M sodium pyrophosphate, 1mM β-glycerophosphate and 1mM sodium orthovanadate, was diluted in distilled water to 1.5X concentration with one Roche Complete Mini Protease Inhibitor tablet (Roche, Basal, Switzerland) per 10ml. Keeping the flasks on ice, DMEM was aspirated and cells were washed twice with ice-cold PBS, then 100µl 1.5X cell lysis buffer was added to each flask. Flasks were rocked on ice for 10 minutes before the cells were scraped and the lysate transferred into an ice-cold Eppendorf. Lysates were spun at 1°C at 18,500 x g for 10 minutes to pellet the cell debris. The supernatant was then transferred to another chilled Eppendorf and lysates stored at -80°C.

2.4.2 Sample preparation

A protein assay was performed in order to determine the protein concentration of the lysates and prepare samples with equal concentrations of total protein. Bovine

serum albumin (BSA) protein standards within a concentration range of 6.25-800µg/ml were made up, as well as a blank water sample, with all standards containing 3.3% v/v 1.5X cell lysis buffer. Protein concentration of the cell lysate was determined using the Bio-Rad DC Protein Assay Kit (Bio-Rad, Hemel Hempstead, UK), as per manufacturer's instructions. Absorbance was read at 750nm with 10 second pre-shake using the iMark™ Microplate Absorbance Reader (Bio-Rad, CA, USA). Samples were then prepared with a concentration 50µg of protein per 20µl. 5X Laemmli sample buffer, containing 62mM Tris-HCl pH 6.8, 10% v/v glycerol, 5% v/v 2-mercaptoethanol, 10% w/v SDS and 0.01% bromophenol blue, was added to the samples so each sample contained 5µl Laemmli buffer per total 25µl. Samples were then boiled for 5 minutes and stored at -20°C.

2.4.3 **SDS-PAGE and transfer**

Proteins were separated by sodium-dodecyl-sulphate polyacrylamide gel electrophoresis (SDS-PAGE), with varying concentrations of acrylamide gels depending on size of the protein of interest. Gel components are shown in Table 2.5. Gels were set up and run using Mini-Protean 3 Electrophoresis equipment (Bio-Rad, Hemel Hempstead, UK) according to the manufacturer's protocol. Gels were first run for 15 minutes at 100V, then increased to 180V and run for approximately 45-60 minutes, allowing the sample dye to run completely through the gel. Tanks were filled with running buffer (components shown in Table 2.6). The samples were run alongside the Precision Plus Protein™ Dual Colour Standard (Bio-Rad Hemel Hempstead, UK) in order to determine the sizes of the proteins detected in the samples.

Separated proteins were then transferred from the acrylamide gel onto an Immobilon® polyvinylidene difluoride (PVDF) membrane. The membrane was firstly pre-soaked in methanol, rinsed in distilled water and then soaked in transfer buffer (components shown in Table 2.6). The gels and membranes were placed within a transfer cassette in between pre-soaked filter paper and sponges, and then transfer was performed using a Transblot Cell (Bio-Rad, Hemel Hampstead, UK), running in transfer buffer at 100V for 90 minutes.

Table 2.5 Components of gels used for SDS-PAGE

Component	Source
30% Acrylamide/1%Bis	National Diagnostics, Hessle, UK
Resolving Buffer 1.5M Tris, pH 8.0 0.4% SDS	National Diagnostics, Hessle, UK
Stack Buffer 0.5% Tris pH 6.8 0.4% SDS	National Diagnostics, Hessle, UK
Ammonium Persulfate 0.5g/ml	Sigma Merck KGaA, Darmstadt, Germany
TEMED	Sigma Merck KGaA, Darmstadt, Germany

Table 2.6 Components of running and transfer buffers used for SDS-PAGE

Buffer	Component	Source
Running + Transfer	192mM Glycine	National Diagnostics, Hessle, UK
Running + Transfer	25mM Tris	National Diagnostics, Hessle, UK
Running	0.1% (w/v) SDS	Sigma Merck KGaA, Darmstadt, Germany
Transfer	20% (w/v) methanol	Sigma Merck KGaA, Darmstadt, Germany

2.4.4 **Protein detection**

After protein transfer, the membrane was removed from the transfer equipment and soaked in 5% milk in Tween wash buffer (TSBT) (components shown in Table 2.7) for 1 hour on a rocker, in order to prevent non-specific binding. Antibodies for the protein of interest (see Table 2.8) were diluted in 0.5% milk in Tris-Buffered Saline -Tween 20 (TBST), and membranes were incubated in 5ml of correctly diluted antibody for an appropriate time period (see Table 2.8). Membranes were then washed three times to remove unbound antibody with TBST, on a rocker, for 10 minutes each wash. Membranes were incubated in 5ml of 1:1000 diluted horseradish peroxidise- (HRP-) conjugated secondary antibody depending on the species of the primary antibody. Details of secondary antibodies used are shown in Table 2.9. Following secondary incubation, membranes were again washed three times with TBST to remove unbound antibody. LumiGLO Peroxidase Chemiluminescence Substrate (KPL, Maryland, USA) was then used according to the manufacturer's protocol; membrane were exposed to an x-ray film in a cassette for an appropriate length of time dependent on the strength of protein expression. Exposed films were developed using a Compact X4 Film Processor. Developed films were scanned for analysis and figure assembly using the SilverFast® Ai Studio 9 software (Lasersoft Imaging AG).

Table 2.7 Components Tris-Buffered saline - Tween 20 (TBST)

Component	Source
50mM Tris, HCl pH 7.4	National Diagnostics, UK
150mM sodium chloride	BDH, VWR, Poole, UK
0.1% Tween 20	Sigma Merck KGaA, Darmstadt, Germany

Table 2.8 Details of primary antibodies used for western blotting

Source	Target protein	Host species	Dilution	Incubation
Cell Signaling Technology #5345	Neutral amino acid transporter (ASCT2)	Rabbit	1:1000	Overnight, 4°C
Cell Signaling Technology #20843	Asparagine Synthetase (ASNS)	Rabbit	1:1000	Overnight, 4°C
Cell Signaling Technology #11815	Activating Transcription Factor 4 (ATF4)	Rabbit	1:1000	Overnight, 4°C
Cell Signaling Technology #88964	Glutaminase 1 (GLS1)	Rabbit	1:1000	Overnight, 4°C
ProteinTech 16757-1-AP	Glutamic-pyruvic transaminase (GPT2)	Rabbit	1:1000	Overnight, 4°C
Cell Signaling Technology #5347	Large neutral amino acid transporter (LAT1)	Rabbit	1:1000	Overnight, 4°C
Abcam ab126707	Pyruvate carboxylase (PC)	Rabbit	1:1000	Overnight, 4°C
Cell Signaling Technology #6924	Phosphoenolpyruvate carboxykinase 2 (PCK2)	Rabbit	1:1000	Overnight, 4°C
Cell Signaling Technology #3820	Pyruvate dehydrogenase kinase 1 (PDK1)	Rabbit	1:1000	Overnight, 4°C
Sigma Merck KGaA, Darmstadt, Germany T9026	α-tubulin	Mouse	1:10,000	1 hour, room temperature

Table 2.9 Details of secondary antibodies used for western blotting

Source	Antibody	Host species	Dilution
Sigma Merck KGaA, Darmstadt, Germany	Anti-Mouse IgG Peroxidase	Goat	1:1000
Sigma Merck KGaA, Darmstadt, Germany	Anti-Rabbit IgG Peroxidase	Goat	1:1000

2.4.5 **Stripping and reprobing**

Membranes were stripped of antibodies for reuse by incubating in stripping buffer (250mM glycine, 1% w/v SDS, pH2) at room temperature for up to an hour, followed by two 10-minute washes in TBST and incubation in 5% milk in TBST for up to one hour. Membranes were reprobed either with antibodies for proteins of a different size to the original probe, or with the antibody for α-tubulin, in order to produce loading control bands. Membranes were not stripped and reprobed more than twice (including one for α-tubulin).

2.4.6 **Western blot image analysis**

Western blot images were quantified using a method by Hossein Davarinejad, available online (249). Density of bands detected by western blotting was measured using the "measure" function in ImageJ. A box was drawn around the largest band to be analysed and this box was used to measure the "mean grey value" of each band, as well as the mean grey value of the background next to each band (keeping the exact same sized box for each measurement). Mean grey value is measured on a scale from 0-255, where 0 is black and 255 is white. Therefore, the values were inverted by subtracting each value from 255, so that a darker band correlated with a higher reading. The net density of each band was then calculated by subtracting the background measurement from the band measurement. This process was then repeated for the loading control bands from each sample. Net protein expression was then calculated relative to the loading control by dividing the protein band measurement by the loading control measurement.

In order to compare data from this process from independent experiments, protein expression changes were calculated as relative changes from the control

conditions in each replicate. For example, net protein expression in the aspirin treated cells was divided by net protein expression in the control medium cells, so protein expression with aspirin was expressed as a fold-change. Results from at least three independent experiments was analysed with this method, as the values presented as a bar graph with standard error. One-sample t-tests comparing to a hypothetical mean of 1 were performed in each condition to determine statistical significance. P-values of less than 0.05 were considered significant.

2.5 mRNA quantificaiton

2.5.1 Isolation of RNA

Cells were washed once with PBS and then treated with 1ml TRI-reagent per T25 flask. Cells were scraped and placed in an RNase free Eppendorf. Samples were either stored at -80°C or processed immediately. 200µll chloroform was added to the sample, before shaking for ~10 seconds and incubating at room temperature for 2-3 minutes. Samples were then centrifuged at 11,500rpm at 4°C for 15 minutes. The resulting top later in the Eppendorf containing the RNA was transferred to a new Eppendorf tube. 0.5ml of 100% isopropanol was then added and mixed with the sample, followed by 10-minute incubation at room temperature. Samples were again centrifuged at 11,500rpm at 4°C for 10 minutes. The supernatant was removed leaving the pelleted RNA in the Eppendorf. The pellet was then dissolved in 1ml 75% ethanol, then the sample was centrifuged at 8,500rpm at 4°C for 5 minutes. The supernatant was discarded, and the pellet allowed to air-dry. The pellet was then resuspended in 100µl RNase free water. Traces of phenol and ethanol were removed using the Qiagen® RNeasy® clean up kit, with an additional on-column DNase digestion, (Qiagen, Manchester, UK) according to the manufacturer's protocol.

2.5.2 Synthesis of cDNA

Concentration of RNA samples was determined by NanoDrop (Thermo Scientific Karlsruhe, Germany). For each sample, 2µg of RNA and 1µl of oligo dT primer (Promega, WI, USA) were combined in a pair of RNase free PCR tubes. These were placed at 70°C for 5 minutes, then subsequently kept on ice. To each sample in the pair, 5µl of M-MLV 5x reaction buffer (Promega), 5µl dNTP (Promega, WI, USA) and 0.63µl of Recombinant RNasin Ribonculease Inhibitor (Promega, WI, USA) were added. Then to one tube in the pair was added 1µl ddH_2O, which would

act as the no reverse transcription (no RT) control. To the other tube was added 1µl reverse transcriptase, M-MLV RT (Promega, WI, USA). The samples were made up to a total volume of 25µl by adding RNase free water. Samples were mixed before incubation at 40°C for 60 minutes, for synthesis of cDNA strands. 175µl RNase free water was then added to each sample to dilute cDNA to 0.01µg/µl. cDNA samples were stored at -20°C until analysis.

2.5.3 **qPCR**

cDNA samples were analysed by quantitative real time polymerase chain reaction (qPCR) to determine the levels of mRNA for specific genes in the original samples. This was done using Quantifast SYBR green (Qiagen, Manchester, UK) containing dNTPs, SYBR green I dye, ROX dye and hot start Taq polymerase. Primers for genes of interest were purchased from Qiagen (see Table 2.10). Samples were diluted appropriately using RNase free water. 2µl cDNA, per 12.5µl reaction, was added to each sample along with SYBR green mastermix and primers in a 96 well polypropylene plate (Agilent Technologies, CA, USA), and the plate spun down to mix the samples. Each sample was carried out in triplicate alongside a no RT control, to test for contaminating DNA. qPCR analysis was performed using the MxPro 3005P Real-time Thermal Cycler (Agilent Technologies, CA. USA), as per the program set up shown in Table 2.11, for 40 cycles. Resulting data was analysed using the MxPro software. ROX was used as a reference dye and each gene of interest was normalised to the house-keeping genes TBP or HPRT. One-sample t-tests comparing to a hypothetical mean of 1 were performed in each condition to determine statistical significance. P-values of less than 0.05 were considered significant.

Table 2.10 Catalogue numbers of primers used for qPCR analysis, purchased from Qiagen, UK

Gene name	Catalogue number
ATF4	QT00074466
GPT2	QT00066381
GLS1	QT00019397
HPRT	QT00059066
PC	QT01005592
PCK2	QT00013125
PDK1	QT00069636
SLC7A11	QT00002674
SLC7A5	QT00089145
TBP	QT00000721

Table 2.11 qPCR program

Step	Time	Temperature
PCR Initial Activation Step	15 mins	95°C
Three-step cycle (40 cycles): • Denaturing • Annealing (fluorescence detection) • Extension	 15 secs 30 secs 30 secs	 94°C 55°C 72°C

2.6 Stable isotope tracer analysis

Cells were seeded in 6cm plates and cultured in the appropriate growth medium (10% DMEM with or without aspirin) for a total of 72 hours, in triplicate for each condition. At the appropriate time point prior to extraction, growth medium was aspirated cells were washed twice with PBS. Medium was then replaced with phenylalanine-free DMEM supplemented with 10% dialysed fetal calf serum

(dFCS), 100 units/ml penicillin, 100µg/ml streptomycin, 0.4mM phenylalanine, 10mM glucose, and 2mM glutamine. Either glucose or glutamine were replaced with uniformly labelled versions (U-[^{13}C]-glucose/glutamine, Cambridge Isotopes). For sample extraction, media was aspirated, and the cells were washed twice with ice-cold 9g/L saline solution. 800µl of ice-cold 80% methanol was then added to each flask, and cells were scraped and transferred into a 1.5ml Eppendorf. Extracted cells were spun at 1°C at 18,500 x g for 10 minutes to pellet the cell debris. The supernatant was then transferred to another chilled Eppendorf, and stored at -80°C until required. Samples were then dried down using a SpeedVac™ to concentrate the metabolites and analysed by gas chromatography mass spectrometry (GCMS) at the Metabolomics Core Facility at McGill University, Canada, as described in (250, 251).

Parallel flasks with identical treatment were used to count cell number at the time of extraction in order to normalise metabolite abundance data to cell number in each sample.

Mass spectrometry data was analysed using the Agilent ChemStation software. This was then further analysed using a Microsoft Excel spreadsheet developed by Shawn McGuirk et al. to determine metabolite abundances, mass isotopomer distribution (MID) and ^{13}C abundance in each metabolite.

2.7 Extracellular flux analysis

Extracellular flux analysis was performed using a Seahorse XFp analyser (Agilent, Santa Clara, CA, USA) according to the manufacturer's protocol.

60,000 cells were seeded and adhered to the cell culture plate immediately before analysis, in order to allow direct comparison of results without the requirement of normalising the results to cell number.

An 8-well Cell Culture Miniplate (Agilent, Santa Clara, CA, USA) was pre-treated with Corning® Cell-Tak Tissue adhesive. 3.22µl adhesive was mixed with 0.25ml PBS. 10µl of this solution was then added to each well the plate, followed by 20µl $NaCO_3$. After 20 minutes, the solution was removed from the wells by pipetting. Each well was washed twice with PBS then left to air dry. Plates were refrigerated until use and were warmed to room temperature before seeding. The sensor

cartridge was hydrated with calibrant and incubated in a CO_2 free incubator at 37°C overnight.

On the day of analysis, cells were trypsinised, counted and resuspended in Seahorse XF Base Medium (Agilent, Santa Clara, CA, USA) supplemented with 10mM Seahorse XF glucose, 1mM Seahorse XF pyruvate and 2mM Seahorse XF glutamine (Agilent, Santa Clara, CA, USA). 60,000 cells were seeded in 80µl medium, and centrifuged at 200g for 1 minute, with no braking on the centrifuge. One well contained cell-free medium to be used as a blank measurement in the analyser. A further 100µl of supplemented Seahorse medium was then added to each well, making a total well volume of 180µl. The plate was incubated in a non-humidified incubator at 37°C and 5% CO_2 for approximately 45 minutes prior to analysis.

Stocks of oligomycin, carbonyl cyanide-*p*-trifluoromethoxyphenylhydrazone (FCCP), rotenone/antimycin A and monensin (purchased from Sigma Merck KGaA, Darmstadt, Germany) were made in DMSO and diluted in Seahorse medium before loading into the injection ports of the sensor cartridge in order to carry out the Cell Mito Stress Test. Details of the volumes and concentrations of these compounds are shown in Table 2.12.

Table 2.12 Details of injection compounds used for extracellular flux analysis in the Mito Stress Test

Port	Compound	Injection port concentration	Injection port volume	Final well concentration	Final well volume
A	Oligomycin	20µM	20µl	2µM	200µl
B	FCCP	20µM	22µl	2µM	222µl
C	Rotenone/ antimycin A	10µM/10µM	25µl	1µM/1µM	247µl
D	Monensin	200µM	27µl	20µM	274µl

2.7.1 Bioenergetics analysis

Oxygen consumption rate (OCR) and extracellular acidification rate (ECAR) data generated from extracellular flux analysis was used to estimate ATP production from glycolysis and oxidative phosphorylation (oxphos) using a spreadsheet produced by Eric H Ma and Kelsey Williams in the Russell Jones lab (252, 253), accessible from https://russelljoneslab.vai.org/tools/.

2.8 Statistical analysis

Results are expressed as mean values +/- standard error of the mean (SEM) where three or more independent experiments were performed. Where a single experiment was performed, the mean of technical replicate readings +/- standard deviation (SD) is expressed. p-values greater than or equal to 0.05 ($p \leq 0.05$) were considered statistically significant (*). Two asterisks indicate $p \leq 0.01$ (**), three asterisks indicate $p \leq 0.001$ (***) and four asterisks indicate $p \leq 0.0001$ (****). GraphPad Prism (GraphPad Software Inc, California, USA) was employed for statistical analysis including calculation of SD, SEM and t-tests.

2.9 Proteomic data analysis

Raw proteomics data were analysed and organised by Dr Phil Lewis in the Proteomics Facility at the University of Bristol. Analysis of gene lists from proteomic data was performed using Webgestalt.org. A list of significantly regulated genes in both long-term 2mM and 4mM aspirin (shown in Appendix 7.1) was entered into the “Gene List” section. “Method of Interest” entered was Over-representation analysis, and “Functional Database” entered was Pathway and KEGG. Genes involved in central carbon metabolism were selected from the “Central carbon metabolism in cancer” and “Pyruvate metabolism” categories. Analysis using Ingenuity Pathway Analysis (IPA) was performed by Phil Lewis in the Proteomics Facility at the University of Bristol.

Chapter 3 Results 1

Investigating the effect of aspirin on metabolic protein expression

3.1 Introduction

As discussed in section 1.3.1, the impact of aspirin treatment on CRC incidence is affected by many factors, particularly the length of time for which aspirin is taken. Patients may take aspirin for many years for the prevention of cardiovascular disease, and the chemo-preventative role is only reported after around 10 years after commencing aspirin treatment (154). While the effects of aspirin on many aspects of cell biology have been studied in detail (described in section 1.3.2), treatment times of cells *in vitro* have been short (usually <1 week). Given different lengths treatment have differing effects on CRC incidence and mortality, it was hypothesised that longer term exposure to aspirin may have distinct effects on cell biology and may lead to distinct adaptations. Work has been previously carried out in the Williams lab in order to investigate this hypothesis (unpublished).

Three CRC cell lines (SW620, LS174T, HCA7) were cultured with either 2mM or 4mM aspirin alongside untreated controls for approximately 52 weeks, this was defined as long-term exposure. Proteomic analysis was performed on SW620 cells after 52 weeks of treatment, in order to investigate the effects of long-term aspirin exposure and identify novel mechanisms of action or potential adaptations using an unbiased approach (experiments carried out by Dr Eleanor Mortensson and Dr Kate Heesom). The design of this experiment is shown in Figure 3.1.

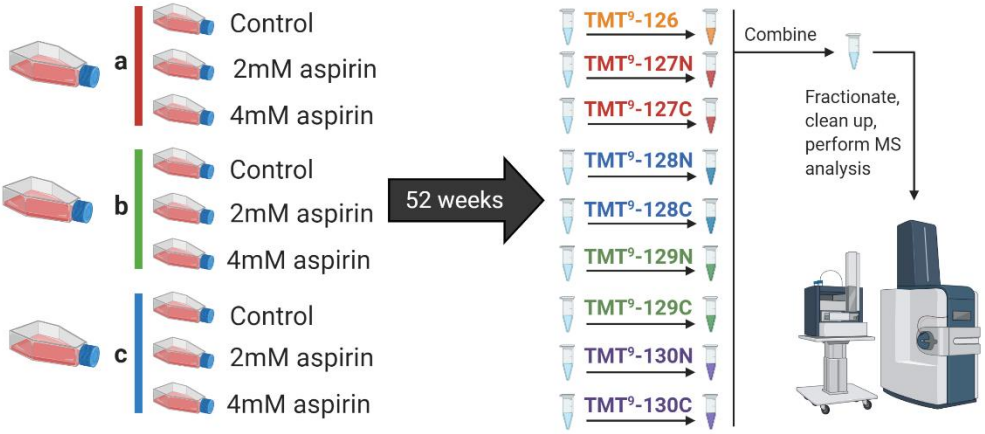

Figure 3.1 Experimental design for proteomic analysis of long-term aspirin treated SW620

Adapted from Dr Eleanor Mortensson, unpublished. Created with BioRender.com.

Volcano plots showing regulation of proteins in this experiment are shown in Figure 3.2. These show a dose-dependent effect of aspirin on the number of significantly up- and downregulated proteins.

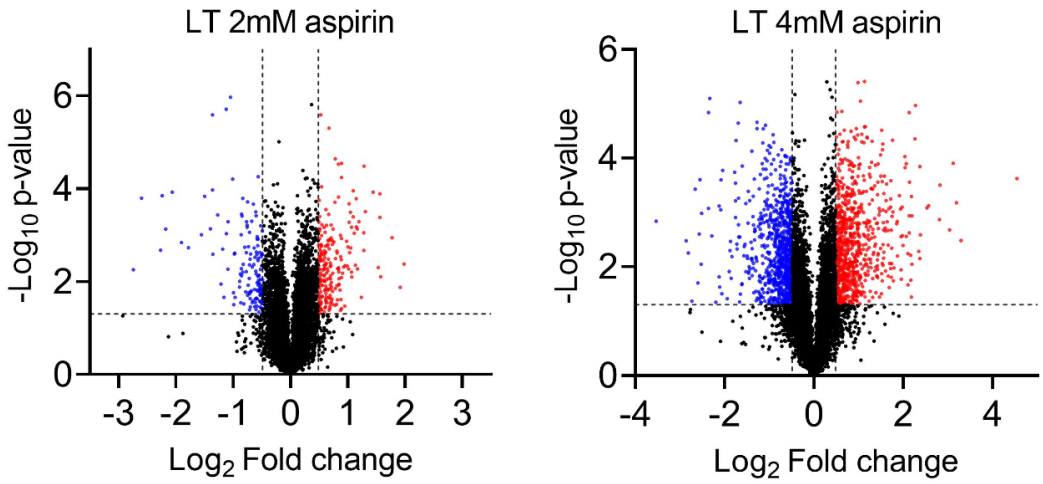

Figure 3.2 Volcano plots from proteomic analysis of long-term (52-week) aspirin treated SW620 cells

Data produced by Dr Eleanor Mortensson, unpublished.

Over-representation analysis of the proteins that were significantly regulated ($p<0.05$, fold change>1.4) in both 2mM and 4mM aspirin using the online tool Webgestalt highlighted “metabolic process” as having the most regulated proteins in gene ontology (GO) biological processes (Figure 3.3). This suggests that regulation of cell metabolism may be a key mechanism of long-term aspirin treatment in these cells, and therefore warrants further investigation. This chapter aims to further analyse the proteomic data set, building on original analysis by Dr Eleanor Mortensson, to further understand the effect of aspirin on cell metabolism, and to validate these findings in the laboratory.

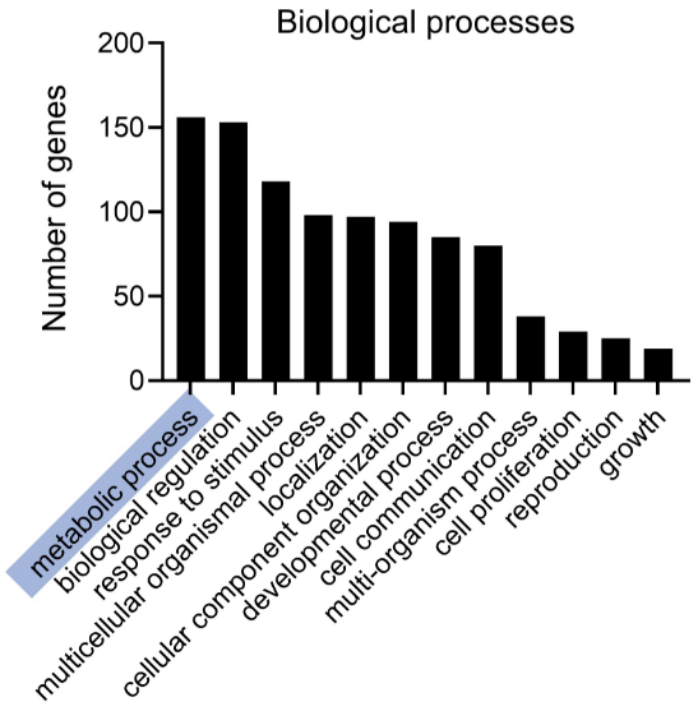

Figure 3.3 Overrepresentation analysis of significantly regulated proteins with long-term (52-week) aspirin treatment in SW620 cells

Comparison with gene ontology (GO) biological process categories shows “metabolic process” has the highest number of regulated genes with long-term aspirin treatment. Analysis performed by Dr Eleanor Mortensson.

3.2 Aims

Proteomic analysis of long-term aspirin treated SW620 cells highlighted regulation of genes involved in “metabolic processes”, suggesting that prolonged exposure to aspirin might reprogram cellular metabolism. As this could be key to understanding the mechanism underlying the anti-cancer effect of aspirin, the aims of this chapter are:

i. To perform analysis of proteomic data from SW620 cells treated long-term with aspirin to investigate the effect of aspirin exposure on expression of metabolic proteins

ii. To validate proteomic results using western blotting and qPCR in a number of different colorectal cancer cell lines

iii. To investigate the effects of short-term aspirin treatment on metabolic protein expression, and to compare this with the effects of long-term treatment

iv. To investigate the stability of protein expression changes in long-term aspirin treated cells after the removal of aspirin

3.3 Results

3.3.1 Long-term aspirin exposure regulates metabolic proteins

Preliminary analysis of the proteome of SW620 cells treated with long-term (52-week) 0, 2 and 4mM aspirin highlighted regulation of a number of proteins involved in metabolism (Dr Eleanor Mortensson, personal communication). Therefore, the initial aim of the project was to further analyse the proteomic data to investigate the effect of long-term exposure to aspirin on cellular metabolism. From the proteomics results, a list was generated of proteins that were significantly regulated ($p<0.05$, fold change>1.4) in both 2mM and 4mM long-term aspirin treated cells compared to controls. The full list with the fold changes and p-values is shown in Appendix 7.1.

Analysis of these proteins using the 'pathway enrichment analysis' function in Webgestalt (further described in section 2.8) identified several enzymes involved in central carbon metabolism, shown in Figure 3.4. Several enzymes involved in glucose metabolism were upregulated, including the glucose transporter 1 (GLUT1/SLC2A1), the glycolysis enzyme hexokinase 1 (HK1), and pyruvate carboxylase (PC). Pyruvate dehydrogenase kinase 1 (PDK1) was downregulated, suggesting an increase in activation of pyruvate dehydrogenase (PDH). These changes collectively indicate a potential increase in glucose import, glycolysis, and entry of glucose-derived carbon into the TCA cycle. Interestingly, glutaminase 1 (GLS1), which catalyses the first step of glutaminolysis, allowing entry of glutamine into the TCA cycle, was also upregulated. These changes suggest there may be an overall increase in entry of carbon derived from both glucose and glutamine into the TCA when the cells are treated with long-term aspirin.

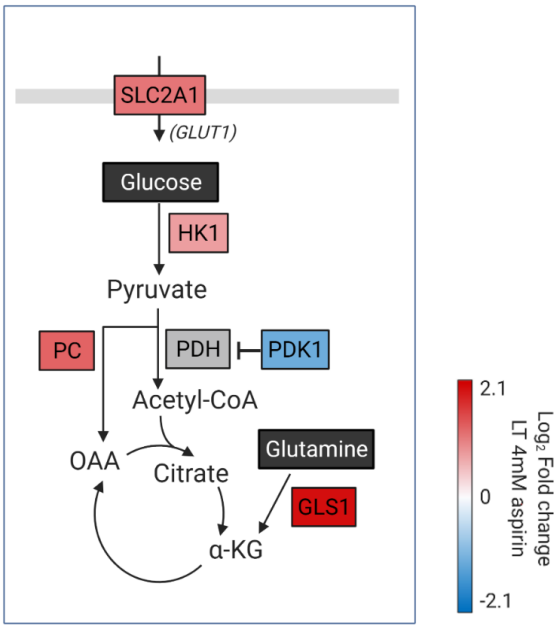

Figure 3.4 Proteins involved in central carbon metabolism are significantly regulated in long-term (52-week) aspirin treated SW620 cells

Proteins involved in central carbon metabolism that are significantly regulated with both LT 2mM and 4mM aspirin in proteomic data set ($p<0.05$, fold change>1.4). Colour scale shows log_2 fold changes from proteomic data set in long-term (LT) 4mM aspirin compared to controls. Created with BioRender.com.

Due to the large increase in GLS1 expression, expression of other proteins involved in glutamine metabolism was also investigated, to establish whether there was a clear overall increase in the glutaminolysis pathway as a whole. Figure 3.5 shows regulation of enzymes involved in catalysing the two steps of glutaminolysis (254) (conversion of glutamine into glutamate, and subsequently α-ketoglutarate), as well as transporters of both glutamine and glutamate, with long-term 4mM aspirin. The full list of these proteins with the fold changes and p-values is shown in Appendix 7.2.

Despite the strong upregulation of GLS1, several other key glutaminolysis enzymes, including asparagine synthetase (ASNS), glutamic-pyruvic transaminase 2 (GPT2), and phosphoserine aminotransferase 1 (PSAT1), were downregulated, making it unclear whether there is an overall increase in the glutaminolysis pathway with aspirin treatment. Interestingly, the cystine/glutamate antiporter xCT (SLC7A11) and large neutral amino acid transporter LAT1 (SLC7A5/SLC3A2) were also both downregulated with aspirin.

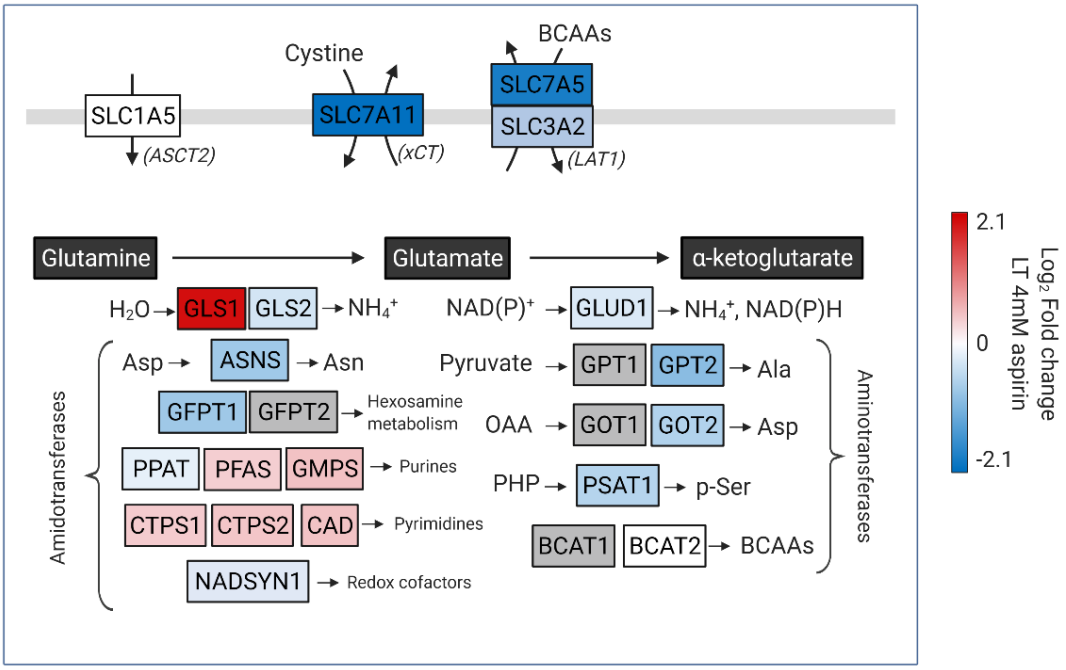

Figure 3.5 Glutaminolysis proteins are regulated in long-term (52-week) aspirin treated SW620 cells

Regulation of proteins involved in glutaminolysis in long-term (LT) 4mM aspirin treated cells compared to controls in proteomic data set, colour scale shows log_2 fold changes. Created with BioRender.com.

3.3.2 Long-term aspirin is associated with reduced ATF4 signalling

Several of the proteins downregulated in the proteomic data are transcriptional targets of activating transcription factor 4 (ATF4), suggesting aspirin may have an overall inhibitory effect on ATF4 signalling. This was further investigated by analysis of the proteomic data using Ingenuity Pathway Analysis (IPA), which showed inhibition of ATF4 signalling with aspirin (p= 0.0116, z-score=-2.894). This supports the hypothesis that aspirin may have a metabolic reprogramming effect, as ATF4 is an important regulator of cell metabolism and amino acid homeostasis (255). The transcriptional targets of ATF4 that were identified in the proteomic data set by IPA, along with their fold changes with aspirin treatment, are shown in Figure 3.6. The full list with the fold changes and p-values is shown in Appendix 7.3.

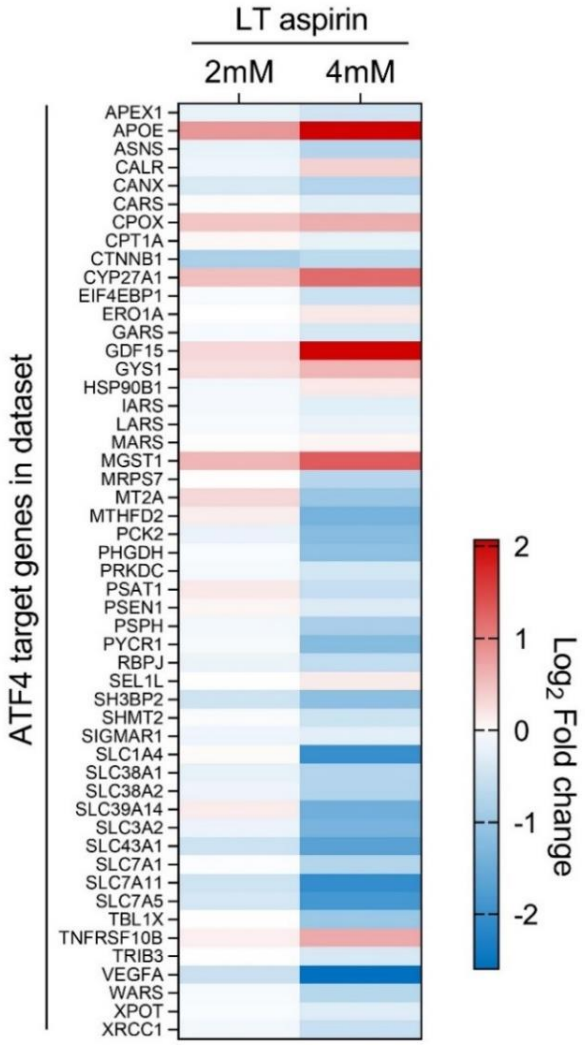

Figure 3.6 ATF4 target genes are regulated in long-term (52-week) aspirin treated SW620 cells

Colour scale shows log_2 fold changes from proteomic data set of transcriptional targets of ATF4 in 4mM aspirin compared to controls, as identified by Ingenuity Pathway Analysis (IPA).

3.3.3 Long-term aspirin regulates expression of metabolic enzymes in SW620 cells

As several key metabolic enzymes show regulation with long-term aspirin treatment in the proteomic data, a sample of these were validated by western

analysis. Validation of the antibodies for GLS1, PC and PDK1 used for this analysis by performing siRNA knockdown is shown in Appendix 7.4, and for GPT2 in Figure 3.17. Samples were taken 72 hours after seeding long-term (~52-week) aspirin treated SW620 cells in the relevant aspirin dose (2mM, 4mM or control).

These results (shown in Figure 3.7) confirm significant regulation of several proteins in line with the proteomic data, including downregulation of PDK1 and GPT2, and upregulation of GLS1. Western blotting identified two distinct splice variants of GLS1 (known as $GLS1^{GAC}$ and $GLS1^{KGA}$). As $GLS1^{GAC}$ was the dominantly expressed isoform in these cells, this isoform was used for statistical analysis. PC and LAT1 were not significantly regulated, but showed a trend towards upregulation and downregulation respectively, in line with the proteomic data. In contrast, despite showing downregulation in the proteomic data, ASNS and PCK2, both targets of ATF4, did not show consistent regulation by western blotting. Furthermore, although not significantly regulated in proteomic data, western analysis showed a trend towards downregulation of the glutamine transporter SLC1A5/ASCT2 (alanine-serine-cystine transporter 2), though this was not significant. Interestingly, despite regulation of a number of transcriptional targets of ATF4, the ATF4 protein levels were not found to be consistently regulated with aspirin treatment by western blotting, consistent with the function of ATF4 being modified by post-translational regulation (256). ATF4 protein was not detected in the proteomic data set.

To investigate whether the metabolic proteins of interest undergo transcriptional regulation, expression of a selection of genes of interest were also investigated by qPCR (Figure 3.8). Neither GLS1, PC nor PDK1 showed significant regulation of mRNA levels, suggesting post-translational regulation on exposure to aspirin. GLS1 showed a trend towards upregulation, suggesting there may be some transcriptional regulation of GLS1. Interestingly, four transcriptional targets of ATF4 (GPT2, PCK2, SLC7A11, SLC7A5) all showed strong and significant downregulation with both long-term 2mM and 4mM aspirin, further supporting the previous findings that aspirin may inhibit ATF4 signalling (section 3.3.2). ATF4 itself did not show transcriptional regulation, again consistent with post-translational regulation.

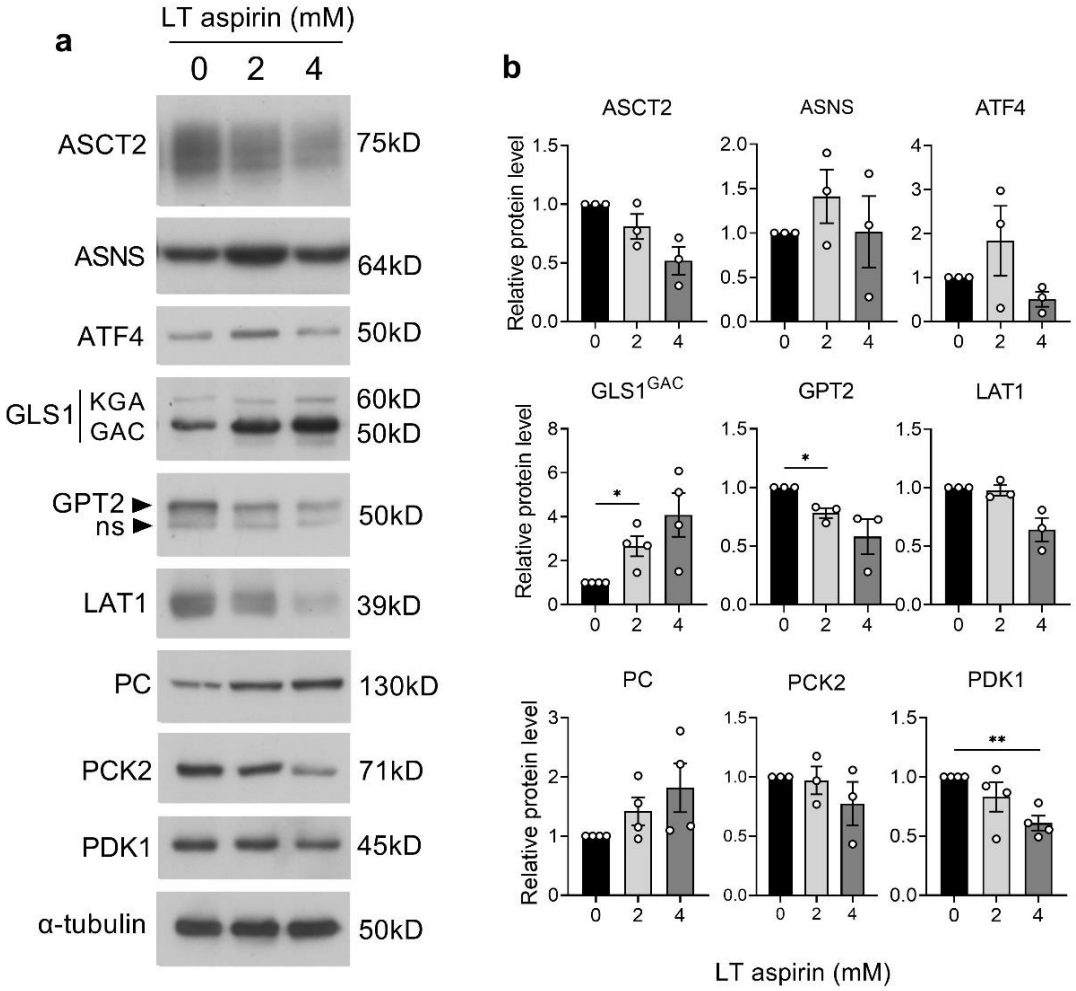

Figure 3.7 Long-term (52-week) aspirin treatment regulates metabolic enzymes in SW620 cells

a Western analysis of long-term (LT) aspirin treated SW620 cells, representative of at least 3 independent experiments. ns=non-specific band. **b** Quantification by densitometry, to show protein expression relative to control. Error bars represent standard error, *=p≤0.05, **=p≤0.01.

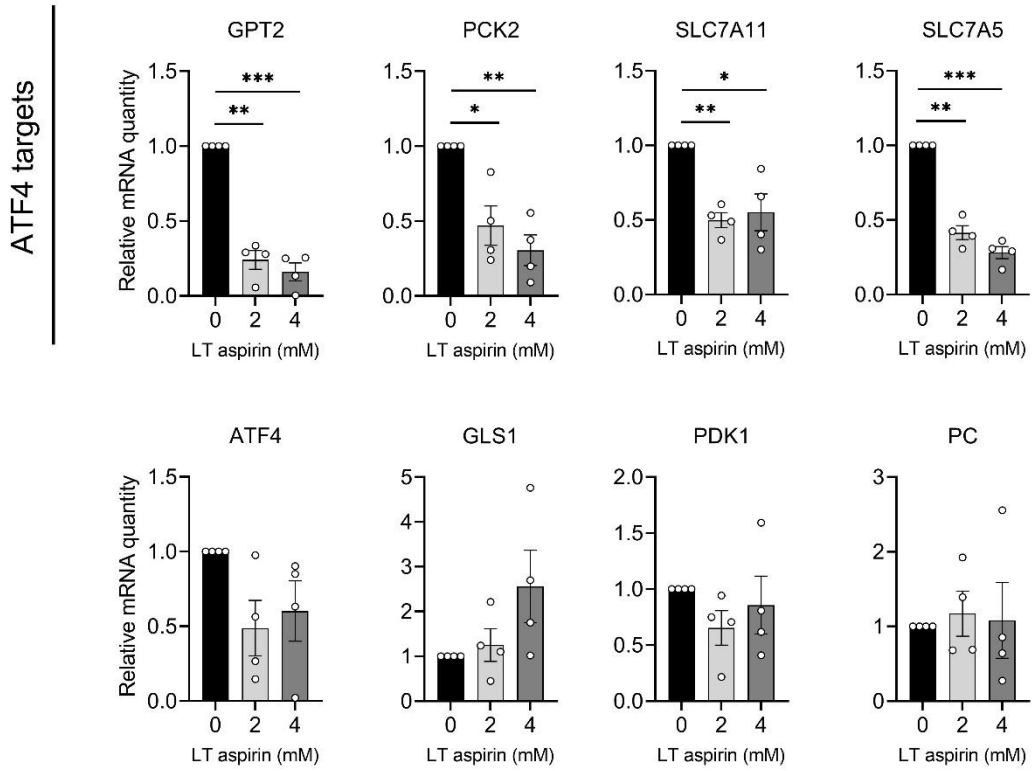

Figure 3.8 Long-term (52-week) aspirin treatment regulates transcription of ATF4 target genes in SW620 cells

qPCR analysis of long-term (LT) aspirin treated SW620 cells, showing expression of mRNA with aspirin treatment relative to control. Data show 4 independent experiments. Error bars represent standard error, *=p≤0.05, **=p≤0.01, ***=p≤0.001.

3.3.4 **Short-term aspirin regulates metabolic proteins in SW620 cells**

As western blotting and qPCR results confirmed significant regulation of metabolic proteins with long-term aspirin, it was next investigated whether this regulation also occurred with short-term aspirin treatment. This is an important question when considering therapeutic use of aspirin, as there is a need to determine whether aspirin may have benefit for patients who have not previously been taking aspirin. In order to investigate this, SW620 cells were seeded in media containing either 0mM (control), 2mM or 4mM aspirin, and cultured for 72 hours prior extraction and western blotting. These results are shown in Figure 3.9.

GLS1^{GAC} showed significant upregulation with short-term 2mM aspirin, though this was to a lesser extent than in the long-term treatment. PC also showed significant upregulation with 2mM aspirin, despite PC not being significantly regulated with long-term treatment. ASCT2 shows a trend towards downregulation with 4mM, again in line with the effect observed with long-term aspirin treatment, though this was not significant. None of the other proteins investigated, including those that were significantly regulated with long-term aspirin, showed significant regulation with short-term aspirin treatment, including ASNS, GPT2, LAT1, PCK2 and PDK1. This suggests that while short-term aspirin treatment is sufficient to induce some of the changes seen with long-term aspirin treatment (such as induction of GLS1^{GAC} expression), longer exposure times are required to regulate expression of other proteins, and/or to have the same level of regulation.

Investigation of transcriptional regulation of metabolic genes was performed with short-term aspirin treated SW620 cells (Figure 3.10). The ATF4 target genes SLC7A5 and GPT2 that were strongly transcriptionally regulated with long-term aspirin, also showed significant downregulation with short-term aspirin (although to a slightly lesser extent, consistent with the protein expression). Despite showing downregulation with long-term aspirin treatment, PCK2 and SLC7A11 did not show any significant transcriptional regulation with short-term aspirin treatment. These results suggest that short-term aspirin treatment is sufficient to induce some regulation of metabolic genes, particularly targets of ATF4, suggesting short-term as well as long-term aspirin treatment may inhibit ATF4 signalling, but to a lesser extent. As LAT1 (SLC7A5) and GPT2 did not show any regulation at the protein level with short-term aspirin but did show transcriptional regulation, this suggests the treatment may need to be extended in order to see protein level regulation, and that the full long-term treatment (52 weeks) may not be required for this effect.

Overall, these results show that short-term (72-hour) aspirin treatment has a similar effect on regulation of some of the metabolic enzymes that are also regulated with long-term (52-week) aspirin treatment in SW620, though longer treatment has a stronger effect on regulation. In particular GLS1, PC and PDK1 show relatively consistent regulation and therefore the next experiments were designed to investigate the effect of a time course of aspirin treatment on expression of these enzymes.

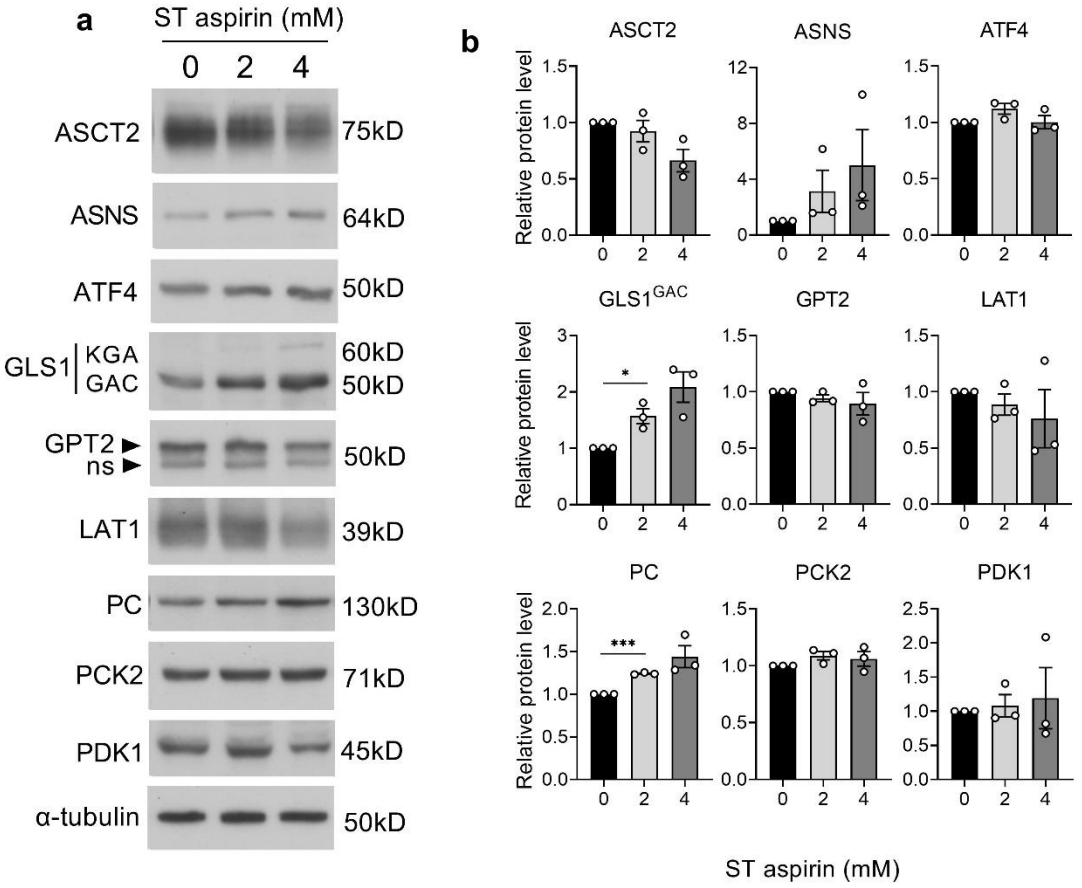

Figure 3.9 Short-term (72-hour) aspirin treatment regulates metabolic enzymes in SW620 cells

a Western analysis of short-term (ST) aspirin treated SW620 cells, representative of 3 independent experiments. ns=non-specific band. **b** Quantification by densitometry, to show protein expression relative to control. Error bars represent standard error, *=p≤0.05, ***=p≤0.001.

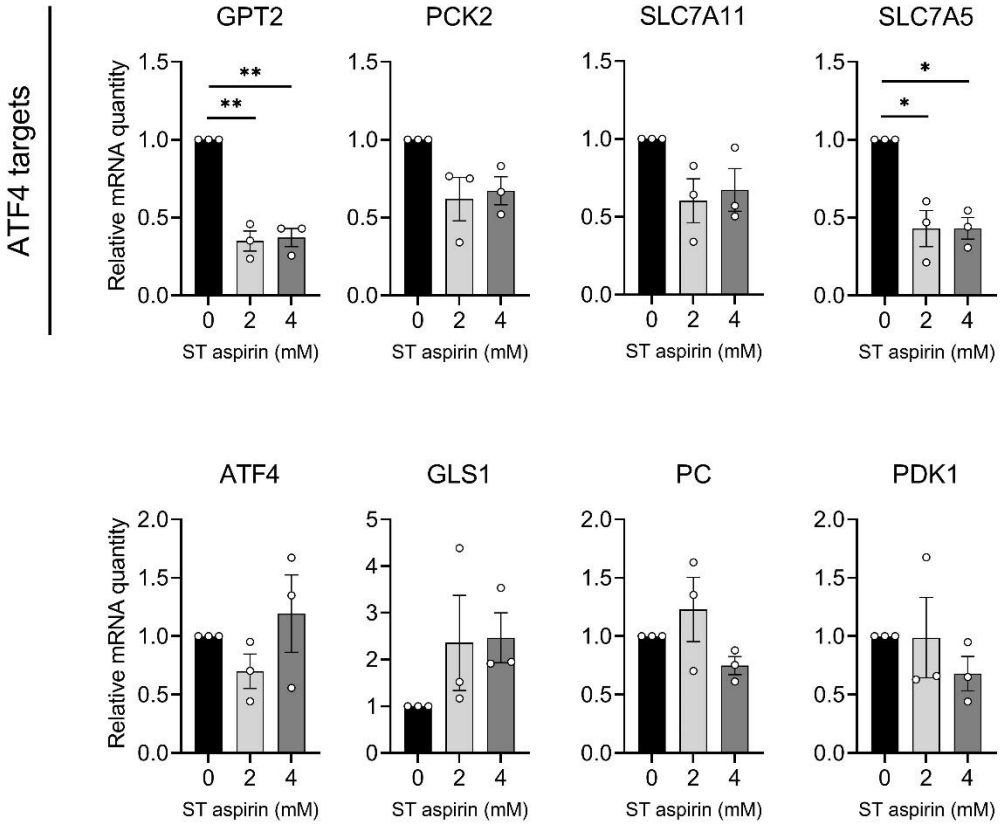

Figure 3.10 Short-term (72-hour) aspirin treatment regulates transcription of ATF4 target genes in SW620 cells

qPCR analysis of short-term (ST) aspirin treated SW620 cells, showing expression of mRNA with aspirin treatment relative to control. Data show 3 independent experiments. Error bars represent standard error, *=p≤0.05, **=p≤0.01.

3.3.5 Metabolic enzyme expression is regulated within 72 hours of aspirin treatment in SW620 cells

To investigate the timing of protein regulation upon aspirin treatment, expression of GLS1, PC and PDK1 was analysed by western blotting after a time course of aspirin treatment (24, 48, 72 and 96 hours) in SW620 cells. These results are shown in Figure 3.11. Expression of $GLS1^{GAC}$ protein showed a trend towards upregulation within 24 hours of 4mM aspirin treatment (though not significant), and was significantly regulated in both 2mM and 4mM by 72 hours. The upregulation at 96 hours was not statistically significant due to variation between replicates. PDK1 was significantly downregulated at 72 hours and 96 hours of aspirin

treatment with 4mM aspirin. PC expression was significantly upregulated at 72 hours of 4mM aspirin treatment, and is upregulated at 96 hours though this is not statistically significant.

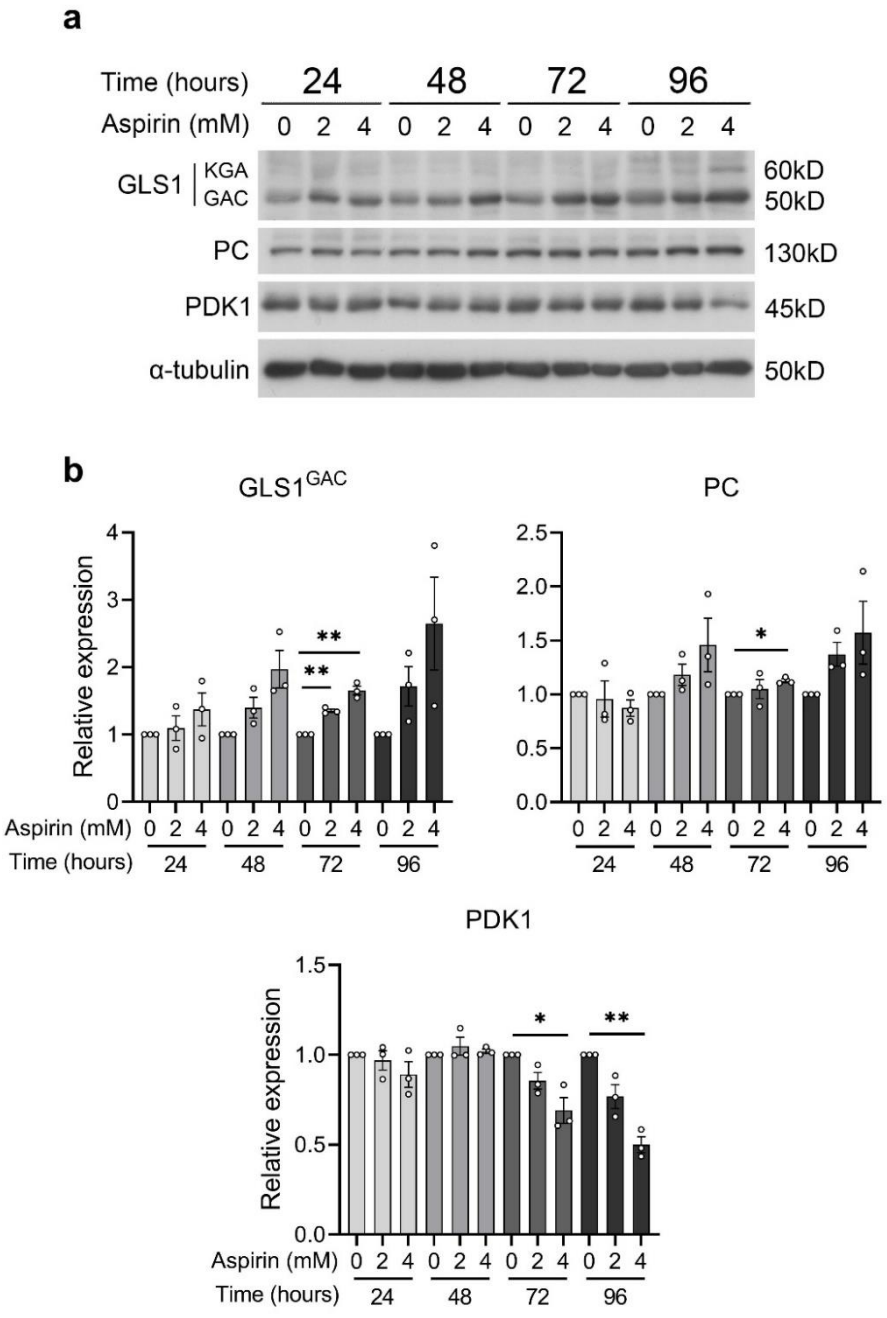

Figure 3.11 Time course of metabolic enzyme regulation with 24- 96 hours of aspirin treatment in SW620 cells

a Western analysis of a time-course of aspirin treatment in SW620 cells, representative of 3 independent experiments. **b** Quantification by densitometry, to show protein expression relative to control. Error bars represent standard error, *=p≤0.05, **=p≤0.01.

3.3.6 Regulation of GLS1 expression with long-term aspirin is stable up to 72 hours post aspirin removal

Results thus far have shown that aspirin treatment causes regulation of metabolic enzymes, particularly GLS1, within a short time frame (72 hours), and this regulation is increased and maintained following long-term treatment with aspirin. It was next asked whether these changes are stable following removal of aspirin in long-term aspirin treated cells. SW620 cells previously treated with long-term aspirin were cultured in aspirin-free media, and protein expression was analysed by western blotting at 24, 48 and 72 hours post aspirin removal. These results are shown in Figure 3.12. $GLS1^{GAC}$ remains upregulated in cells treated previously with both 2mM and 4mM aspirin compared to controls up to 72 hours post aspirin removal, suggesting this regulation is relatively stable. PC shows some upregulation at 24 and 48 hours post aspirin removal, whereas PDK1 does not show any clear regulation. This experiment was performed once, therefore further replication and longer aspirin removal times would be required to fully investigate the stability of GLS1 induction.

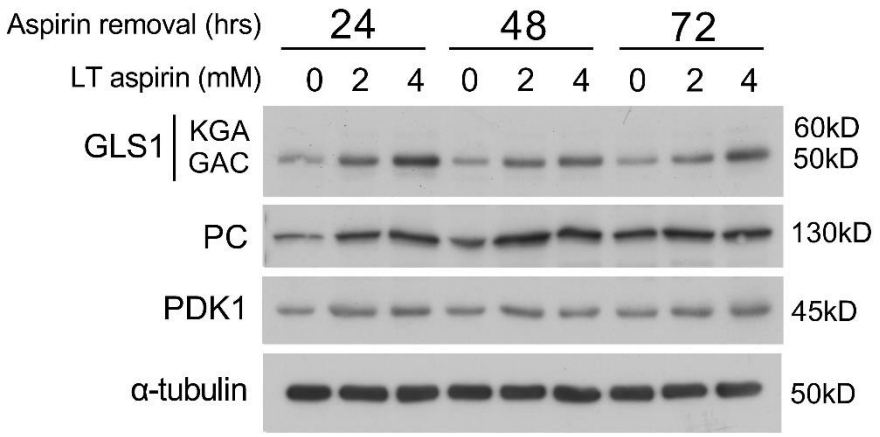

Figure 3.12 Regulation of GLS1 expression with long-term (52-week) aspirin is stable up to 72 hours post aspirin removal

Western analysis of long-term (LT) aspirin treated SW620 cells, cultured in the absence of aspirin for up to 72 hours. Expression of GLS1, PC and PDK1 was analysed 24, 48 and 72 hours post aspirin removal.

3.3.7 **Aspirin regulates metabolic proteins in CRC cell lines LS174T and HCA7**

As results so far have shown significant regulation of metabolic enzymes with aspirin treatment in the CRC cell line SW620, it was next investigated whether the same regulation occurs in two further CRC cell lines, LS174T and HCA7. These experiments were conducted to determine whether this was a cell line specific effect or more broadly applicable to CRC cells.

Expression of GLS1, PC and PDK1 was analysed by western blotting in LS174T (Figure 3.13) and HCA7 (Figure 3.14), with both short-term (72-hour) and long-term (>26 weeks) aspirin treatment. In LS174T cells, $GLS1^{GAC}$ showed a trend towards upregulation in both short- and long-term 4mM aspirin, consistent with results from SW620 cells, though this was only significant in short-term 4mM aspirin. PC and PDK1 do not show significant regulation.

In HCA7 cells, $GLS1^{GAC}$ showed some upregulation with both short- and long-term aspirin treatment, but this was not significant. PDK1 was significantly downregulated with long-term 4mM aspirin treatment, again consistent with results seen in SW620. However, in contrast to SW620 cells, PC was significantly downregulated in HCA7 with long-term 4mM aspirin.

Despite some differences, these results show that regulation of metabolic enzymes with aspirin treatment occurs in the three CRC cell lines investigated, and that short-term treatment is sufficient to induce some regulation. Induction of GLS1 expression is particularly consistent across cell lines and treatment times.

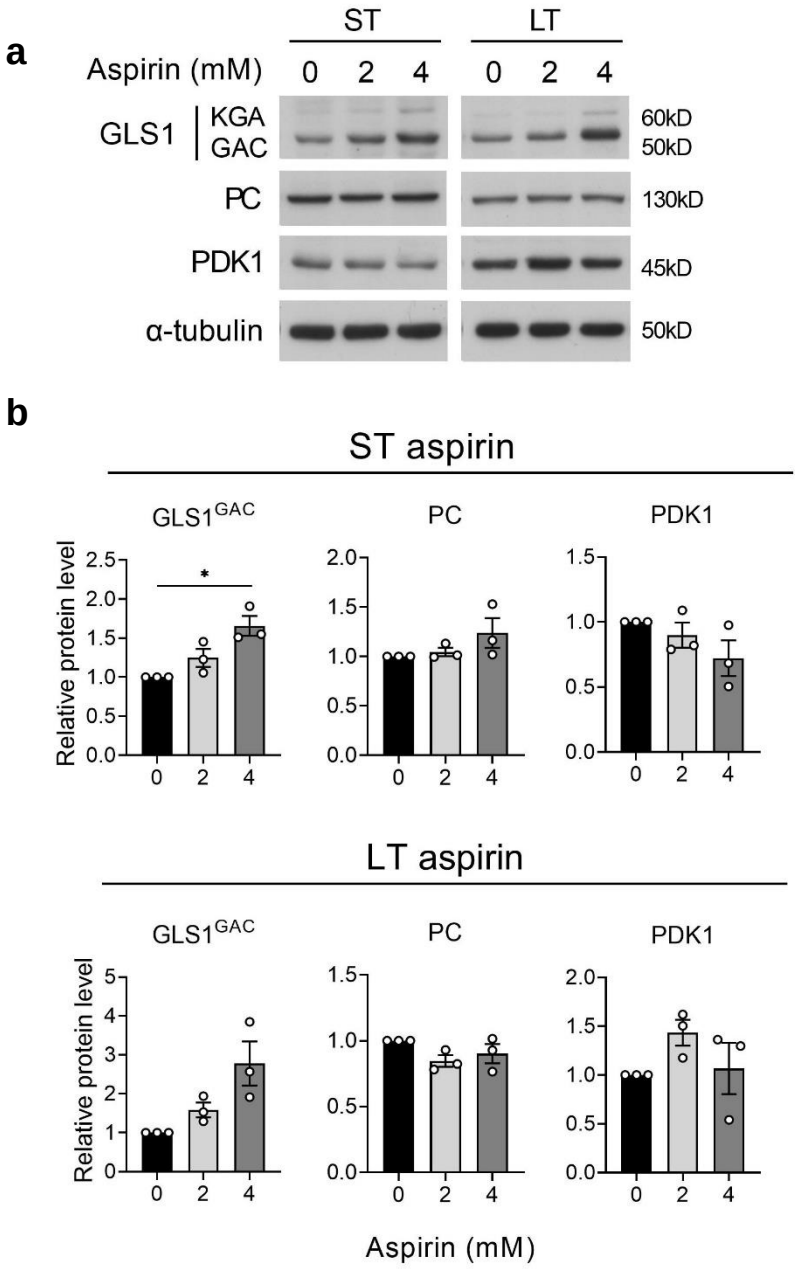

Figure 3.13 Short-term (72-hour) and long-term (>26-week) aspirin treatment regulates GLS1^{GAC} in LS174T cells

a Western analysis of short-term (ST) and long-term (LT) aspirin treated LS174T cells, representative of 3 independent experiments. **b** Quantification by densitometry, to show protein expression relative to control. Error bars represent standard error, *=p≤0.05.

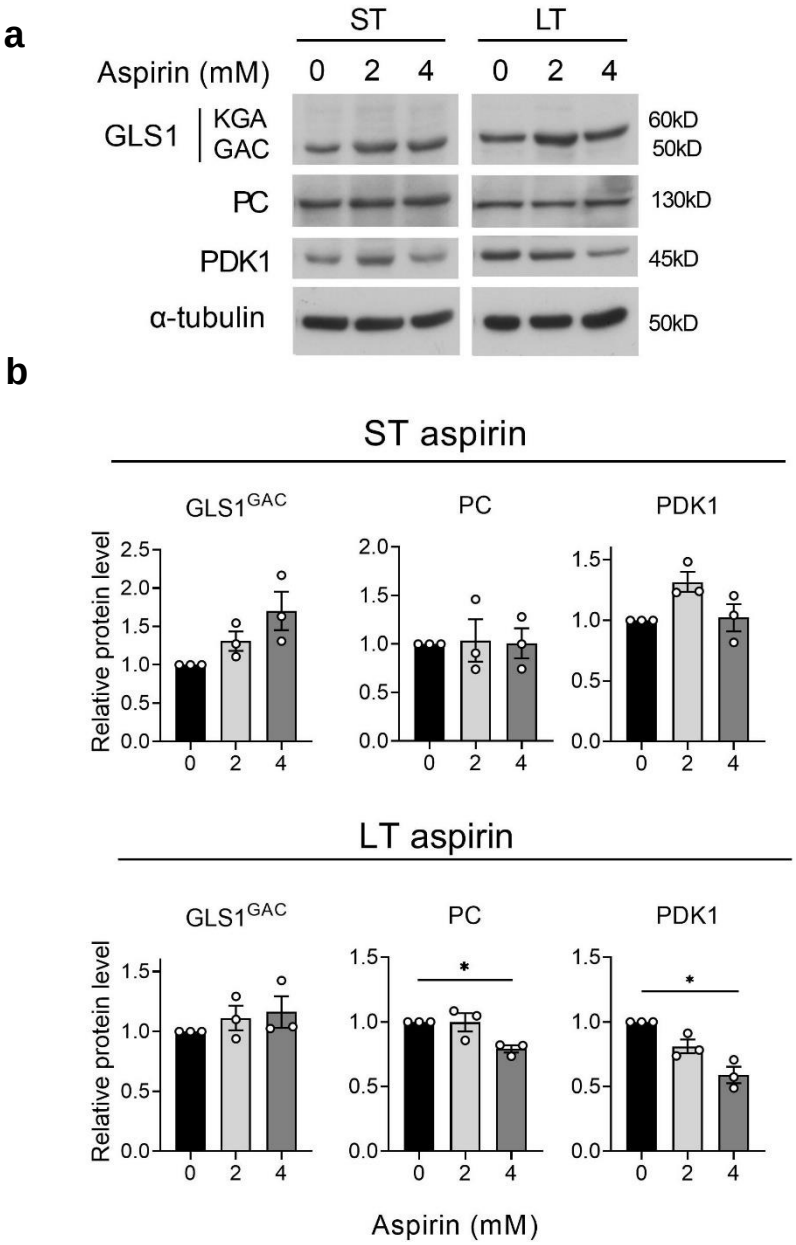

Figure 3.14 Short-term (72-hour) and long-term (>26-week) aspirin treatment regulates metabolic enzymes in HCA7 cells

a Western analysis of short-term (ST) and long-term (LT) aspirin treated HCA7 cells, representative of 3 independent experiments. **b** Quantification by densitometry, to show protein expression relative to control. Error bars represent standard error, *=p≤0.05.

3.3.8 **Long-term aspirin regulates metabolic enzymes in colorectal adenoma cell line RG/C2**

Having investigated regulation of metabolic enzymes with aspirin treatment in CRC cell lines and shown some variation in response, it was next asked whether the same effect occurs in colorectal adenoma cells. This is an important question when considering aspirin as a preventative as well as therapeutic agent for colorectal cancer. Expression of GLS1, PC and PDK1 were analysed by western blotting in the colorectal adenoma cell line RG/C2 following long-term aspirin treatment (120 weeks). These results are shown in Figure 3.15. Both splice variants of GLS1 ($GLS1^{KGA}$ and $GLS1^{GAC}$) were expressed in this cell line, with $GLS1^{KGA}$ being the more highly expressed isoform. This is in contrast to the carcinoma cell lines, where $GLS1^{GAC}$ was dominantly expressed. Interestingly, both isoforms of GLS1 showed upregulation with long-term 4mM aspirin in this cell line, consistent with results seen in the carcinoma cell lines, though this was only significant in the KGA isoform. Neither PC nor PDK1 showed consistent regulation.

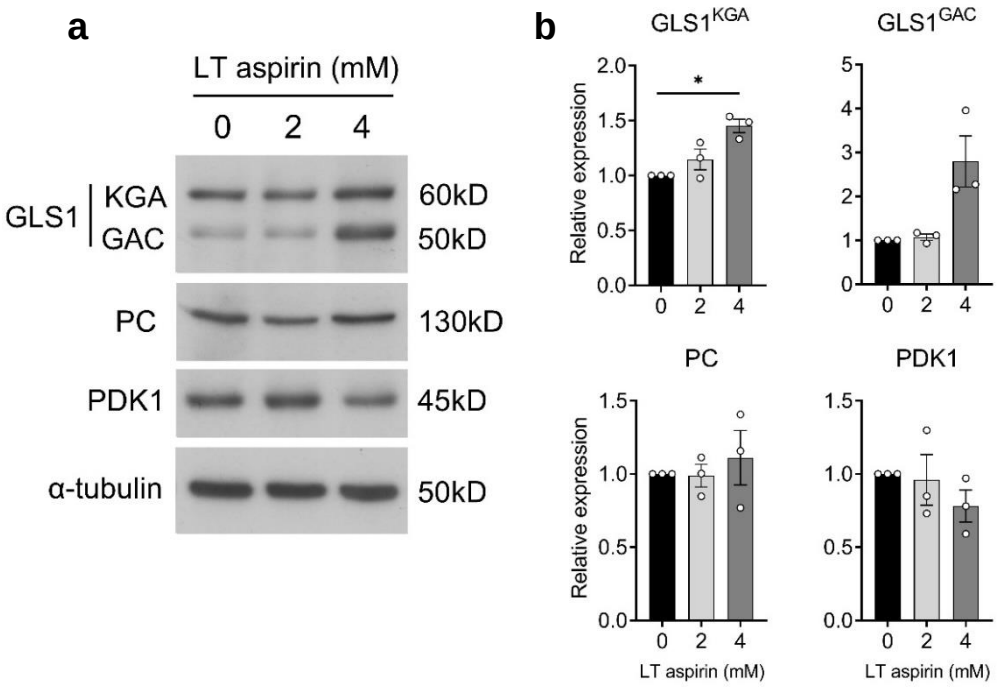

Figure 3.15 Long-term (120-week) aspirin treatment regulates $GLS1^{GAC}$ in RG/C2 cells

a Western analysis of long-term (LT) aspirin treated RG/C2 cells, representative of 3 independent experiments. **b** Quantification by densitometry, to show protein expression relative to control. Error bars represent standard error, *=p≤0.05.

3.3.9 Knockdown of ATF4 or GPT2 does not induce upregulation of GLS1 expression

As described in section 1.2.8.3, GLS1 is often upregulated in cancer, particularly CRC, and is thought to promote tumorigenesis. It is therefore interesting that GLS1 is upregulated with aspirin treatment, as aspirin has anti-tumorigenic effects, decreasing cell proliferation and inducing apoptosis *in vitro* (257), as well as decreasing CRC risk in patients (as described in section 1.3.1). It was therefore hypothesised that GLS1 may be upregulated with aspirin treatment in response to other proteins involved in glutaminolysis being downregulated as a compensation mechanism, rather than a direct effect of aspirin. Proteomic data, and subsequent validation, suggests that ATF4 signalling is inhibited with aspirin treatment. As ATF4 regulates many genes involved in amino acid metabolism, it was investigated whether GLS1 may be upregulated in response to ATF4 inhibition. Furthermore, GPT2 (a transcriptional target of ATF4) was also found to be downregulated with aspirin. GPT2 has been previously shown to be upregulated in response to GLS1 inhibition or knockdown (258), suggesting that the reverse effect may also occur, and that GLS1 may also be upregulated with aspirin treatment specifically in response to downregulation of GPT2. It was therefore also investigated whether GLS1 is upregulated in response to downregulation of GPT2 (shown in section 3.3.3).

To investigate this, knockdown of ATF4 using siRNA was performed in SW620 cells, and GPT2 and GLS1 expression were analysed over a time course (48-96 hours), shown in Figure 3.16. Gene expression was analysed by both western blotting and qPCR, which showed that although there was not a strong knockdown of ATF4 at the protein level, there was an approximate 80% knockdown at the mRNA level. These results show that ATF4 knockdown reduces levels of GPT2 mRNA and protein after 72 and 96 hours of knockdown, as expected. However, GLS1 expression is not induced, and is actually decreased at the protein level.

A time course of GPT2 knockdown was also performed (48-96 hours) and GPT2 and GLS1 expression was analysed by western blotting (Figure 3.17). This shows strong knockdown of GPT2 protein, however there is no clear change in expression of GLS1. These results suggest that upregulation of GLS1 expression with aspirin treatment is not a direct response to inhibition of ATF4 signalling or downregulation of GPT2.

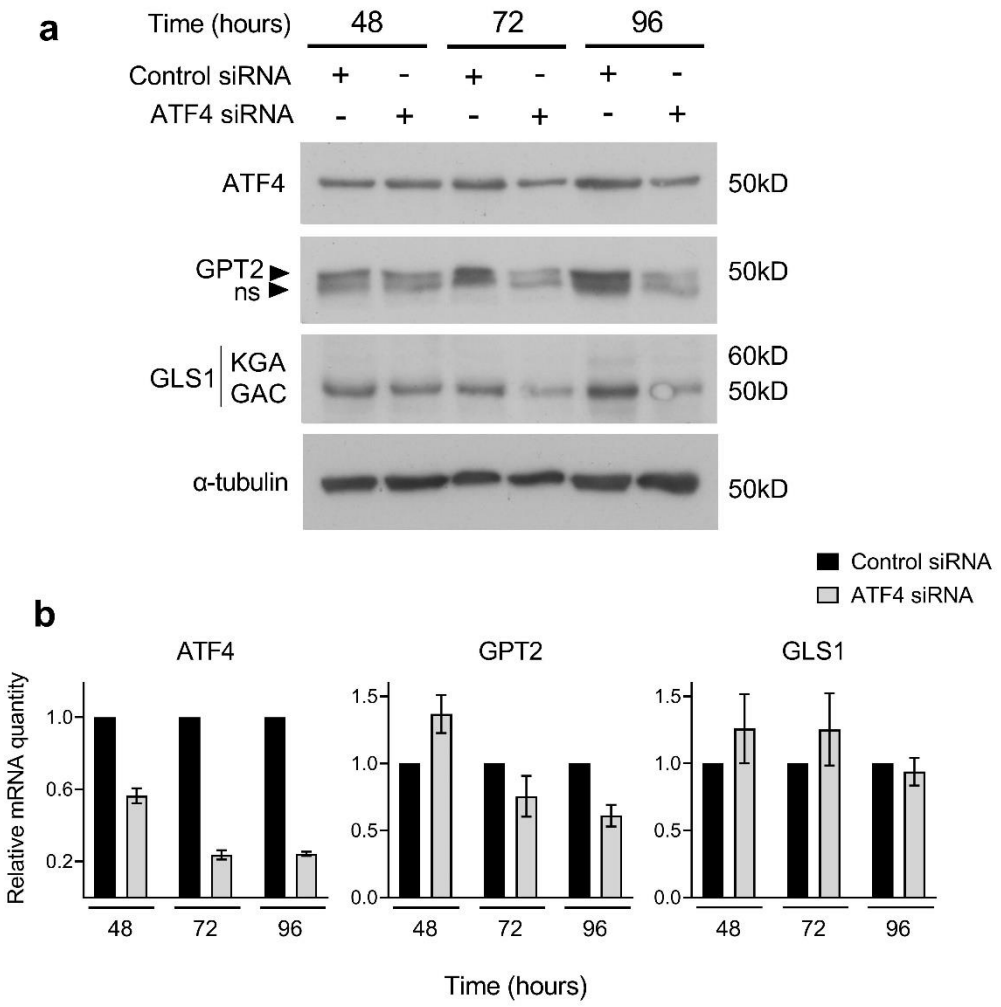

Figure 3.16 Knockdown of ATF4 does not induce expression of GLS1

a Western analysis of ATF4, GPT2 and GLS1 expression in SW620 cells after knockdown of ATF4 with siRNA, after 48, 72 and 96 hours after knockdown. ns=non-specific band. **b** qPCR analysis of ATF4, GPT2 and GLS1 expression in SW620 cells after knockdown of ATF4, at 48, 72 and 96 hours after knockdown. **a** shows representative blots from 2 independent experiments. **b** shows technical replicates from one individual experiment, (n=2 for ATF4 48hr, n=3 for all other conditions), error bars show standard deviation.

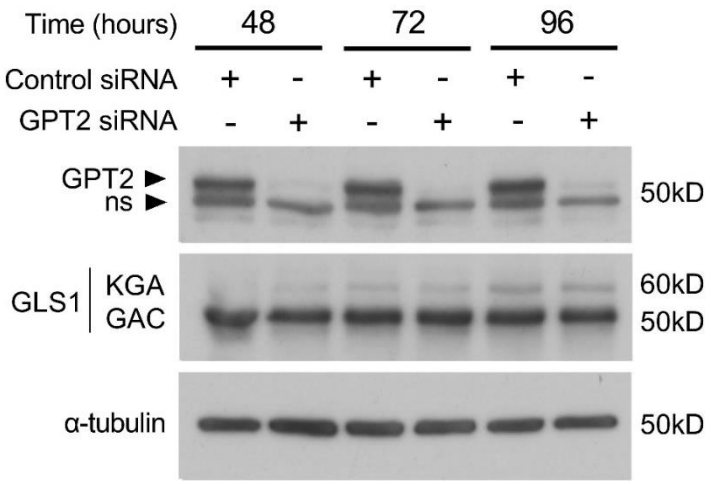

Figure 3.17 Knockdown of GPT2 does not induce expression of GLS1

Western analysis of GPT2 and GLS1 expression in SW620 cells after knockdown of GPT2 with siRNA, at 48, 72 and 96 hours after knockdown. ns=non-specific band.

3.4 Discussion

The aim of this chapter was to build on previous proteomic analysis performed in the Williams lab to investigate novel effects of long-term aspirin exposure in CRC cells. Previous analysis of these data highlighted that aspirin regulates proteins involved in metabolic processes (Dr Eleanor Mortensson, unpublished), leading to the hypothesis that aspirin could act to reprogram cellular metabolism of CRC cells. Due to the large amount of research interest in targeting cancer metabolism, as well as further understanding anti-cancer mechanisms of aspirin, this hypothesis warranted further investigation. Identification and characterisation of metabolic reprogramming downstream of aspirin treatment would help to further understand its anti-cancer mechanisms, which could help in maximising clinical benefit of aspirin use in CRC prevention and treatment, such as identifying optimum treatment timing and patient subgroups. This is particularly important when considering the associated risks of aspirin treatment, such as increased risk of severe bleeding.

Analysis of the significantly regulated proteins within the proteomic data highlighted regulation of key metabolic enzymes: GLS1, GLUT1, HK1, PC and PDK1. The directions of these changes suggested there may be an overall increase in carbon entry derived from both glucose and glutamine into the TCA when the cells are treated with long-term aspirin. However, metabolic activity cannot always be inferred from metabolic enzyme expression alone. Therefore, further investigation is required in order to confirm this, which is carried out in the following chapter (Chapter 4).

As GLS1 showed strong upregulation, the regulation of other proteins in the glutaminolysis pathway was also investigated in order to determine whether there was a consistent global effect on glutaminolysis enzymes with aspirin treatment. However, it was found that several other glutaminolysis proteins were downregulated with aspirin, including ASNS and GPT2. Therefore, without measuring metabolic activity (see Chapter 4) no clear conclusion can be made on the overall effect of aspirin on glutaminolysis from these data.

Further analysis of the proteomic data using IPA highlighted an inhibition of ATF4 signalling with aspirin treatment. Regulation of several transcriptional targets of ATF4 was confirmed in this chapter by qPCR, providing further evidence that aspirin treatment has an inhibitory effect on ATF4 signalling. Despite the consequences of this for cellular metabolism or tumorigenicity not having been

confirmed, this finding further supports the hypothesis that long-term aspirin treatment may have a metabolic reprogramming effect, as ATF4 is a key regulator of cellular metabolism.

Validation of the proteomic results by western blotting and qPCR confirmed that long-term aspirin treatment significantly regulated many of the proteins highlighted in the proteomic data. This was shown in three distinct CRC cell lines (SW620, LS174T, HCA7) with a variety of mutational backgrounds (see section 2.1.1). This suggests that the potential metabolic reprogramming effect of aspirin, and any clinical benefit of this effect, may be applicable to multiple subtypes of CRC tumours. Regulation of GLS1 in the colorectal adenoma cell line RG/C2 suggests this may also be relevant for prevention of CRC.

It was also found that short-term treatment with aspirin was sufficient to induce some of the changes in metabolic enzyme expression seen with long-term aspirin. This suggests that this mechanism may not be limited to patients who take aspirin for chronic conditions, but may also be relevant in patients who might take a shorter course of aspirin as part of an adjuvant treatment regime for CRC for example.

Upregulation of GLS1 expression was the most consistent and significant change seen with aspirin treatment, which is of interest as this appears to be in direct opposition to aspirin's antitumourigenic role (257). GLS1 expression is thought to promote cell proliferation and is often increased in cancers. Its upregulation may therefore not be a direct effect of aspirin treatment, but this requires further investigation. GLS1 may be upregulated as a compensation mechanism in response to the effect of aspirin on other metabolic pathways. It was hypothesised in this chapter that GLS1 upregulation may be a response to inhibition of ATF4 signalling by aspirin, or more specifically, downregulation of the ATF4 target GPT2, as these could potentially inhibit amino acid synthesis and particularly glutaminolysis. However, it was found that GLS1 expression was not upregulated in response to either ATF4 or GPT2 knockdown in these cells. This suggests that there may be other effects of aspirin that lead to the upregulation of GLS1. Of note, knockdown of ATF4 by siRNA did not significantly reduce levels of ATF4 protein, so the effect of ATF4 inhibition still needs to be determined. There may be a more efficient way of inhibiting this signalling pathway, which could then result in GLS1 upregulation, for example, inhibition of ATF4 activating enzymes by small molecule inhibitors (259). Further investigation to determine the specific underlying

mechanism for the induction of GLS1 expression upon aspirin treatment is of importance.

GLS1 upregulation was also found to be maintained following 72 hours of aspirin removal from long-term aspirin treated cells. It would be interesting to further investigate the stability of this change after the cessation of long-term aspirin treatment. It has been suggested that CRCs that develop in the presence of long-term aspirin use may have some level of resistance to the therapeutic benefits of aspirin (discussed in section 1.3.1). Any stable cellular changes that are maintained after the removal of aspirin exposure may help to explain the possible aspirin-resistant phenotype of cancer cells. However, GLS1 expression would only be considered in this context if the regulation was stable for a much longer time than has been demonstrated here. This does however warrant further investigation.

This work adds to a growing body of literature on the effects of aspirin on cancer cellular metabolism (described in section 1.4). Of particular interest are the previous studies that show aspirin affects metabolism of glucose and glutamine. In line with the findings in this chapter, aspirin has previously been shown to inhibit PDK1 in breast cancer cells (203). However, aspirin has also been found to downregulate GLUT1 in hepatoma cells (210), which is opposite to the effect seen here in the proteomic data with long-term aspirin treatment. Interestingly, a recent study by Boku et al in 2020 also investigated the effect of aspirin on glutamine metabolism (212). Consistent with the findings of this chapter, they also find that aspirin treatment upregulates GLS1 expression. However, they also find that aspirin upregulates other glutaminolysis enzymes, which were found in this chapter to be downregulated, such as GPT2. They also find that aspirin promotes ATF4 signalling, whereas results in this chapter suggests that aspirin has an inhibitory effect on ATF4 signalling. As different CRC cell lines were used by Boku et al. to those used in this chapter (HCT-15, HCT-116, SW480), this suggests there may be some cell line specificity in the effects of aspirin, or other context dependent factors such as the length of treatment time. It is therefore important to further understand the mechanisms driving the regulation of metabolism by aspirin, to identify whether there are specific subgroups of patients who will most benefit from therapeutic use of aspirin and what the optimum timing of treatment is. Overall, the work in this chapter adds to a growing body of evidence that aspirin can significantly affect expression of metabolic enzymes in cancer cells.

Importantly, the conclusions that can be drawn from the results in this chapter on the metabolic reprogramming effect of aspirin are limited, as enzyme expression levels do not necessarily correlate with pathway activity. Though there are several previous studies highlighting an effect of aspirin on expression of metabolic enzymes, these studies have not directly measured the effect of aspirin on metabolic pathway activity. Most studies to date have inferred pathway activity based on changes to enzyme expression. However, this is not always reliable as many other factors can affect pathway activity such as post-translational modification of enzymes, activity of other enzymes in the same pathway, or substrate and product availability. Consistent with other studies, results in this chapter show that aspirin regulates several metabolic enzymes, however the effect of aspirin on metabolic pathway activity within cells is still unknown. This will be further investigated in the next chapter.

Chapter 4 Results 2

Investigating the effect of aspirin on metabolic pathways

4.1 Introduction

Results in section 3.3 show that aspirin regulates proteins involved in metabolic pathways, suggesting aspirin treatment might cause cellular metabolic reprogramming. However, these results do not show whether these changes relate to changes in metabolic pathway activity. More direct methods of investigating metabolic pathway activity were therefore employed in order to determine whether aspirin induces metabolic reprogramming in tumour cells, which have not been utilised in previously published studies investigating the effect of aspirin on cellular metabolism. These methods are described in this section.

4.1.1 Extracellular flux analysis

Extracellular flux analysis allows measurement of activity of the two main pathways in cells that produce ATP, glycolysis and oxphos. Activity of oxphos is shown by measuring the oxygen consumption rate (OCR) of the cells. As previously discussed in section 1.2.1, TCA cycle activity and oxphos activity are intimately linked by the balance of NAD/NADH levels, therefore OCR is also considered a proxy measurement for TCA cycle activity. Extracellular acidification rate (ECAR), measuring the rate of proton production from the cells into the medium, infers the rate of lactate secretion from the cells, an indication of glycolytic activity. OCR and ECAR can be measured in real time using a Seahorse Bioanalyzer.

Using the Seahorse Bioanalyzer, further information about cellular metabolism and mitochondrial function can be gained by performing a Mito Stress Test, involving sequential injection of metabolic inhibitors (260). The effects of the inhibitors and the metabolic parameters they can determine are illustrated in Figure 4.1. The first inhibitor injected in the Mito Stress Test is oligomycin, an inhibitor of ATP synthase. This shows the proportion of baseline OCR that is attributable to ATP production. The next drug is FCCP, which is an uncoupler of the ETC. It allows the flow of protons across the inner mitochondrial membrane, which pushes OCR to its maximum rate. This shows the theoretical maximum respiration rate of the cells, and allows calculation of ‘spare respiratory capacity’, which is the difference between the baseline OCR of the cells and their theoretical maximum. The next injection is of rotenone and antimycin A, which are inhibitors of complex I and III of the ETC respectively. These cause the ETC to be completely shut down, meaning that any remaining oxygen consumption is due to non-mitochondrial respiration. The final injection used, in addition to the standard Mito Stress Test, is monensin, which was determined by Mookerjee et al. to produce a maximal level of glycolysis,

allowing calculation of spare glycolytic capacity (261). The Na^+/K^+ ATPase pump produces a gradient of Na^+ and K^+ across the cell membrane, which consumes a large proportion of ATP in the cell. Monensin allows leak of the ions across the membrane, therefore causing the Na^+/K^+ ATPase pump to work at maximal capacity, which maximises ATP demand. As ATP can no longer be produced from oxphos due to the addition of rotenone and antimycin A, glycolysis is pushed to its maximal level with the addition of monensin, in order to meet ATP demand.

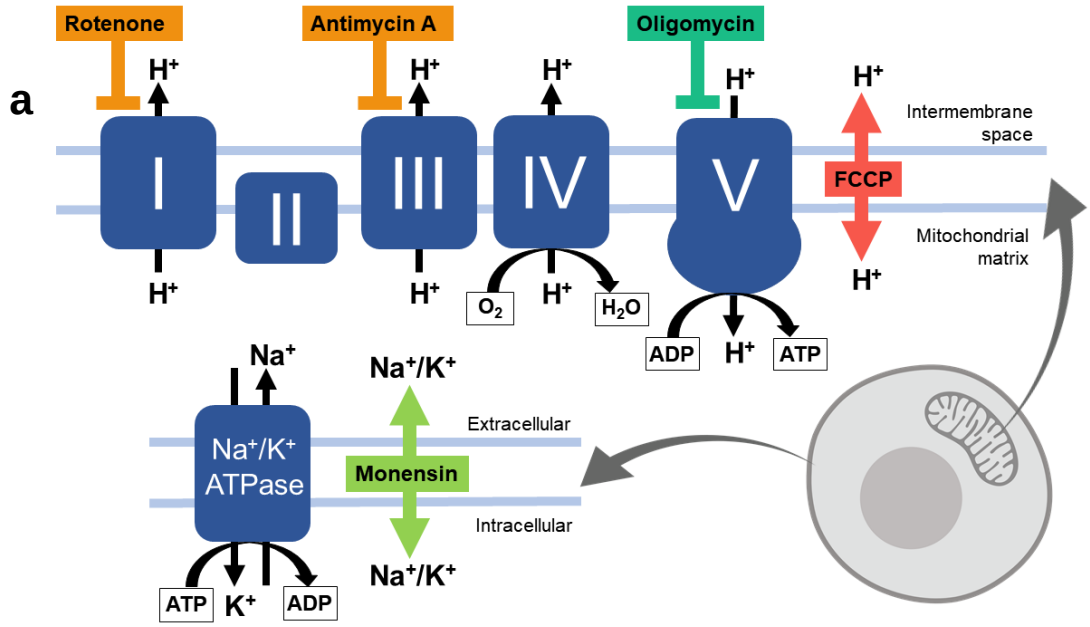
a
Rotenone
Antimycin A
Oligomycin
H+
I
II
III
IV
V
FCCP
Intermembrane space
Mitochondrial matrix
O2
H2O
ADP
ATP
Na+
Na+/K+
Na+/K+ ATPase
Monensin
Extracellular
Intracellular
K+

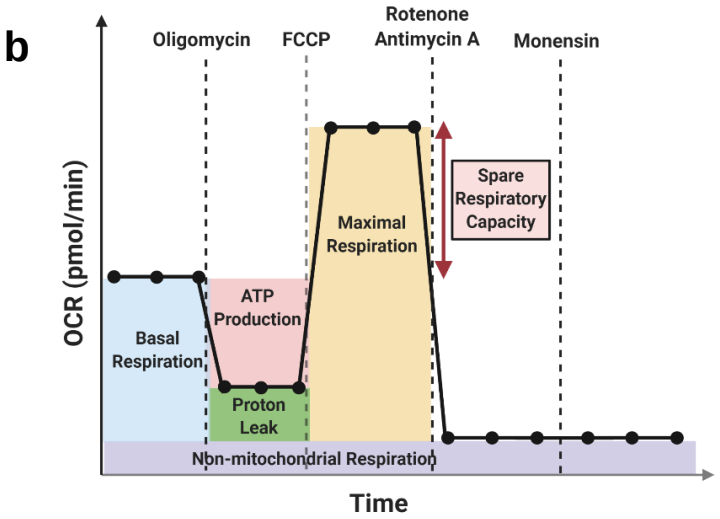
b
Oligomycin
FCCP
Rotenone
Antimycin A
Monensin
OCR (pmol/min)
Basal Respiration
ATP Production
Proton Leak
Maximal Respiration
Spare Respiratory Capacity
Non-mitochondrial Respiration
Time

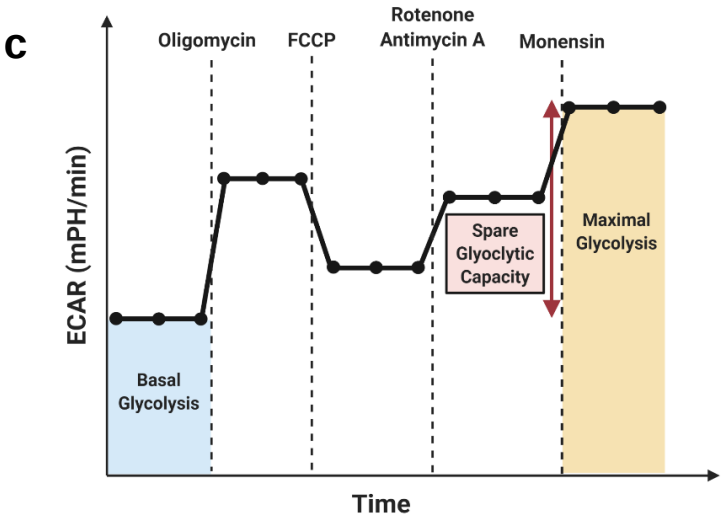
c
Oligomycin
FCCP
Rotenone
Antimycin A
Monensin
ECAR (mPH/min)
Basal Glycolysis
Spare Glyoclytic Capacity
Maximal Glycolysis
Time

Figure 4.1 Principles of extracellular flux analysis and the Mito Stress Test

a Oligomycin inhibits ATP synthase (complex V), blocking the electron transport chain (ETC) and oxphos. FCCP uncouples oxygen consumption from ATP production, maximising oxygen consumption and providing a measure of maximal respiration. Rotenone and antimycin A block complexes I and III respectively, completely blocking ETC function and all mitochondrial oxygen consumption. Monensin allows Na^+/K^+ leak across the cell membrane, maximising the ATP required by the Na^+/K^+ ATPase pump. As oxphos is already inhibited by rotenone/antimycin A, this maximises the demand of ATP from glycolysis, therefore providing a method of measuring maximum glycolytic capacity. **b** OCR trace with drug injections. **c** ECAR trace with drug injections. Adapted from (260).

4.1.2 **Bioenergetics analysis**

Extracellular flux analysis data provide a proxy for the outputs of the main two ATP producing pathways (glycolysis and oxphos), however, there are several reasons why these measurements do not represent the absolute amount of ATP produced from either pathway (253). For example, not all extracellular acidification is from lactate production; CO_2 production from the TCA cycle will also acidify the extracellular environment. Also, not all pyruvate produced in glycolysis is converted to lactate (some will directly enter the TCA cycle), and production of pyruvate that is not converted to lactate still produces ATP from glycolysis. Glycolysis and oxphos also produce very different amounts of ATP per glucose molecule, so measuring the pathway activity by OCR and ECAR does not allow their relative contributions to overall ATP production to be measured. To take these factors into account, OCR and ECAR can be converted into total ATP production using bioenergetics calculations detailed by Mookerjee et al. (253), using a spreadsheet produced by Eric H Ma and Kelsey Williams in the Russell Jones lab (252) (see section 2.7.1). This allows calculation of total ATP production (J_{ATP}), ATP production from glycolysis ($J_{ATP\text{-}GLYC}$) and ATP production from oxphos ($J_{ATP\text{-}OX}$). With glycolysis and oxphos in the same units, their contributions to total ATP production can be compared, and conclusions can be drawn about the overall bioenergetic phenotype of the cells. These measurements are made from the basal OCR and ECAR data, as well as the maximal measurements (OCR with FCCP, ECAR with monensin). This provides information about the maximum possible contribution of each pathway to ATP production, and how far each pathway is to this theoretical maximum at basal levels.

4.1.3 **Stable isotope tracer analysis**

While abundances of intracellular metabolites can be readily measured and compared, this does not provide information about metabolic pathway activity. A change in metabolite level could be due to either a change in rate of production or consumption, and these cannot be distinguished by metabolite abundance alone. One method of investigating pathway activity or "flux" through metabolic pathways is using nutrients that are labelled with stable (non-radioactive) isotopes, such as ^{13}C. This is referred to as stable isotope tracer analysis (SITA). This method can be used to perform "flux analysis", which involves computational estimation of metabolic fluxes based on labelling data combined with other known features about the cells such as growth rates etc. (262). However, ^{13}C labelling data from SITA can also be directly interpreted in order to compare metabolic pathway activity and nutrient contributions between different conditions (262). Using this method, the labelling patterns of downstream metabolites (as determined by mass spectrometry) after incubation with an isotopically labelled nutrient can provide information about the metabolic fate of that nutrient.

4.2 Aims

Given that aspirin regulates key metabolic enzymes, it was next investigated whether this was sufficient to regulate metabolic pathway activity in CRC cells, as hypothesised in section 3.1. Aims of this chapter are:

i. To investigate the effect of long-term aspirin treatment on utilisation of glycolysis and oxidative phosphorylation (oxphos) for ATP production

ii. To investigate the effect of long-term aspirin treatment on nutrient utilisation, using stable isotope tracer analysis (SITA) to trace the metabolic fate of glucose and glutamine in CRC cell lines

4.3 Results

4.3.1 Long-term aspirin treatment does not alter the overall levels of glycolysis or oxidative phosphorylation in SW620 cells

Having shown that long-term aspirin treatment alters expression of metabolic enzymes in CRC cell lines, it was investigated whether this led to any effect on the pathways used for ATP production: glycolysis and oxidative phosphorylation (oxphos). Long-term (~52-week) aspirin treated SW620 cells underwent extracellular flux analysis using a Seahorse XFp analyzer. This involved real-time measurements of extracellular acidification rate (ECAR), as a proxy for lactate production from glycolysis, and oxygen consumption rate (OCR), as a measurement of oxphos. These measurements were also taken after serial injection of the metabolic inhibitors oligomycin, FCCP, rotenone/antimycin A, and monensin, to measure different metabolic parameters in the cells (described in section 4.1).

Prior to performing this experiment, conditions for analysis were optimised. Optimum cell number was determined, in order to produce basal OCR readings in the ideal range for the machine (20-150 pmol/min) and ideal confluency of the cells (50-90%) (263). This was found to be 60,000 cells per well (Figure 4.2). Optimum concentration of FCCP to produce maximal OCR was also determined, as this can vary between cell lines. If the FCCP concentration is too low, OCR will not be maximally induced. However, if the dose is too high, this will induce cell death, and therefore not produce maximal OCR. Optimisation of FCCP concentration was carried out according to the manufacturer's protocol (263), using serial injection of increasing FCCP concentrations in order to produce a dose response curve. These results (shown in Figure 4.3) show that in SW620 cells, the optimum concentration of FCCP to produce maximal OCR is 1-2µM.

.

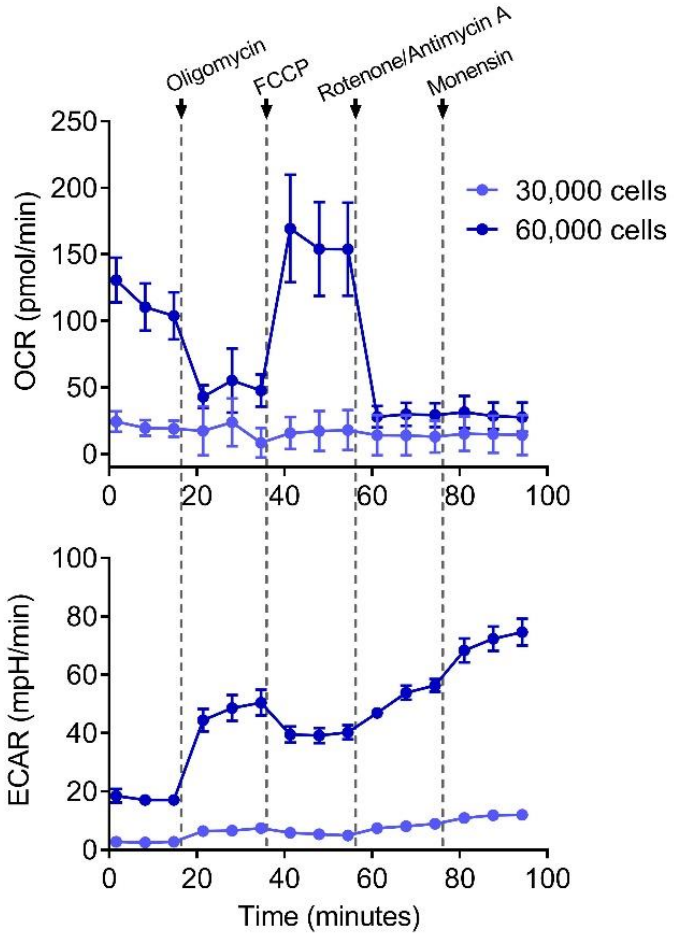

Figure 4.2 Cell number optimisation for extracellular flux analysis in SW620

Oxygen consumption rate (OCR) and extracellular acidification rate (ECAR) were measured using two different cell densities (30,000 and 60,000 cells). 60,000 cells showed basal OCR in the ideal range (20-150pmol/min) and was therefore used for subsequent experiments. Data represent technical replicates from one experiment (n=3), error bars represent standard deviation.

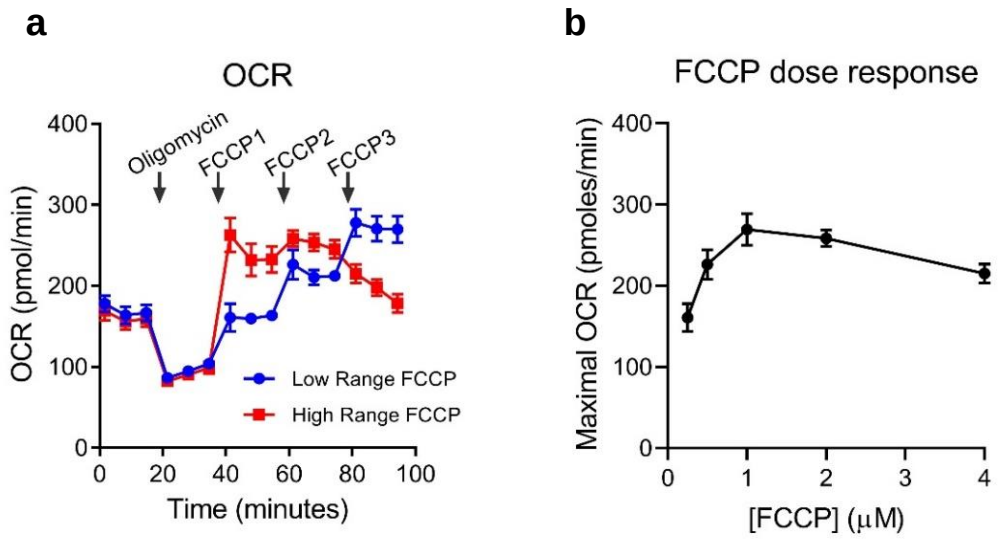

Figure 4.3 FCCP concentration optimisation in SW620

a OCR trace over time of FCCP dose response experiment. The first injection port was used to inject oligomycin in all conditions. The plate was divided into high and low FCCP concentrations. In low FCCP, the second two ports injected 0.25µM FCCP (FCCP1 and FCCP2), and the last port (FCCP3) injected 0.5µM FCCP, leading to cumulative FCCP concentrations of 0.25µM, 0.5µM and 1µM. In the high dose FCCP, the second two injection ports injected 1µM FCCP, and the third injection port injected 2µM FCCP, leading to cumulative FCCP concentrations of 1µM, 2µM and 4µM. **b** Dose response produced from data in **a**. Data represent technical replicates from one experiment, (n=3 for low range FCCP, n=4 for high range FCCP), error bars represent standard deviation.

Using these determined conditions, extracellular flux analysis was then performed in long-term (~52-week) aspirin treated SW620 cells. These results are shown in Figure 4.4a-b. OCR was not changed by long-term aspirin exposure; baseline OCR, and following injection of each drug, does not change in the 2mM or 4mM aspirin treated cells compared to the control. This suggests that aspirin does not alter the levels of oxphos, or any of the other parameters measured such as maximal oxphos. There is a slight increase in average ECAR in the 4mM treated cells across the trace, though this is not statistically significant. This suggests glycolysis at baseline and maximal glycolysis are not significantly changed with aspirin treatment.

Bioenergetics analysis of these data shows the relative contributions of glycolysis and oxphos to overall ATP production, calculated from OCR and ECAR (detailed in section 4.1.2). Results from this analysis are shown in Figure 4.4c-h.

Bioenergetic scope ($J_{ATP-GLYC}$ x J_{ATP-OX}), and bioenergetic capacity (total basal and maximal J_{ATP}) allow the relative contributions of glycolysis and oxphos to be compared at both basal and maximal levels. Spare respiratory capacity provides a measurement of how close the basal ATP production from oxphos is to the theoretical maximum, which shows how able the cells are to increase ATP output from oxphos if required, such as in response to stress. Glycolytic index reports the proportion of total ATP production that comes from glycolysis. Supply flexibility index indicates the bioenergetic plasticity of the cells, which is their ability to adapt to limitation of nutrients such as glucose and glutamine. This is calculated by measuring their ability to switch their ATP production between either glycolysis or oxphos, which depends on how close these pathways are to their potential maximum when at basal levels.

Although these results do not show any significant changes with aspirin treatment, they do highlight some interesting characteristics of the cells. A key observation is that at basal levels, less than 50% of ATP is produced from glycolysis. This is interesting as cancer cells are classically thought to undergo the Warburg effect and become highly glycolytic in the presence of sufficient oxygen. Typically, glycolytic cells would be defined as cells that produce more than 50% of their ATP from glycolysis (253). Under this definition, these cells are not considered glycolytic. These data show that they produce a significant amount of ATP from oxphos, which also opposes the classic Warburg effect. This supports the more updated view of cancer metabolism that although cancer cells may increase levels of aerobic glycolysis, they are still also largely dependent on oxphos for ATP production (26). Another interesting observation is that the cells have large spare respiratory capacity and spare glycolytic capacity, as their maximal $J_{ATP-GLYC}$ and J_{ATP-OX} are considerably higher than their basal levels. This also means they have very high supply flexibility index (~100%), meaning they could theoretically maintain their ATP production levels by switching between glycolysis and oxphos if necessary. This means they have the ability to adapt to nutrient depletion, another key characteristic of cancer cells, as they often encounter this in the tumour microenvironment due to poor vascularisation. This ability does not appear to be hindered by long-term aspirin treatment.

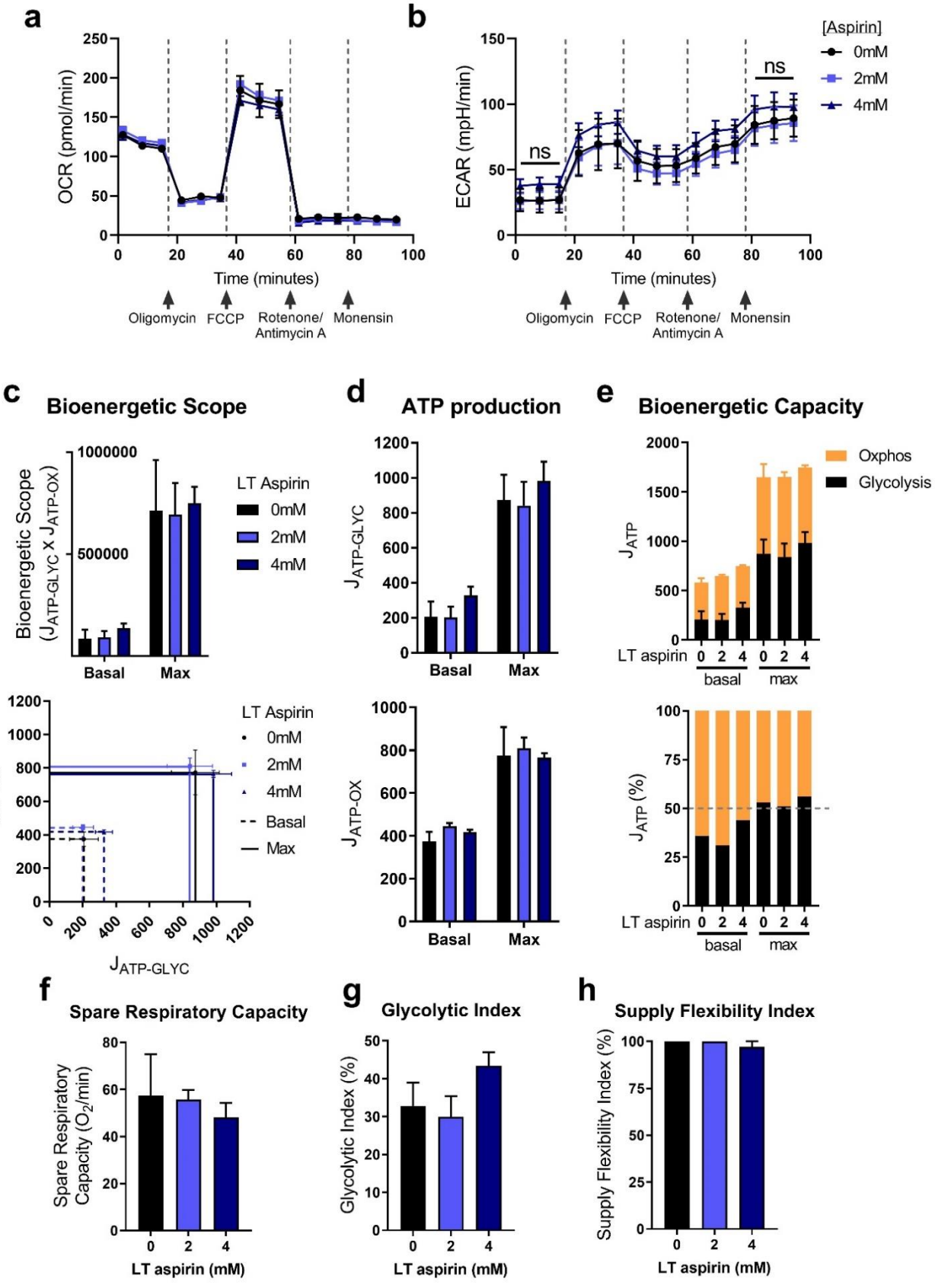
a
OCR (pmol/min)
Time (minutes)
Oligomycin
FCCP
Rotenone/ Antimycin A
Monensin
b
ECAR (mpH/min)
ns
[Aspirin]
0mM
2mM
4mM
c
Bioenergetic Scope
Bioenergetic Scope ($J_{ATP-GLYC}$ x J_{ATP-OX})
LT Aspirin
Basal
Max
J_{ATP-OX}
$J_{ATP-GLYC}$
d
ATP production
$J_{ATP-GLYC}$
J_{ATP-OX}
e
Bioenergetic Capacity
Oxphos
Glycolysis
J_{ATP}
J_{ATP} (%)
LT aspirin
basal
max
f
Spare Respiratory Capacity
Spare Respiratory Capacity (O_2/min)
LT aspirin (mM)
g
Glycolytic Index
Glycolytic Index (%)
h
Supply Flexibility Index
Supply Flexibility Index (%)

Figure 4.4 Extracellular flux analysis and bioenergetics analysis of long-term (52-week) aspirin treated SW620 cells

a-b Oxygen consumption rate (OCR) and extracellular acidification rate (ECAR) were measured as proxies to oxphos and glycolysis respectively, at basal levels and with mitochondrial stress test. Ns = not significant. **c-h** Bioenergetics analysis converted these measurements into ATP production (J_{ATP}) from each pathway, $J_{ATP\text{-}OX}$ (ATP production from oxphos) and $J_{ATP\text{-}GLYC}$ (ATP production from glycolysis). Max measurements are oxphos with FCCP and glycolysis with monensin. Data represent 3 independent experiments, error bars represent standard error (n=3).

These results suggest that long-term aspirin treatment does not affect the use of glycolysis or oxphos for ATP production. It was next investigated whether aspirin has any acute effect on OCR and ECAR, which may then equilibrate over the course of long-term treatment. To investigate this, extracellular flux analysis was performed with SW620 cells that had not been previously treated with aspirin, using the first injection port to inject either 2mM or 4mM aspirin, or vehicle control. This allowed measurement of the real-time effect of aspirin treatment on OCR and ECAR. These results are shown in Figure 4.5. These data were not normalised to cell number, so the OCR and ECAR measurements cannot be directly compared, but comparison can be made in any change that occurs in OCR or ECAR over time with addition of aspirin. Therefore, OCR and ECAR at each time point were calculated relative to the average of the basal measurements in each aspirin condition. Measurements were taken for approximately 2 hours following injection of aspirin, however there appeared to be no change in either OCR or ECAR in this time, suggesting no acute effect of aspirin on OCR or ECAR.

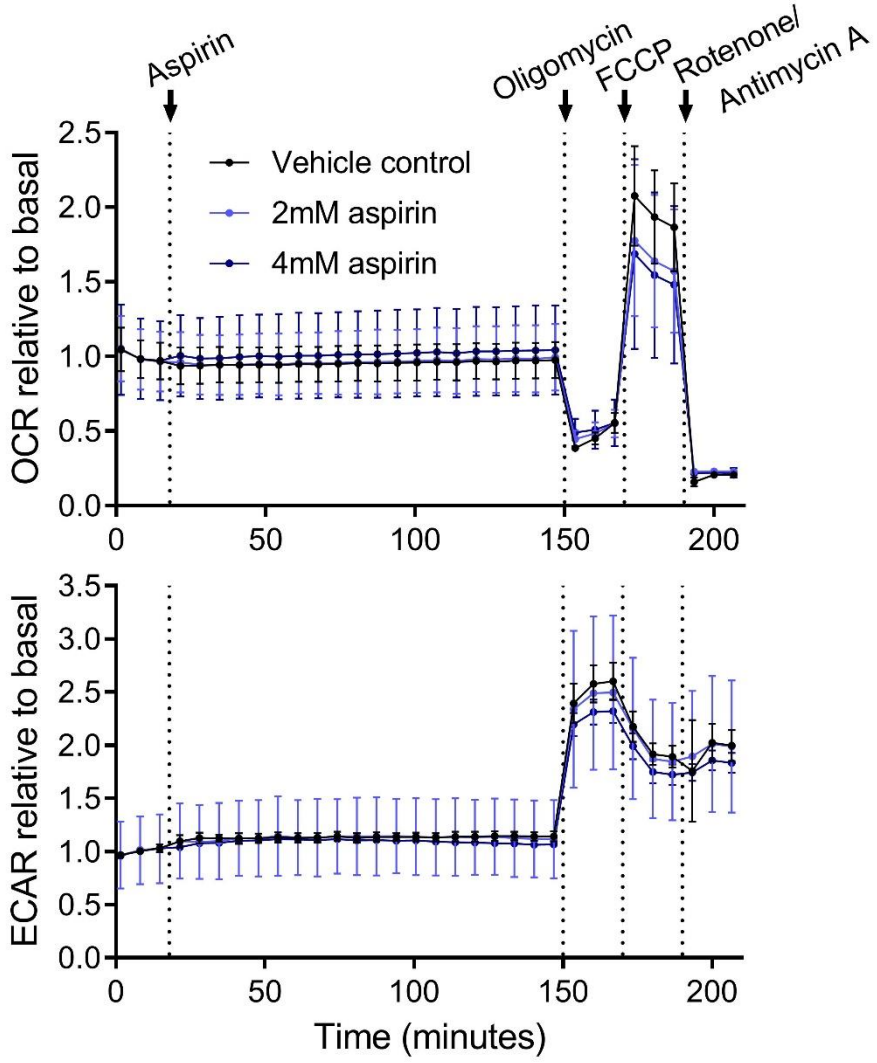

Figure 4.5 Extracellular flux analysis of SW620 cells with aspirin injection

OCR and ECAR at each time point were calculated relative to the average of all basal measurements in each aspirin condition. Data represent technical replicates from one experiment (n=3 for vehicle control, n=2 for 2mM and 4mM aspirin), error bars represent standard deviation.

4.3.2 **Long-term aspirin treatment alters utilisation of glucose and glutamine in SW620 cells**

The effect of long-term aspirin treatment on the metabolic fate of glucose and glutamine was investigated using SITA in SW620 cells. The design of this experiment is illustrated in Figure 4.6. Parallel sets of plates were seeded with control or long-term 4mM aspirin treated SW620s and were cultured for a total of 72 hours before extraction. At selected time points (1, 2, 4, 8, and 24 hours prior to extraction), the cells were treated with media supplemented with either glucose or glutamine with ^{13}C replacing the usual ^{12}C (U[^{13}C]-glucose/glutamine), maintaining aspirin treatment and consistent glucose/glutamine concentrations between all treatment conditions. Three replicate plates of cells were treated in each condition (control and 4mM aspirin) and at each time-point. Three parallel plates in each condition were also treated with unlabelled media and the number of cells was counted at the same time point as extraction, in order to normalise the metabolite levels to cell number. The abundance of metabolites and the incorporation of ^{13}C was quantified by gas-chromatography mass spectrometry (GC-MS).

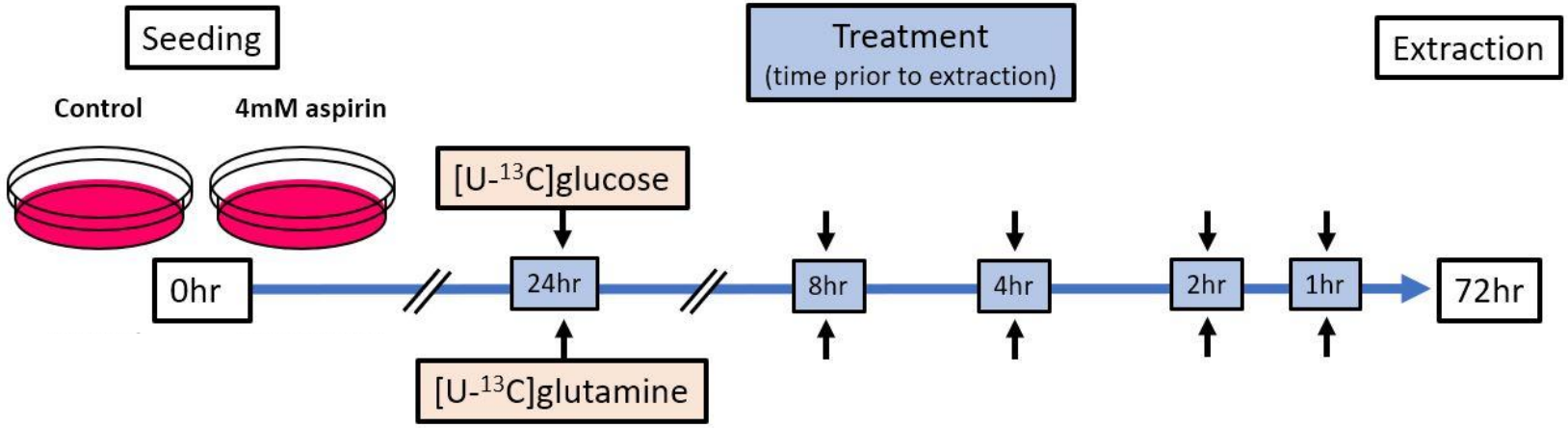

Figure 4.6 Experimental design for stable isotope tracer analysis time course

SW620 cells previously treated with aspirin for ~52 weeks were seeded in the relevant aspirin dose (either control or 4mM) and cultured for a total of 72 hours prior to extraction. As various time points before extraction (1, 2, 4, 8 and 24 hours), the cells were treated with media containing either [U-^{13}C]glucose or [U-^{13}C]glutamine.

The ^{13}C labelled nutrients become incorporated in downstream pathways and metabolites over time, as shown in Figure 4.7, which illustrates labelling patterns with either U[^{13}C]-glucose or U[^{13}C]-glutamine following incorporation into one turn of the TCA cycle. Ideally, SITA experiments should be performed at 'metabolic steady state', where metabolite abundances and metabolic fluxes in the cells remains stable over time (262). Experiments are often performed in standard cell culture conditions, where metabolites may accumulate or deplete over time, this is therefore known as 'pseudo metabolic steady state' (262). In metabolic steady state, the isotope labelling of downstream metabolites increases until it reaches a plateau, where the amount of ^{13}C labelling in each metabolite pool is stable over time, which is known as 'isotopic steady state' (262).

The time course in this experiment (Figure 4.6) provides the information required to determine at which time point isotopic steady state occurs. It is important that comparisons of nutrient contributions between conditions are made at isotopic steady state, as differences prior to this point can be affected not only by pathway activity, but also by metabolite pool size ('dynamic labelling') (262). Isotopic steady state may be reached at different time points for different pathways, e.g. steady state for glycolytic intermediates will be reached much more quickly than TCA cycle intermediates when labelling with U[^{13}C]-glucose (262).

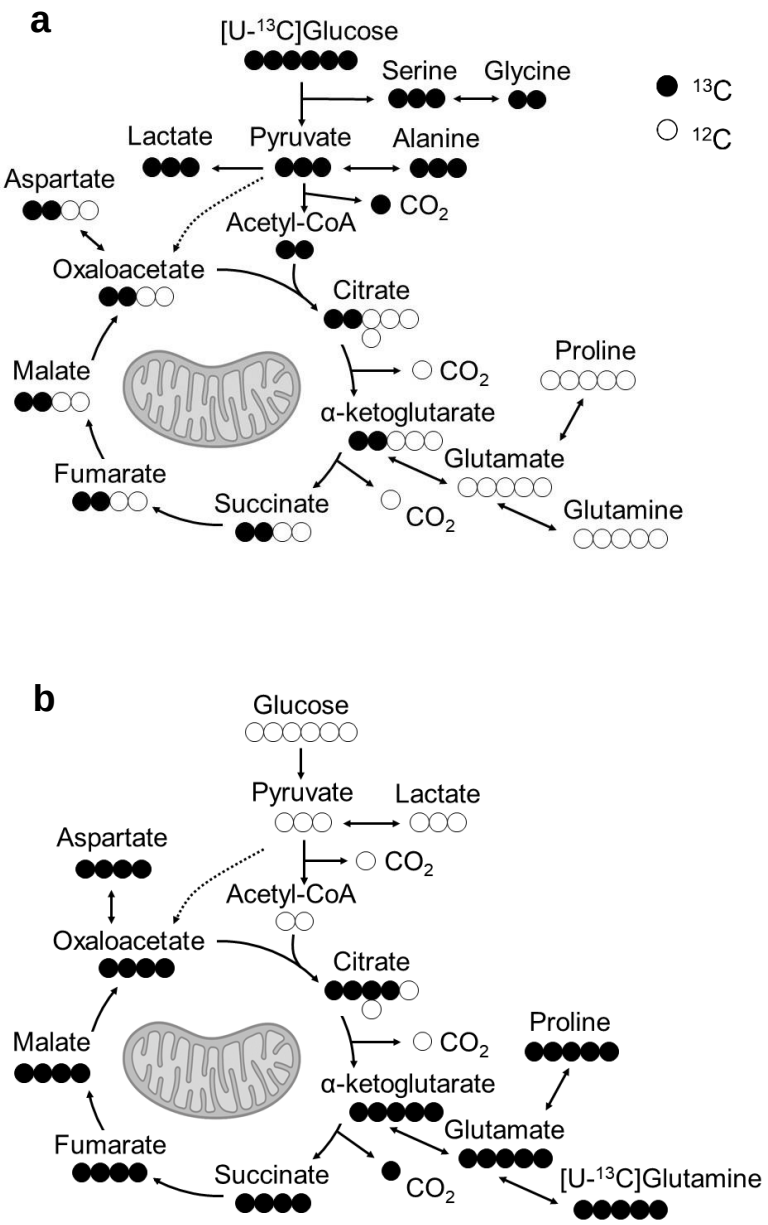

Figure 4.7 Labelling patterns in downstream metabolites when treating with [U-^{13}C]glucose (a) or [U-^{13}C]glutamine (b), after one turn of the TCA cycle

Figure 4.8 shows a time course of incorporation of ^{13}C from glucose and glutamine in three example metabolites to represent the TCA cycle and glutaminolysis (citrate, glutamate and malate), shown by the percentage of ^{13}C in the metabolite pools over time. Full metabolite data is provided in Appendix 7.5 . As expected, incorporation of ^{13}C increases over time, followed by a plateau as the cells reach isotopic steady state. In both the glucose and glutamine tracing results, isotopic steady state in TCA cycle metabolites appears to be reached by 8 hours, so this time point was used for further analysis and for subsequent experiments. Further enrichment of ^{13}C from glucose and a decrease in enrichment from glutamine occurs after the 8-hour isotopic steady state time point, possibly due to pseudo-metabolic steady state conditions.

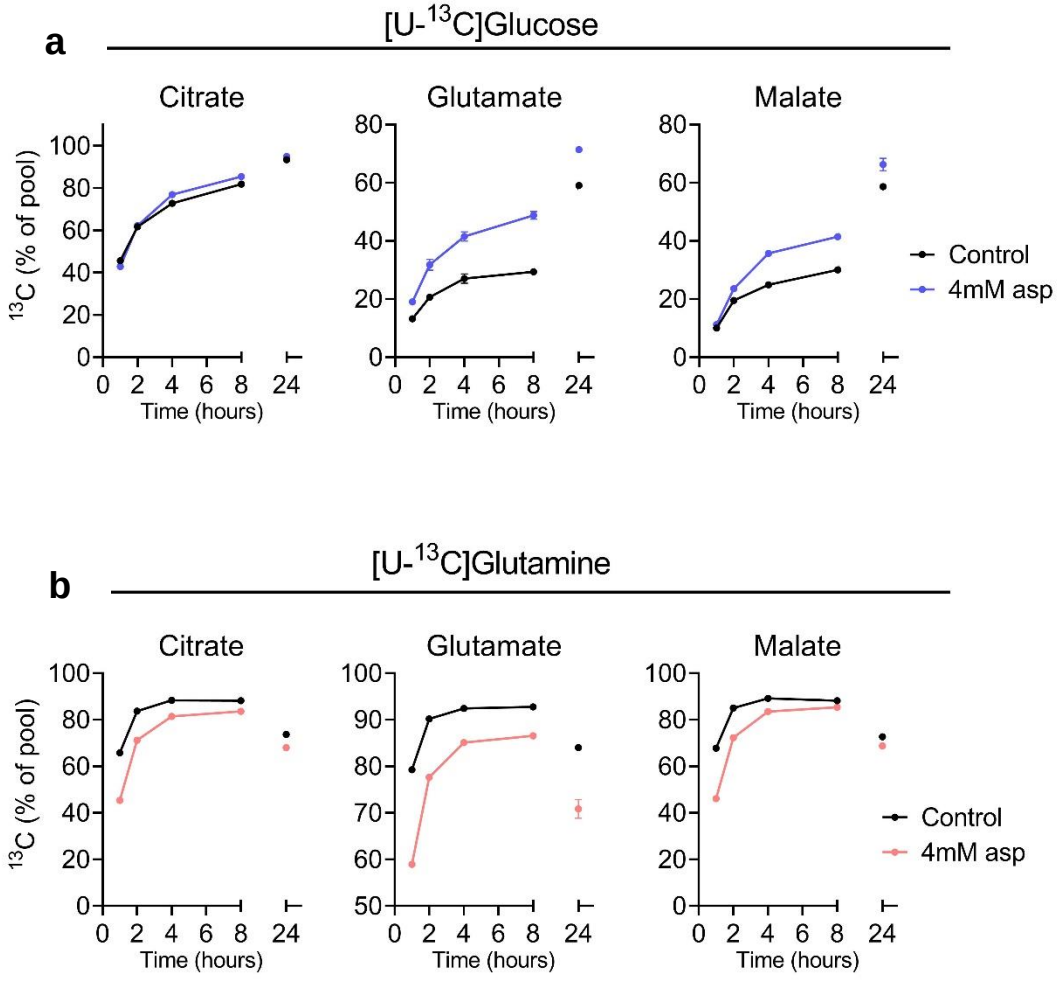

Figure 4.8 Time course of ^{13}C incorporation into citrate, glutamate and malate from [U-^{13}C]glucose (a) or [U-^{13}C]glucose (b) in long-term (52-week) aspirin treated SW620 cells

Long-term (LT) 4mM aspirin treatment compared to control. Error bars represent standard error (n=3).

Figure 4.9 and Figure 4.10 show the percentages of ^{13}C and ^{12}C in the metabolite pools at isotopic steady state (8 hours). At isotopic steady state, the proportion of a metabolite that is labelled with ^{13}C represents the contribution of the labelled nutrient (either glucose or glutamine) to the carbon pool of that particular metabolite (262). These data show that with aspirin treatment, the relative contribution of glucose to the metabolites shown is generally increased, and the relative contribution of glutamine is generally decreased. For example, at 8 hours, the proportion of ^{13}C labelling from glucose is increased with aspirin treatment particularly in TCA cycle metabolites including α-ketoglutarate, succinate, fumarate and malate. Although interestingly, it is slightly decreased in alanine. Conversely, the proportion of ^{13}C labelling from labelled glutamine decreases with aspirin treatment in several metabolites including proline, α-ketoglutarate, glutamate and succinate.

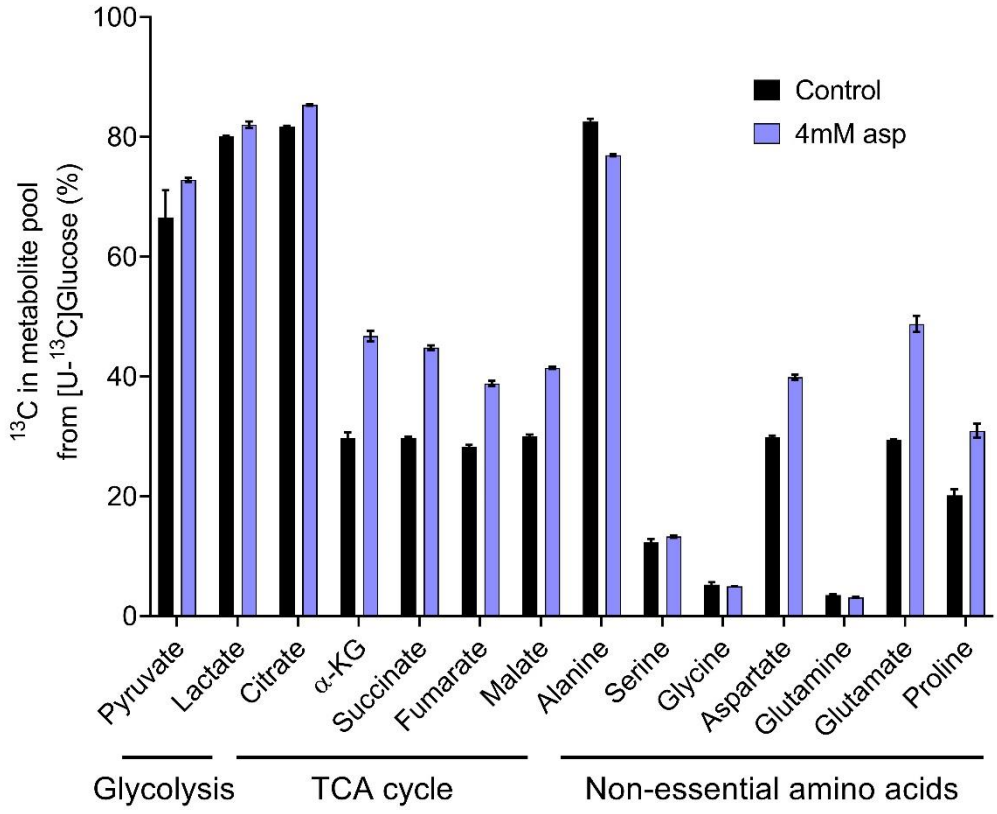

Figure 4.9 Contribution of ^{13}C relative to the total metabolite abundance after 8hrs incubation with [U-^{13}C]glucose in long-term (52-week) aspirin treated SW620 cells

Long-term 4mM aspirin treatment compared to control. Error bars represent standard error (n=3).

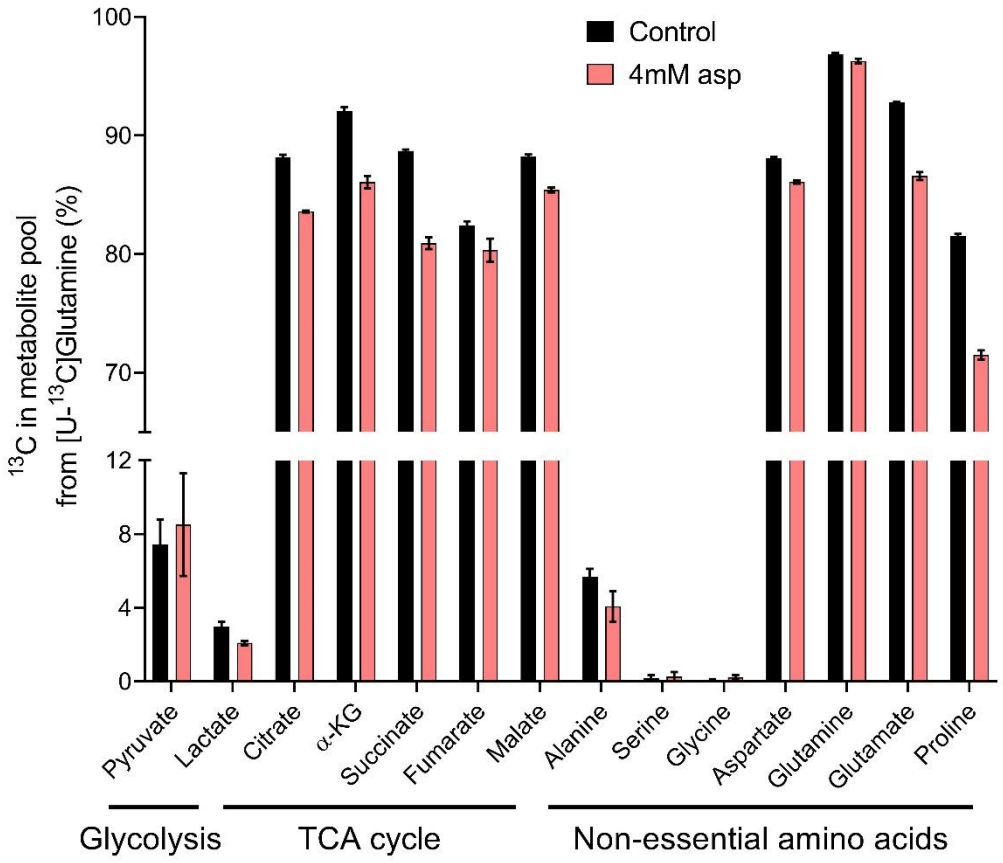

Figure 4.10 Contribution of ^{13}C relative to the total metabolite abundance after 8hrs incubation with [U-^{13}C]glutamine in long-term (52-week) aspirin treated SW620 cells

Long-term 4mM aspirin treatment compared to control. Error bars represent standard error (n=3).

Figure 4.11 shows the mass isotopomer distribution (MID) data for three example metabolites (citrate, glutamate and malate) with labelled glucose and glutamine. MID data for all metabolites are shown in Appendix 7.5. MID data show the proportion of each mass isotopomer contribution to the overall metabolite pool. Mass isotopomers (also known as isotopologues) are the possible forms of each metabolite depending on how many of the carbon atoms are labelled with ^{13}C. For example, a metabolite with no labelled carbons is m+0, with one labelled carbon is m+1, etc.

MID data show a decrease in the proportion of m+0 citrate, glutamate and malate, as well as m+2 citrate, and an increase in other labelled isotopologues with labelled glucose, indicating increased incorporation of glucose. With labelled glutamine, the m+0 portion of these metabolites is increased with aspirin treatment, and there is a decrease in the more highly labelled isotopologues, indicating decreased incorporation of glutamine.

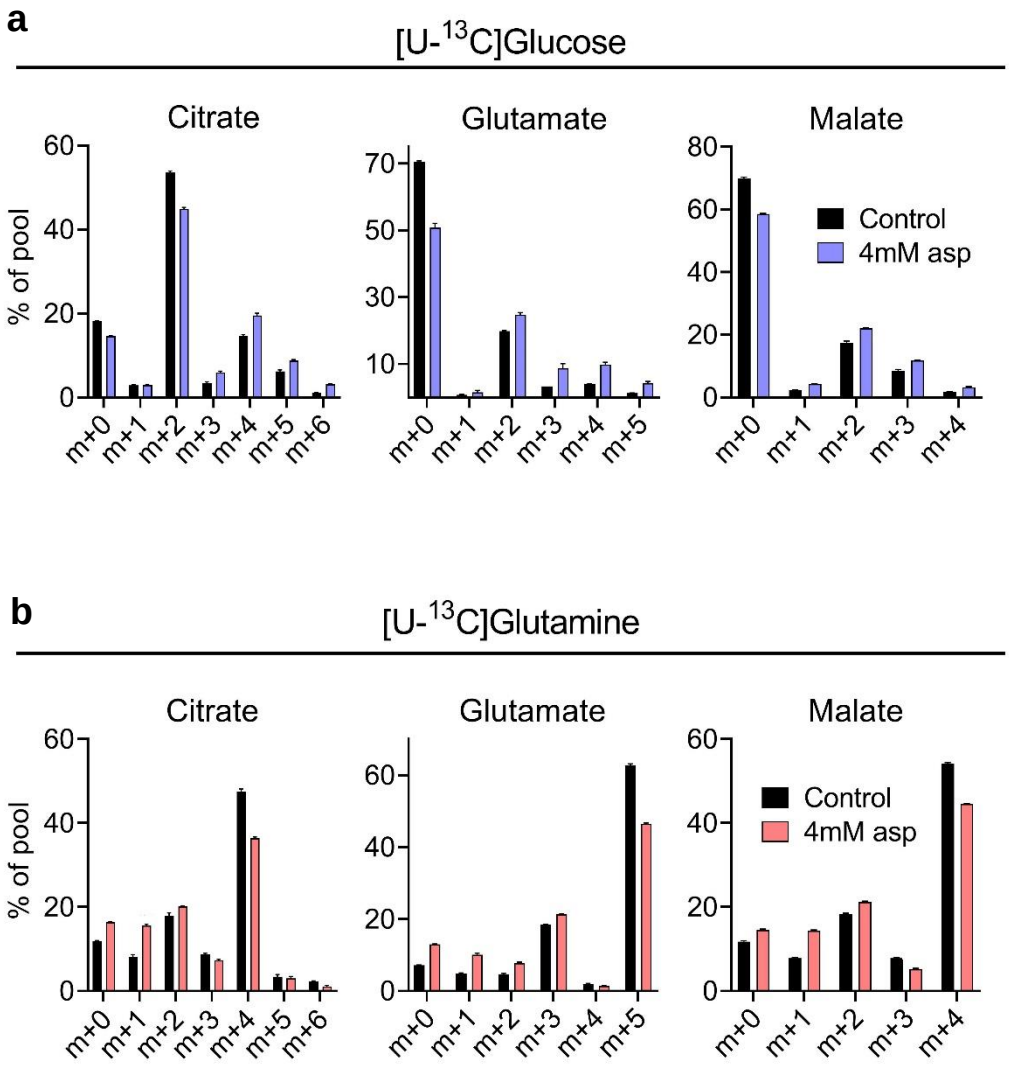

Figure 4.11 MID data for citrate, glutamate and malate from [U-^{13}C]glucose (a) or [U-^{13}C]glutamine (b) in long-term (52-week) aspirin treated SW620 cells

Long-term (LT) 4mM aspirin treatment compared to control. Error bars represent standard error (n=3).

As well as showing overall nutrient contributions to metabolites, MID data can give information on specific pathway activity based on the expected resulting labelling patterns. Due to the increase in PC expression with aspirin treatment, these data were used to determine whether there was an increase in the activity of this pathway, that converts pyruvate directly into oxaloacetate as an alternative entry point into the TCA cycle, known as pyruvate anaplerosis. One method of measuring activity of this pathway by SITA is to use a [3,4-^{13}C]glucose tracer, as this can only produce m+1 TCA cycle intermediates if it enters via PC, and does not produce any labelling via acetyl-coA (see Figure 4.12a).

When using [U-^{13}C]glucose, PC activity results in the production of m+3 oxaloacetate, whereas the usual entry of glucose into the TCA cycle via acetyl-coA produces m+2 oxaloacetate after one turn (see Figure 4.12b). Therefore, comparing the amount of m+3 intermediates that are present can also indicate whether there is a difference in PC activity. This assumption is complicated by the fact that m+3 intermediates can also be produced after labelled acetyl-coA has undergone multiple turns in the TCA cycle (see Figure 4.13). However, it has previously been shown that levels of m+3 malate from [U-^{13}C]glucose are a reliable indicator of PC activity, as they correlate with PC mRNA levels, and the levels of m+1 citrate produced from [3,4-^{13}C]glucose (264). Using this method, these data suggest that there may be an increase in PC activity with aspirin treatment, as the proportion of m+3 labelled malate is increased in the aspirin treated cells compared to controls at isotopic steady state (8 hours), as shown in Figure 4.11a.

Interestingly, when looking at the proportion of m+3 malate across the time course of the experiment, this shows that there is no difference in the aspirin treated cells at the early time points (1-2 hours), as shown in Figure 4.14. If there was a difference in PC activity with aspirin treatment, you might expect to see this difference at an early time point, as later time points allow for multiple TCA cycles to have occurred and therefore contribute to the m+3 malate pool. It is therefore unclear from these data whether PC activity is increased, or whether there is a general increase in glucose incorporation into the TCA cycle with aspirin treatment. Further experiments, using a [3,4-^{13}C]glucose tracer, are required to confirm this.

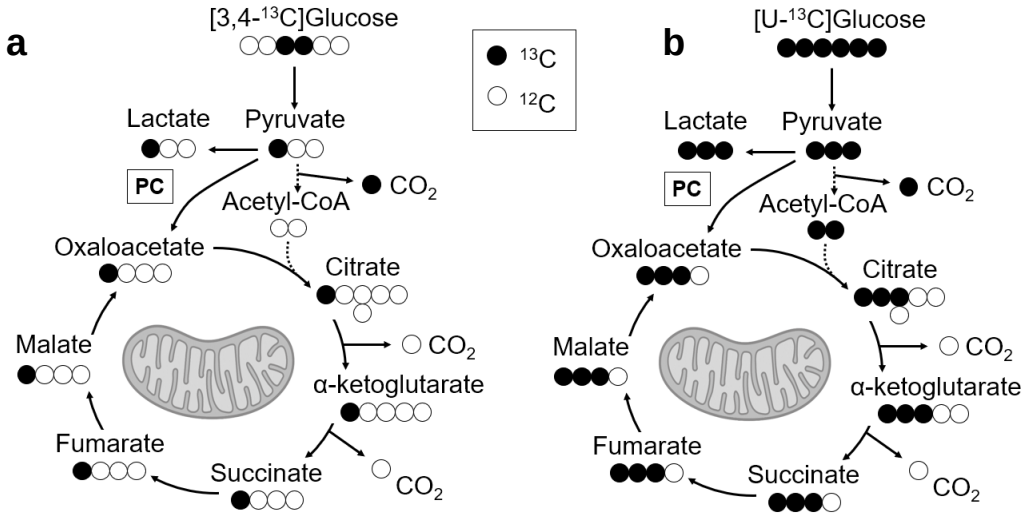

Figure 4.12 Labelling patterns produced by pyruvate carboxylase (PC) activity

a) [3,4-^{13}C]glucose is the gold-standard method to detect PC activity via SITA. This tracer can only produce labelled (m+1) TCA cycle intermediates when it enters via PC. When pyruvate enters via acetyl-coA, the labelled carbons are lost to CO_2. b) [U-^{13}C]glucose can also indicate PC activity, this tracer produces m+3 TCA cycle intermediates after one turn, whereas entry via acetyl-coA produces m+2.

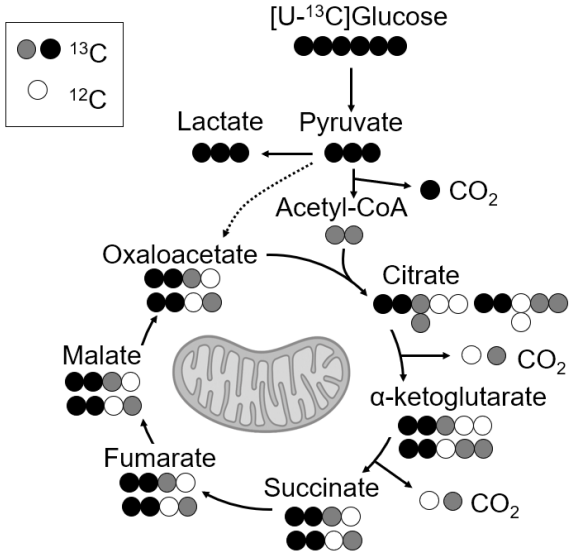

Figure 4.13 Labelling patterns produced from a second turn of the TCA cycle

When [U-^{13}C]glucose enters the TCA cycle via acetyl-coA, m+3 intermediates can be produced after two turns of the cycle. Black indicates labelled carbons originating from the first turn of the TCA cycle, and grey indicates labelled carbons originating from the second turn.

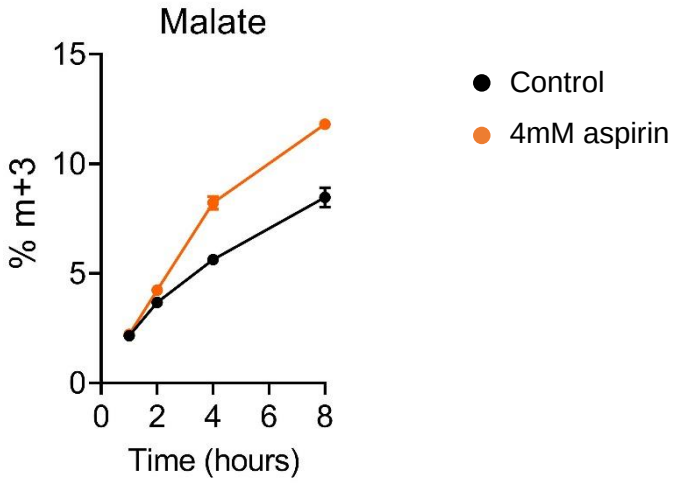

Figure 4.14 Proportion of m+3 malate over a time course of incubation with [U-^{13}C]glucose in long-term (52-week) aspirin treated SW620 cells

Error bars represent standard error (n=3).

This experiment also provides information on intracellular metabolite abundances. Metabolite abundances alone cannot be used to infer pathway activity, as it is impossible to determine whether an accumulation of a metabolite is due to its increased production or decreased consumption, and vice versa. However, interestingly in these results there is a consistent increase in abundance of aspartate and a decrease in abundance of alanine with 4mM aspirin treatment (Figure 4.15). This would be consistent with a decrease in activity of the glutaminolysis enzymes ASNS and GPT2 respectively, which were both found to be downregulated with aspirin treatment (see section 3.3), so could potentially indicate decreased activity of these enzymes, although further experiments would be required to confirm this. Full metabolite abundance data are shown in Appendix 7.5.

Overall, these data suggest that with long-term aspirin treatment, cells undergo a partial switch in their nutrient utilisation away from glutamine and towards glucose. There is an increase in glucose entry into the TCA cycle, including potentially via the anaplerotic pathway catalysed by PC. Opposingly, glutamine incorporation into glutamate and TCA cycle metabolites is reduced with aspirin treatment.

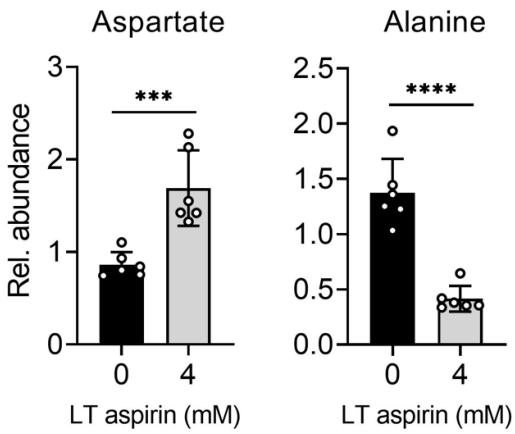

Figure 4.15 Intracellular abundance (relative to cell number) of aspartate and alanine in long-term (52-week) aspirin treated SW620 cells from SITA experiments

Error bars represent standard error, ***=p<0.001, ****=p<0.0001.

4.3.3 Long-term aspirin treatment alters utilisation of glucose and glutamine in further CRC cell lines LS174T and HCA7

SITA data in SW620 cells show a clear effect of long-term aspirin treatment on utilisation of glucose and glutamine. Results in section 3.3.7 show that aspirin treatment also regulates metabolic proteins in the CRC cell lines LS174T and HCA7. It was therefore investigated whether aspirin has the same effect on nutrient utilisation in these cell lines. The experiments were performed using the same experimental design as shown in Figure 4.6, however using only the 8-hour time point of incubation with U[^{13}C]-glucose/glutamine, as this was found to be sufficient for isotopic steady state in TCA cycle metabolites.

Figure 4.16 and Figure 4.17 show the relative contributions of ^{13}C to the metabolite pools from [U^{13}C]-glucose and [U^{13}C]-glutamine respectively in LS174T cells. In line with the results seen in SW620, long-term aspirin treated cells have an increase in incorporation of glucose into several metabolites (α-KG, fumarate, malate, aspartate, proline), and a decrease in incorporation of glutamine into citrate, α-KG, fumarate, malate, alanine, aspartate, glutamate and proline. This suggests an inhibition of glutamine metabolism with aspirin, from the first step of

glutaminolysis (due to decreased incorporation of glutamine into glutamate), and an increase in entry of glucose into the TCA cycle. Interestingly, these data show a decrease in incorporation of glucose into serine and glycine with long-term aspirin treatment in LS174T cells, suggesting impairment of the serine biosynthesis pathway. This effect was not seen in SW620 cells. MID and relative abundance data for LS174T cells are shown in Appendix 7.5.

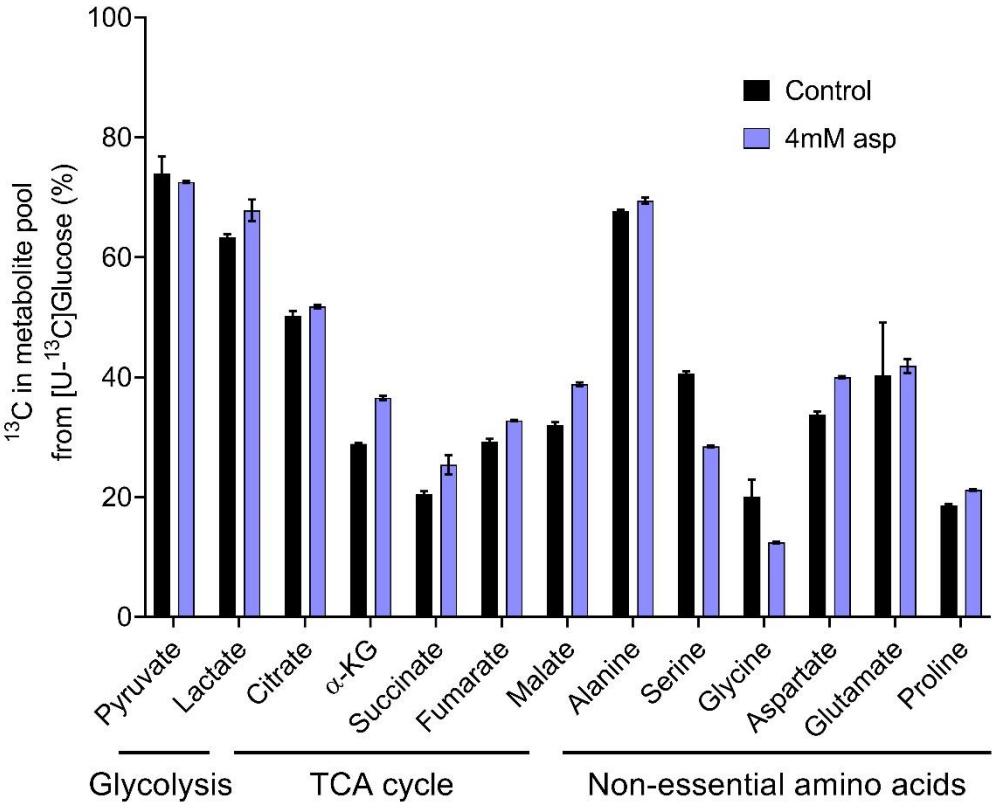

Figure 4.16 Contribution of ^{13}C relative to the total metabolite abundance after 8hrs incubation with [U-^{13}C]glucose in long-term (52-week) aspirin treated LS174T cells

Long-term 4mM aspirin treatment compared to control. Error bars represent standard error (n=3). *=p<0.05, **=p<0.01, ***=p<0.001.

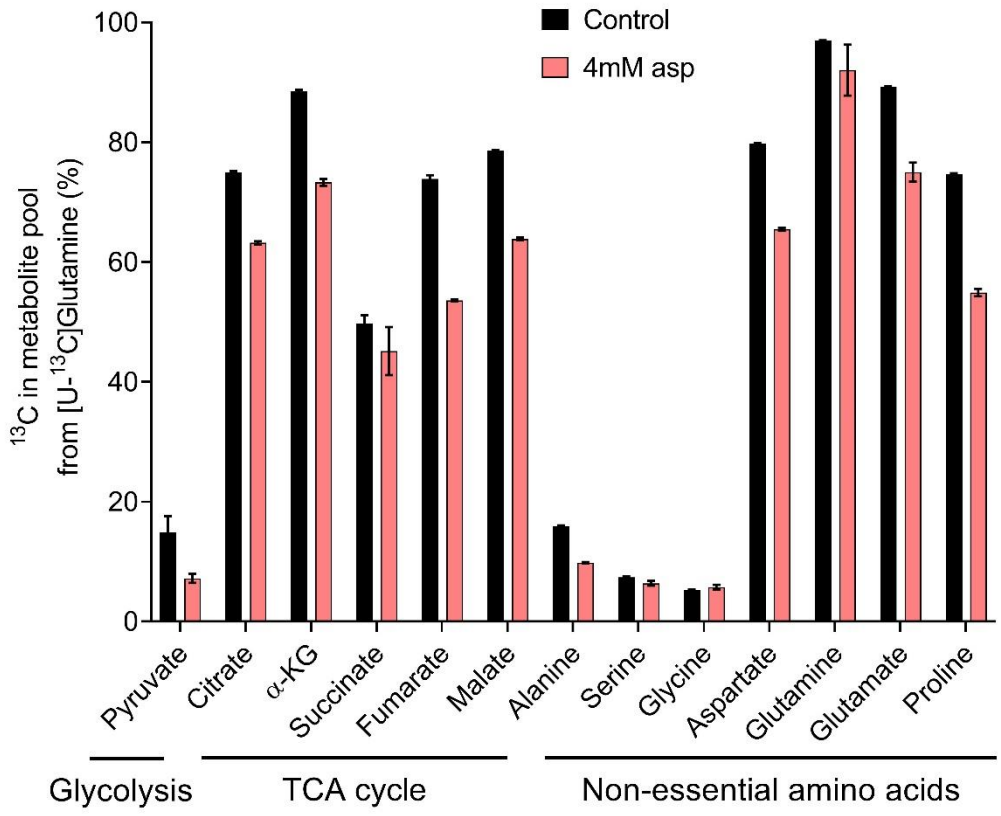

Figure 4.17 Contribution of ^{13}C relative to the total metabolite abundance after 8hrs incubation with [U-^{13}C]glutamine in long-term (52-week) aspirin treated LS174T cells

Long-term 4mM aspirin treatment compared to control. Error bars represent standard error (n=3).

Similar results were also seen in HCA7 cells, with an increase in incorporation of glucose into several metabolites (citrate, α-KG, malate, glutamate, aspartate, Figure 4.18), and a decrease in incorporation of glutamine into several metabolites (citrate, α-KG, fumarate, malate, alanine, glutamate, aspartate, Figure 4.19). Interestingly, there is also a decrease in incorporation of glucose into serine in HCA7, similar to results seen in LS174T, as well as decrease incorporation of glucose into glycine. Again, this suggests a potential impairment of serine biosynthesis from glucose with long-term aspirin treatment in these cell lines. MID and relative abundance data for HCA7 cells are shown in Appendix 7.5.

Overall, these results show that long-term aspirin treatment has a similar effect on nutrient utilisation in three distinct CRC cell lines, causing a reduction in glutaminolysis and an increase in glucose utilisation.

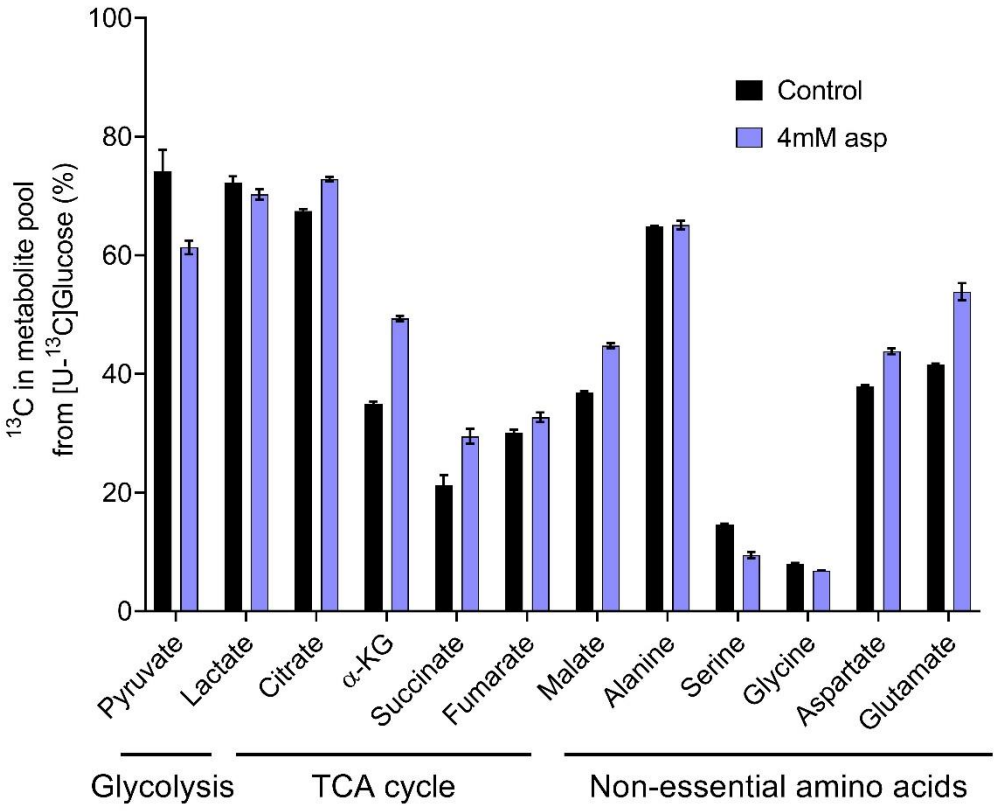

Figure 4.18 Contribution of ^{13}C relative to the total metabolite abundance after 8hrs incubation with [U-^{13}C]glucose in long-term (52-week) aspirin treated HCA7 cells

Long-term 4mM aspirin treatment compared to control. Error bars represent standard error (n=3). **=p<0.01, ***=p<0.001.

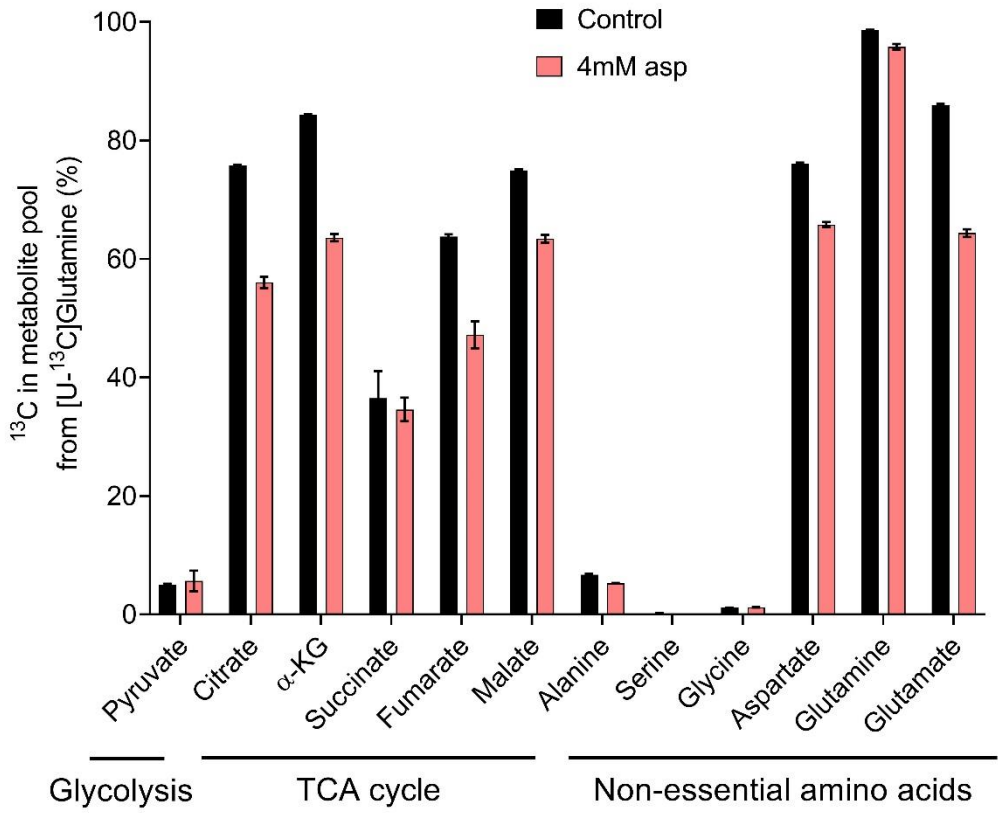

Figure 4.19 Contribution of ^{13}C relative to the total metabolite abundance after 8hrs incubation with [U-^{13}C]glutamine in long-term (52-week) aspirin treated HCA7 cells

Long-term 4mM aspirin treatment compared to control. Error bars represent standard error (n=3). *=p<0.05, **=p<0.01, ***=p<0.001, ****=p<0.0001.

4.4 Discussion

This is the first time to our knowledge that extracellular flux analysis and SITA have been used to investigate the metabolic effect of aspirin on cancer cells. A few previous studies have implied that metabolic pathways in cancer cells are altered by aspirin due to changes seen in metabolic enzyme expression (discussed in section 1.4), but this is not always a reliable indicator of pathway activity. Previous studies have therefore not been able to establish with certainty that aspirin leads to metabolic reprogramming. Results presented in this chapter demonstrate for the first time a clear metabolic reprogramming effect of aspirin in CRC cell lines.

SITA results presented here show that in three CRC cell lines, aspirin causes a shift in nutrient utilisation, consisting of a general reduction in the contribution of glutamine to TCA cycle metabolites and amino acids, and a concomitant increase in utilisation of glucose. Interestingly, extracellular flux analysis shows no effect of aspirin on production of ATP by glycolysis or oxphos. This suggests that the original hypothesis in section 3.1, that aspirin may increase carbon entry into the TCA cycle and increase reliance on oxphos, is not correct, and that aspirin does not lead to a reversal of the Warburg effect in these cells. However, these results do support the hypothesis that aspirin significantly reprograms cellular metabolism.

SITA data suggest that aspirin has an inhibitory effect on glutaminolysis and this leads to a compensatory upregulation of glucose utilisation. Glucose and glutamine are known to cooperate in fuelling the TCA cycle; decrease in entry of one nutrient can lead to a compensatory increase in the other (254, 265). This suggests that increasing entry of glucose carbon may be a compensation mechanism for the reduction of glutamine anaplerosis with aspirin to maintain carbon entry into the TCA cycle. As there was no overall effect on oxphos (as measured by OCR), this suggests the cells are able to maintain TCA cycle function in the presence of aspirin through a switch in their carbon source, favouring glucose over glutamine. This highlights the metabolic plasticity of the cells, allowing them to minimise the impact on ATP production and proliferation in the presence of aspirin. Furthermore, this suggests that impairment of ATP production is not a mechanism by which long-term aspirin reduces cell proliferation and induces apoptosis (as shown by Dr Eleanor Mortensson, unpublished).

Inhibition of the glutaminolysis pathway with aspirin also supports the hypothesis that GLS1 upregulation shown in Chapter 3 is not a direct effect of aspirin

treatment, but a compensatory response perhaps to increase rates of glutaminolysis as it is being impaired due to the effect of aspirin on other enzymes. This also highlights the importance of directly measuring metabolic pathways, as enzyme expression does not reflect overall pathway activity in this context.

It is important that this effect on nutrient utilisation with aspirin treatment shown in the SITA data was replicated consistently in three CRC cell lines (SW620, LS174T, HCA7), with different mutational statuses (see section 2.1.1). This suggests that this mechanism of aspirin is more likely to be broadly applicable to CRC cells, and therefore to a wide range of CRC patients. It is particularly important that both *KRAS* mutant (SW620, LS174T) and *KRAS* wild-type (HCA7) cells, and *PIK3CA* wild-type (SW620 and HCA7) and *PIK3CA* mutant cells (LS174T) are represented, as *KRAS* and *PIK3CA* mutations have been previously shown to impact reliance on glutamine metabolism in CRC cells (32, 41). Further work to determine whether this effect is specific to certain contexts will be important to inform patient stratification of aspirin use for CRC treatment and prevention. This is important when considering the significant risk and side effects associated with aspirin use (266).

Some other interesting observations were made from the SITA data, alongside the overall switch from glutamine to glucose utilisation. For example, despite most metabolites showing increased incorporation of glucose, alanine showed decreased contribution from glucose with aspirin treatment in SW620 cells. It has been recently shown that knockout of GPT2 leads to a decrease in glucose incorporation into alanine in K562 cells (267) (GPT2 catalyses the conversion of pyruvate and glutamate to alanine and α-KG). As aspirin treatment leads to downregulation of GPT2 (as shown in Chapter 3), this could be an explanation for this result. This effect on glucose incorporation into alanine was not seen in the other two cell lines (LS174T and HCA7), however, GPT2 expression with aspirin treatment was not investigated in these cells. It is therefore possible that aspirin does not regulate GPT2 expression in other cell lines and there is therefore no effect on alanine synthesis.

Furthermore, it was observed in LS174T and HCA7 cells (but not SW620), that aspirin treatment reduced the incorporation of glucose carbon into serine and glycine. This suggests that aspirin may impair the serine biosynthesis pathway which produces serine and glycine from the glycolytic intermediate 3-phosphoglycerate (see Figure 1.5). Interestingly, PSAT1, a key component of this

pathway, showed downregulation with aspirin treatment in SW620 cells in the proteomic data (shown in Figure 3.5). While this did not appear to affect serine biosynthesis in SW620 cells, this enzyme may also be downregulated with aspirin in LS174T and HCA7 cells leading to reduced serine biosynthesis. Further investigation into whether impaired serine biosynthesis may be a key anti-tumorigenic effect of aspirin in LS174T and HCA7 cells would be of particular interest. For example, it would be interesting to determine whether supplementation with cell-permeable serine could rescue the effect of aspirin treatment on proliferation of these cells.

As previously discussed, data in this chapter show that with aspirin treatment cells maintain ATP production. Therefore, reduced ATP production is not the reason for the growth inhibitory effect of aspirin. The cells undergo reprogramming of nutrient utilisation, which suggests the cells may have sufficient metabolic plasticity to maintain ATP production despite the metabolic effects of aspirin, such as the inhibition of glutaminolysis. It is not clear from these results whether the metabolic reprogramming observed is a causative factor of the reduced cell proliferation with aspirin. However, it does suggest that aspirin may force the cells to adapt their metabolism and therefore be under increased metabolic pressure and decreased metabolic flexibility. This may make the cells vulnerable to further metabolic perturbations, as their ability to adapt further may be limited. Aspirin treated cells may therefore be more sensitive to inhibition of particular compensatory pathways.

It has been repeatedly found in the literature that cancer cells are very metabolically flexible and this provides a survival advantage when the cells are exposed to metabolically stressful conditions in the tumour microenvironment. Examples of these conditions include nutrient deprivation, hypoxia, and the diverse metabolic conditions encountered during metastasis in the bloodstream and at secondary sites (38). This ability allows cancer cells to adapt to single therapeutic agents that target cellular metabolism (38). Therefore, combining complementary metabolic therapies has been found to be a successful approach in targeting cancer metabolism as this reduces the ability of the cells to adapt and continue to proliferate. Several studies have also shown success when combining metabolic interventions with conventional chemotherapies (268-270) as well as immunotherapies (271). There is also increasing interest in the impact of diet on tumour metabolism and how this may interact with and complement metabolic therapies (272). This suggests that exploiting the metabolic effect of aspirin to

increase the efficacy of other cancer therapies, particularly inhibitors of metabolic pathways, could be a potential approach to enhance the clinical benefits of aspirin. This possibility will be explored in the next chapter.

A limitation of the work in this chapter is that investigations are performed in conditions that are not entirely representative of cancer cells *in situ*. Cellular metabolism is particularly responsive to environmental conditions. The high nutrient and oxygen levels in standard cell culture do not always represent the tumour microenvironment, which is often hypoxic and low in many key nutrients such as glucose and glutamine. While *in vitro* cell culture is an invaluable model system, it is not certain that the same results will be produced in more physiological systems. While the metabolic reprogramming effect of aspirin is evident from the data in this chapter, further work is required to establish whether this effect is physiologically relevant. This will also be further explored in the next chapter.

Overall, the findings in this chapter show that aspirin reprograms cellular metabolism, particularly by causing cells to adapt their utilisation of glucose and glutamine. This suggests that aspirin treated cells may be less metabolically flexible, exposing potential metabolic vulnerabilities. This will be investigated in the next chapter.

Chapter 5 Results 3

Investigating the effects of combining aspirin with metabolic inhibitors

5.1 Introduction

Results in Chapter 3 and Chapter 4 show that aspirin treatment has a significant metabolic effect on CRC cells, including regulation of metabolic enzymes and reprogramming of nutrient utilisation pathways. It is not clear from these data whether metabolic reprogramming is important for the anti-cancer effects of aspirin, or whether these changes are a causative factor of impaired cell proliferation or tumorigenesis with aspirin. Nonetheless, these effects may be relevant in optimising therapeutic use of aspirin. Uncovering novel strategies to target cellular metabolism for cancer therapy is an active area of research, with varying degrees of success. A common theme in the literature is that due to the metabolic flexibility of cancer cells, they are often able to adapt and to continue to proliferate unimpeded when treated with single metabolic agents. As such, using combinations of complementary therapies is often much more effective. It was therefore hypothesised that the observed metabolic effects of aspirin could render the cells more reliant on specific metabolic pathways, making them vulnerable to treatment with further metabolic therapies and therefore aspirin could be utilised to enhance the effectiveness of existing metabolic cancer drugs. This will be investigated in this chapter.

Some of the previous work in the field of targeting cancer metabolism is discussed in this section, including progress in strategies targeting different aspects of cellular metabolism, and where combination therapies have proved successful. This section will also discuss the difficulties of studying metabolic cancer therapies experimentally.

5.1.1 Targeting glucose metabolism in cancer

Despite the well-established dependence of cancer cells on glycolysis (the Warburg effect), new cancer therapies exploiting this fact have had limited impact. This is because of the excessive toxicity of drugs that inhibit glycolysis due to a lack of specificity, as many proliferative and highly energy consuming tissues within the body rely heavily on glycolysis (273). Examples of glycolysis targeting drugs that have been investigated in clinical trials include the HK inhibitor 2-deoxyglucose (2-DG) (274) and PDK1 inhibitor dichloroacetate (DCA) (275), though DCA has shown limited efficacy on CRC cell lines in vitro (276). There are also many cellular mechanisms for adapting to inhibition of glucose metabolism. For example, in the absence of glucose, cancer cells utilise the gluconeogenic enzyme

phosphoenolpyruvate carboxykinase (PEPCK/PCK2) to fuel biosynthetic pathways using glutamine-derived carbon (251). It has also been shown that cancer cells can increase reliance on oxphos for ATP production, largely fuelled by glutamine and glutamate, in response to inhibition of glycolysis (277).

However, there are examples where inhibition of glycolysis and/or glucose metabolism have been successful when combined with other therapies. For example, suppression of PKM2 has recently been found to increase the efficacy of 5-flurouracil (5-FU) in CRC cells, a common chemotherapy drug for treating CRC (270). As described in section 1.2.5.3, PKM2 is often upregulated in cancer and slows the rate of pyruvate production, leading to increased reliance on glycolysis over oxphos. This study showed that suppression of PKM2 reduced levels of ATP, increasing accumulation of 5-FU in the cells (270). PKM2 suppression has also been found to synergise with oxaliplatin, another common chemotherapy drug for CRC, in CRC cell lines (268). Multiple studies have also found that suppression of reliance on glycolysis via inhibition of HIF-1α increases efficacy of irradiation, and decreases CRC cell radioresistance as well as their resistance to oxidative stress (278, 279).

5.1.2 **Targeting glutamine metabolism in cancer**

Due to the clear importance of glutaminolysis in cancer (discussed in section 1.2.8), targeting this process is a promising approach for therapies, with more positive outcomes than targeting glycolysis. Several classes of compound that affect glutamine metabolism have been studied including glutamine mimetics, glutamine transporter inhibitors and GLUD inhibitors. Some have shown promise in preclinical models, however they are often limited by toxicity (103). Early attempts at inhibiting glutamine metabolism for cancer therapy used 6-Diazo-5-oxo-L-norleucine (DON), a glutamine antagonist that inhibits glutamine utilising reactions. This proved to be too toxic to be used clinically, but more recently a pro-drug has been developed (JHU083) which gets activated in the tumour microenvironment and has shown efficacy in mouse models (280).

Glutaminase inhibitors have been of particular interest and have showed some promise. BPTES (bis-2-(5-phenylacetamido-1,3,4-thiadiazol-2-yl)ethyl sulfide) is an allosteric glutaminase inhibitor that has shown efficacy in mouse models of hepatocellular carcinoma (144). Another allosteric glutaminase inhibitor that has been studied is compound-968, however, more recently a more potent GLS1 selective and stable inhibitor has been developed known as CB-839, which has

shown preclinical effects on triple-negative breast cancer (281) and acute myeloid leukaemia (AML) (282). It has moved into phase I clinical trials (103) including for patients with advanced CRC (283).

Though showing initial promise, the success of CB-839 has been varied between different models and tumour types. One reason for its limited efficacy in certain conditions is again due the metabolic flexibility of the cells and their ability to adapt to inhibition of GLS1. For example, some cancer cells can depend on GLS2 instead of GLS1 (284), which is not sensitive to CB-839 (103). Upregulation of GPT2 via activating transcription factor 4 (ATF4) has also been shown to compensate for inhibition of GLS1 (258). Furthermore, just as glutamine metabolism compensates for a reduction in glucose availability, glucose can also support inhibition of glutaminolysis. It has been shown that pyruvate carboxylase (PC) activity which provides an alternative entry point for glucose into the TCA cycle (see Figure 1.6), supports glutamine independence and adaptation to GLS1 inhibition (265). Asparagine synthetase (ASNS), which can synthesise glutamate independently of GLS1, has been found to be upregulated in response to GLS1 inhibition in HeLa cells (258). A study using pancreatic cancer models thoroughly investigated cellular responses to inhibition of GLS1 using proteomics and metabolomics and highlighted a wide range of compensatory mechanisms (285).

There is a large body of work investigating the efficacy of combining GLS1 inhibition with complementary therapies (286). One particularly comprehensive study published recently investigating combination therapies found that inhibition of GLS2, amidotransferases, or glycolysis enzyme HK2 synergises with inhibition of GLS1 (287). Inhibition of GLS1 has also been found to have synergistic effects with inhibition of mTOR signalling in triple-negative breast cancer cells (288) and glioblastoma cells (289). GLS1 inhibition has been found to activate autophagy in CRC cells and inhibition of autophagy, as well as asparagine depletion, had synergistic effects with GLS1 inhibition (290). More recently, GLS1 inhibition has been shown to induce autophagy by activation of ATF4 and inhibition of mTOR in CRC cells; prevention of this response by inhibition of ATF4 signalling was found to be synergistic with GLS1 inhibition (291). In liver cancer cells, the combination of CB-839 and an inhibitor of glutamine transporter ASCT2 has been found to be effective (292). In breast cancer cells, CB-839 has been shown to synergise with inhibition of fatty acid oxidation (293). GLS inhibition has also been shown to increase the efficacy of chemotherapy drugs in ovarian cancer cells (131) and CRC cells (269).

5.1.3 **Studying metabolic cancer therapies**

Determining efficacy of metabolic cancer therapies experimentally can be challenging due to the distinct metabolic phenotypes of cells in different models. As previously discussed, cancer cells are metabolically flexible and reprogram their metabolism in response to the environment. Metabolic phenotype and therefore response to metabolic therapies, is highly dependent on the environmental conditions. It is particularly recognised that metabolic phenotypes of cells vary greatly between cell culture and *in vivo* conditions, which is largely down to the metabolite composition of traditional cell culture medium. Cell culture medium contains supraphysiological concentrations of many nutrients including glucose and glutamine and lacks many micronutrients found *in vivo.* This is because culture medium was originally designed to maximise the growth of cells *in vitro*, not necessarily to reflect physiological conditions (294). This leads to distinct metabolic phenotypes and potentially conflicting results when investigating the effectiveness of metabolic inhibitors *in vitro* and *in vivo*.

Inhibitors that target glutamine metabolism are particularly affected by this problem. Cell culture media are thought to increase the reliability of the cells on glutamine metabolism due to the high concentrations of glutamine and cysteine (120). This can lead to drugs such as CB-839 showing efficacy *in vitro* but being less effective *in vivo*.

Recently, efforts have been made by multiple research groups to address this issue. Consequently, two novel cell culture media have been developed to more closely replicate the metabolite composition of human plasma; Plasmax (295) and human plasma-like medium (HPLM) (119). Both of these studies compare the metabolic phenotypes of cells in these media compared to traditional media and find significant metabolic reprogramming of the cells, including dramatic changes in the utilisation of nutrients. For example, supraphysiological levels of pyruvate in DMEM-F12 medium leads to stabilisation of HIF-1α and a pseudohypoxic response, which does not occur with Plasmax (295). The lack of certain metabolites in traditional media also has significant effects; uric acid, which is present in human plasma at much higher concentrations that those found in RPMI, was found to significantly inhibit pyrimidine synthesis and increase sensitivity of the cells to 5-FU when they were cultured in the physiologic levels of uric acid in HPLM (119). It is thought that the metabolic phenotypes of the cells in Plasmax or HPLM will be more representative of cells *in vivo* and therefore results gained from

in vitro studies using these media will be more likely to be replicated in mouse models and patient studies.

Further study has shown that nutrient availability for cancer cells in the tumour interstitial fluid can differ still from the plasma and can even vary between tumour sites and tissue of origin (296). Therefore, further work will be required to replicate physiological conditions for the particular cells or tumour type of interest for *in vitro* study. Furthermore, lifestyle and dietary factors can significantly affect the metabolite composition of the human plasma and tumour interstitial fluid (296). Metabolic disorders such as type 2 diabetes, which is linked to an increased risk of several cancer types, leads to changes in the metabolite composition of the plasma and this can occur many years before diagnosis of the disease (297). This further complicates the challenge of replicating physiological metabolic phenotypes *in vitro*, as well as uncovering potential links between metabolic phenotypes of patients and their risk of developing cancer.

However, the knowledge that diet can impact plasma metabolite levels allows for the potential of combining dietary interventions with metabolic cancer therapies in order to improve their efficacy, and there is a lot of ongoing work in this area. For example, dietary restriction of serine and glycine has been found to synergise with therapies that target serine/glycine biosynthesis (272, 287). Restriction of dietary methionine has also been showed to affect plasma metabolites and interact with responses to chemo- and radiotherapy (298).

Targeting cancer metabolism and studying metabolic therapies *in vitro* is a rapidly advancing area of research. Some of the principles discussed here will be used in this chapter to investigate the potential translational implications of the metabolic effects of aspirin and whether aspirin may enhance the efficacy of existing metabolic therapies.

5.2 Aims

The aim of this chapter is to investigate whether aspirin treatment renders CRC cells vulnerable to further metabolic perturbation. Results so far suggest that cells undergo metabolic reprograming upon aspirin treatment, which suggests they may be less able to further adapt their metabolism to support proliferation in the presence of additional metabolic stress. Specific aims of this chapter are:

i. To investigate the sensitivity of aspirin treated cells to metabolic inhibitors

ii. To investigate the mechanisms by which aspirin may increase sensitivity to metabolic inhibitors

iii. To investigate the effect of nutrient depletion on aspirin treated cells

5.3 Results

5.3.1 Aspirin enhances the efficacy of MPC inhibitor UK-5099

As SITA data in Chapter 4 suggest that aspirin treatment increases glucose entry into the TCA cycle, possibly to compensate for reduced glutamine entry, it was hypothesised that aspirin treated cells may be more sensitive to inhibition of this pathway. Mitochondrial pyruvate carrier (MPC) is required for transporting pyruvate produced from glycolysis into the mitochondria so it can enter the TCA cycle. An inhibitor of MPC known as UK-5099 has been developed (299) and has been shown to reduce oxphos and increase glycolysis in cancer cells (300). It was hypothesised that aspirin treated cells may be more sensitive to UK-5099 treatment as they may be more reliant on entry of glucose into the TCA cycle.

This hypothesis was tested by performing proliferation experiments in the long-term (~52-week) aspirin treated cell lines: SW620, LS174T and HCA7. 20,000 cells were seeded in all conditions, except 4mM aspirin treated HCA7 cells, of which 40,000 cells were treated due to significantly reduced growth. Cells were treated with a range of concentrations of UK-5099 in comparison to a DMSO control for 72 hours before measuring cell number by crystal violet staining. In each aspirin dose, the growth of the cells in each UK-5099 dose was calculated relative to the DMSO control.

Results for SW620 cells (Figure 5.1) show that UK-5099 alone (up to 80µM) had no effect on cell number. However, doses between 20-80µM significantly reduced cell number compared to controls in the 4mM aspirin treated cells and 80µM significantly reduced cell number compared to control in 2mM aspirin treated cells. This suggests that long-term aspirin treatment does sensitise the cells to UK-5099.

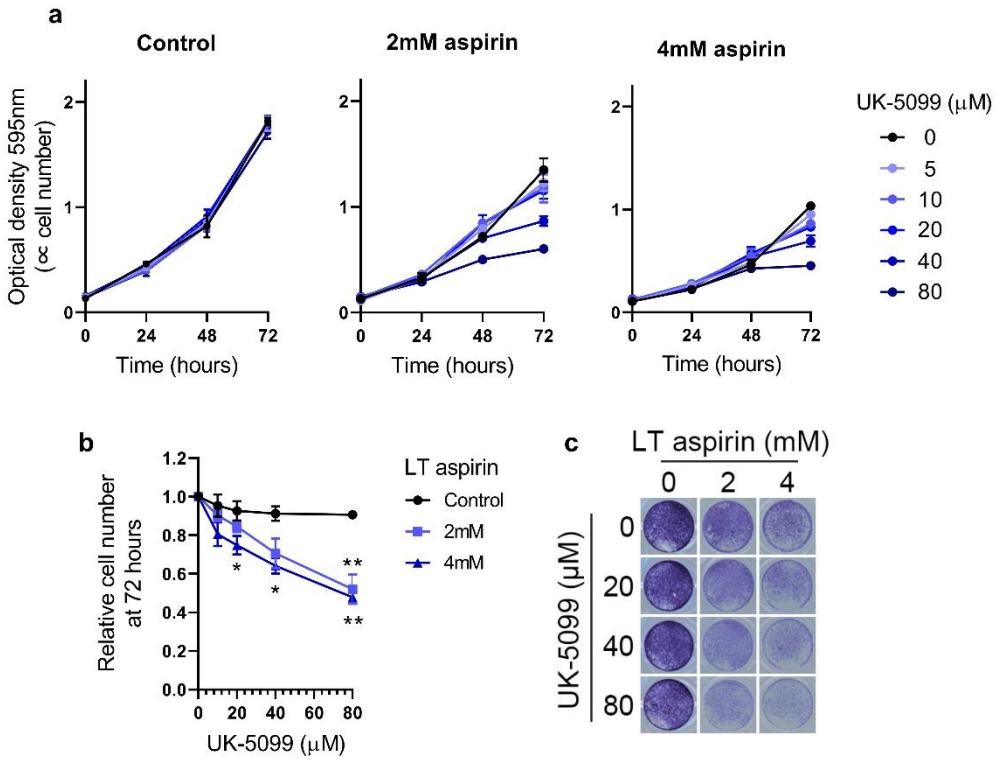

Figure 5.1 Proliferation of the long-term (~52-week) aspirin treated cell line SW620 in combination with MPC inhibitor UK-5099

a Proliferation assay curves measured by optical density of crystal violet staining, showing one replicate representative of three independent experiments, error bars represent standard deviation (n≥3). **b** Cell number in treated cells relative to DMSO control in each long-term (LT) aspirin condition after 72 hours of treatment, from three independent experiments. Error bars represent standard error (n=3). *=p≤0.05, **= p≤0.01. **c** Representative images of stained cells after 72 hours of treatment.

Results for LS174T cells (Figure 5.2) show that in contrast to the SW620 cells, LS174T cells are sensitive to UK-5099 even in the absence of aspirin and long-term aspirin treatment does not significantly increase their sensitivity to the drug. As aspirin had similar metabolic effects in this cell line (such as increased glucose utilisation), this suggests there is cell line specificity in the sensitivity to this drug and the ability of the cells to adapt when treated with the combination of drugs.

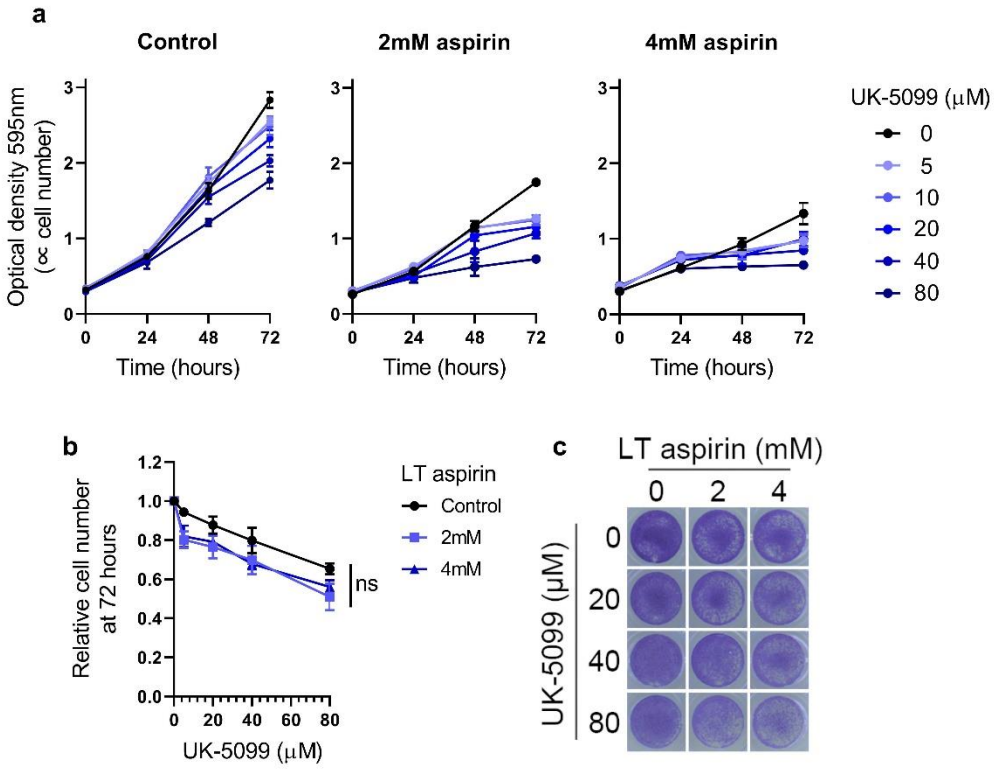

Figure 5.2 Proliferation of the long-term (~52-week) aspirin treated cell line LS174T in combination with MPC inhibitor UK-5099

a Proliferation assay curves measured by optical density of crystal violet staining, showing one replicate representative of three independent experiments, error bars represent standard deviation (n≥3). **b** Cell number in treated cells relative to DMSO control in each long-term (LT) aspirin condition after 72 hours of treatment, from three independent experiments. Error bars represent standard error (n=3). ns=not significant. **c** Representative images of stained cells after 72 hours of treatment.

Results for HCA7 cells (Figure 5.3) show more similar findings to those in SW620; the cells not treated with aspirin show no sensitivity to UK-5099 even in the highest doses, but long-term 4mM aspirin treated cells show sensitivity to all doses of UK-5099. 2mM aspirin treated cells also show significantly reduced cell numbers with 40µM UK-5099. This suggests that despite not seeing similar results in LS174T, this effect is not specific to just one cell line.

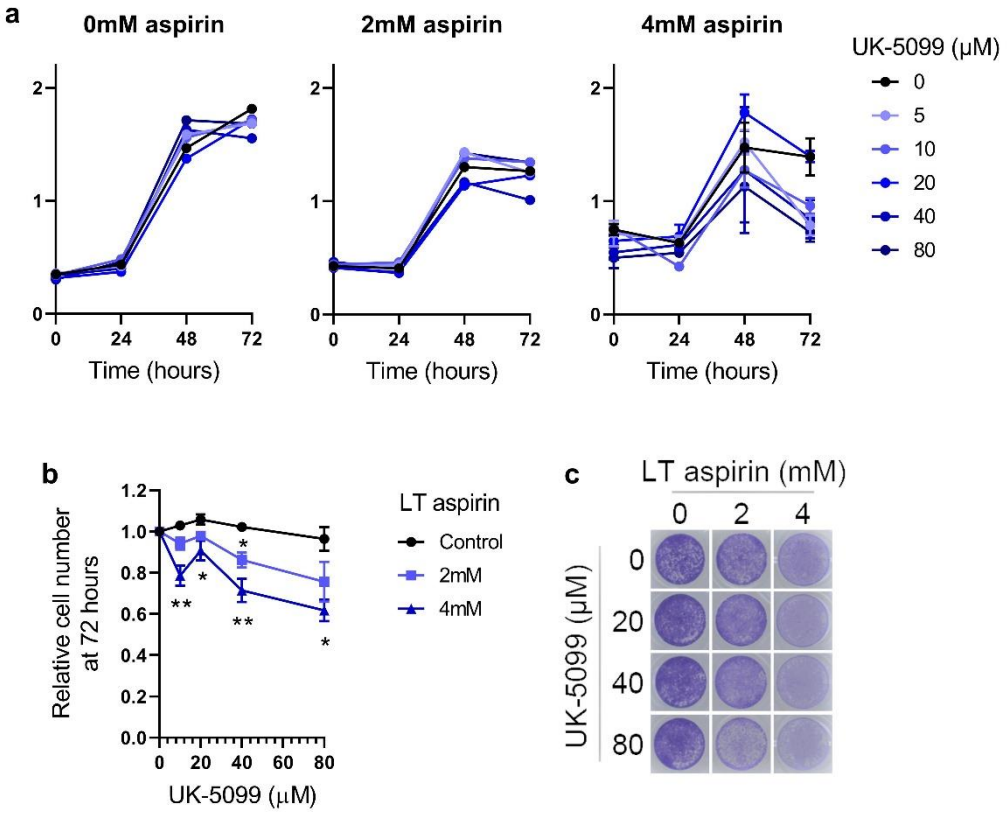

Figure 5.3 Proliferation of the long-term (~52-week) aspirin treated cell line HCA7 in combination with MPC inhibitor UK-5099

a Proliferation assay curves measured by optical density of crystal violet staining, showing one replicate representative of three independent experiments, error bars represent standard deviation (n≥3). **b** Cell number in treated cells relative to DMSO control in each long-term (LT) aspirin condition after 72 hours of treatment, from three independent experiments. Error bars represent standard error (n=3). *=p≤0.05, **= p≤0.01. **c** Representative images of stained cells after 72 hours of treatment.

It was also shown in Chapter 3 that short-term (72-hour) aspirin treatment had similar effects on metabolic enzyme expression as long-term (52-week) treatment, therefore, it was next investigated whether short-term treatment could also increase sensitivity to UK-5099 in SW620 cells. In this experiment, SW620 cells that had not previously been treated with aspirin were treated with both aspirin and UK-5099 for a total of 72 hours. These results (Figure 5.4) show very similar findings to those in SW620 cells treated with long-term aspirin; control cells show no sensitivity to UK-5099, but 4mM aspirin treated cells had significantly reduced cell numbers at all UK-5099 doses tested in comparison to control. 2mM aspirin treated cells also had significantly reduced cell numbers at 40µM and 80µM UK-5099. This suggests that short-term aspirin treatment is sufficient to induce sensitivity to UK-5099 in SW620 cells.

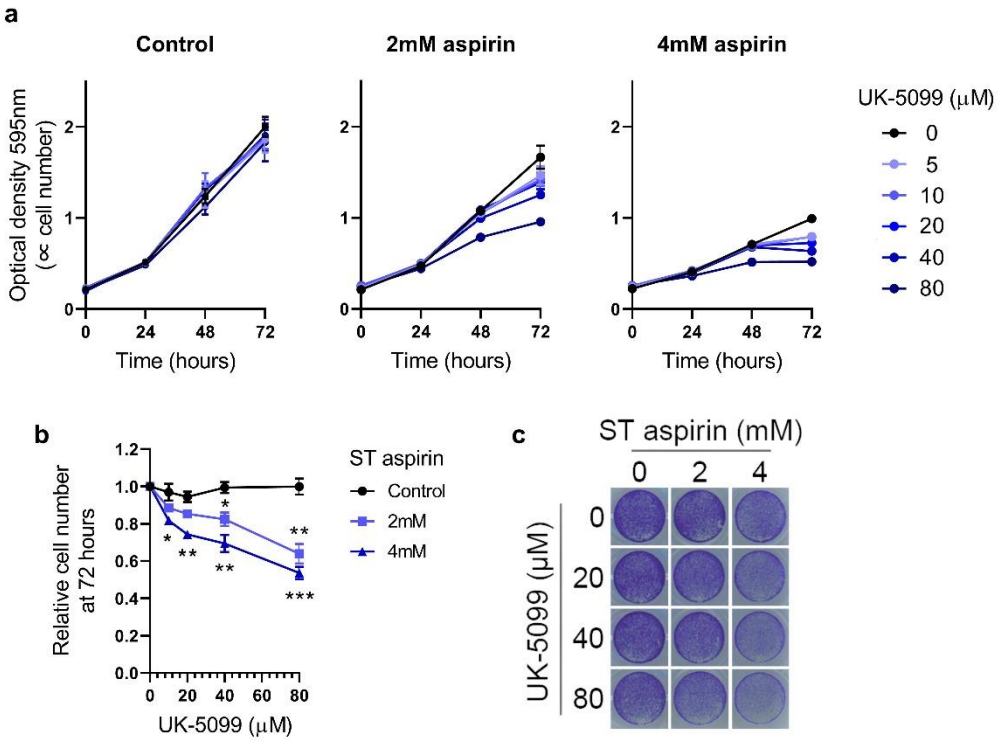

Figure 5.4 Proliferation of the short-term (72-hour) aspirin treated cell line SW260 in combination with MPC inhibitor UK-5099

a Proliferation assay curves measured by optical density of crystal violet staining, showing one replicate representative of three independent experiments, error bars represent standard deviation (n≥3). **b** Cell number in treated cells relative to DMSO control in each short-term (ST) aspirin condition after 72 hours of treatment, from three independent experiments Error bars represent standard error (n=3). *=p≤0.05, **= p≤0.01, ***=p≤0.001. **c** Representative images of stained cells after 72 hours of treatment.

5.3.2 Aspirin enhances the efficacy of glutaminase inhibitor CB-839

The data from Chapter 3 show that aspirin increases expression of GLS1, although results in Chapter 4 show that aspirin inhibits glutaminolysis. This suggests that GLS1 expression may be increased with aspirin treatment as a compensation mechanism to try and restore glutaminolysis in the aspirin treated cells. This would suggest that the cells may be more reliant on this enzyme and therefore more susceptible to its inhibition. This hypothesis was tested by combining aspirin treatment with CB-839, an inhibitor of GLS1 which is currently in phase I clinical

trials in cancer patients including in patients with advanced colorectal cancer (283). Proliferation experiments were performed on long-term (~52-week) aspirin treated cell lines SW620, LS174T and HCA7, combining aspirin with a range of concentrations of CB-839 (or DMSO vehicle control) for a period of 72 hours, followed by crystal violet staining to quantify the relative number of viable cells. The proliferation of each CB-839 treatment was calculated relative to the growth of the same aspirin concentration with DMSO control, as before.

Results from SW620 cells are shown in Figure 5.5. In line with previous results in the literature (290), these data show that up to 10μM CB-839 had no effect on the growth of control SW620 cells. However, both 5μM and 10μM CB-839 significantly decreased the growth of the cells treated with 2mM and 4mM aspirin compared to aspirin treatment with DMSO control. Unlike the results with UK-5099, sensitivity to the drug combination was enhanced with increased concentration of aspirin; the 4mM aspirin treated cells were much more sensitive to CB-839 than the 2mM aspirin treated cells.

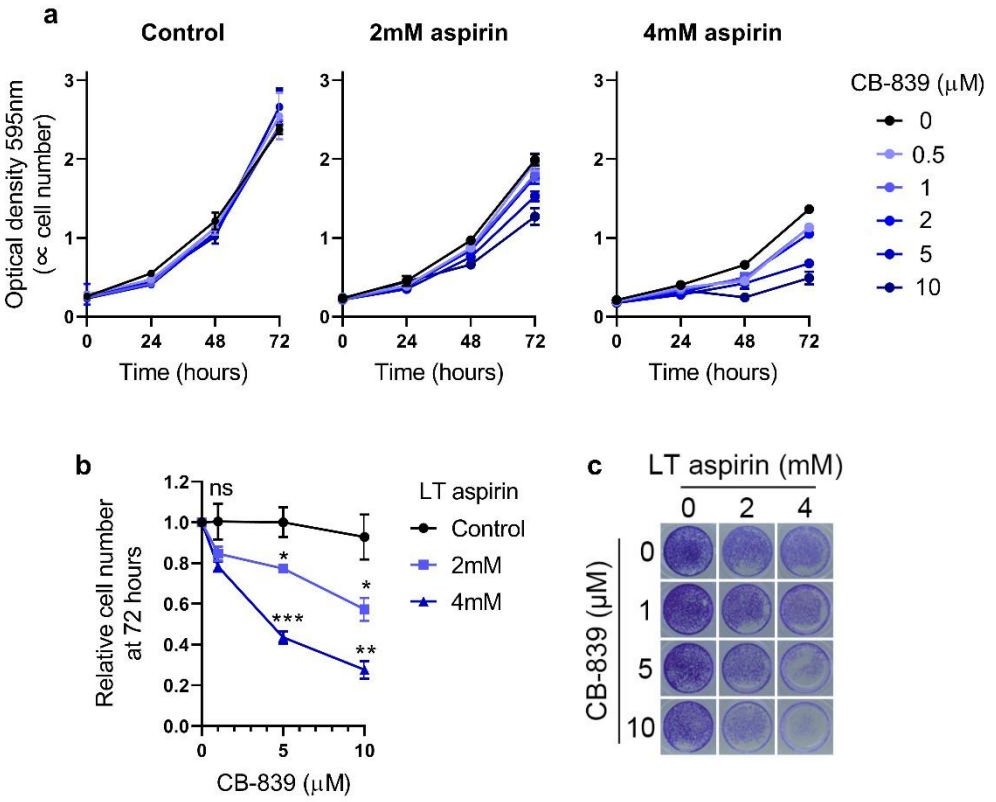

Figure 5.5 Proliferation of the long-term (~52-week) aspirin treated cell line SW260 in combination with GLS1 inhibitor CB-839

a Proliferation assay curves measured by optical density of crystal violet staining, showing one replicate representative of three independent experiments, error bars represent standard deviation (n≥3). **b** Cell number in treated cells relative to DMSO control in each long-term (LT) aspirin condition after 72 hours of treatment, from three independent experiments. Error bars represent standard error (n=3). *=p≤0.05, **= p≤0.01, ***=p≤0.001. **c** Representative images of stained cells after 72 hours of treatment.

Results for LS174T cells are shown in Figure 5.6. Similarly, to the results found with UK-5099, LS174T cells have decreased cell numbers with CB-839 even in the absence of aspirin. However, aspirin treatment did increase sensitivity to the drug; cell numbers were significantly reduced with 2μM and 5μM CB-839 compared to controls in the 4mM aspirin treated cells, although this was not detected at the higher dose of 10μM CB-839. Of note, even though more sensitive to CB-839 alone, the combination with aspirin did not increase the sensitivity of the LS174T cells to the same extent as detected in the SW620 cells.

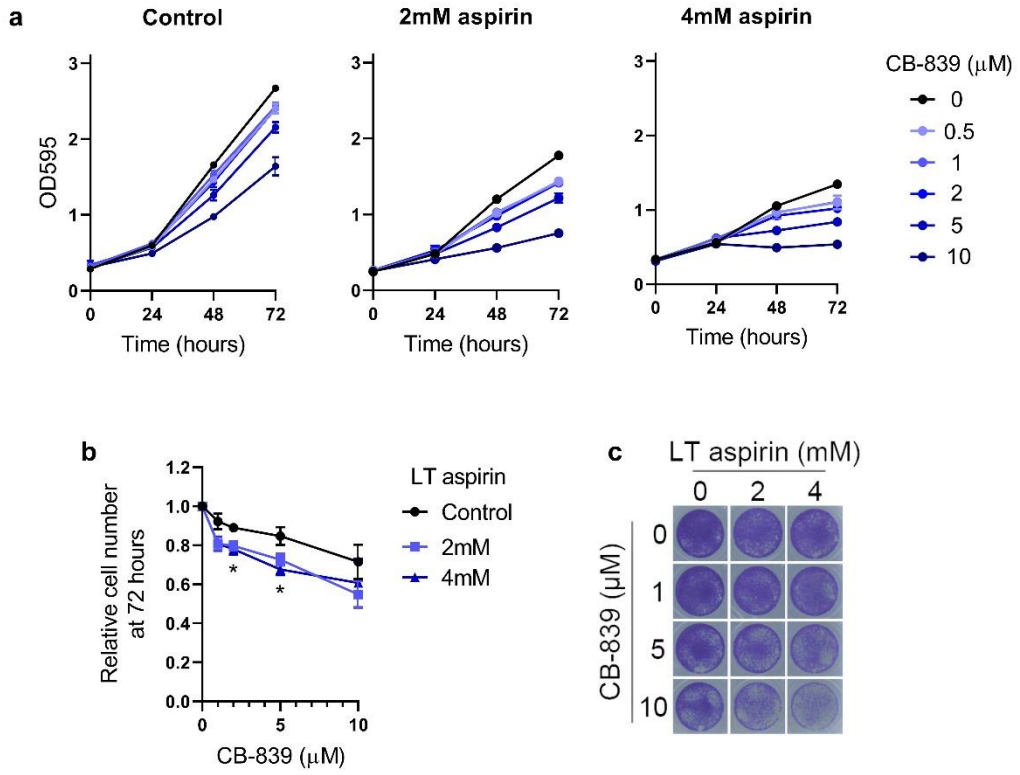

Figure 5.6 Proliferation of the long-term aspirin treated cell line LS174T in combination with GLS1 inhibitor CB-839

a Proliferation assay curves measured by optical density of crystal violet staining, showing one replicate representative of three independent experiments, error bars represent standard deviation (n≥3). **b** Cell number in treated cells relative to DMSO control in each long-term (LT) aspirin condition after 72 hours of treatment, from three independent experiments. Error bars represent standard error (n=3). *=p≤0.05. **c** Representative images of stained cells after 72 hours of treatment.

Results for HCA7 cells (Figure 5.7) show similar results to those seen in SW620 cells; in the absence of aspirin, the cells show little sensitivity to CB-839, but in 4mM aspirin treated cells cell number was significantly reduced in 5μM and 10μM CB-839 in comparison to control. Overall, these results show that long-term aspirin treatment can increase the sensitivity of three CRC cell lines to the GLS1 inhibitor CB-839.

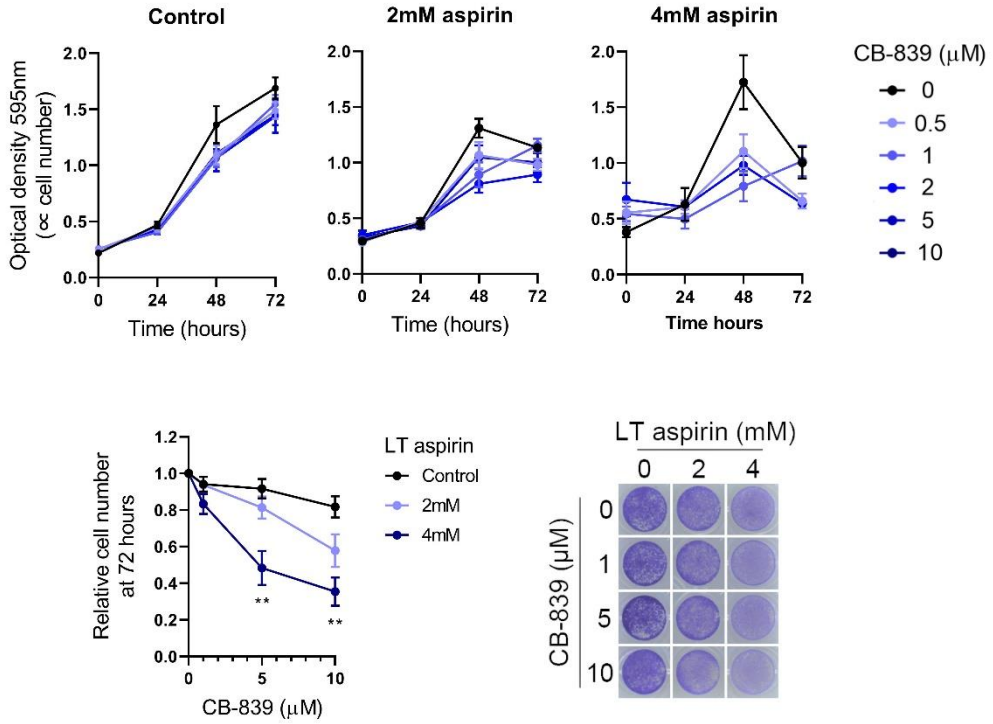

Figure 5.7 Proliferation of the long-term (52-week) aspirin treated cell line HCA7 in combination with GLS1 inhibitor CB-839

a Proliferation assay curves measured by optical density of crystal violet staining, showing one replicate representative of three independent experiments, error bars represent standard deviation (n≥3). **b** Cell number in treated cells relative to DMSO control in each long-term (LT) aspirin condition after 72 hours of treatment, from three independent experiments. Error bars represent standard error (n=3). **= p≤0.01. **c** Representative images of stained cells after 72 hours of treatment.

Importantly, previous results have also shown that short-term (72-hour) aspirin treatment leads to an increase in GLS1 expression (Figure 3.9). It was therefore investigated whether short-term aspirin treatment was also sufficient to increase sensitivity to CB-839. This is important for establishing whether aspirin treatment may be clinically useful in enhancing efficacy of CB-839 in patients who have not been previously treated with aspirin.

This was tested by treating SW620 cells with both aspirin and CB-839 for 72 hours. The results from this experiment are shown in Figure 5.8. This again shows no

effect of CB-839 on control cells, however there is a significant decrease in cell number compared to control in all CB-839 doses with 4mM aspirin and with 5µM and 10µM in 2mM aspirin treated cells. The cells are less sensitive to CB-839 in comparison to cells treated with long-term aspirin and there is no difference in CB-839 sensitivity between 2mM and 4mM aspirin treated cells. Therefore, short-term treatment with aspirin is sufficient to increase the cell's sensitivity to CB-839, however, to a lesser extent than long-term aspirin treatment.

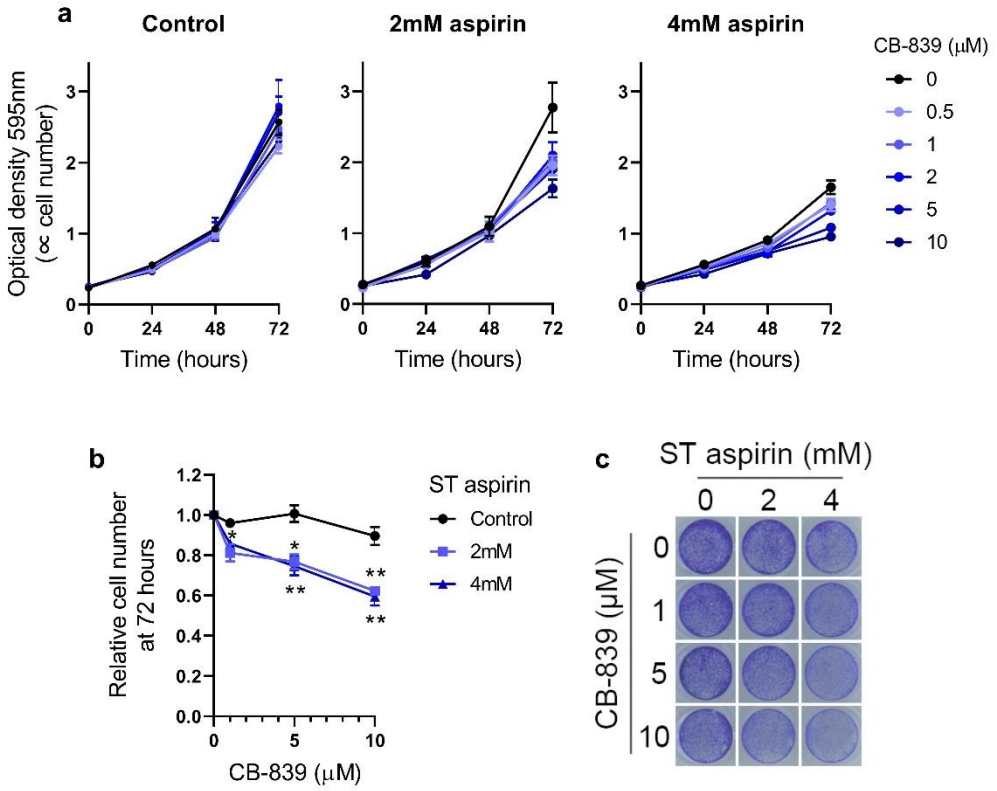

Figure 5.8 Proliferation of the short-term (72-hour) aspirin treated cell line SW260 in combination with GLS1 inhibitor CB-839

a Proliferation assay curves measured by optical density of crystal violet staining, showing one replicate representative of three independent experiments, error bars represent standard deviation (n≥3). **b** Cell number in treated cells relative to DMSO control in each short-term (ST) aspirin condition after 72 hours of treatment, from three independent experiments. Error bars represent standard error (n=3). *=p≤0.05, **= p≤0.01, ***=p≤0.001. **c** Representative images of stained cells after 72 hours of treatment.

5.3.3 The combination of aspirin and CB-839 induces apoptosis in SW620 cells

It was next investigated whether the combination of aspirin and CB-839 induces apoptosis in CRC cells, to determine whether the combination causes cell death or simply cell cycle arrest. This was investigated using an Incucyte analyser to measure cell confluence in parallel with fluorescence produced from a stain detecting active caspase-3/7 in real time. Prior to performing the experiment, the caspase-3/7 dye was validated, and concentration was optimised using the apoptosis inducer ABT-737 as a positive control for active caspases in SW620 cells. The results from the validation are shown in Figure 5.9 and Figure 5.10. ABT-737 did not significantly affect confluence at the concentrations used (Figure 5.9a), but apoptosis was induced as measured by the fluorescence produced from the caspase-3/7 stain (as quantified by “green object count”), particularly at the later time points (72 hours onwards) (Figure 5.9b). This confirms the caspase-3/7 stain is able to detect apoptotic cells. The range of concentration used for the stain (2-8µM, as recommended by the manufacturer) had no effect on the level of apoptosis detected, therefore the lowest concentration (2µM) was used for subsequent experiments. This was shown by the green object count in Figure 5.9b, and also by the images of the green fluorescence shown in Figure 5.10.

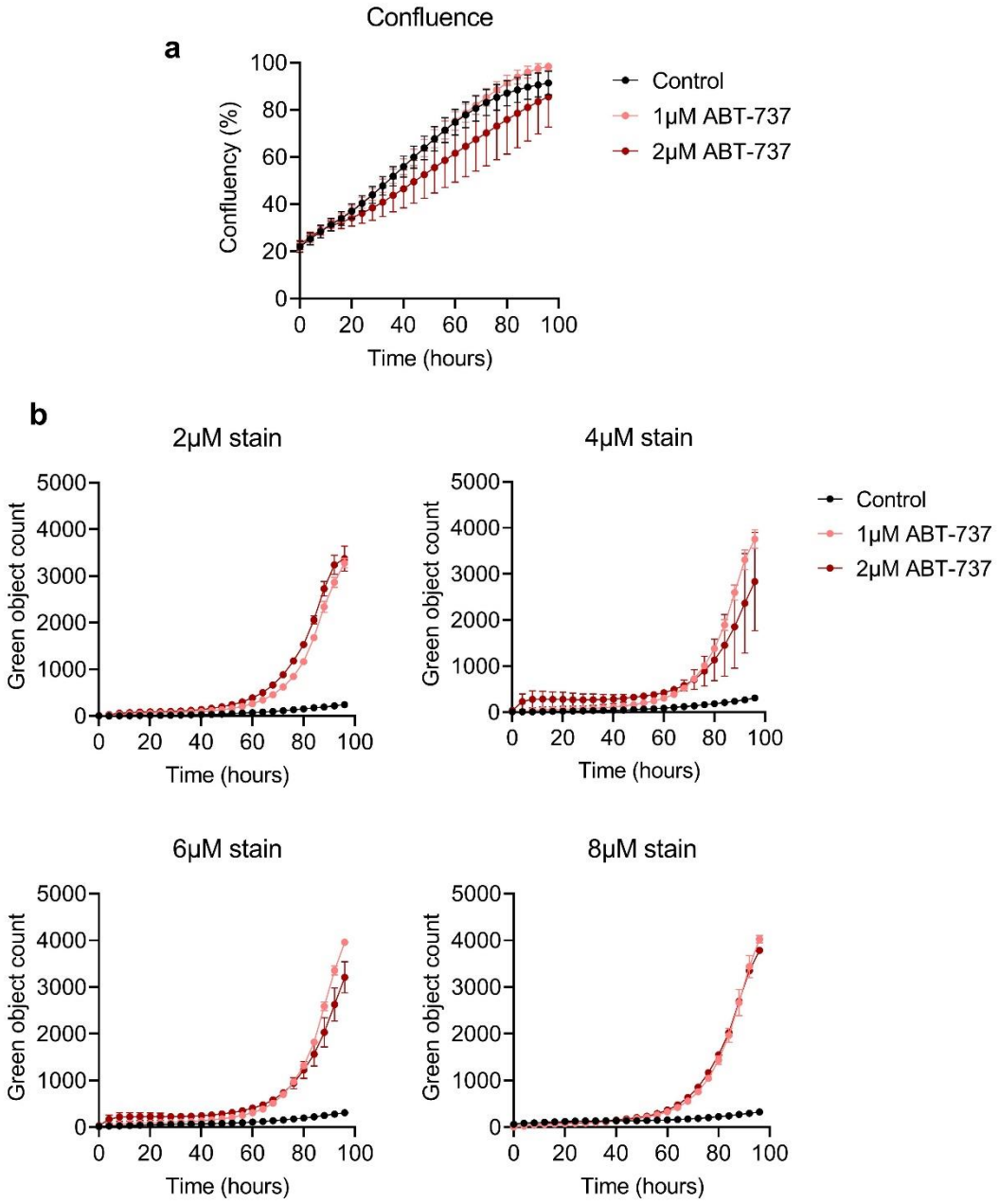

Figure 5.9 Confluence and detection of apoptosis when treating with ABT-737 and a stain for active caspase-3/7 in SW620 cells

a Confluence of the cells over time after treatment with ABT-737 analysed in an Incucyte for 96 hours. Error bars represent standard deviation (n≥24). **b** Fluorescence measured by green object count over time with each concentration of caspase-3/7 stain. Data represent technical replicates from one experiment (n=4 for control, n=3 for 1μM and 2μM ABT-737), error bars represent standard deviation.

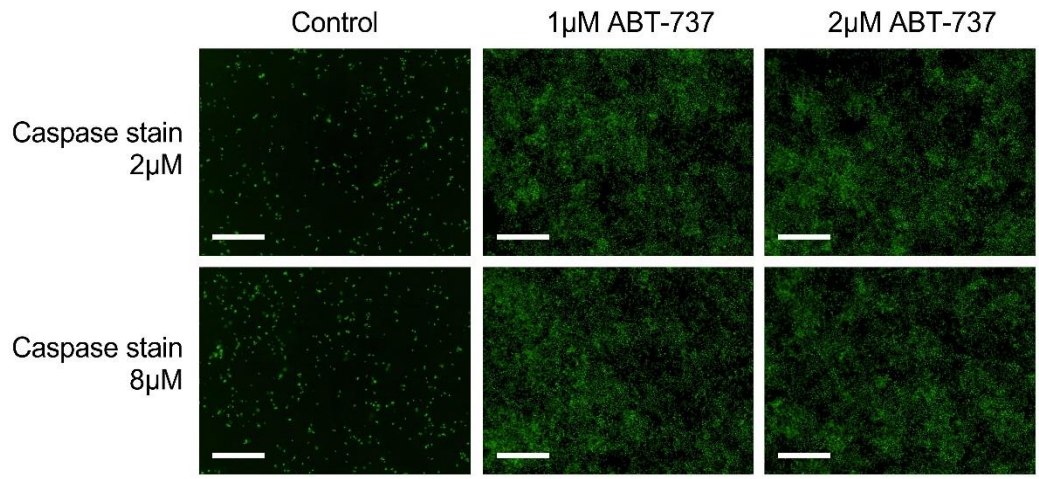

Figure 5.10 Fluorescence detected using a stain for active caspase-3/7 when treating with ABT-737 to induce apoptosis in SW620 cells

Representative images of green fluorescence after 96 hours of ABT-737 treatment, with the highest and lowest concentrations of caspase-3/7 stain used. Scale bar represents 300μm.

Using the optimised concentration of caspase-3/7 stain, this assay was performed to determine levels of apoptosis when treating long-term (~52-week) aspirin treated SW620 cells with CB-839. These results are shown in Figure 5.11. Confluency and fluorescence (indicating apoptotic cells) were measured over approximately 72 hours. In line with previous experiments, the combination of aspirin and CB-839 reduced confluency compared to the control conditions (Figure 5.11a). Green object count was calculated relative to the cell confluency, to normalise the number of apoptotic cells to the total number of cells in the wells. This showed a significant induction of apoptosis in the cells treated with a combination of aspirin and CB-839, compared to all other conditions (Figure 5.11b). Neither aspirin nor CB-839 alone significantly induced apoptosis in this experiment, when comparing fluorescence at the end time-point. Both aspirin alone and aspirin combined with CB-839 show a slight increase in apoptosis at the early time points (approximately 24 hours onwards), though apoptosis upon treatment with the combination increases dramatically at the later time points (Figure 5.11c). These data show that the combination of aspirin and CB-839 reduces cell number over time at least in part by inducing apoptosis.

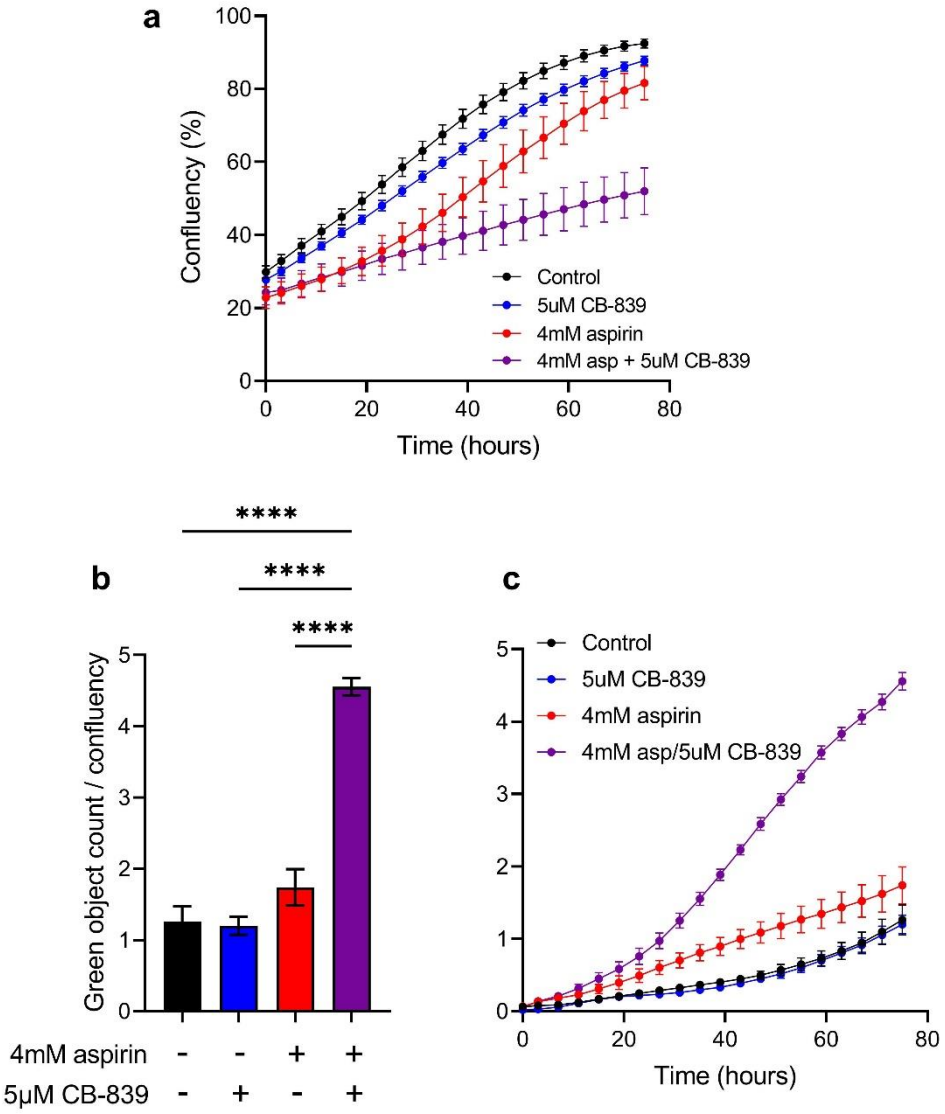

Figure 5.11 Combining long-term (~52-week) aspirin treatment and 72-hour CB-839 treatment induces apoptosis in SW620 cells

a Confluency of the cells over time after treatment with long-term 4mM aspirin and/or CB-839 compared to control. **b** Green object count relative to confluency, to indicate the relative amount of apoptotic cells in each condition and the end time point (~72 hours). **c** Relative apoptotic cells over time. Error bars represent standard error (n=3). ****=p<0.0001.

5.3.4 **The effect of cell density on UK-5099 and CB-839 sensitivity**

Results so far in this chapter suggest that the presence of either short or long-term aspirin treatment can increase the sensitivity of cells to two metabolic inhibitors. However, aspirin treatment alone reduces cell number (as shown in Figures 5.1 – 5.8), it is therefore possible that this decrease in cell density may in itself increase the cells' sensitivity to the inhibitors, rather than any specific effect of aspirin (Tracey Collard, personal communication). To investigate this possibility, the effect of the inhibitors used was tested on varying cell densities in SW620 cells, starting with the seeding density used in previous experiments (20,000 cells per well), and decreasing down to 2,500 cells per well. The results from this experiment are shown in Figure 5.12. Cell number was calculated in the treated wells relative to the vehicle control wells with the same cell density.

Decreasing cell density did not have a large effect on the sensitivity of the cells to UK-5099; relative cell number was close to 1 even at the lowest seeding density. This suggests the sensitising effect of aspirin treatment to UK-5099 was not due to decreased cell density. Decreasing cell density did increase sensitivity to treatment with CB-839. In the lowest cell density (2,500 cells seeded), relative cell number with CB-839 treatment dropped to an average of 65%. However, this density is much lower than that seen upon aspirin treatment alone in the previous experiments. Using the data in Figure 5.5 for comparison, the density of the aspirin treated cells is comparable to the 10,000 cells/well seeding density used here (Figure 5.5 and Figure 5.12). With 10,000 cells, relative cell number upon CB-839 treatment was an average of 75% in comparison to control at 72 hours, whereas CB-839 treatment reduces cell number to 57% of control in 2mM aspirin and 28% in 4mM aspirin (Figure 5.5). The effect of the CB-839 treatment is considerably higher with aspirin treatment than with 10,000 cells/well seeding density. This suggests that it is not reduced cell density alone that increases the cells' sensitivity to CB-839 when treated with aspirin. It is therefore likely that the specific effects of aspirin on the cells are also responsible for the increase the sensitivity of the cells to CB-839.

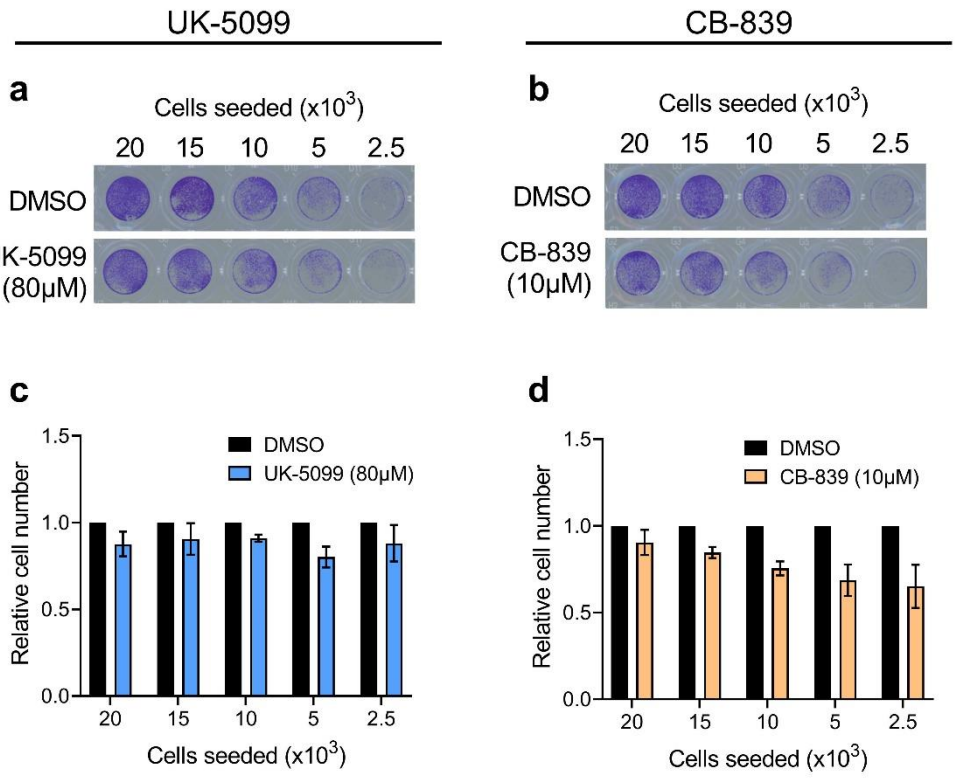

Figure 5.12 Effect of seeding density on sensitivity to CB-839 or UK-5099 in SW620 cells

a-**b** Representative crystal violet stained wells after 72 hours treatment with UK-5099 and CB-839 respectively, compared to DMSO control. **c-d** Relative cell number in the drug treated condition compared to the vehicle control in each cell seeding density. Error bars represent standard deviation (n=3).

5.3.5 Aspirin does not sensitise SW620 cells to suppression of GLS1 expression

Both long- and short- term aspirin treatment were found to increase sensitivity to CB-839, which is hypothesised to be due to increased reliance of cells on GLS1 upon aspirin treatment. CB-839 is thought be a specific inhibitor of GLS1, however there is a possibility that this inhibitor has off-target effects that could be related to the sensitisation effect of aspirin. If aspirin treated cells are more sensitive to inhibition of GLS1, then suppression of GLS1 expression using siRNA would potentially have the same effect as CB-839. This hypothesis was tested by knocking down GLS1 in cells and treating them with 4mM aspirin in comparison to

control medium. The cells were cultured for a total of 8 days, with 7 days of aspirin treatment, and then stained using crystal violet to measure cell number. The results of this experiment are shown in Figure 5.13. GLS1 knockdown had no effect on cell yield after 7 days, and although 4mM aspirin treatment reduced cell number, there was no difference in cell number between the cells transfected with siRNA targeting GLS1 in comparison to cells transfected with control siRNA in either control or aspirin treated cells. Western analysis of GLS1 expression shows that aspirin treatment induces GLS1 expression in the control transfected cells (as previously shown in Chapter 3) and that siRNA targeting GLS1 reduced expression of GLS1 in both control and aspirin treated conditions.

In this model, GLS1 knockdown did not affect cell number in the aspirin treated cells, which contrasts with the effect of CB-839 in aspirin treated cells. There are several possible explanations for this result. Firstly, CB-839 may have off-target effects that make aspirin treated cells more sensitive to it, however, the literature suggests that CB-839 is a selective inhibitor (281). Secondly, knockdown by siRNA may not be sufficient to fully inhibit GLS1 activity. Western analysis shows some GLS1 protein expression remains following knockdown and the activity in the remaining protein may be sufficient to prevent the impact on the cells. Thirdly, reduced expression of GLS1, that occurs upon knockdown but not upon inhibition with a small-molecule, may cause the cell to adapt and compensate in a way that inhibition of enzyme activity alone does not.

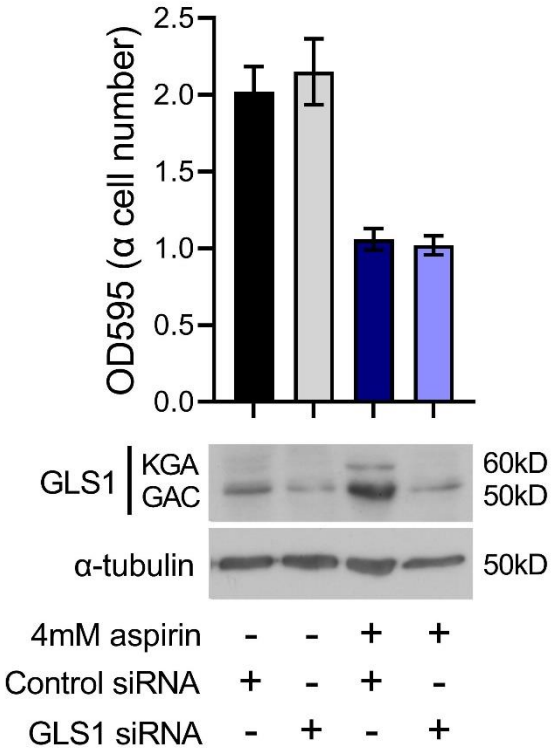

Figure 5.13 Aspirin treatment does not sensitise cells to knockdown of GLS1 by siRNA

Optical density at 595nm (OD595) in each condition after crystal violet staining, to indicate the relative number of cells after 7 days of knockdown and aspirin treatment. Error bars represent standard deviation (n=15). Western analysis of GLS1 expression compared to α-tubulin loading control.

5.3.6 **Aspirin sensitises SW620 cells to CB-839 in physiological medium**

The sensitisation of the cells to CB-839 when treated with aspirin is of particular interest as CB-839 is currently undergoing clinical trials for various cancer types (283). Therefore, as both drugs are known to be safe for patients, this combination may be easily clinically translatable if the same effect occurs *in vivo* as has been shown here *in vitro*. As previously discussed in section 5.1.3, due to the distinct metabolic phenotypes *in vitro* and *in vivo*, metabolic inhibitors can have different efficacies between conditions. Therefore, it was next investigated whether aspirin sensitises cells to CB-839 when treated in human plasma-like medium (HPLM), recently developed by Cantor et al. to have similar metabolite composition to human plasma (discussed in section 5.1.3) (119). Using physiological media takes

the *in vitro* system a step closer to *in vivo* conditions, therefore, it is an attempt to better reflect what would occur *in vivo*.

Cells were cultured in HPLM (supplemented with 10% dialysed FBS) for at least 48 hours prior to setting up the experiment in order to allow them to adjust to the conditions, as recommended by Cantor et al. (119). SW620 cells were then seeded in HPLM and the following day treated with combinations of aspirin and CB-839 in HPLM and cultured for 72 hours (as before). Medium was changed every 24 hours during the experiment as low levels of nutrients in the medium are depleted more quickly than when using normal DMEM. Cells were fixed and stained with crystal violet to quantify cell number at 0-, 24-, 48- and 72-hours post treatment. The results from this experiment are shown in Figure 5.14. Growth curves were produced by calculating cell number at each time point relative to the cell number at the 0-hour time point in each condition (Figure 5.14a). Consistent with previous results, in the absence of aspirin, CB-839 did not reduce cell proliferation. Both 2mM and 4mM aspirin alone reduced cell proliferation in comparison to control and this was reduced further upon addition of CB-839. To better visualise the relative effect of CB-839 treatment in combination with aspirin, cell number at 72 hours was calculated in the CB-839 treated cells relative to the vehicle control in each aspirin condition separately (Figure 5.14b). This shows that relative cell number does not change with CB-839 in the absence of aspirin, but CB-839 significantly reduced cell number in both 2mM and 4mM aspirin in a dose dependent manner. These results show that aspirin treatment sensitises cells to CB-839 in HPLM, which reassuringly is consistent with results using DMEM. This suggests this effect is more likely to translate to *in vivo* models and have future clinical utility. Importantly, these results also increase confidence in other results from experiments using DMEM, supporting its use in *in vitro* model systems, despite the discussed caveats.

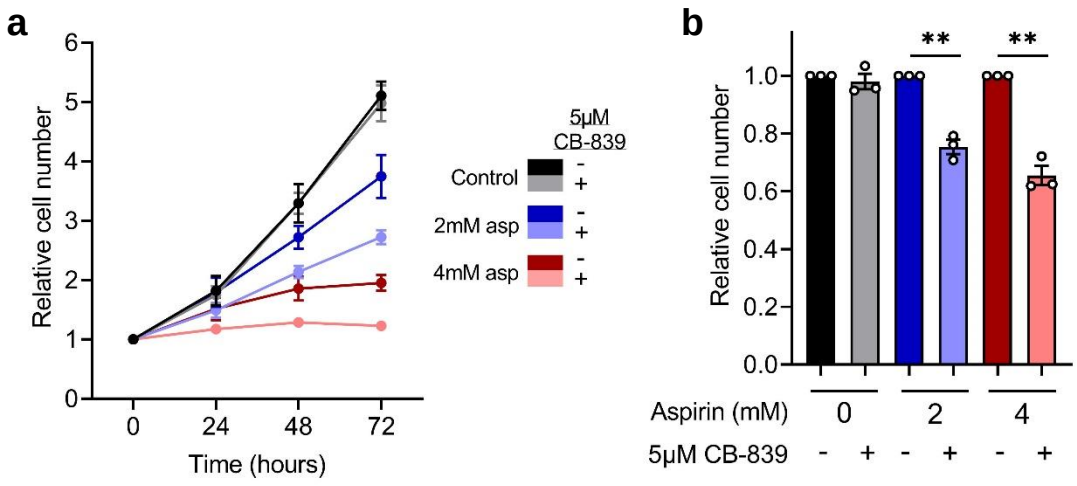

Figure 5.14 Aspirin sensitises SW620 cells to CB-839 in human plasma-like medium (HPLM)

a Cell number over time after treatment, relative to the 0-hour time point in each condition. **b** Cell number after 72 hours of CB-839 and aspirin treatment, relative to the DMSO control in each aspirin condition. Error bars represent standard error (n=3). **=p<0.01.

5.3.7 Aspirin does not affect changes in OCR and ECAR in response to CB-839

To further investigate the mechanism behind the increased sensitivity to CB-839 caused by aspirin treatment, the effects of CB-839 on levels of glycolysis and oxphos were investigated in long-term (~52-week) aspirin treated SW620 cells using extracellular flux analysis. Control and long-term aspirin treated cells were placed in the Seahorse XFp analyser and 10µM CB-839 was injected using the first injection port to measure the acute effect on OCR and ECAR of CB-839 addition, followed by the mitochondrial stress test (described in Figure 4.1). These results are shown in Figure 5.15. OCR and ECAR, following injection of CB-839, was calculated relative to basal OCR and ECAR, in order to allow comparison between conditions. In all conditions, there is a slight decrease in basal oxphos and increase in basal glycolysis with injection of CB-839. These results are consistent with inhibition of GLS1, as this limits entry of glutamine to the TCA cycle (reducing oxphos) and an increase in glycolysis would compensate for this subsequent reduction in ATP synthesis. Results show a similar response to CB-839 in OCAR and ECAR levels in both the aspirin treated and control cells. There is also no change in the maximal OCR between the control and 4mM aspirin

treated cells when they had been acutely treated with CB-839. This suggests that aspirin does not sensitise the cells to CB-839 due to reduced ability to produce ATP.

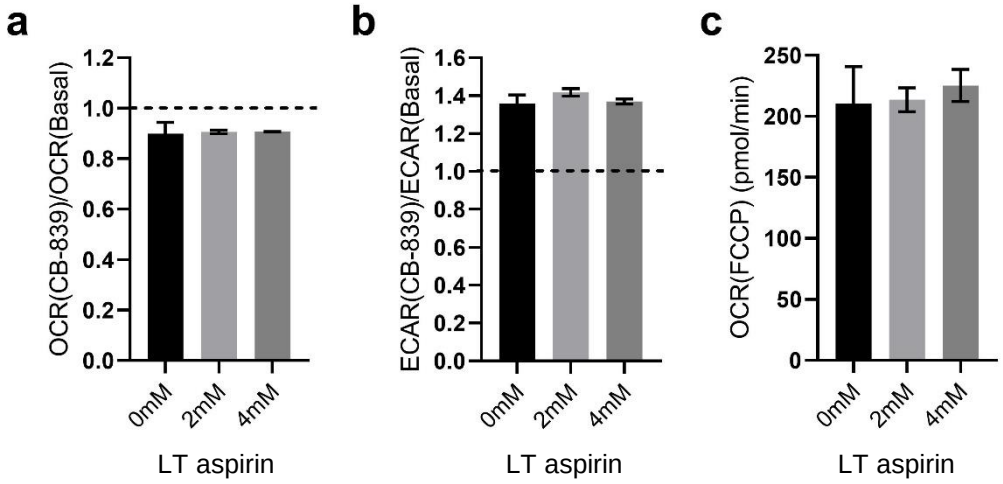

Figure 5.15 Extracellular flux analysis of long-term (LT) (~52-week) aspirin treated SW620 cells with CB-839 injection

a-b OCR and ECAR in control and long-term (LT) aspirin treated cells after injection of 10μM CB-839, relative to basal OCR and ECAR. Baseline measurement was recorded after 15 minutes, and CB-839 was injected in the first injection port at 20 minutes, and OCR and ECAR recorded immediately afterwards. **c** Maximal OCR (after injection of CB-839, oligomycin and FCCP) in each aspirin condition. Data represent technical replicates from one independent experiment (n=3 for 0mM aspirin, n=2 for 2mM and 4mM aspirin), error bars represent standard deviation.

5.3.8 Proliferation is not rescued by supplementation with non-essential amino acids or a ROS scavenger when treating with aspirin and CB-839

As aspirin treatment does not change OCR and ECAR in response to CB-839, the mechanism behind the sensitisation of aspirin treated cells to CB-839 remained unclear. It was next hypothesised that the combination of drugs could lead to an increase in reactive oxygen species (ROS) production, leading to cell death. Glutaminolysis is important for the production of glutathione, an important ROS scavenger that regulates ROS levels. Therefore, combining aspirin and CB-839 may limit glutathione production and increase ROS levels, potentially leading to the induction of apoptosis shown in Figure 5.11.

To test this hypothesis, SW620 cells were treated with aspirin and CB-839 with the addition of N-acetyl cysteine (NAC) for 72 hours before fixing and staining with crystal violet in order to quantify cell number. NAC is another ROS scavenger that could rescue cell proliferation in the presence of aspirin and CB-839 by regulating ROS levels, if this hypothesis were correct. These results are shown in Figure 5.16. Cell number was calculated relative to the drug-free condition. As shown in previous experiments, CB-839 alone does not affect cell number whereas aspirin alone does and the combination of aspirin and CB-839 further reduces cell number. Adding NAC had no effect on cell number in any of the drug treatment conditions and did not rescue cell number with the combination of aspirin and CB-839 treatment. This suggests that aspirin does not sensitise the cells to CB-839 by inducing high levels of ROS.

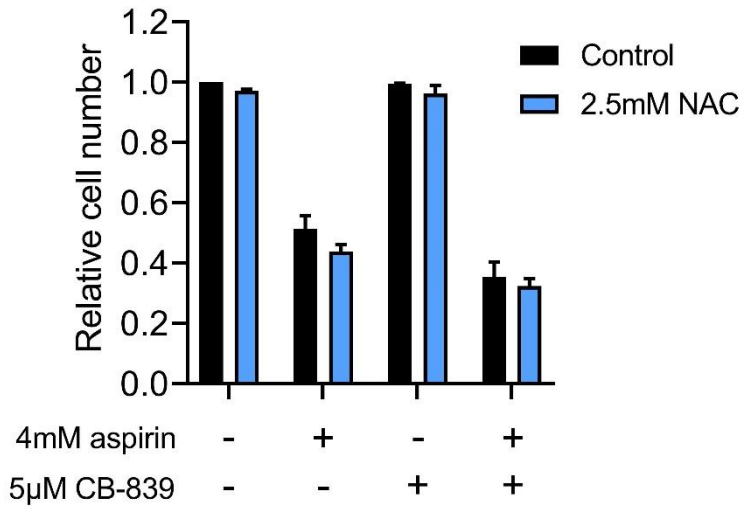

Figure 5.16 NAC does not rescue cell growth when treating with aspirin and CB-839 in SW620 cells

Cell number after 72 hours relative to the control (no drugs) condition, quantified by crystal violet staining. Error bars represent standard error (n=2).

It was next hypothesised that the cells may be sensitive to the combination of aspirin and CB-839 due to a deficiency in amino acid synthesis, as GLS1 inhibition would potentially inhibit synthesis of amino acids derived from glutamine, and aspirin inhibits many amino acid synthesising enzymes (as shown in Chapter 3). This hypothesis was tested by treating SW620 cells with aspirin and CB-839 with the addition of non-essential amino acids (NEAAs) for 72 hours before fixing and staining with crystal violet in order to quantify cell number. If NEAA synthesis deficiency causes the reduction of cell growth with aspirin and CB-839, then the addition of NEAAs may rescue this effect. A 100X stock of NEAAs was added to the medium so that the final concentration was 1X. The results from this experiment are shown in Figure 5.17. These results are similar to those in the previous experiment (Figure 5.16); aspirin alone and the aspirin/CB-839 combination reduce cell number as expected, but supplementation with NEAAs does not affect cell number in any condition and does not rescue the effect of aspirin and CB-839 in combination. This suggests that the aspirin treated cells are not more sensitive to CB-839 due to a deficiency in NEAA synthesis.

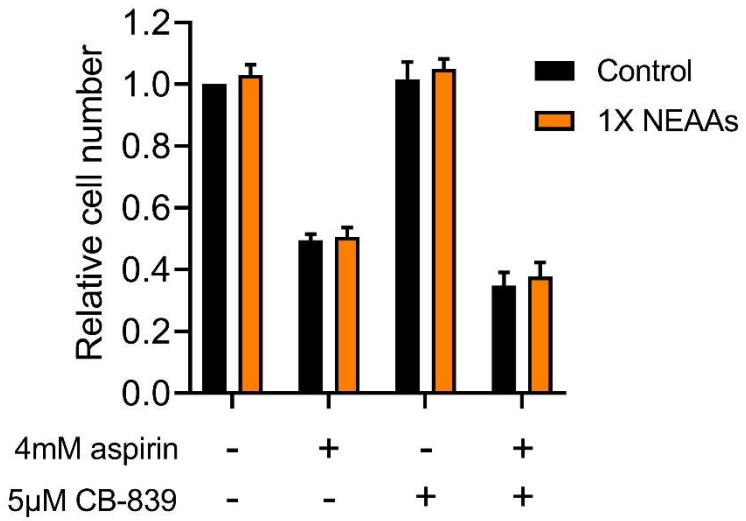

Figure 5.17 NEAA supplementation does not rescue cell growth when treating with aspirin and CB-839 in SW620 cells

Cell number after 72 hours relative to the control (no drugs) condition, quantified by crystal violet staining. Error bars represent standard error (n=2).

5.3.9 **Knockdown of GPT2 does not sensitise SW620 cells to CB-839**

It has been previously shown in the literature that cancer cells can upregulate GPT2 as a response to knockdown of GLS1 or inhibition with CB-839 (258). It was shown in Chapter 3 that aspirin treatment leads to downregulation of GPT2. It was therefore hypothesised that aspirin treated cells may be more sensitive to CB-839 as they have lower levels of GPT2 expression and are therefore unable to compensate for inhibition of GLS1. This hypothesis was investigated by testing whether knocking down GPT2 with siRNA (to mimic the effect of aspirin treatment) also sensitised the cells to treatment with CB-839. The results of this experiment are shown in Figure 5.18. Interestingly, CB-839 had no effect on cell number in either GPT2 knockdown conditions or control, suggesting that GPT2 knockdown does not sensitise the cells to CB-839. Western analysis showed a clear knockdown of GPT2 in the GPT2 siRNA treated cells compared to control siRNA. Overall, these results suggest that aspirin treatment does not sensitise the cells to CB-839 solely because of the downregulation of GPT2.

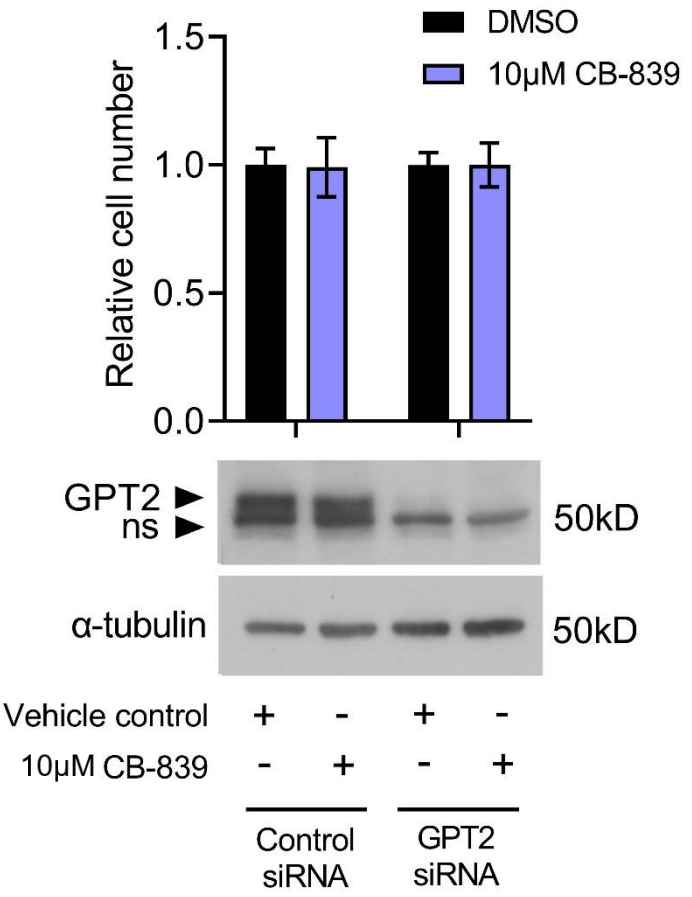

Figure 5.18 GPT2 knockdown does not sensitise SW620 cells to CB-839

Cell number in CB-839 treated cells relative to the DMSO control, measured by crystal violet staining. Error bars represent standard deviation (n=15). Western analysis of GPT2 expression compared to α-tubulin loading control. Representative of two independent experiments. ns=non-specific band.

5.3.10 **Aspirin and CB-839 combination metabolomic analysis**

Investigations so far have not provided an explanation for why aspirin treated cells are more sensitive to treatment with CB-839. Therefore, the metabolic effects of the combination of aspirin and CB-839 were more broadly investigated using SITA. Long-term (~52-week) 4mM aspirin treated SW620 cells were treated with 5μM CB-839 and compared to controls and cells treated with either long-term aspirin or CB-839 alone. Treatment time for CB-839 was reduced to 24 hours, to limit the impact on total cell number. Cells were treated with either [U-^{13}C]glucose or [U-

^{13}C]glutamine for 8 hours prior to extraction, as this allows TCA cycle intermediates to reach isotopic steady state (as previously shown in Chapter 4). As previously described, the proportion of ^{13}C in each metabolite pool represents the contribution of the labelled nutrient to that metabolite. Examples of these data are shown in Figure 5.19. Full metabolite data for ^{13}C proportions, MIDs and relative abundances are shown in Appendix 7.6.

Consistent with previous findings in Chapter 4, ^{13}C incorporation in these examples show that aspirin alone increases the contribution of glucose into the TCA cycle metabolites α-KG and succinate, and decreases contribution of glutamine. Interestingly, CB-839 alone dramatically decreases the contribution of glutamine to TCA cycle metabolites as expected, as this drug inhibits glutaminolysis through GLS1. Concomitantly, CB-839 alone largely increases contribution of glucose to TCA cycle metabolites, possibly to compensate for the reduction in carbon entry from glutamine. It is interesting that CB-839 alone has such a large effect on glucose and glutamine incorporation given that it does not affect cell proliferation (as shown in section 5.3.2). This demonstrates the metabolic flexibility of these cancer cells. The combination of aspirin and CB-839 leads to a further decrease in contribution of glutamine to TCA cycle metabolites and a further increase in contribution of glucose, however, this is not largely different from the effect of CB-839 alone, in contrast to the drastic difference seen in cell proliferation seen between these two conditions, seen in section 5.3.2. The nutrient contributions therefore do not explain the effect of aspirin and CB-839 on proliferation and apoptosis.

Interestingly, these results show that long-term aspirin treated cells have reduced contribution of glucose to serine and glycine. There was no difference in this seen in the previous experiment with long-term aspirin treated SW620 cells in Chapter 4, however this effect did occur in long-term aspirin treated LS174T and HCA7 cells. This suggests that long-term aspirin treatment may affect serine and glycine biosynthesis in all three cell lines. Glutamine contribution to serine and glycine is extremely low, however, it is interesting that this is increased when cells are treated with the combination of aspirin and CB-839.

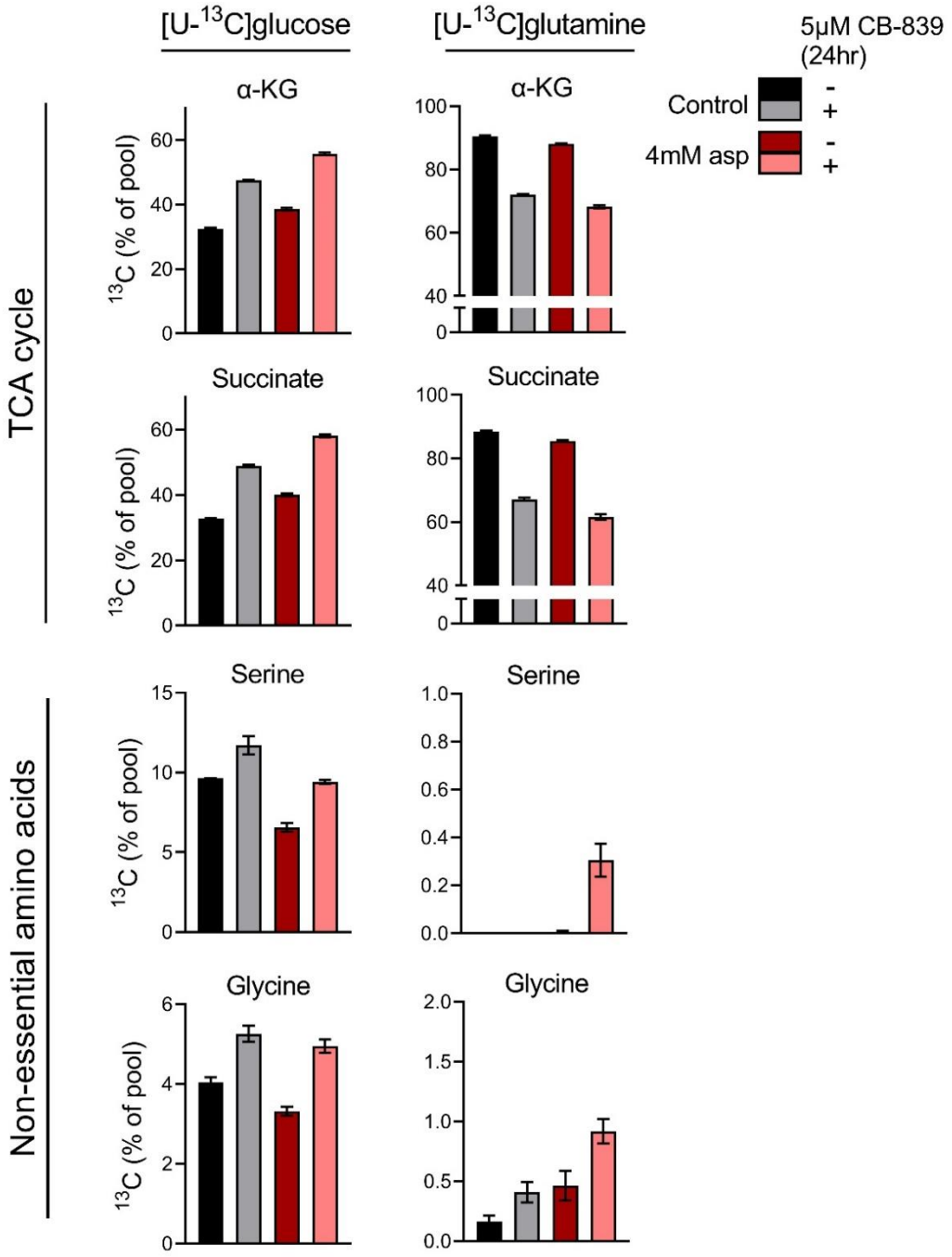

Figure 5.19 Contribution of ^{13}C relative to the total metabolite abundance after 8hrs incubation with [U-^{13}C]glucose or [U-^{13}C]glutamine in SW620 cells treated with long-term (52-week) aspirin and CB-839

% of ^{13}C in metabolite pools in long-term 4mM aspirin treatment and 24-hour 5μM CB-839 treatment compared to control and combination treatment. Error bars represent standard error (n=3).

Relative abundances (shown in Appendix 6, Figure 7.18, Figure 7.21) also do not show any clear differences in the aspirin and CB-839 combination treatment condition could explain the induction of apoptosis. However, interestingly there is a dramatic reduction in abundance of aspartate, and to a slightly lesser extent reducted abundance of alanine, with CB-839 treatment either with or without aspirin. This suggests a possibile deficiency in alanine/aspartate synthesis with CB-839 treatment, which could impair synthesis of proteins and nucleotides (301). However, this does not clearly explain the difference in proliferation, as the same effect occurs with both CB-839 alone and CB-839/aspirin.

Overall, these results show that CB-839 has the expected effect on both glutamine and glucose metabolism. However, there is not a further notable effect on metabolism upon combination of aspirin and CB-839 that could explain the large reduction in cell number and induction of apoptosis shown in Chapter 4.

Samples from this experiment were also analysed by western blotting to investigate expression of GLS1 and GPT2 when aspirin and CB-839 are combined. These results are shown in Figure 5.20. Consistent with previous results in Chapter 3, long-term aspirin treatment induces a large increase in expression of GLS1 and reduces expression of GPT2. CB-839 alone does not have any significant effects on expression of these enzymes, although there is a slight trend towards increased expression of GLS1. Expression of GLS1 and GPT2 with aspirin and CB-839 in combination is not significantly different from aspirin alone, so again these results do not help to explain the dramatic reduction of proliferation in this condition.

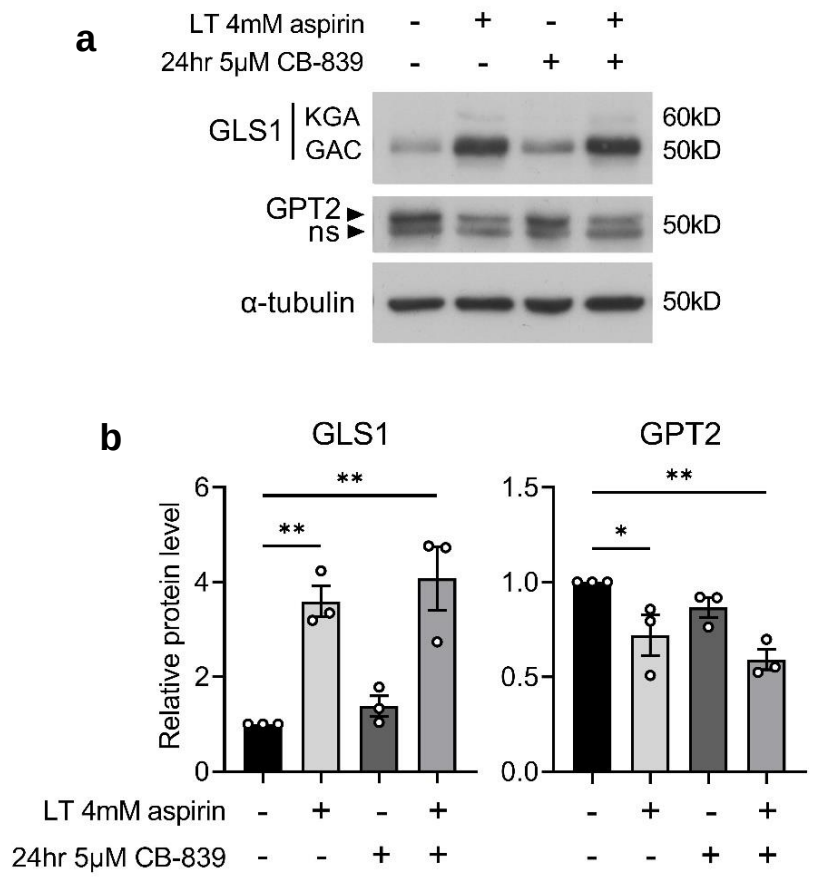

Figure 5.20 Western analysis of SW620 cells treated with long-term (~52-week) aspirin and CB-839

a Western analysis of GLS1 and GPT2 expression in long-term (LT) 4mM aspirin treated cells that were treated with 5μM CB-839 for 24 hours. Representative of three biological replicates. **b** Quantification of relative protein expression compared to control in three biological replicates. Error bars represent standard error (n=3). *=p<0.05, **=p<0.01.

5.3.11 **Effect of nutrient depletion on long-term aspirin treated cells**

Results in this chapter show that aspirin treatment, particularly long-term, makes cells more vulnerable to metabolic inhibitors. It was therefore investigated whether long-term aspirin treatment had any effect on the ability of the cells to cope with depletion of the two main carbon sources: glucose and glutamine. Levels of these nutrients in the tumour microenvironment can often be low due to poor vascularisation and rapid consumption by tumour cells as well as stromal and immune cells. Cancer cells must adapt to survive and grow in these low nutrient conditions. Metabolic therapies may be effective if they limit the ability of the cells to cope with low nutrient conditions.

Long-term (~52-week) aspirin treated SW620 cells were grown in decreasing concentrations of glucose for 72 hours. Cells were fixed and stained with crystal violet at 0-, 24-, 48- and 72 hours of treatment to produce growth curves (Figure 5.21a). Cell number at the 72-hour time point was calculated in each glucose concentration relative to the control concentration (25mM, used in normal DMEM) to compare the effect of glucose depletion in each aspirin condition (Figure 5.21b). These results show that glucose depletion reduced cell growth, but the effect of glucose depletion was not significantly different between aspirin conditions. This suggests that long-term aspirin treatment doesn’t affect the ability of the cells to cope with glucose depletion.

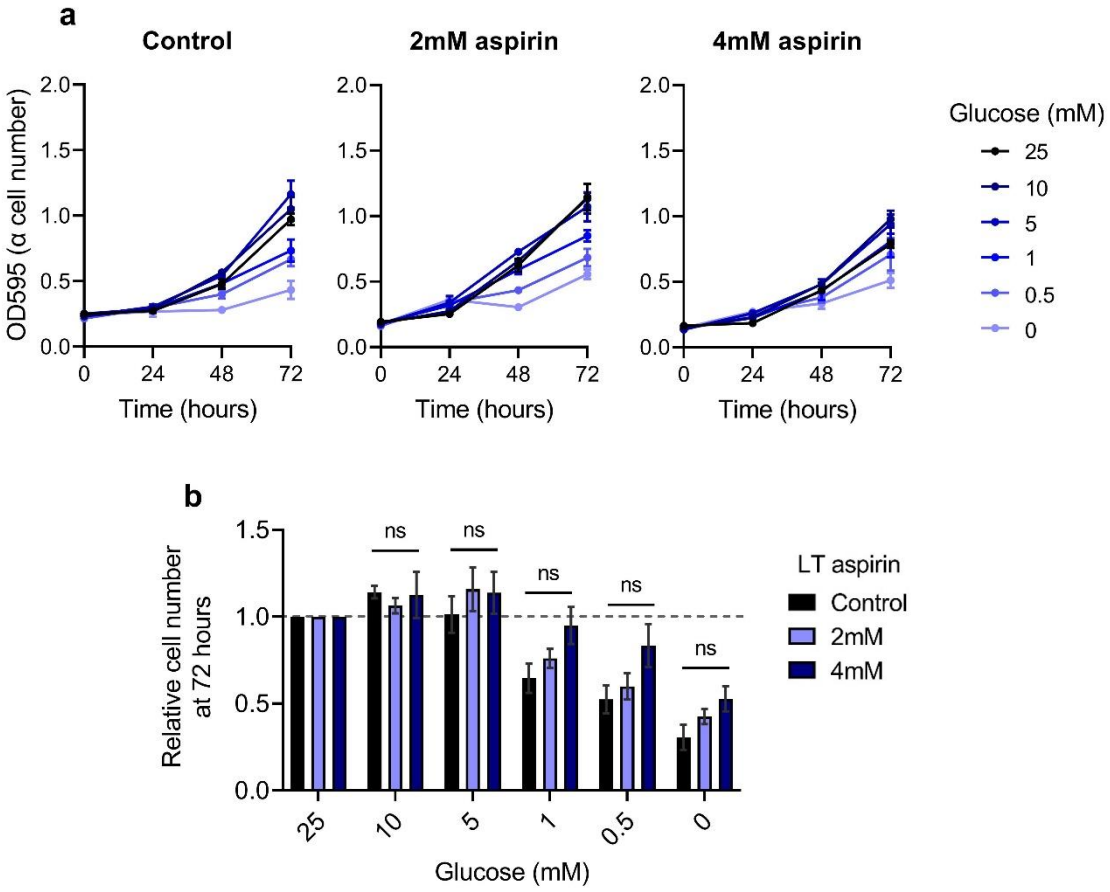

Figure 5.21 Proliferation of the long-term (~52-week) aspirin treated cell line SW620 with depletion of glucose

a Proliferation assay curves measured by optical density of crystal violet staining, showing one replicate representative of three independent experiments, error bars represent standard deviation (n≥3). **b** Cell number relative to 25mM glucose in each long-term (LT) aspirin condition at 72 hours, from three independent experiments. Error bars represent standard error (n=3). ns=not significant.

The effect of aspirin treatment on response to glutamine depletion was also investigated. Long-term (~52-week) aspirin treated SW620 cells were grown in decreasing concentrations of glutamine for 72 hours. Cells were fixed and stained with crystal violet at 0-, 24-, 48- and 72 hours of treatment to produce growth curves (Figure 5.22a). Cell number at the 72-hour time point was calculated in each glutamine concentration relative to the control concentration (2mM, used in normal DMEM) to compare the effect of glutamine depletion in each aspirin condition (Figure 5.22b). These results show that glutamine depletion reduced cell growth, but that the control cells were significantly more affected by glutamine depletion

compared to long-term aspirin treated cells at all concentrations of glutamine (apart from 0mM glutamine, in which all conditions showed no proliferation). This suggests that despite being more sensitive to inhibition of GLS1 (as shown in section 5.3.2), long-term aspirin treated cells appear to be more resistant to glutamine depletion.

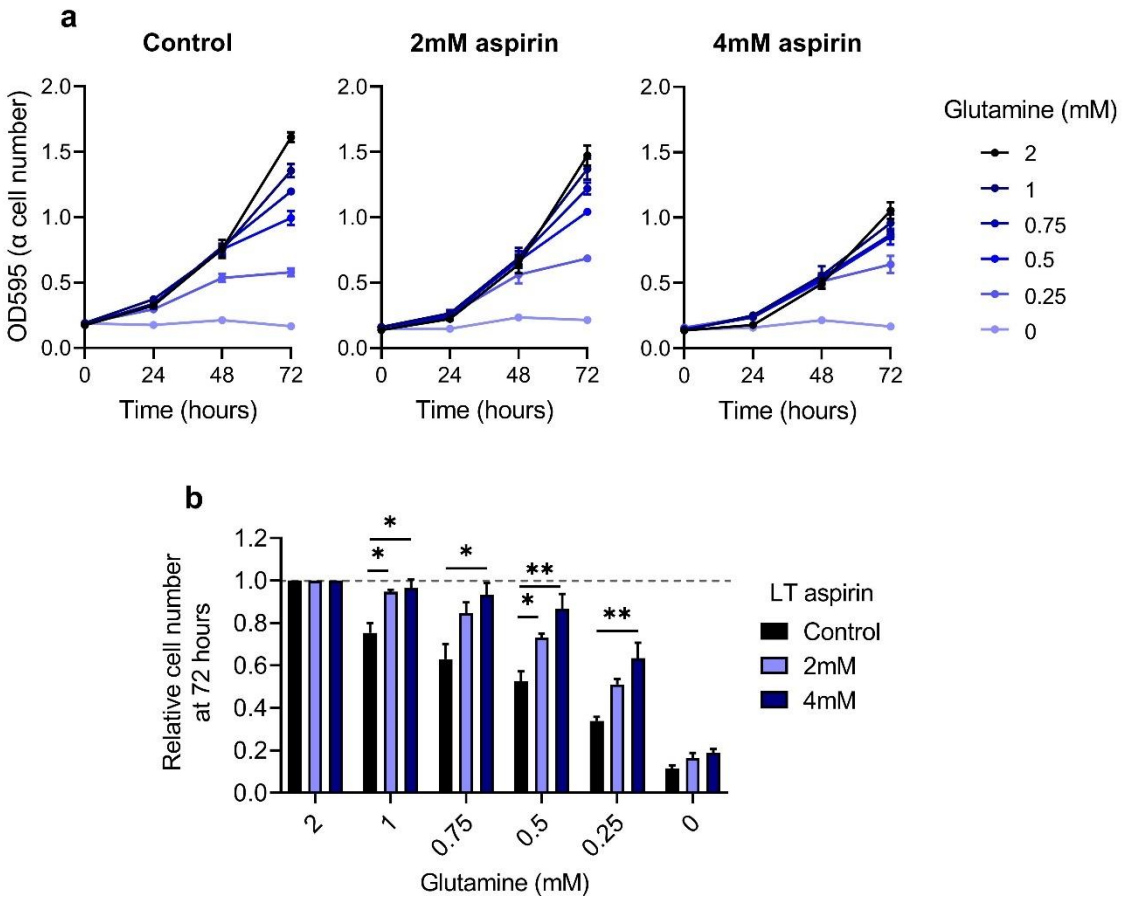

Figure 5.22 Proliferation of the long-term (~52-week) aspirin treated cell line SW620 with depletion of glutamine

a Proliferation assay curves measured by optical density of crystal violet staining, showing one replicate representative of three independent experiments, error bars represent standard deviation (n≥3). **b** Cell number relative to 2mM glutamine in each long-term (LT) aspirin condition at 72 hours, from three independent experiments. Error bars represent standard error (n=3). *=p≤0.05, **=p≤0.01.

5.4 Discussion

5.4.1 Efficacy of combining aspirin with metabolic inhibitors

This chapter has investigated the hypothesis that the metabolic effects of aspirin shown in previous chapters may render cells vulnerable to further metabolic perturbation. This hypothesis was pursued due to a large body of work showing that combinations of complementary metabolic interventions are often more effective than single interventions as they limit the ability of the cells to metabolically adapt. Aspirin is a good candidate for combining with other interventions as its clinical use is well established and it has a good safety profile.

Results in this chapter show that aspirin treatment increases the sensitivity of the cells to two metabolic inhibitors: UK-5099 and CB-839. These drugs were chosen as they target pathways that were shown to be upregulated upon aspirin treatment (glucose utilisation and GLS1 expression respectively). It was thought that the cells may be using these pathways as compensation mechanisms against the effects of aspirin treatment on other metabolic pathways. It was therefore thought that aspirin treated cells may be more sensitive to inhibition of these pathways. Increased sensitivity to these drugs suggests that the cells are more reliant on these pathways when treated with aspirin.

It is of particular interest that aspirin treatment appears to increase the efficacy of CB-839 as this drug is currently in clinical trials and this finding could therefore have direct clinical relevance. Treating patients with a combination of aspirin and CB-839 may prove more effective than treatment with CB-839 alone for CRC. Importantly, both drugs also have relatively good safety profiles and are already used in patients (aspirin routinely, and CB-839 on trial basis), which would make clinical translation of this treatment much less time-consuming and expensive than development of a completely novel therapy. Work published in 2020 by Boku et al. supports our findings that aspirin increases sensitivity of CRC cell lines to CB-839, suggesting that this approach may be broadly applicable to CRC patients, as this increases the number of different cell lines with which this treatment has shown efficacy. Interestingly, they also show that aspirin increases sensitivity to two further metabolic inhibitors: SASP (xCT inhibitor) and AOA (aminotransferase inhibitor) (212). The potential for aspirin to increase the efficacy of existing metabolic therapies may therefore be wide ranging and there may be other potential candidates of drugs that may have enhanced efficacy when combined with aspirin warranting further investigation.

As previously discussed, metabolic interventions that are effective *in vitro* may not necessarily show the same results *in vivo* due to different nutrient availability and metabolic phenotypes of the cells. Findings in this chapter show that the combination of aspirin and CB-839 is effective in HPLM, which has not previously been reported and therefore builds further on the work done by Boku et al. (212). This increases confidence that this combination may be clinically translatable. It also provides confidence in other results gained in this project that have been performed in DMEM, despite the discussed limitations of these conditions. Due to cost and practicality limitations, HPLM cannot currently replace DMEM as the standard laboratory cell culture media. Reproducing similar results in HPLM as found in DMEM supports the continued use of DMEM as a standard condition and shows that it can produce insightful results. Nonetheless, more physiological conditions are certainly worth pursuing and further work, such as investigating the efficacy of this combination in *in vivo* models, will be required to assess the potential of this approach for clinical application.

5.4.2 **Mechanism underlying efficacy of aspirin and CB-839**

Work in this chapter also aimed to investigate in more detail the mechanisms by which aspirin sensitised CRC cells to CB-839. Results show that the combination of drugs induced apoptosis in SW620 cells. However, investigations into the underlying metabolic mechanisms of the combination did not show any clear explanations for its efficacy. One possibility that was investigated was that aspirin and CB-839 may affect TCA cycle function, therefore inhibiting production of sufficient ATP. However, extracellular flux analysis showed that aspirin did not further impact OCR or ECAR upon CB-839 treatment, suggesting the combination does not impair ATP production and in this way induce apoptosis.

Glutamine metabolism and amino acid metabolism more generally, are important for the regulation of ROS levels in cancer cells, for example by the synthesis of ROS scavenger glutathione (302). It was therefore hypothesised that the combination of CB-839 and aspirin may affect ROS balance by inhibiting glutathione production, as both of these drugs inhibit glutaminolysis. Balancing ROS levels is particularly important in cancer cells. Although ROS are important for many signalling pathways involved in tumorigenesis, excessive ROS levels lead to cell death (303). Induction of excessive ROS levels has been shown to underly the efficacy of combining inhibitors of glutamine transporter ASCT2 and GLS1 in cancer cells (292). CB-839 has also been found to induce ROS in pancreatic

cancer cells *in vitro* and the effect of the drug could be rescued by addition of a ROS scavenger (285). It was therefore considered that build-up of ROS levels due to glutathione deficiency could be responsible for the induction of apoptosis seen with aspirin and CB-839. NAC is a ROS scavenger that can regulate ROS levels and has been previously shown to rescue cell proliferation where high ROS levels have been induced (292). It was therefore investigated whether NAC may rescue proliferation in the presence of aspirin and CB-839. However, NAC was not found to have any effect on proliferation in any treatment condition, suggesting excessive ROS levels are not the cause of apoptosis induced by aspirin/CB-839. It would nevertheless be interesting to directly investigate whether ROS levels are affected by treatment with aspirin and/or CB-839, which can be performed by flow cytometry assays, including detection of mitochondrial and total cell ROS levels. Of course, it is possible that the NAC concentration used here was not sufficient to reduce ROS levels in these cells, as only one concentration of NAC was investigated in these experiments (taken from Jin et al. (292)).

Another possibility was that the combination of aspirin and CB-839 led to a critical deficiency in amino acid synthesis. Glutamine is important for the synthesis of many non-essential amino acids (NEAAs), such as asparagine and aspartate. Despite being called non-essential (due the ability of cells to synthesise them), these amino acids are crucial for the proliferation of cancer cells. As aspirin and CB-839 may both inhibit the ability of the cells to synthesise other amino acids from glutamine, it was hypothesised that this may be the cause of the induction of apoptosis. This was investigated by determining whether supplementation of the growth media with NEAAs was sufficient to rescue proliferation in the presence of aspirin and CB-839. However, this was not found to be the case.

One consideration from these results is that some amino acids are not readily transported into the cell, and therefore some components of the NEAA mixture may have remained extracellular and been unable to impact intracellular metabolism, for example this is the case with aspartate (86). Repeating this investigation using cell permeable amino acids such as aspartate β-methyl ester hydrochloride (βMD) (304) to determine if this were able to rescue cell proliferation with aspirin and CB-839 would be of interest, particularly as relative intracellular abundance of aspartate dropped dramatically in the CB-839 treated conditions (as shown in Figure 7.18 and Figure 7.21). It is therefore still possible that lack of ability to synthesise aspartate is the cause of the efficacy of the aspirin CB-839 combination. However, it would still be unclear as to why CB-839 treatment alone

can dramatically reduce aspartate levels, without affecting proliferation or apoptosis. It may be that in the absence of aspirin, cells are able to compensate for the lack of aspartate synthesis and aspirin impairs this ability. Further investigation is therefore required to fully understand the significance of the effect on aspartate abundance.

It was also suggested here that aspirin treatment may prevent the cells from metabolically compensating to CB-839 treatment due to the reduced expression of GPT2 with aspirin. Upregulation of GPT2 has previously been shown to be a compensation mechanism in response to GLS1 inhibition in cancer cells (258). Therefore, if aspirin prevents this response, it could render the cells more sensitive to GLS1 inhibition by this mechanism. However, knockdown of GPT2 by siRNA did not sensitise the cells to CB-839, suggesting the inhibition of GPT2 expression by aspirin was not the sole reason for the sensitisation of the cells to CB-839

To further investigate whether GPT2 is involved in sensitising CRC cells to CB-839, it would be interesting to determine whether overexpression of GPT2 can rescue proliferation upon aspirin and CB-839 treatment. Similarly, it could also be investigated whether overexpression of LAT1 could rescue proliferation, given the downregulation of LAT1 with aspirin (shown in Chapter 3) and the importance of LAT1 in CRC cells for glutamine metabolism (41). These investigations would provide further insight into the mechanisms by which aspirin sensitises cells to CB-839. Aspirin reduces expression of many different metabolic enzymes (as shown in Chapter 3) therefore it could be that a combination of these changes affect the ability of the cells to respond to and compensate for GLS1 inhibition, rather than any one specifically.

5.4.2.1 **Metabolomic analysis and SITA**

Metabolomic analysis of cells treated with aspirin and CB-839, tracing the metabolic fates of glucose and glutamine, was performed in order to assess more broadly the metabolic effects of combining these drugs. However, these results did not provide a clear explanation for the increase in cell death. CB-839 alone appeared to have a similar effect metabolically to the combination of CB-839 with aspirin, despite CB-839 alone having no discernible effect on proliferation or apoptosis. Specifically, CB-839 treatment unsurprisingly inhibited utilisation of glutamine, as well as reducing intracellular abundance of alanine and aspartate. While there was not a large difference in this effect with the addition of aspirin, it could be that aspirin somehow impairs the ability of the cells to metabolically

compensate for the effects of CB-839. What specific compensation mechanisms may be impaired are not clear from these data and therefore have yet to be determined.

Overall, while aspirin does appear to increase the reliance of the cells on activity of GLS1, more work is required to further understand the mechanism by which the combination of aspirin and CB-839 dramatically decreases cell proliferation and induces apoptosis.

One particularly interesting finding from the metabolomic analyses was that aspirin treatment alone impaired the incorporation of glucose carbon into serine and glycine. This was not observed in previous experiments (in SW620 cells in Chapter 4), although this effect was shown in the other two cell lines investigated in the same chapter (LS174T an HCA7). This suggests that aspirin treatment may impair the serine biosynthesis pathway in all three cell lines investigated. As previously discussed in section 4.4, proteomic data showed that aspirin treatment reduces expression of PSAT1 in SW620 cells (Figure 3.5), which catalyses a key step in the serine biosynthesis pathway, which could be a potential explanation for the impairment of this pathway. Another possibility is that aspirin treatment causes the cells to increase entry of glucose into the TCA cycle, potentially to compensate for decreased entry of glutamine carbon, and one of the consequences of this may be diversion of glucose away from other biosynthetic pathways such as serine biosynthesis. As previously discussed, it would be interesting to investigate whether impairment of serine biosynthesis is a key anti-cancer mechanism of aspirin treatment. Experiments would include determining whether the effect of aspirin could be partially rescued by supplementation with cell-permeable serine, as well as investigating the underlying cause for the impairment of the pathway such as by overexpression of PSAT1. The serine biosynthesis pathway is regulated by ATF4 signalling (272) and aspirin was found to inhibit ATF4 signalling in Chapter 3. This could therefore possibly explain the inhibition of serine synthesis with aspirin. Inhibition of serine synthesis has been shown to synergise with serine deprivation in cell lines and this can also be applied to dietary restriction of serine *in vivo*, which leads to decreased abundance of serine in the bloodstream (272). This suggests that aspirin treatment could potentially synergise with serine deprivation in cell lines or dietary serine restriction for CRC therapy.

5.4.3 **Effect of nutrient deprivation**

Work in this chapter also investigated the effect of aspirin treatment on the ability of the cells to cope with nutrient depletion. Key nutrients such as glucose and glutamine are often limited in the tumour microenvironment and this can affect how the cells respond to different therapies. Interestingly, glutamine withdrawal had a greater impact on cell proliferation in untreated cells than aspirin treated cells. This could be due to the fact that not only do aspirin treated cells have a decreased rate of proliferation, they also have decreased levels of glutamine utilisation (as shown in Chapter 4). This means they are less likely to use up the glutamine available to them in the media than the controls cells. Therefore, instead of being more sensitive to low glutamine levels, control cells may deplete glutamine from the medium more quickly and therefore the low glutamine levels in the growth medium may rapidly become limiting for cell proliferation. This effect was also shown in a recent study, which found that *KRAS* mutant CRC organoids had a much higher rate of glutamine utilisation than *KRAS* wild type and were therefore more sensitive to glutamine depletion from growth medium (41). This distinction highlights a limitation of standard cell culture conditions, in that nutrients are depleted and replenished over time, rather than maintained at more constant rates as they would be *in vivo*.

Overall, work in this chapter has shown that aspirin sensitises CRC cell lines to metabolic inhibitors, which supports the proposal that aspirin induces significant metabolic reprogramming in CRC cells, and renders them more reliant on certain metabolic pathways. More importantly, this suggests that aspirin may be clinically beneficial in enhancing efficacy of existing metabolic therapies, including CB-839. This may prove to be a valuable treatment option for reducing disease progression and increasing survival and quality of life in CRC patients, increasing the efficacy of CB-839 and reducing the likelihood of development of resistance. This application is of particular importance due to the currently limited treatment options for advanced CRC.

Chapter 6 General Discussion

This project aimed to elucidate cellular mechanisms of aspirin in a model of long-term aspirin treatment, where CRC cell lines were maintained in aspirin for 52 weeks. Long-term use of aspirin has been shown to significantly decrease the risk of developing CRC approximately 10 years after initiation of treatment (as discussed in section 1.3.1). Development of the long-term aspirin treated cell lines aimed to investigate, for the first time *in vitro,* whether distinct effects occurred in cells that have been exposed to aspirin for an extended period.

Proteomic analysis of long-term aspirin treated SW620 cells that was performed previously in the lab by Dr Eleanor Mortensson highlighted a potential impact of long-term aspirin on cellular metabolism. Due to the importance of metabolism in cancer biology and potential for new therapies (discussed in section 1.2) metabolic reprogramming of cancer cells by aspirin was investigated in this project. Understanding the effect of aspirin on cancer cell metabolism could increase understanding of the cellular mechanisms of aspirin in cancer prevention. Understanding this is important for optimised use, such as improved patient stratification, timing of treatment and potential combination therapies.

6.1 Aspirin and metabolic reprogramming in CRC cells

Initial investigations in Chapter 3 confirmed that long-term aspirin exposure leads to regulation of a number of metabolic enzymes. Interestingly, this effect was also seen with short term (72-hour) treatment, suggesting the effect on cellular metabolism is not solely a result of long-term aspirin exposure. These results add to an increasing number of studies in the literature highlighting regulation of metabolic enzymes in cancer cells when treated with aspirin, as reviewed in section 1.4. Of particular note was the induction of GLS1 expression, which occurred consistently with both long- and short-term aspirin treatment across multiple cell lines. This was recently corroborated by findings published by Boku et al. in 2020 showing that aspirin induces expression of GLS1 in other CRC cell lines as well (212).

GLS1 is generally thought to be an oncogene that promotes tumorigenesis, so it is somewhat counterintuitive that it is upregulated with aspirin treatment, which is known to have anti-tumorigenic effects. Along with the observation of reduced glutaminolysis with aspirin shown in Chapter 4, this led to hypothesis that GLS1 upregulation may be an indirect effect of aspirin treatment, perhaps to compensate

for other metabolic effects of aspirin. The maintenance of GLS1 upregulation up to 72 hours post aspirin removal (as shown in Figure 3.12) may also suggest that this is due to an indirect effect of aspirin treatment. It would be interesting to investigate further the length of time for which GLS1 maintains upregulation following removal of aspirin and to determine what specifically this is in response to, as data here suggest it is does not occur in response to inhibition of ATF4 signalling or downregulation of GPT2.

It is important to stress that enzyme expression levels cannot report metabolic pathway activity, and therefore this project directly investigated the effect of aspirin treatment on activity of metabolic pathways (the first study to do this to our knowledge). Using a combination of extracellular flux analysis and stable isotope tracer analysis (SITA), this project has shown that aspirin impacts nutrient utilisation of CRC cells; SITA data show that glutaminolysis was reduced with aspirin treatment (as shown by decreased ^{13}C labelling in glutamate and TCA cycle metabolites), despite seeing strong upregulation of GLS1. This highlights the issue with inferring pathway activity from enzyme expression levels alone. This also supports the hypothesis that GLS1 induction is not a direct effect of aspirin treatment but most likely a compensatory response, as activity of the pathway is actually decreased.

Although expression of GLS1 protein is increased with aspirin, it is interesting to speculate whether the activity of the enzyme is affected. As discussed in section 1.2.8.3, activity of glutaminases is affected by post-translational modification, which can be regulated by pathways such as NFκB. Aspirin has been shown to modulate NFκB signalling in a context-dependent manner (described in section 1.3.2.2), therefore it is possible that aspirin treatment leads to decreased activity of the GLS1 enzyme via activation of NFκB, resulting in subsequent upregulation of the protein to compensate for the loss of activity. It would be interesting to investigate this possibility further, for example by determining GLS1 enzyme activity in the presence of aspirin treatment using an enzyme activity assay, and the effect of aspirin on NFκB signalling in these cells by using an NFκB reporter assay.

SITA data also highlighted an increase in entry of glucose into the TCA cycle with aspirin treatment. It is hypothesised that this is a compensation mechanism in response to decreased entry of glutamine-derived carbon, in order to maintain carbon flux through the cycle. Interestingly, extracellular flux analysis showed no

effect of aspirin on OCR or ECAR, suggesting no change in oxphos or lactate production. This suggests that by switching the carbon source for the TCA cycle and replacing glutamine carbon with glucose carbon, cells are able to maintain levels of TCA cycle flux and oxphos in order to maintain ATP production in the presence of aspirin. This highlights the extent to which cancer cells are able to adapt their metabolism in response to environmental perturbations, in order to maintain activity of the necessary metabolic pathways and maximise proliferation. Although aspirin treatment does reduce cell proliferation, it may have a stronger effect if the cells were unable to induce compensatory metabolic pathways.

A summary of the metabolic reprogramming effect of aspirin treatment as shown by the data in Chapter 3 and Chapter 4 of this project is shown in Figure 6.1.

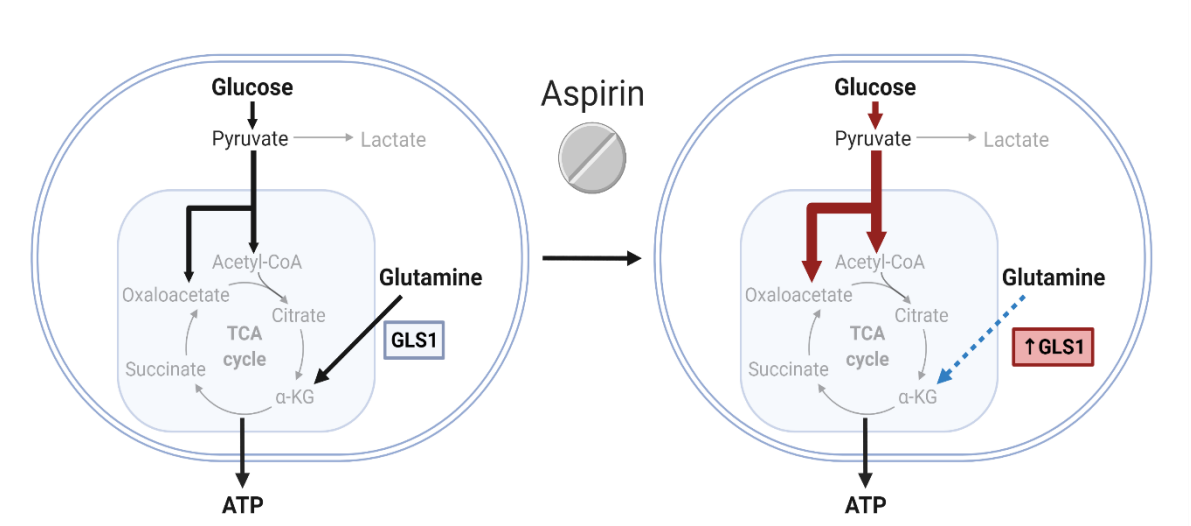

Figure 6.1 Summary of the effect of long-term aspirin exposure on metabolic reprogramming in CRC cells

Data in this project have shown that aspirin treatment leads to regulation of metabolic enzymes, particularly the upregulation of glutaminase 1 (GLS1). It has also been shown that aspirin leads to a decrease in glutaminolysis (indicated by blue dotted arrow) and an increase in glucose entry into the TCA cycle (indicated by red arrows). ATP production from oxphos (as measured by OCR) was not found to be affected by aspirin. It is therefore hypothesised that aspirin leads to an increase in GLS1 expression and glucose utilisation as compensatory responses to inhibition of glutaminolysis, and that this allows maintenance of TCA cycle flux and ATP production from oxphos in the presence of aspirin. Created with BioRender.com.

SITA and extracellular flux analysis were performed in long-term aspirin treated cells but not in short-term treated cells. Data in Chapter 3 show that short-term aspirin is sufficient to regulate metabolic enzymes, which suggests short term aspirin would have a similar effect on nutrient utilisation as long-term treatment. However, further experiments would be required to confirm this. This is important for determining the clinical relevance of the metabolic effect of aspirin. For example, whether it is only applicable to patients who have taken aspirin for a long time period, or whether acute use of aspirin could have the same beneficial effects.

6.2 Combining aspirin with metabolic inhibitors

Having established that aspirin treatment induces metabolic reprograming in CRC cells, it was hypothesised that this effect could be utilised in order to increase efficacy of existing metabolic inhibitors. It was found that aspirin treatment leads to an increase in glucose utilisation and GLS1 expression and as a result, it was suggested that the cells would be more reliant on these pathways in the presence of aspirin and therefore be more sensitive to targeted inhibitors. The effect of aspirin treatment was therefore investigated in combination with UK-5099 and CB-839, inhibitors of glucose utilisation (via MPC) and GLS1 respectively. Mechanisms of action of these two inhibitors are illustrated in Figure 6.2.

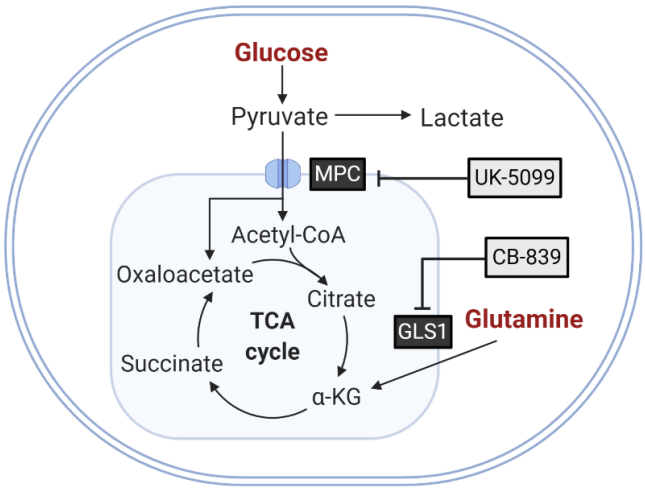

Figure 6.2 Mechanisms of action of two metabolic inhibitors combined with aspirin

UK-5099 inhibits the mitochondrial pyruvate carrier (MPC), therefore inhibiting entry of pyruvate into the TCA cycle. CB-839 inhibits glutaminase 1 (GLS1).

Importantly, results in Chapter 5 confirmed that aspirin treatment increased sensitivity of CRC cell lines to both of these inhibitors. This supports the hypothesis that aspirin treatment makes the cells more reliant on these pathways. Interestingly, a similar effect was also found with short-term aspirin treatment. This suggests that combining aspirin with complementary metabolic inhibitors could be an effective therapeutic approach and could include patients who had not previously taken aspirin. This is reassuring and suggests that short-term aspirin has a similar effect on metabolic reprogramming and nutrient utilisation as shown with long-term aspirin in Chapter 4, despite this not having been directly investigated.

These results add to a large body of work showing efficacy of various combinations of drugs targeting metabolism (as discussed in section 5.1), as well as work showing that aspirin can enhance efficacy of a range of cancer treatments including chemotherapies (192, 305), targeted therapies (306), immunotherapies (271) and metabolic inhibitors (212).

While UK-5099 is not used clinically, these results suggest that aspirin treated cells are more sensitive to inhibition of glucose metabolism, and therefore this principle may be applicable to other clinical inhibitors of glycolysis, such as 2-DG. CB-839 on the other hand is under investigation in clinical trials for various cancers, and therefore it is of significant clinical relevance that aspirin may enhance its efficacy. Interestingly, the study published by Boku et al. in 2020 also found that aspirin increased sensitivity of CRC cells to CB-839 (212). Different cell lines were used in this study, suggesting this effect may be broadly applicable to CRC and not necessarily specific to certain subtypes, therefore suggesting that this approach may benefit a large proportion of CRC patients rather than only particular subgroups.

Further investigations in this project showed that the combination of aspirin and CB-839 induces apoptosis in SW620 cells, however investigations into the underlying mechanism of this effect were inconclusive. However, importantly, it was shown that the combination of aspirin and CB-839 was effective at reducing cell proliferation when the cells were grown in HPLM, which has a metabolite composition that closely reflects human plasma. Excitingly, this result provides more confidence that this approach may be effective in treating patients.

6.3 Remaining questions and future work

A key question emerging from this work is whether the combination of aspirin and CB-839 will be an effective treatment for CRC. Work to investigate this question should focus studying the effects of this combination in more physiological models, to build on the work here using physiological cell culture medium. For example, studying the effect of the combined treatment in a variety of patient derived organoids or patient derived xenografts will help identify whether there is a difference in response between tumours with different genetic backgrounds or CMS subtypes, improving the process of patient stratification and increasing the potential for personalised medicine. Investigations are ongoing in collaboration with the Owen Samson lab at the Beatson Institute (Glasgow, UK), to determine whether the treatment with a combination of aspirin and CB-839 is tolerable and safe, as well as an effective treatment for inhibiting tumour progression in mouse models of CRC. If further investigations show promising results, this could warrant a clinical trial investigating the efficacy of aspirin and CB-839 treatment in CRC patients.

As discussed in section 1.2.8.2, glutamine metabolism is important for the maintenance of normal healthy intestinal tissue, and a large proportion of glutamine metabolism in the body occurs within the intestine. The epithelial lining of the intestine has a rapid turnover due to exposure to the digestive tract. Inhibition of GLS1 with CB-839 could therefore impact normal intestinal epithelial homeostasis. While CB-839 has thus far been found to be relatively well-tolerated, this issue could explain the side-effects relating to the digestive system that have been reported with the drug, such as nausea, loss of appetite and diarrhoea (307). Phase I trials of the drug involving dose escalation studies are ongoing in order to fully determine the risks and side effects.

What also remains to be determined is the cellular mechanism by which the combination of aspirin and CB-839 reduces proliferation and induces apoptosis. Interestingly, intracellular aspartate abundance was dramatically reduced by CB-839 treatment (see Figure 7.18 and Figure 7.21). It would therefore be interesting to investigate whether cell-permeable aspartate may be able to rescue proliferation with aspirin and CB-839 treatment. Lack of aspartate could affect ability of the cells to synthesise nucleotides (301), which could be a possible explanation for the reduction in proliferation with aspirin and CB-839.

Another possible mechanism to investigate is the effect of aspirin on ATF4 signalling. A recent study found that inhibition of ATF4 signalling was synergistic with inhibition of GLS1 (291). As data in Chapter 3 suggested that aspirin inhibits ATF4 signalling, this mechanism could be linked with the synergy of aspirin and CB-839. Interestingly, Boku et al. reported the opposite effect, that aspirin induced ATF4 signalling in CRC cells (212). This suggests that this effect may be cell line specific or there may be differences between long-term and short-term aspirin treatment. GLS1 inhibition has also been found previously to synergise with mTOR inhibition (288, 289), and aspirin has been shown to inhibit mTOR signalling in work by Din et al. (227). Together, these findings suggest that the effects of aspirin on mTOR and ATF4 signalling, and how these interacts with CB-839 sensitivity, warrant further investigation. If this mechanism were further understood, it could help to identify other combinations of existing drugs that could be repurposed for the treatment of advanced CRC, for which there are currently limited treatment options.

Another interesting avenue for future investigations will be whether drugs similar to aspirin have similar effects on cellular metabolism, and whether they can also increase efficacy of CB-839. Of particular interest is 5-aminosalicylic acid (5-ASA), also known as mesalazine or mesalamine, which is an NSAID that is structurally similar to aspirin (see Figure 6.3). Unlike aspirin, 5-ASA is a weak inhibitor of COX enzymes and therefore does not have the same side effects that are associated with aspirin use such as increased risk of severe bleeding, which limit the clinical utility of aspirin as a prophylactic agent for CRC (308).

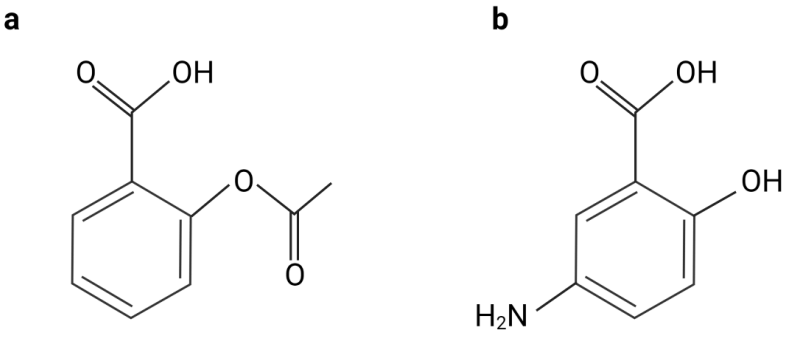

Figure 6.3 Chemical structures of aspirin (acetylsalicylic acid) (a) and 5-ASA (5-aminosalicylic acid) (b)

Created with BioRender.com.

5-ASA is used routinely for the treatment of inflammatory bowel disease (Crohn's disease and ulcerative colitis). These conditions lead to an increased risk of developing CRC, known as colitis associated cancer (CAC) (309). There is evidence to suggest that 5-ASA reduces risk of CAC (310, 311), although it is not clear whether 5-ASA is effective in preventing CRC in patients who do not have inflammatory bowel disease. Recent work in the Williams lab has shown that 5-ASA can reduce the cancer stem cell phenotype in colorectal adenoma cells, suggesting it might slow progression of benign adenomas into invasive carcinomas (308). Unpublished proteomic data produced in the Williams lab has also shown that short-term 5-ASA treatment regulates metabolic enzymes in colorectal adenoma cells, and suggest that 5-ASA may have a similar effect on metabolism, including upregulation of GLS1 and downregulation of GPT2, LAT1 and PDK1. These results have also been validated by western blotting and qPCR (Lucy Jobson-Wood, unpublished). As 5-ASA is more well-tolerated than aspirin and has fewer side effects, it will be worthwhile to investigate whether 5-ASA has a similar effect on metabolic reprogramming in CRC cells in more detail, such as using extracellular flux analysis and SITA. It would also be important to investigate whether 5-ASA can also increase the efficacy of CB-839 in CRC cell lines, as this may be a more safe and well-tolerated treatment than combining CB-839 with aspirin.

6.4 **Concluding remarks**

This project has outlined a detailed model by which CRC cell lines undergo metabolic reprogramming when treated with aspirin. This is a significant contribution to a large body of work attempting to further elucidate mechanisms of action of aspirin on tumour cells, and how these may relate to the use of aspirin in cancer prevention and treatment. This work provides insight into the therapeutic use of aspirin to reprogramme tumour cell metabolism and emphasises its potential for increasing efficacy and reducing side effects of both novel and existing therapies.

Of particular importance, it is reported here that aspirin increases sensitivity of CRC cells to CB-839, which has significant clinical implications and potential for translation. This project has paved the way for future investigations to determine the clinical utility of this approach, which would be rapidly translatable due to the well-established clinical use of aspirin and the ongoing clinical trials for CB-839.

This approach has the potential to improve outcomes for CRC patients, particularly those with advanced disease, for which current treatment options are very limited. It could also provide a tolerable preventative measure for those at high risk of developing CRC, such as those with Lynch syndrome or diagnosed with multiple benign polyps in the colon at bowel screening clinics.

Chapter 7 Appendices

7.1 Appendix 1

Significantly regulated proteins in both long-term (52-week) 2mM and 4mM aspirin treated SW620 cells, from proteomic data set produced by Dr Eleanor Mortensson (unpublished).

Table 7.1 Regulation of proteins in proteomic data set of long-term (52-week) aspirin treated SW620 cells.

Includes only proteins significantly regulated (log fold change>1.4, t test p-value<0.05) in both 2mM and 4mM aspirin treated cells. Key central carbon metabolism enzymes shown in Figure 3.4 are highlighted in yellow.

		2mM/0mM aspirin		4mM/0mM aspirin	
Best Accession	Gene symbol	Log_2 fold change	T test	Log_2 fold change	T test
Q8WTS1	ABHD5	-0.86759788	0.02848584	-2.06146649	0.031441407
P33121	ACSL1	0.51295313	0.000731105	1.593629994	0.001935896
Q9ULC5	ACSL5	0.586985907	0.002610386	1.553450139	0.001547599
Q9NR19	ACSS2	0.68930781	0.00125447	0.76667801	0.017761108
P07311	ACYP1	0.590541204	0.0021616	1.378533644	0.00013603
Q13444	ADAM15	-0.63494631	0.00190657	-1.74330389	4.76993E-05
O75689	ADAP1	-1.18310319	0.00200039	-1.03931975	0.000579751
Q96A54	ADIPOR1	-0.59906514	0.006769716	-0.5441016	0.000460585
Q86V24	ADIPOR2	-1.90269398	0.00145445	-3.53032709	0.00145307
Q02952	AKAP12	0.557358553	0.021153507	2.103087338	0.021398808
Q04828	AKR1C1	0.838007556	0.005417627	1.427824524	0.000469499
P13196	ALAS1	1.022332888	0.000213035	1.758061645	4.71015E-05
P47895	ALDH1A3	0.979567403	0.001363416	1.580273935	0.000215906
Q92685	ALG3	0.509538707	0.047354461	1.259615177	0.00022252
Q5XXA6	ANO1	-1.27062034	0.000367046	-2.1254935	0.015459335
A0A0S2Z377	ANXA6	-0.96418339	0.021915305	-1.01522294	0.010167509
P56377	AP1S2	1.145650759	0.000665032	0.570226464	0.008415673
P02649	APOE	0.839480713	0.005047091	2.065453776	0.000126509
P78540	ARG2	1.279220821	0.002136859	1.548880202	0.00934285
V9GYF0	ARHGEF2	-0.71405837	0.004368338	-0.82632979	0.04706704
P49407	ARRB1	0.504988734	0.000822019	0.793721204	0.000162462
O95671	ASMTL	0.595109988	0.003069132	0.911757387	0.000638513
Q5SQI0	ATAT1	0.928114527	0.004846223	1.472902998	0.000960666
O00244	ATOX1	0.631108992	0.00061111	1.39073715	0.03009468
P23634	ATP2B4	0.673143954	0.001296155	1.470640168	0.036006789
O94766	B3GAT3	0.710848374	0.001163649	1.288879833	0.000119896
O43505	B3GNT6	0.867031338	0.015333479	1.015976974	0.016136383
O43286	B4GALT5	0.849580232	0.00867484	1.640145727	0.001481167
O14874	BCKDK	0.521456506	0.030197887	0.822031013	0.01276674
A0A024RDG9	BDH2	-0.72079057	0.008510733	-0.74028185	0.003645579
Q8TD16	BICD2	0.547074559	0.000598656	0.717369853	0.009437674
Q96D05	C10orf35	0.892102565	0.008173026	2.135379672	0.001155002
A0A024R978	C1orf24	-1.08880291	0.000513467	-2.33035894	7.95637E-06
Q5T0Z8	C6orf132	-0.63831967	0.004315723	-0.77909438	0.014569747
Q6UWU4	C6orf89	0.873705224	0.001015633	2.373511186	0.000144221
Q9BVT8	C7orf21	0.59130684	0.0075026	1.063420076	0.000933036

P16070	CD44	1.774978679	0.001134034	2.196353155	0.008980205
P19256	CD58	0.586553663	0.004472318	0.789689847	0.000362444
P27701	CD82	1.171304933	0.005371323	1.364188847	0.004189068
P32320	CDA	1.145863186	0.000164962	2.132742064	1.45754E-05
Q99618	CDCA3	0.69264669	0.019960082	0.759493144	0.005141664
P12830	CDH1	-2.1750688	0.000741075	-2.11311771	0.023522577
Q9UQ88	CDK11A	0.600829092	0.002447008	1.356177416	0.002842001
Q14011	CIRBP	-0.50261907	0.002606122	-1.10811734	0.000241813
Q8NCR9	CLRN3	-0.74733892	0.000193922	-1.43207798	0.01090151
Q8IYK4	COLGALT2	0.489309902	0.000748178	1.233045782	0.042878972
Q5HYK3	COQ5	0.888094636	5.77974E-05	0.617754632	0.001229997
E9PD68	CRMP1	-1.39757557	0.000733329	-1.72463911	0.003821807
O75718	CRTAP	0.585383354	0.005385251	1.180316472	0.001630317
P35221	CTNNA1	-1.11961438	0.000936416	-1.11584441	0.00088455
P35222	CTNNB1	-0.85931931	0.005282715	-0.66799493	0.004953668
P07711	CTSL	0.68602745	0.034462246	2.13047493	0.002375222
A0A097ZMP6	CUX1-RETa	0.778787679	0.032131862	3.117977222	0.000125568
O43169	CYB5B	0.54147515	0.00101868	0.688976537	0.005795734
Q02318	CYP27A1	0.510056442	0.000399061	1.187863439	4.15555E-05
A0A024R529	DAK	-0.51268131	0.018023849	-0.69260198	0.005608824
B1AKK2	DDAH1	-1.09344618	0.00540696	-2.08235402	0.000253335
O94830	DDHD2	0.589431886	0.009768802	0.903965412	0.000473016
Q9NR30	DDX21	-0.56533836	0.003546284	-0.89654696	0.003900903
Q96LJ7	DHRS1	0.890141916	2.88568E-05	1.359708232	0.000326361
Q5CZB5	DKFZp686M0430	0.506159576	0.028184657	1.95514848	0.016908006
Q63HQ8	DKFZp686M21196	-0.99118269	0.03127114	-0.49901404	0.029313917
Q68D38	DKFZp686O15119	1.439096177	0.000119527	2.38269295	0.002590556
P25686	DNAJB2	0.546173966	0.02065952	1.144262962	0.007533747
Q9UQ16	DNM3	1.30853531	0.000313098	2.25969303	4.45699E-05
Q92608	DOCK2	0.839620475	0.000152115	1.131758406	2.67855E-05
P51452	DUSP3	0.494083945	0.00535224	0.756066887	0.000859187
P51808	DYNLT3	0.542371003	0.002669866	1.429800882	0.000275825
Q9UNE0	EDAR	0.844411022	0.006193592	0.685022619	0.013749451
P98172	EFNB1	-0.50205479	0.029673296	-1.18814164	0.001028054
Q9GZV4	EIF5A2	0.689237093	0.029146679	1.150138204	0.017926246
P50402	EMD	0.694129688	0.004743503	0.862513304	0.001828148
H7C2K6	EPB41L1	1.003514897	0.001811594	0.953795578	0.006157173
P16422	EPCAM	-0.7568626	0.00061444	-1.52348969	0.012311876
Q8TE68	EPS8L1	-0.8322759	0.000163328	-0.96063186	0.00962952
B1AK53	ESPN	-1.78285361	0.001872806	-2.28900067	0.002702978
Q9H6T0	ESRP2	-0.51218783	0.018264507	-0.61891813	0.014801292
Q9Y624	F11R	-1.49713472	0.000145822	-1.87995511	0.005047503
Q7Z309	FAM122B	0.653910716	0.014523614	3.192017355	0.000662958
Q96ND0	FAM210A	0.508596273	0.034538248	0.659593255	0.024303389
Q8NEZ5	FBXO22	0.527324069	0.00224323	0.767588542	0.000465104
Q9NRD1	FBXO6	0.618117209	0.026096503	1.564906634	0.000446724
Q9NYL4	FKBP11	0.489204892	0.012890913	0.981186144	0.002403759
Q9NWM8	FKBP14	0.892647272	0.001182064	2.824715919	0.00031478
Q9Y680	FKBP7	0.709159512	0.000604733	0.855569391	0.005799341
O95302	FKBP9	-0.87752601	0.006868021	-0.87164	0.016769556
O75955	FLOT1	-0.5798099	0.001077367	-1.33142955	0.002260798
Q96PY5	FMNL2	0.505438616	0.003681354	0.878973684	0.000141975
Q8IVF7	FMNL3	0.516156242	0.031001667	0.976759525	0.001037128
P15328	FOLR1	-1.2145109	0.011308814	-2.85907776	0.00331216
O75600	GCAT	0.639676522	0.005284927	1.288620784	0.002957228
Q9Y2T3	GDA	1.529219051	0.004974141	2.179782032	0.000510415
O94925	GLS	1.279386474	0.000891622	1.991521543	0.004058203
Q68CQ7	GLT8D1	0.67220323	0.00860085	0.587242426	0.01121574
O60547	GMDS	-0.56239418	0.00321844	-0.83306301	0.010650654

O60234	GMFG	1.56045354	0.000130135	1.715988244	0.000803062
Q9Y223	GNE	1.284430665	3.3058E-05	1.916074849	0.000495441
P59768	GNG2	0.989424659	0.004601232	2.193788832	0.001159664
Q8NFJ5	GPRC5A	-0.73382546	0.001785533	-1.44728378	0.016330527
Q8NBI5	hCG_39762	-0.68593429	0.015796664	-1.4893426	0.007003265
P51858	HDGF	-0.60150576	0.000386555	-0.79121522	0.035648845
P12277	HEL-S-29	1.132505616	0.00440252	1.32051611	0.002046139
P21980	HEL-S-45	1.0501834	0.001895483	2.344309932	0.005193709
P40121	HEL-S-66	0.533102809	0.00160379	0.984180796	0.000216866
Q16777	HIST2H2AC	-0.48688677	0.009202697	-0.51516852	0.008482169
P19367	HK1	0.494178092	0.000526011	0.787304338	0.011606539
Q96ED9	HOOK2	-0.51836535	0.000630344	-0.58813777	0.002499484
P54652	HSPA2	0.543849244	9.1116E-05	1.023530442	0.001639789
Q05084	ICA1	-0.67497482	0.000505857	-1.33207493	0.000244173
Q70UQ0	IKBIP	0.839299261	2.99064E-05	1.1187224	5.24709E-05
Q14116	IL18	-0.57363389	0.007644855	-1.21975203	0.015183812
Q9BT40	INPP5K	0.518498834	0.002677874	0.946149144	0.00029668
Q13568	IRF5	0.600504681	0.009896336	0.918334693	0.001215776
O14896	IRF6	-2.59927701	0.00016134	-2.52561355	0.00898275
P14923	JUP	-0.96922916	0.002451938	-0.97203833	0.001155571
P32004	L1CAM	-0.58433016	0.002623508	-1.54363088	0.003864565
Q9UN81	L1RE1	-0.51298294	0.014614787	-0.92177969	0.000821322
Q9UHA4	LAMTOR3	-0.52696051	0.027053059	-0.51906834	0.002027393
Q6P1M3	LLGL2	-0.64605345	0.000216622	-0.99333475	0.00547481
A0A024R9V7	LOC92689	0.545342163	0.003368731	1.152099987	2.64389E-05
B2RTQ5	LRRC16A	-0.50284944	0.00452445	-0.61001819	0.01145841
Q9BWS2	LSR	-0.53617067	0.002355532	-1.18709776	0.001200189
Q9UNF1	MAGED2	1.072135051	0.008035223	1.854640263	0.00160967
Q14244	MAP7	-0.82550502	0.004280264	-0.61134275	0.025013089
O15264	MAPK13	-0.71623964	0.000872563	-1.00678024	5.95394E-05
Q6P0Q8	MAST2	0.808479038	0.002191191	1.114100435	0.001546643
Q9HCC0	MCCC2	-1.3623165	2.58112E-06	-1.56778668	0.006249487
Q96S19	METTL26	-0.56168051	5.56022E-05	-1.00799646	0.04029155
O75121	MFAP3L	-0.8857872	0.009972404	-1.31458973	0.002175882
Q09327	MGAT3	-0.48781992	0.016102676	-1.00326699	0.002731611
P10620	MGST1	0.590836458	0.045385273	1.314970595	0.01646202
Q9UJG1	MOSPD1	0.873791808	0.041764075	1.595489431	0.002207687
Q9H3R2	MUC13	0.705590432	0.004554918	1.781483255	0.018073434
E5KP27	MUTYH	-0.81324584	0.030364898	-1.01702299	0.019631304
Q9BQG0	MYBBP1A	-0.5228563	0.012851442	-1.00857149	0.01818393
Q8WUY8	NAT14	0.654972193	0.001605055	1.292550745	0.000362994
Q9BTE0	NAT9	0.841473769	0.011844043	1.159220952	0.00906284
Q6PIU2	NCEH1	0.576991604	0.00729233	1.460121983	0.000846441
D3DVC4	NES	-0.5554331	0.010518891	-0.60099023	0.010914982
Q969F2	NKD2	0.73035048	0.030810289	0.962156471	0.01296283
P61916	NPC2	0.58173986	0.009559764	1.062418244	0.000823502
A0A024RBG1	NUDT4	-0.51103878	0.037690911	-0.75290136	0.000854568
P04181	OAT	1.094606214	0.000111031	1.532106714	7.00038E-05
Q9BYG5	PARD6B	-0.49188462	0.00137085	-0.87631651	0.007196586
Q96KB5	PBK	0.498660497	0.0030267	0.917481714	0.006786068
P11498	PC	1.094389804	0.000403151	1.280461982	0.000366459
Q15118	PDK1	-0.70733289	0.003287201	-1.18572567	0.001589109
O00151	PDLIM1	0.695266823	0.0117761	1.629458137	0.000300449
Q53GG5	PDLIM3	0.875221681	0.002937723	1.936250758	0.000861164
P50479	PDLIM4	0.684258921	0.001232576	0.915540189	0.019997549
Q6PCE3	PGM2L1	0.732641973	0.001313615	1.195257032	4.25052E-05
Q6NSJ2	PHLDB3	0.724531302	0.023815194	1.437588256	0.000128331
Q9NRD5	PICK1	-0.49349027	0.025480679	-1.00716928	0.001860316
A6PW57	PIP5K1A	-0.51495668	0.002976676	-0.98981285	0.002384026

O00625	PIR	0.492664408	0.00548466	0.994946005	0.000823862
Q9Y446	PKP3	-0.65888887	0.026005108	-1.02131692	0.01416922
Q8NCC3	PLA2G15	0.621126853	0.01795909	1.173322904	0.00185952
Q6P4A8	PLBD1	0.884076368	0.003365226	2.03767322	9.41077E-05
Q15149	PLEC	0.80740212	0.012302342	1.365035486	0.011937738
Q96AC1	PLEKHC1	0.489671317	0.010949335	0.878780014	0.012272568
Q99541	PLIN2	-1.36109138	0.000107716	-2.36073834	1.458E-05
O00469	PLOD2	0.696269888	0.014451595	1.359526928	0.001288785
O15162	PLSCR1	0.614785939	0.01244919	0.744124667	0.008783388
Q8IY17	PNPLA6	0.527553305	2.61039E-06	0.71723674	0.003796079
O00592	PODXL	-0.56397982	0.001222664	-1.65757971	0.0028281
Q9GZS1	POLR1E	-0.5264384	0.014829991	-0.85664144	0.014081663
Q15165	PON2	0.511106285	0.005428437	0.746916193	0.000496294
P16435	POR	0.607886309	0.001729558	1.244605249	0.000198692
P49593	PPM1F	0.513309943	0.00305232	0.831903931	0.001913962
Q9P0J1	PPM2C	0.613094396	0.002335502	1.127627206	0.029644994
O60831	PRAF2	0.745304386	0.000743003	1.55665191	0.006994175
P42785	PRCP	0.699172272	0.008790613	0.824349629	0.002676983
P07478	PRSS2	-2.74227781	0.005574367	-2.81028277	0.005598757
Q15274	QPRT	0.715145194	0.02646733	1.528828552	0.008679092
Q9NX57	RAB20	-1.12094175	1.96701E-06	-2.12148445	0.000767298
Q13637	RAB32	0.652895495	0.015152484	1.31365856	0.000375721
P09455	RBP1	1.19485503	0.000514012	2.10204674	0.005753314
Q93062	RBPMS	0.94864419	0.033873523	1.122008628	0.009754298
Q14257	RCN2	0.538623582	0.04047159	1.562085725	0.002104402
Q8IZV5	RDH10	0.586498872	0.000686408	1.615913801	0.00095596
Q9BRS2	RIOK1	-0.76616214	0.000517307	-0.71953141	0.007499855
Q8NCN4	RNF169	-0.56715814	0.016143462	-0.6634705	0.002169348
Q9BXT8	RNF17	0.783804802	0.003219722	0.923584583	0.029314381
P23921	RRM1	0.78035873	0.014331567	2.138863865	0.000277908
O76021	RSL1D1	-0.7144086	0.040678344	-0.91377907	0.028380143
Q8WXA3	RUFY2	0.664452246	0.003288724	1.401439322	0.001592572
Q9HCY8	S100A14	-2.26844493	0.002115937	-2.66119625	0.000373137
P33764	S100A3	1.238940125	0.021896323	0.92294456	0.040316
O95171	SCEL	-0.70252911	0.035243369	-1.35693224	0.010714809
Q9BY50	SEC11C	-0.77191541	0.002402057	-1.22114345	0.031243431
Q13228	SELENBP1	0.740058377	0.006599674	0.69554701	0.01560005
Q14563	SEMA3A	0.531471114	0.016796124	2.528511098	0.000829922
Q9C0C4	SEMA4C	-0.5583912	0.007527264	-1.17334583	0.04553368
P36952	SERPINB5	-2.24060003	0.000141831	-2.35955995	0.000845716
Q587I9	SFT2D3	-0.60336678	0.005976592	-0.74372346	0.002772872
Q9BRG2	SH2D3A	-0.6114378	0.023601278	-1.38880725	0.007037675
Q5TCZ1	SH3PXD2A	0.654542996	0.005889638	0.77948196	0.010516466
A1X283	SH3PXD2B	0.606666143	0.015062507	0.899236189	0.012367493
A0A024R6R1	SHCBP1	0.756892453	0.001421683	0.752677429	0.011050103
Q6P1M0	SLC27A4	0.595660736	0.015533466	1.515347481	3.08923E-05
P11166	SLC2A1	0.670746695	0.041035722	1.126282073	0.000256003
Q9HBR0	SLC38A10	0.540945208	0.001726657	0.665662331	0.001660964
Q8IWA5	SLC44A2	1.914904801	0.013351772	3.293760837	0.00327428
P53794	SLC5A3	0.735976667	0.016404996	0.919594718	0.001039495
B7ZLQ5	SMARCA1	0.814318574	0.002422696	0.935519114	0.033272916
Q96SB8	SMC6	0.526685732	0.037954003	0.938824448	0.003779709
P35610	SOAT1	0.603554954	0.036286047	1.142382314	0.013241524
Q92673	SORL1	-0.62891917	0.01485459	-1.03898435	0.003031876
H3BR01	SPINT1	-0.69340581	0.002551803	-0.50529475	0.007207332
O43278	SPINT1	-1.04847798	1.09168E-06	-1.16675024	0.004164153
P16150	SPN	0.730888326	0.001604212	0.86323929	0.000225542
Q9Y5Y6	ST14	-1.55610592	0.000989754	-1.47291343	0.001574531
Q9Y365	STARD10	-0.54097599	0.026277309	-0.76848495	0.015076368

Q9UHE8	STEAP1	-0.48566026	0.041860199	-1.24548046	0.001816653
P27105	STOM	1.983573791	0.004205816	3.034291254	0.002095138
Q8IYJ3	SYTL1	-0.59567513	0.002325633	-1.15028552	0.016584118
Q01995	TAGLN	-0.6910582	0.016435492	-1.1885125	0.044908771
Q9NVG8	TBC1D13	0.61866726	0.000281211	0.611558263	0.044016603
Q01664	TFAP4	-0.6267555	0.034637858	-0.96493433	0.007762722
Q86UB9	TMEM135	0.623283709	0.004008573	1.004622291	0.029123234
Q6UW68	TMEM205	0.544501397	0.040096564	0.696531631	0.003596696
H7C0G1	TMEM245	0.625335709	0.027221778	0.963841017	0.009648978
Q8NCS4	TMEM35B	1.113717986	0.000904978	2.043342476	0.000150058
Q96B21	TMEM45B	1.167649275	0.000735363	1.102058287	0.003990528
P62328	TMSB4X	0.52962206	0.028882174	0.736892455	0.003550527
Q14134	TRIM29	-0.9970298	0.017325948	-1.22796609	0.03963908
W4VSQ9	TRIP10	0.628039951	0.009063813	0.711541407	0.00729167
Q7Z2T5	TRMT1L	-0.52862511	0.019771606	-0.73871413	0.004553294
Q9Y5S1	TRPV2	0.622379671	0.014395465	1.869718577	0.00632711
P19075	TSPAN8	-0.58322153	0.001220016	-1.69779496	2.2655E-05
Q9C0H2	TTYH3	1.024544435	0.00052912	1.155781764	0.001555921
Q16880	UGT8	-0.49638294	0.020197568	-0.67700042	0.002781117
Q9BZM4	ULBP3	-0.89096822	0.013057682	-1.30396962	0.011811443
A0A1W2PP33	UMAD1	0.490024988	0.019243251	0.773988268	0.003880157
Q70J99	UNC13D	-0.74007952	0.011969852	-0.78992963	0.007670933
Q8IZJ1	UNC5B	-0.75889978	0.000676042	-2.73504869	0.043004455
P06132	UROD	0.503680628	0.014019052	0.938771772	0.001049385
P51784	USP11	1.030693815	0.002395903	1.862457926	0.001466025
P09327	VIL1	-0.83135041	0.006297525	-1.52228005	0.000684603
Q9Y3S1	WNK2	-0.84640846	0.000388916	-1.3807738	0.004647202
Q5BJH7	YIF1B	0.625926276	0.029027548	0.996398423	0.000972062
Q9Y548	YIPF1	0.604350274	0.004449919	0.787734502	0.000135329
O95625	ZBTB11	-0.59382855	0.02279597	-1.08958608	0.02168255
O15156	ZBTB7B	-0.77118252	0.006112719	-1.32835853	0.003209604
P37275	ZEB1	1.064631655	0.006310979	1.373162124	0.003818347
Q8NB50	ZFP62	-0.7050216	0.0231471	-0.5637472	0.041045553
Q8NF64	ZMIZ2	-0.85092613	0.007513014	-1.15516211	0.025927234
Q96NG5	ZNF558	-0.5292116	0.011520235	-1.06302816	0.011383099
Q6ZN08	ZNF66	-0.5253411	0.005496993	-1.0018921	0.019875139
Q6ZMW2	ZNF782	-0.78203143	0.016790337	-1.01283544	0.00167768
Q96NB3	ZNF830	-0.48997472	0.000816303	-0.68952189	0.001516091
Q6GV32		1.014759917	0.005320357	1.974227155	0.000796414
Q53FI7		1.575520446	0.007930929	1.7317876	0.002116043
B4DUJ6		0.911126975	0.006582931	1.719034285	0.000564761
B3KUB6		1.558490259	0.000414101	1.420430024	0.00157873
B2RBE0		0.605506801	0.000869111	1.06262473	0.000710296
B3KU38		0.878917928	0.024330099	1.044480214	0.008821245
Q5TBC7		0.653874612	0.001298053	1.024162632	0.028842076
A8K710		0.524380264	0.022167461	1.011869682	0.002591326
B4E2S3		0.537613219	0.001704851	1.008558097	0.000398246
B7Z653		1.066487786	0.000677824	0.988896325	0.001014735
P53004		0.537999694	0.011854853	0.959362982	0.005103302
B3KTS4		-0.61760937	0.002984982	-0.65322323	0.019434077
D7PBN3		-1.00695256	6.23531E-05	-1.4945557	0.006313616
Q59FZ8		-0.85166081	0.00035359	-2.51329912	0.00103763

7.2 Appendix 2

Regulation of proteins involved in the glutaminolysis pathway, in long-term (52-week) 2mM and 4mM aspirin treated SW620 cells, from proteomic data set produced by Dr Eleanor Mortensson (unpublished).

Table 7.2 Regulation of glutaminolysis proteins in proteomic data set of long-term (52-week) aspirin treated SW620 cells.

T-test and false discovery rates above 0.05 are shown in grey.

		2mM/0mM aspirin			4mM/0mM aspirin		
Best Accession	**Gene symbol**	**Log_2 fold change**	**T test**	**False Discovery Rate**	**Log_2 fold change**	**T test**	**False Discovery Rate**
P08243	ASNS	-0.226435	0.0761115	0.233	-0.759381	0.0042552	0.0284764
O15382	BCAT2	0.2902525	0.0116078	0.104	0.154896	0.0845336	0.1578865
P27708	CAD	0.1336736	0.0187802	0.124	0.4791416	0.0010377	0.0168856
P17812	CTPS1	0.0673913	0.0198064	0.125	0.4097526	0.0004206	0.0124454
Q9NRF8	CTPS2	0.0799202	0.2692685	0.462	0.4562391	0.0104329	0.0441935
Q06210	GFPT1	-0.269829	0.0049054	0.078	-0.773599	0.0252347	0.0727009
O94925	GLS	1.2793865	0.0008916	0.043	1.9915215	0.0040582	0.0280969
Q9UI32	GLS2	-0.015280	0.905163	0.948	-0.335740	0.0221464	0.0674526
P00367	GLUD1	0.0332293	0.3426362	0.532	-0.273830	0.0131958	0.0506471
P49915	GMPS	0.0694216	0.0296558	0.149	0.4914607	0.033482	0.086465
P00505	GOT2	0.0060919	0.9292712	0.961	-0.621537	0.0042085	0.0283882
Q8TD30	GPT2	0.0560169	0.4257204	0.609	-0.948971	0.0286558	0.0785507
Q6IA69	NADSYN1	-0.062546	0.0173362	0.119	-0.517483	0.0047628	0.0300691
O15067	PFAS	0.3921961	0.0084398	0.092	0.3848771	0.0060537	0.0338355
Q06203	PPAT	0.0691371	0.1027109	0.273	-0.178137	0.0366128	0.0914524
Q9Y617	PSAT1	0.1708275	0.0604891	0.206	-0.585035	0.0008333	0.0160549
Q15758	SLC1A5	0.1573481	0.2253405	0.419	-0.13826	0.6027307	0.6884131
P08195	SLC3A2	-0.200192	0.2311954	0.424	-1.385034	0.0076751	0.0381713
Q9UPY5	SLC7A11	-0.490845	0.0839939	0.246	-2.085192	0.0009005	0.0164223
Q01650	SLC7A5	-0.421357	0.0739541	0.229	-1.894267	0.0122858	0.0484743

7.3 Appendix 3

Regulation of transcriptional targets of ATF4, as highlighted by Ingenuity Pathway Analysis (IPA), in long-term (52-week) 2mM and 4mM aspirin treated SW620 cells, from proteomic data set produced by Dr Eleanor Mortensson (unpublished).

Table 7.3 Regulation of ATF4 transcriptional targets in proteomic data set of long-term (52-week) aspirin treated SW620 cells.

T-test and false discovery rates above 0.05 are shown in grey.

Best Accession	Gene symbol	2mM/0mM aspirin			4mM/0mM aspirin		
		Log_2 fold change	T test	False Discovery Rate	Log_2 fold change	T test	False Discovery Rate
P27695	APEX1	-0.25068	0.0227	0.132	-0.47766	0.0066	0.03511306
P02649	APOE	0.839481	0.00505	0.078	2.06545	0.0001	0.0088803
P08243	ASNS	-0.22643	0.07611	0.233	-0.75938	0.0043	0.02847639
K7EJB9	CALR	-0.18141	0.7104	0.828	0.35518	0.4805	0.5782313
D6RB85	CANX	-0.37511	0.0558	0.199	-0.77063	0.004	0.02782157
P49589	CARS	0.022778	0.65743	0.791	-0.29401	0.0096	0.04235771
P36551	CPOX	0.45002	0.00077	0.042	0.65187	5E-05	0.00735591
P50416	CPT1A	0.044078	0.47473	0.649	-0.24874	0.0401	0.09636438
P35222	CTNNB1	-0.85932	0.00528	0.079	-0.66799	0.005	0.03072758
Q02318	CYP27A1	0.510056	0.0004	0.037	1.18786	4E-05	0.00735591
Q13541	EIF4EBP1	-0.0896	0.30905	0.500	-0.52677	0.0039	0.02763948
Q96HE7	ERO1A	-0.00622	0.87097	0.927	0.17612	0.0085	0.0397764
P41250	GARS	-0.08782	0.16801	0.355	-0.40582	0.003	0.02497668
Q99988	GDF15	0.324697	0.05207	0.192	2.06429	0.0028	0.02413971
P13807	GYS1	0.249074	0.00276	0.063	0.58094	0.0031	0.02549772
P14625	HSP90B1	-0.12189	0.01722	0.119	0.16411	0.0468	0.1060157
P41252	IARS	-0.11104	0.08698	0.250	-0.31078	0.0035	0.02628176
Q9P2J5	LARS	-0.08266	0.0342	0.158	-0.2105	0.0158	0.0557486
P56192	MARS	0.001207	0.95582	0.978	0.06837	0.0475	0.10691409
P10620	MGST1	0.590836	0.04539	0.180	1.31497	0.0165	0.05727523
Q9Y2R9	MRPS7	-0.01311	0.77869	0.872	-0.73495	0.0001	0.0088803
P02795	MT2A	0.303471	0.21095	0.404	-1.03221	0.0125	0.04902257
P13995	MTHFD2	0.138679	0.12931	0.307	-1.40656	0.0072	0.03676307
Q6IB91	PCK2	-0.2104	0.09235	0.258	-1.22402	0.0004	0.01210151
O43175	PHGDH	-0.0654	0.28265	0.475	-1.14698	5E-05	0.00735591
P78527	PRKDC	-0.10666	0.15398	0.340	-0.44245	0.004	0.02805925
Q9Y617	PSAT1	0.170827	0.06049	0.206	-0.58503	0.0008	0.01605493
P49768	PSEN1	0.066106	0.35266	0.543	-0.35427	0.0234	0.06960721

P78330	PSPH	-0.14226	0.19826	0.389	-0.88452	0.0017	0.01927704
P32322	PYCR1	-0.09946	0.09263	0.258	-1.21909	0.0028	0.02435663
Q06330	RBPJ	-0.191	0.02064	0.127	-0.61298	0.0003	0.01131905
Q9UBV2	SEL1L	-0.00207	0.97779	0.990	0.14956	0.0299	0.08057446
P78314	SH3BP2	-0.48388	0.02317	0.133	-1.16996	0.0013	0.01794106
P34897	SHMT2	-0.05648	0.01522	0.114	-0.51237	0.0032	0.02572887
Q99720	SIGMAR1	-0.16406	0.10374	0.274	-0.28569	0.0235	0.06970668
P43007	SLC1A4	0.027095	0.899	0.945	-2.04226	0.0002	0.00931211
Q9H2H9	SLC38A1	-0.25398	0.16905	0.356	-0.76997	0.0107	0.0446743
Q96QD8	SLC38A2	-0.17064	0.26107	0.455	-0.79777	9E-05	0.0088803
Q15043	SLC39A14	0.145624	0.28162	0.474	-1.46021	0.0131	0.05033527
P08195	SLC3A2	-0.20019	0.2312	0.424	-1.38503	0.0077	0.03817128
O75387	SLC43A1	-0.50963	0.05403	0.196	-1.68721	0.0017	0.01921385
P30825	SLC7A1	-0.04443	0.76869	0.865	-0.75972	0.0121	0.04808008
Q9UPY5	SLC7A11	-0.49085	0.08399	0.246	-2.08519	0.0009	0.01642229
Q01650	SLC7A5	-0.42136	0.07395	0.229	-1.89427	0.0123	0.0484743
O60907	TBL1X	-0.00904	0.9461	0.972	-1.01553	0.0003	0.01171502
O14763	TNFRSF10B	0.116137	0.10916	0.281	0.68277	0.0162	0.05660511
Q96RU7	TRIB3	-0.006	0.95752	0.979	-0.39841	0.034	0.0875501
J3KPA4	VEGFA	-0.53147	0.06877	0.220	-2.599	0.0198	0.06322752
P23381	WARS	-0.07952	0.196	0.387	-0.73199	0.0003	0.01146725
O43592	XPOT	-0.07168	0.43912	0.620	-0.34028	0.0228	0.06856132
P18887	XRCC1	-0.13636	0.0877	0.251	-0.55941	0.0038	0.02748861

7.4 Appendix 4

Validation of antibodies for glutaminase 1 (GLS1), pyruvate carboxylase (PC) and pyruvate dehydrogenase kinase 1 (PDK1) by siRNA knockdown in four colorectal cell lines (SW620, LS174T, HCA7 and RG/C2).

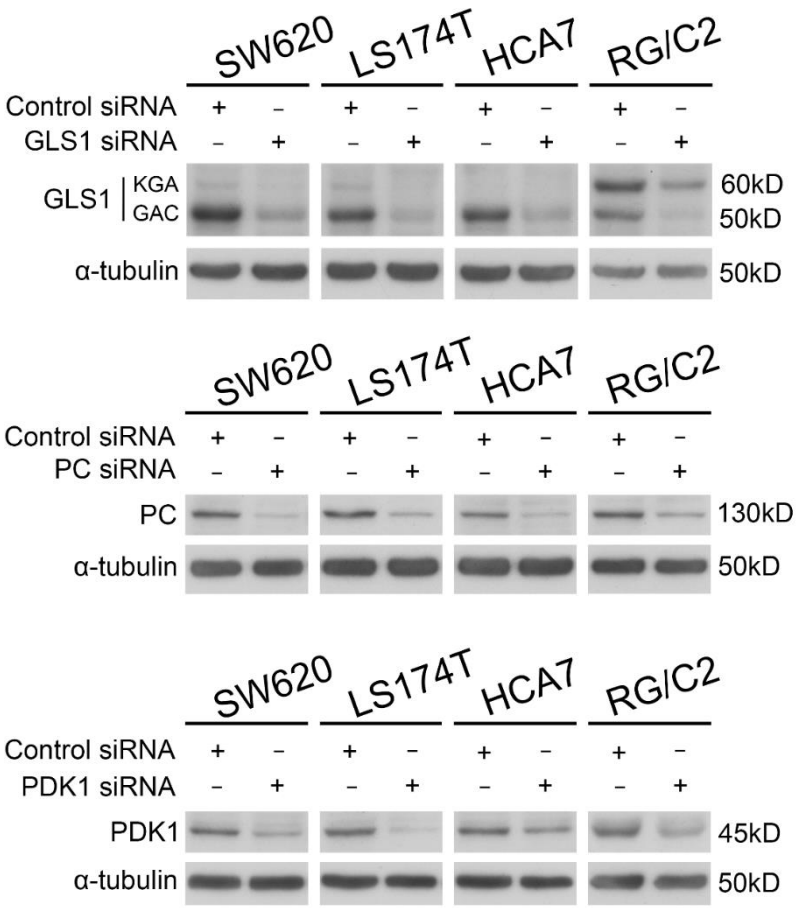

Figure 7.1 Validation of antibodies used for western blotting for GLS1, PC and PDK1 proteins by siRNA knockdown in four cell lines, SW620, LS174T, HCA7 and RG/C2

7.5 Appendix 5

Metabolomics data from long-term (~52-week) 4mM aspirin treated CRC cell lines SW620, LS174T and HCA7.

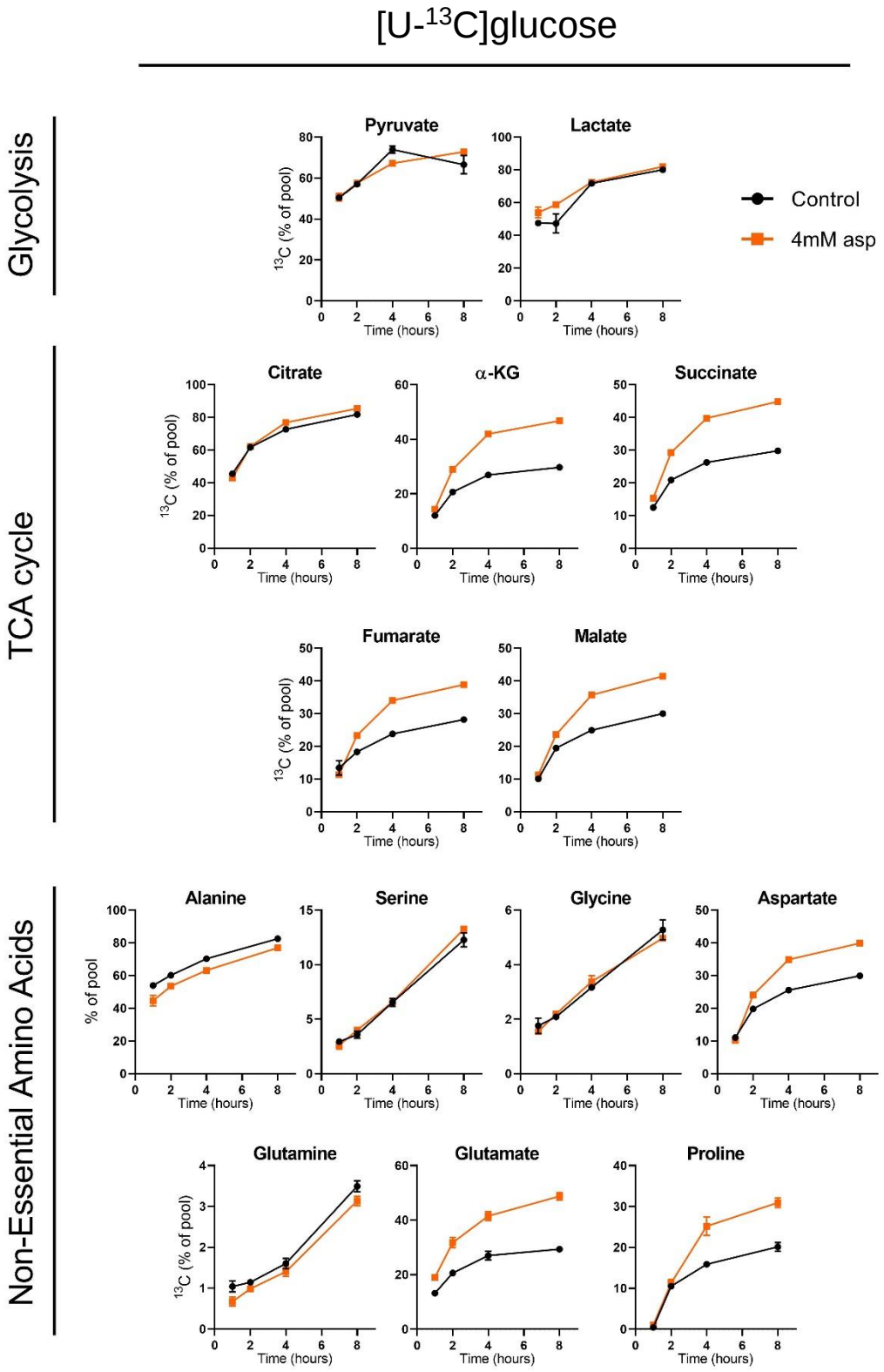

Figure 7.2 Time course of ^{13}C incorporation from [U-^{13}C]glucose in long-term aspirin treated SW620 cells

Long-term (LT) 4mM aspirin treatment compared to control. Error bars represent standard error (n=3).

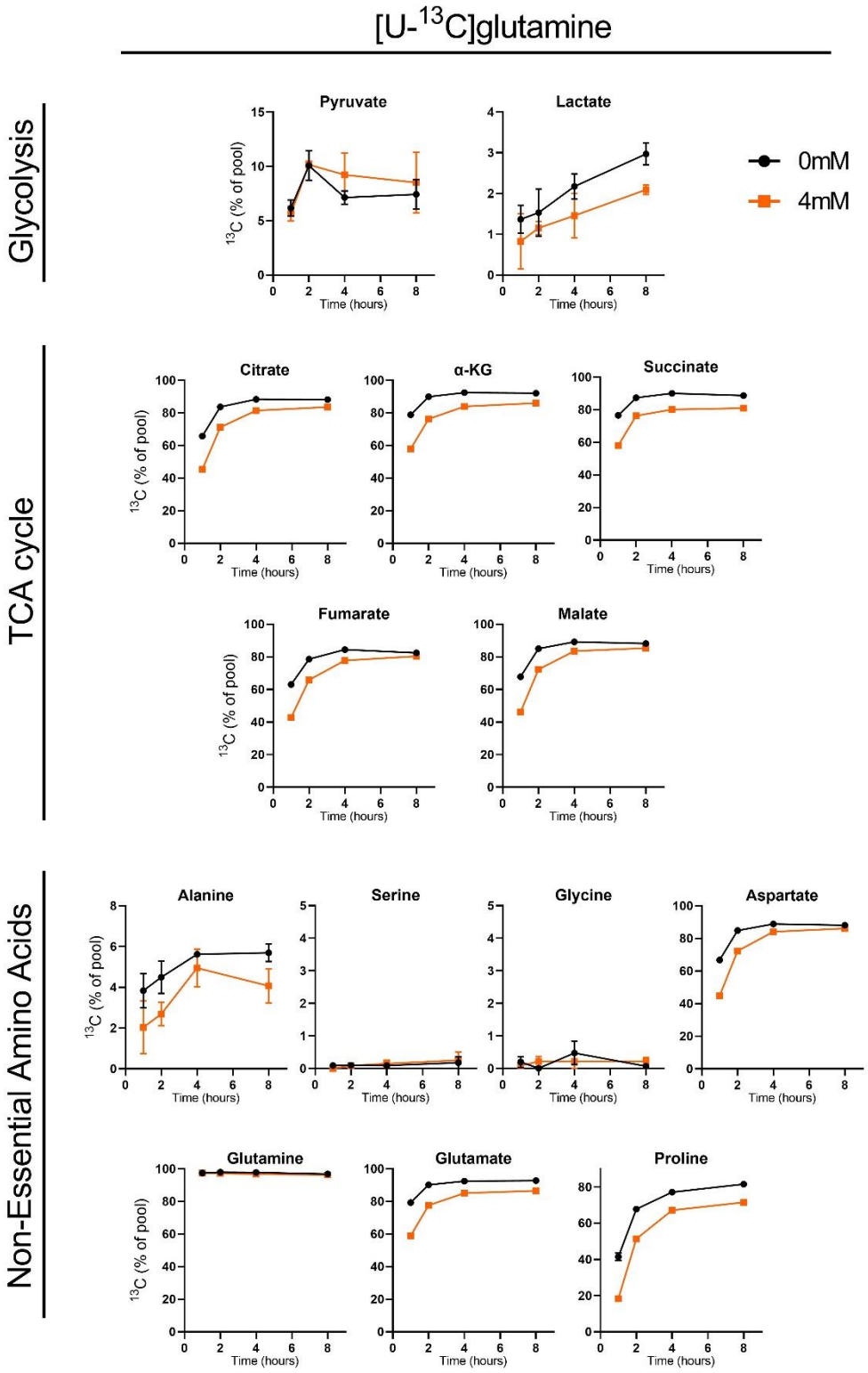

Figure 7.3 Time course of ^{13}C incorporation from [U-^{13}C]glutamine in long-term aspirin treated SW620 cells

Long-term 4mM aspirin treatment compared to control. Error bars represent standard error (n=3).

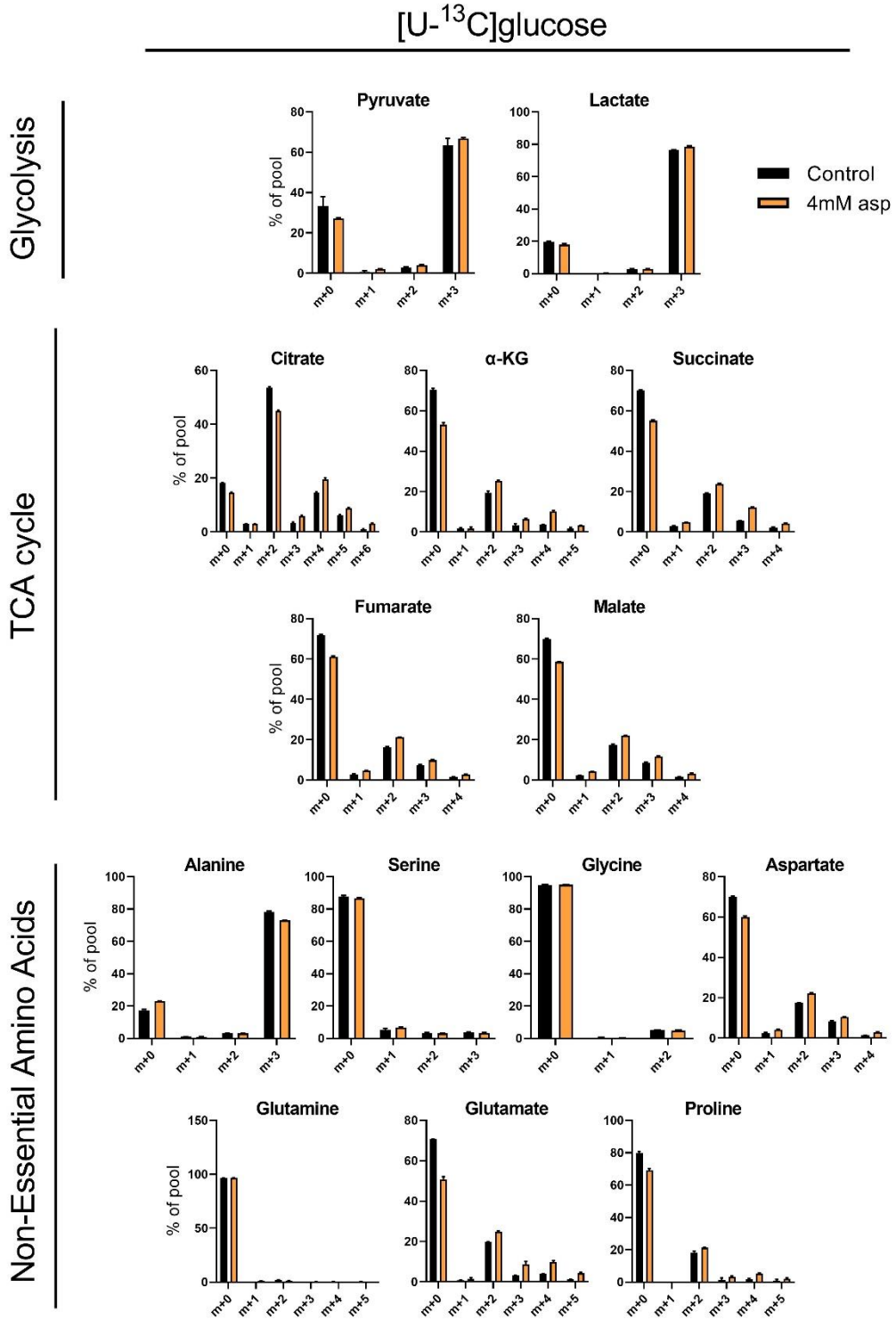

Figure 7.4 Mass isotopomer distribution (MID) data after 8hrs incubation with [U-^{13}C]glucose in long-term aspirin treated SW620 cells

Long-term 4mM aspirin treatment compared to control. Error bars represent standard error (n=3).

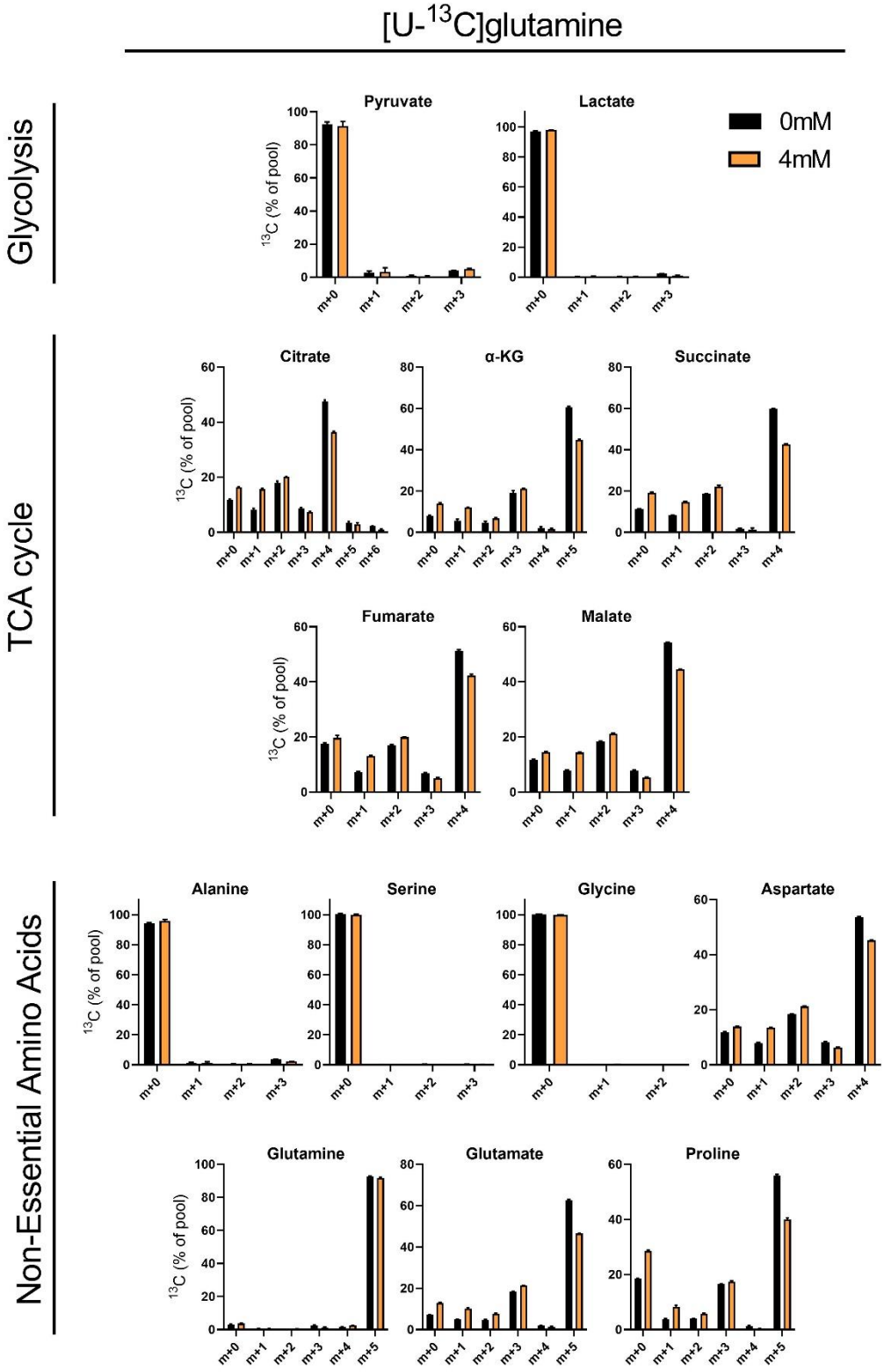

Figure 7.5 Mass isotopomer distribution (MID) data after 8hrs incubation with [U-^{13}C]glutamine in long-term aspirin treated SW620 cells

Long-term 4mM aspirin treatment compared to control. Error bars represent standard error (n=3).

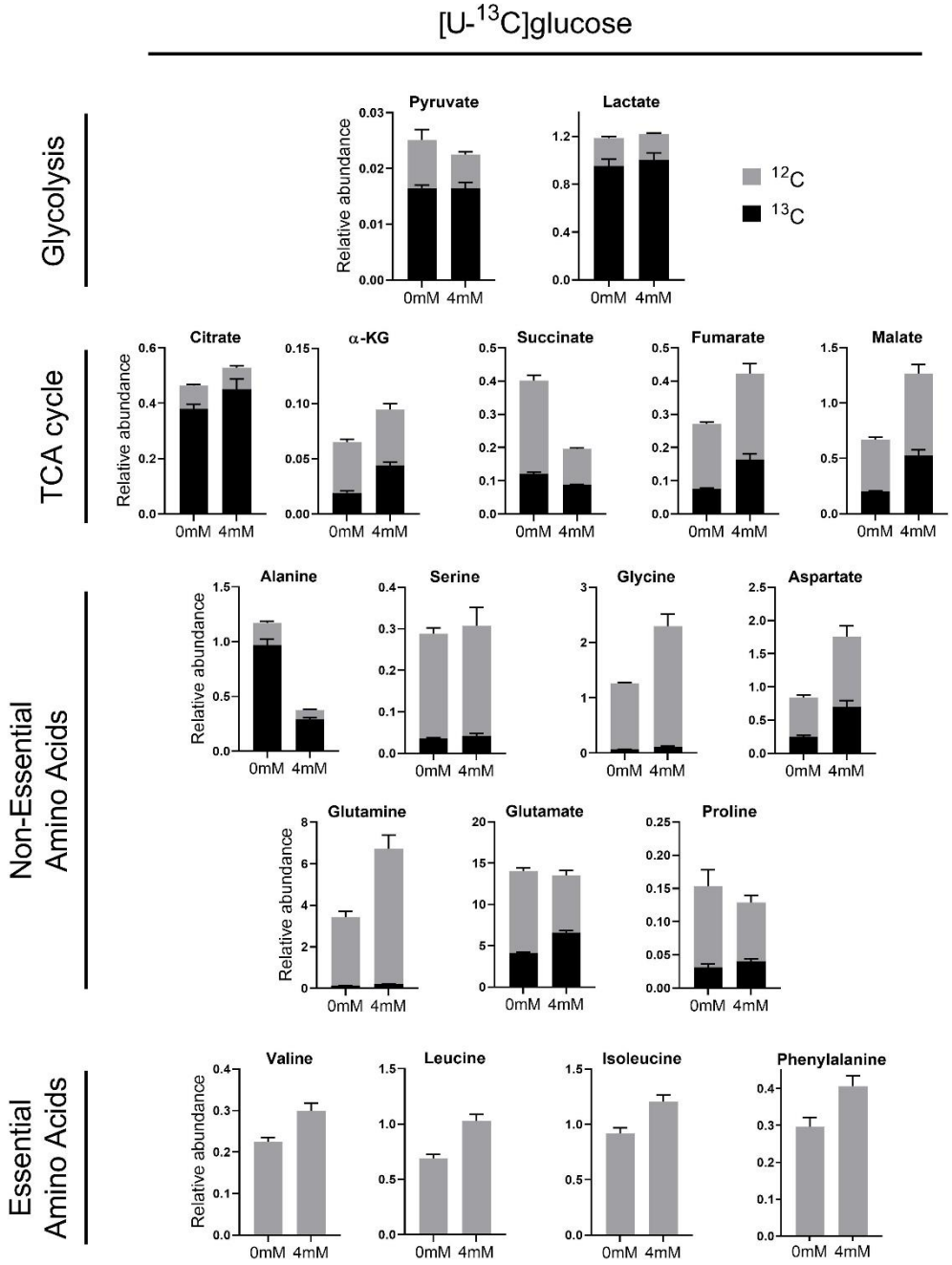

Figure 7.6 Abundance (relative to cell number) of ^{12}C and ^{13}C in metabolite pools after 8hrs incubation with [U-^{13}C]glucose in long-term aspirin treated SW620 cells

Long-term 4mM aspirin treatment compared to control. Error bars represent standard error (n=3).

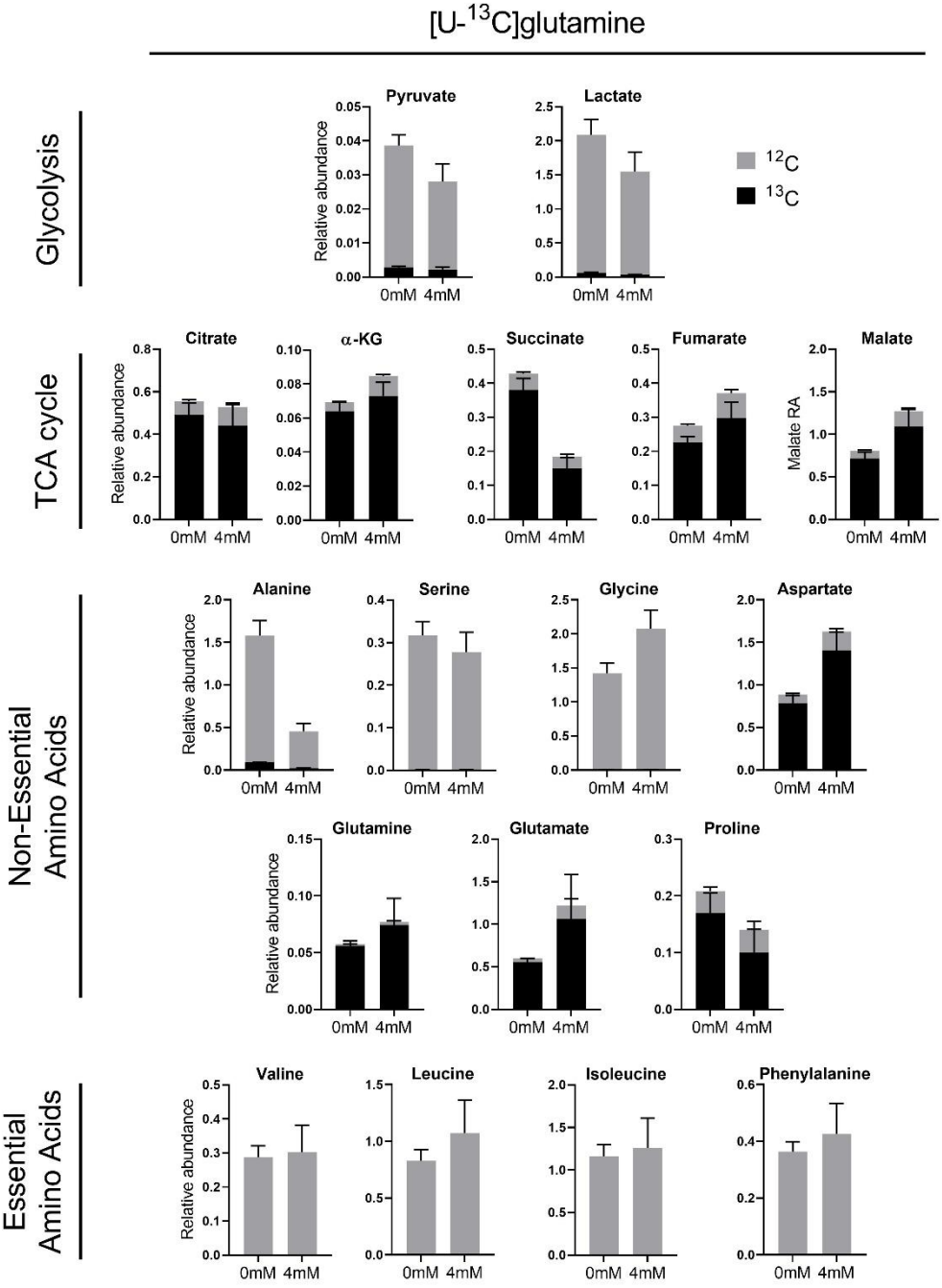

Figure 7.7 Abundance (relative to cell number) of ^{12}C and ^{13}C in metabolite pools after 8hrs incubation with [U-^{13}C]glutamine in long-term aspirin treated SW620 cells

Long-term 4mM aspirin treatment compared to control. Error bars represent standard error (n=3).

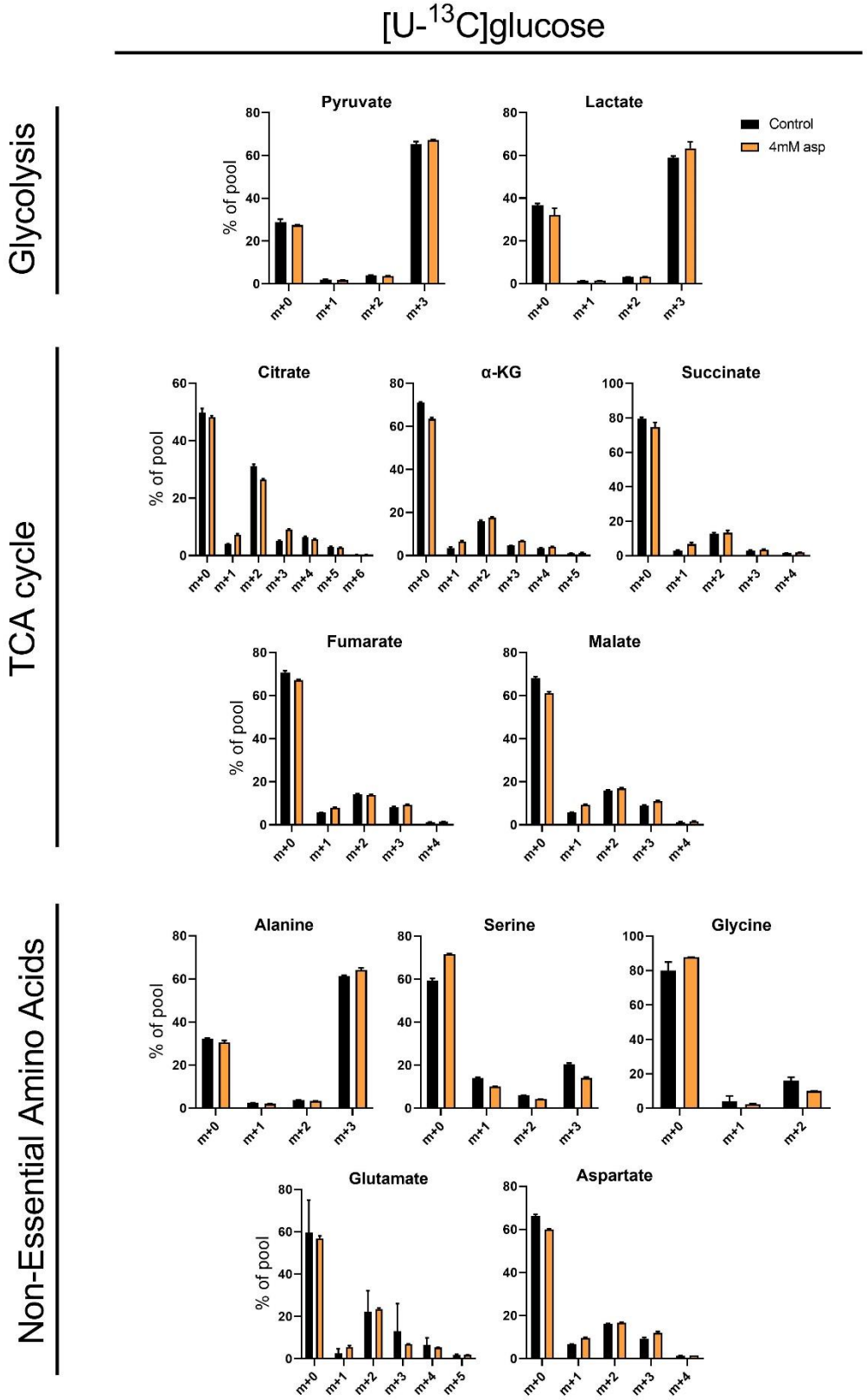

Figure 7.8 Mass isotopomer distribution (MID) data after 8hrs incubation with [U-^{13}C]glucose in long-term aspirin treated LS174T cells

Long-term 4mM aspirin treatment compared to control. Error bars represent standard error (n=3).

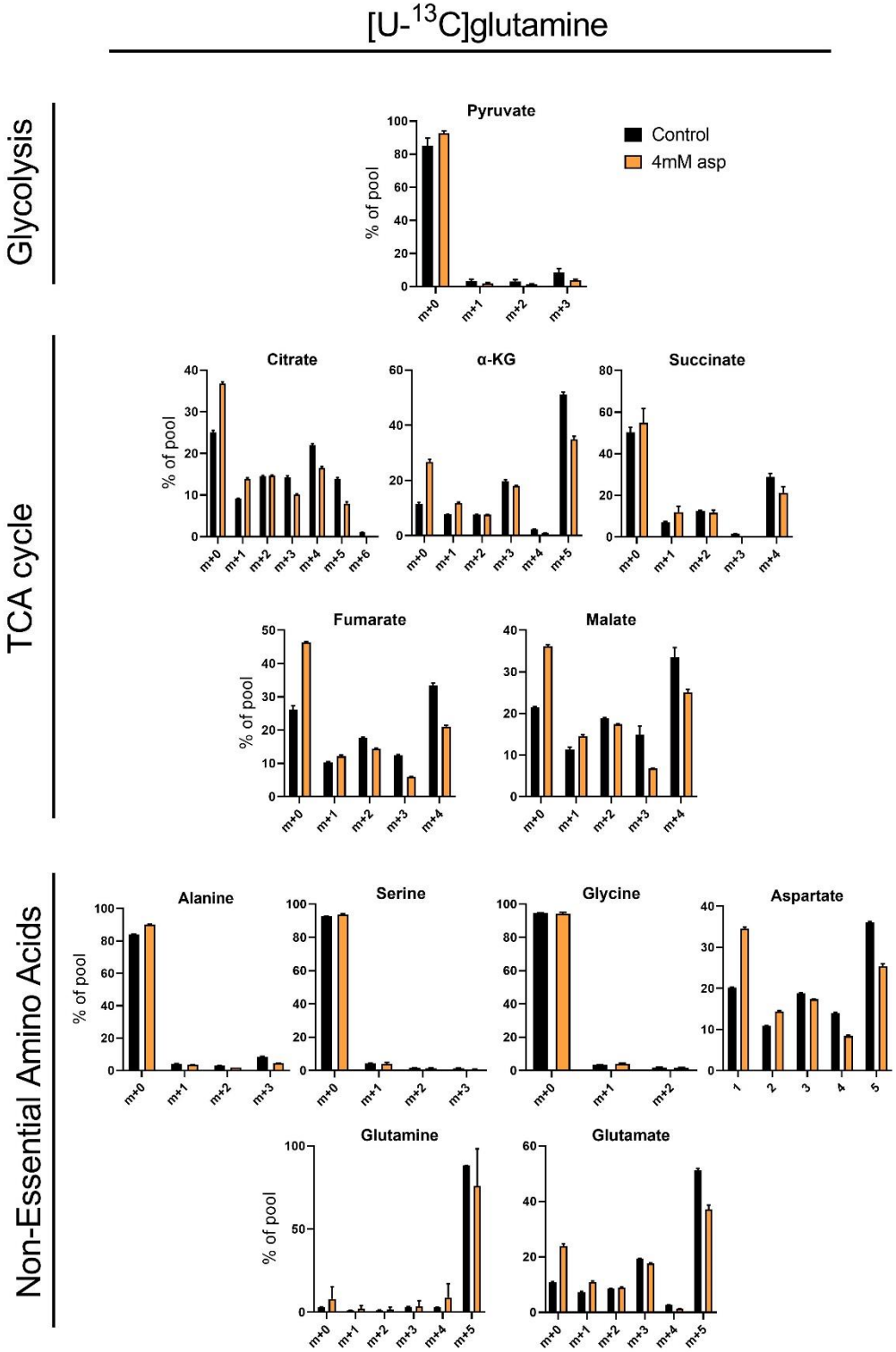

Figure 7.9 Mass isotopomer distribution (MID) data after 8hrs incubation with [U-^{13}C]glutamine in long-term aspirin treated LS174T cells

Long-term 4mM aspirin treatment compared to control. Error bars represent standard error (n=3).

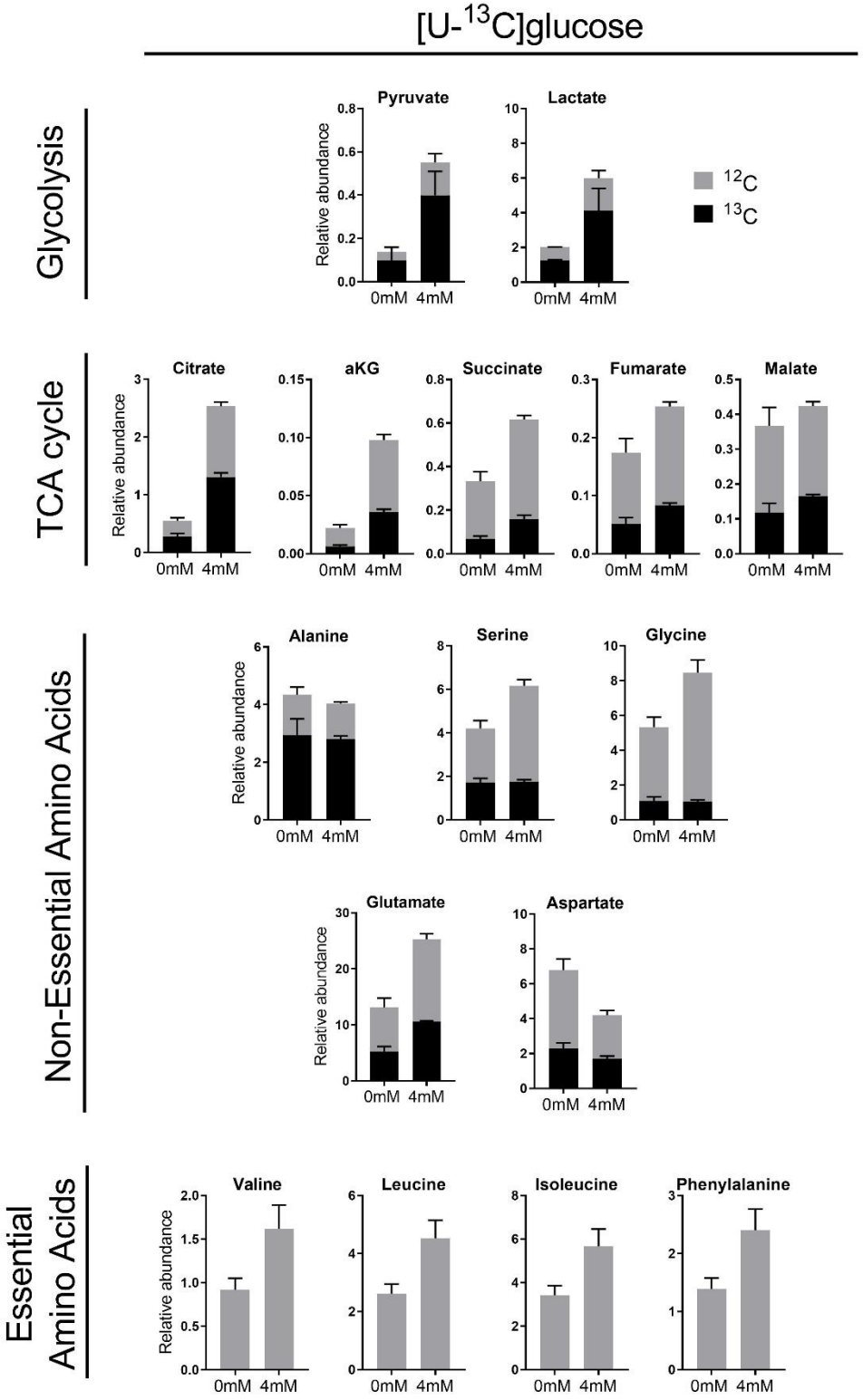

Figure 7.10 Abundance (relative to cell number) of ^{12}C and ^{13}C in metabolite pools after 8hrs incubation with [U-^{13}C]glucose in long-term aspirin treated LS174T cells

Long-term 4mM aspirin treatment compared to control. Error bars represent standard error (n=3).

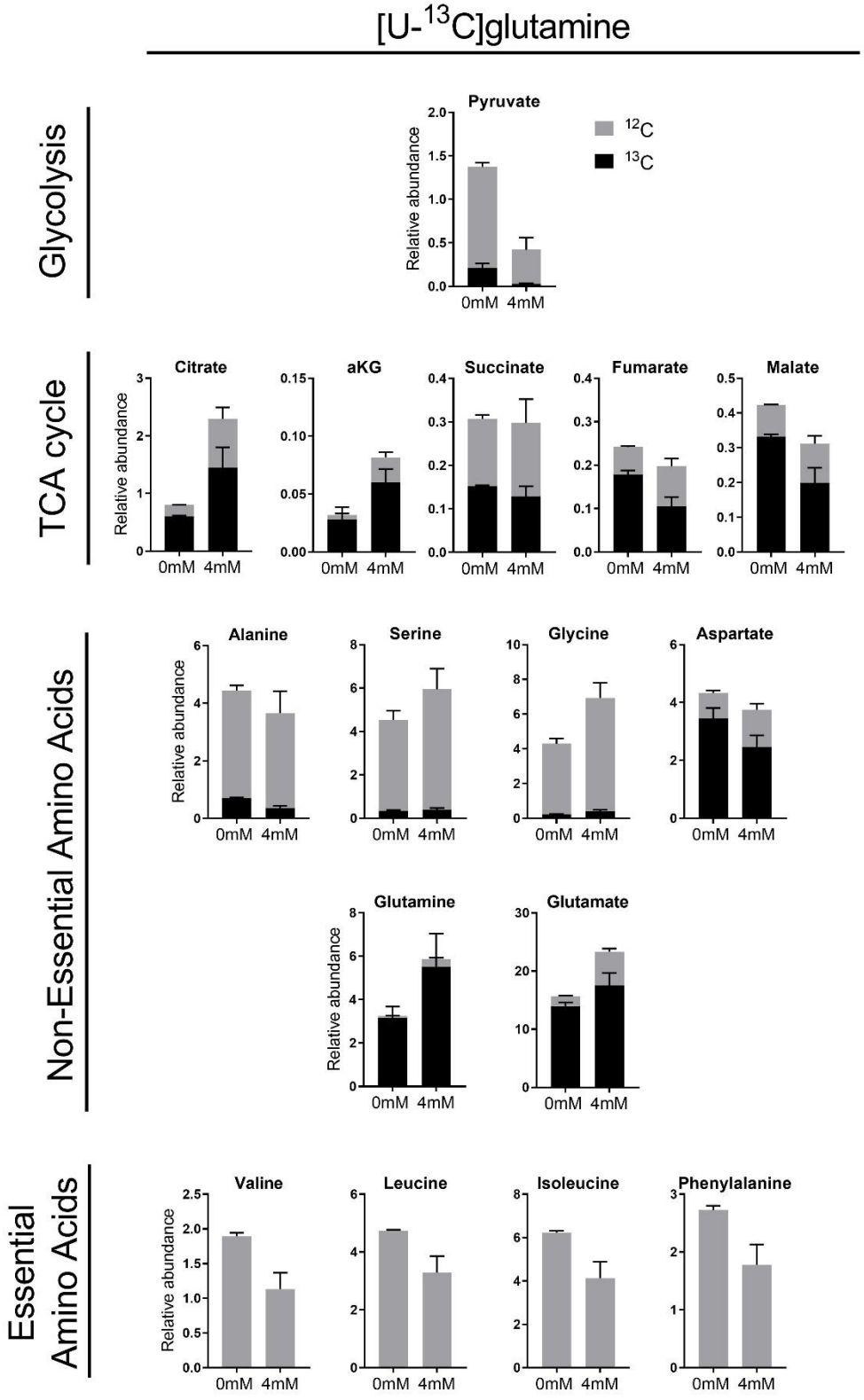

Figure 7.11 Abundance (relative to cell number) of ^{12}C and ^{13}C in metabolite pools after 8hrs incubation with [U-^{13}C]glutamine in long-term aspirin treated LS174T cells

Long-term 4mM aspirin treatment compared to control. Error bars represent standard error (n=3).

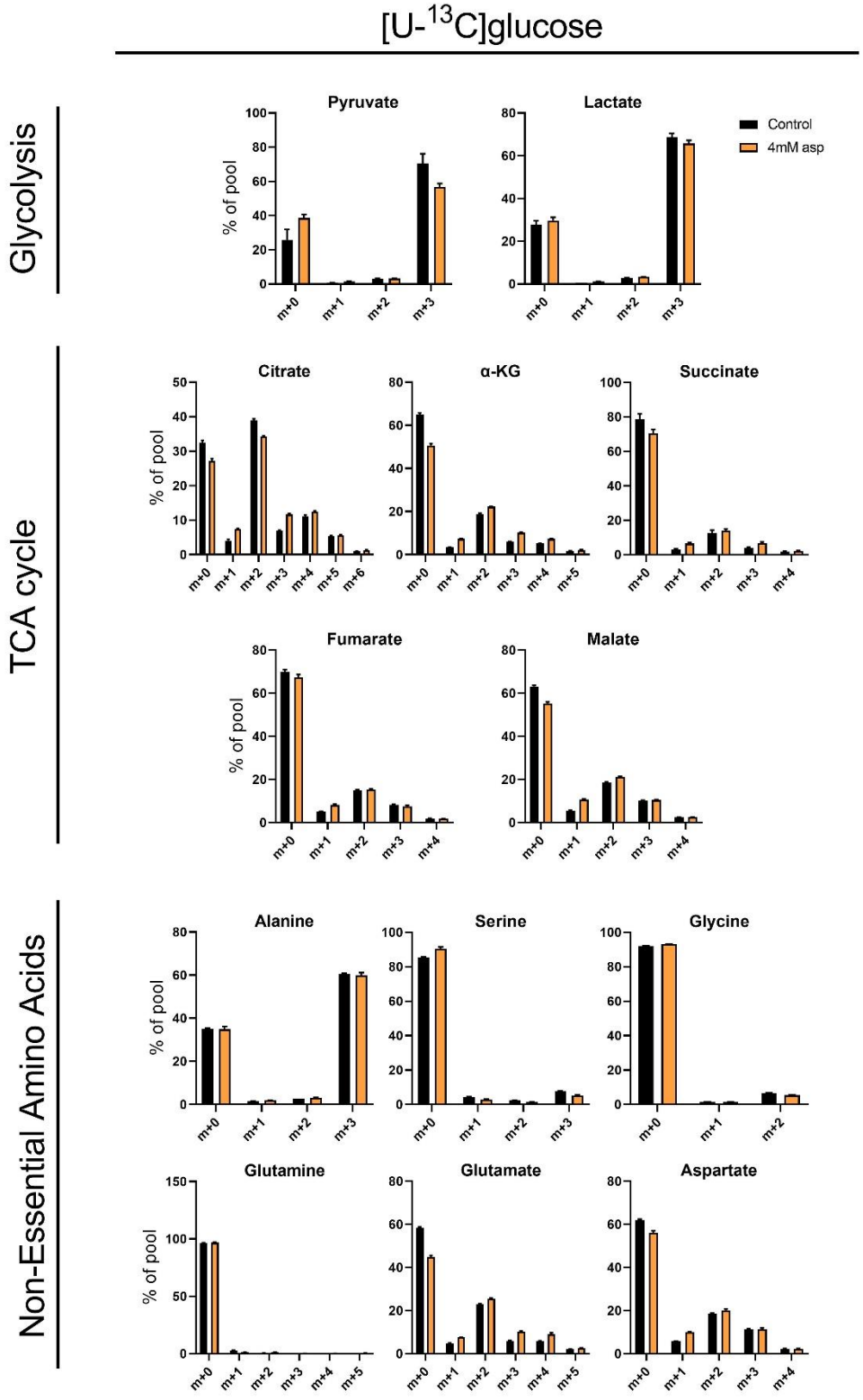

Figure 7.12 Mass isotopomer distribution (MID) data after 8hrs incubation with [U-^{13}C]glucose in long-term aspirin treated HCA7 cells

Long-term 4mM aspirin treatment compared to control. Error bars represent standard error (n=3).

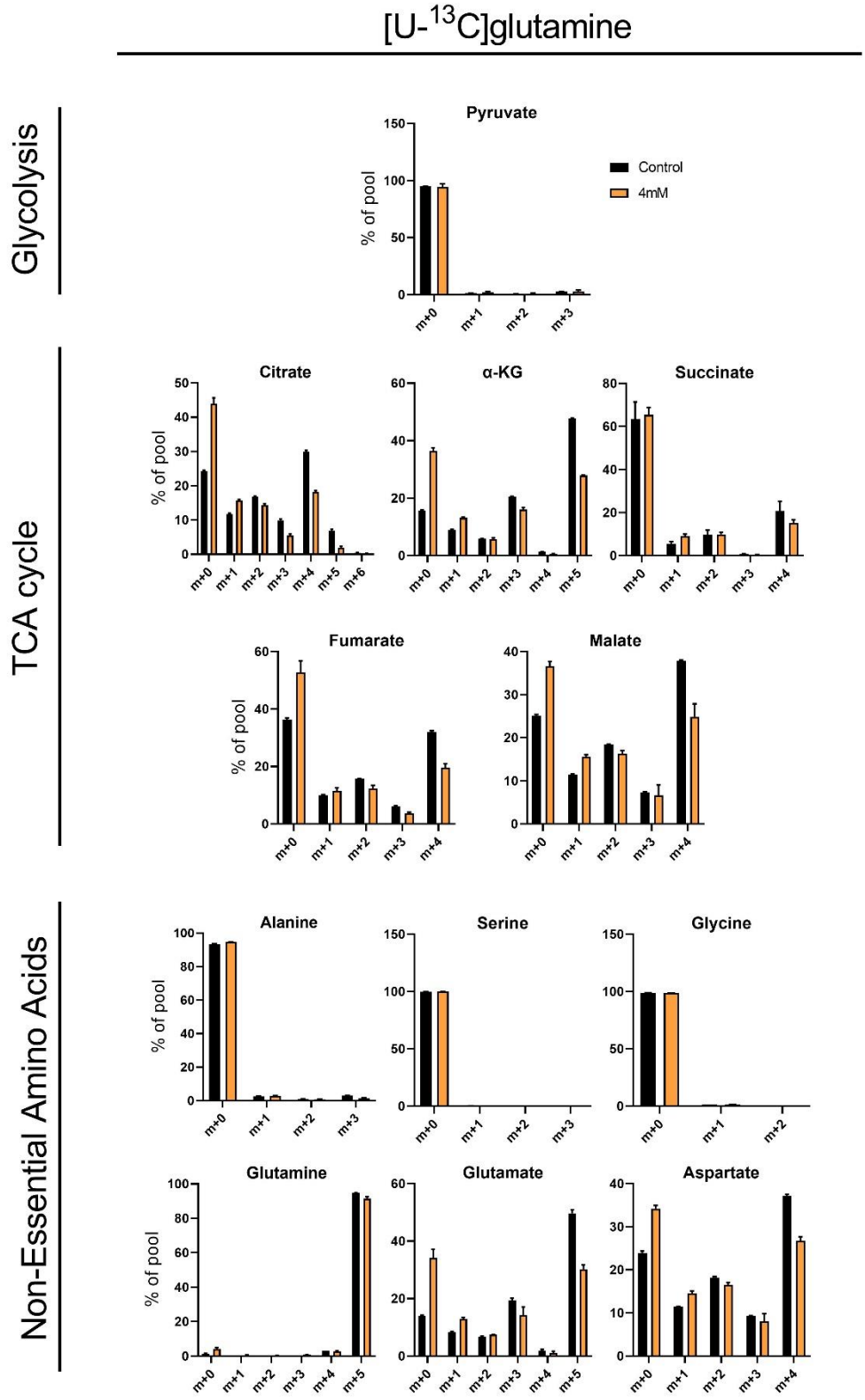

Figure 7.13 Mass isotopomer distribution (MID) data after 8hrs incubation with [U-^{13}C]glutamine in long-term aspirin treated HCA7 cells

Long-term 4mM aspirin treatment compared to control. Error bars represent standard error (n=3).

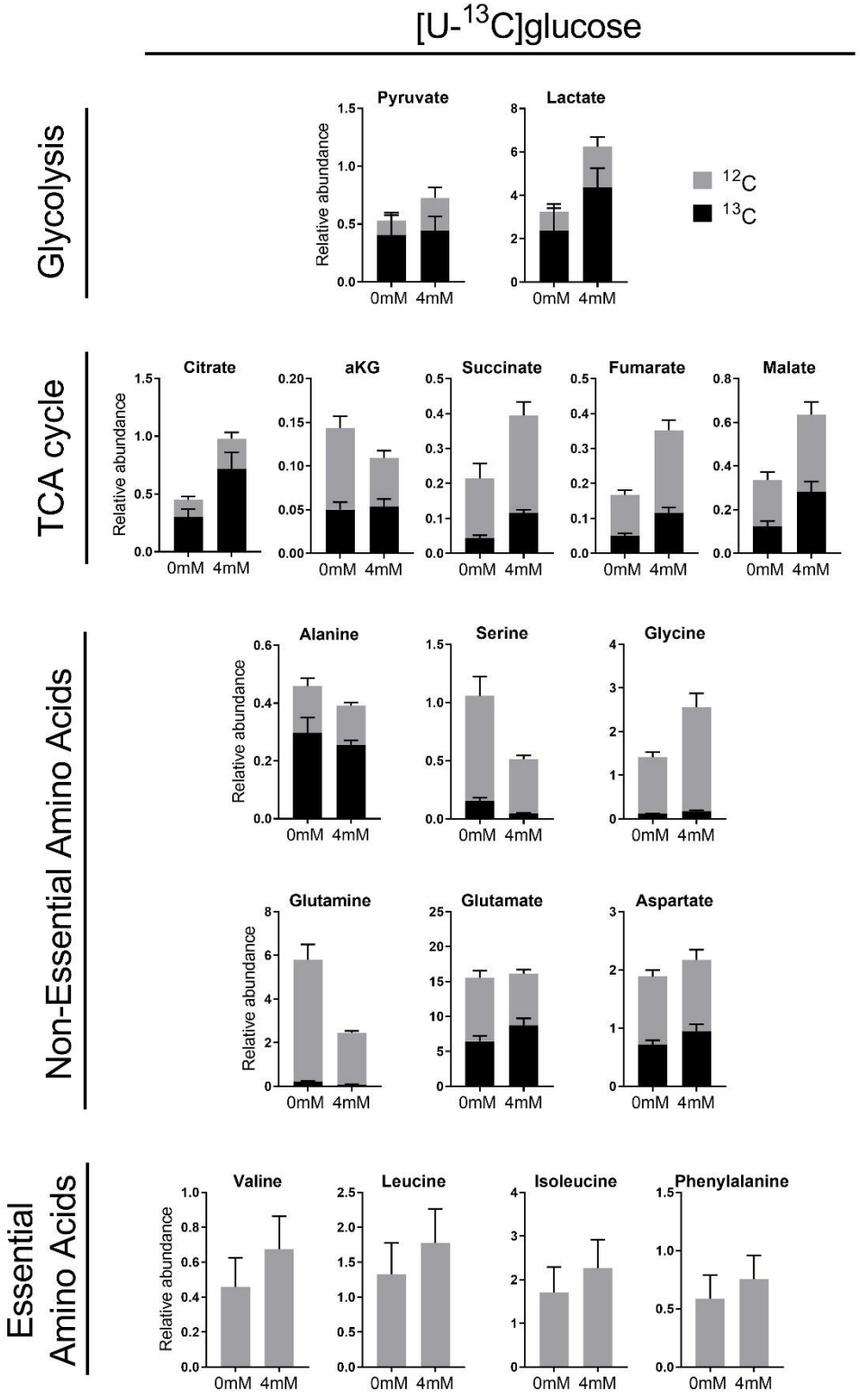

Figure 7.14 Abundance (relative to cell number) of ^{12}C and ^{13}C in metabolite pools after 8hrs incubation with [U-^{13}C]glucose in long-term aspirin treated HCA7 cells

Long-term 4mM aspirin treatment compared to control. Error bars represent standard error (n=3).

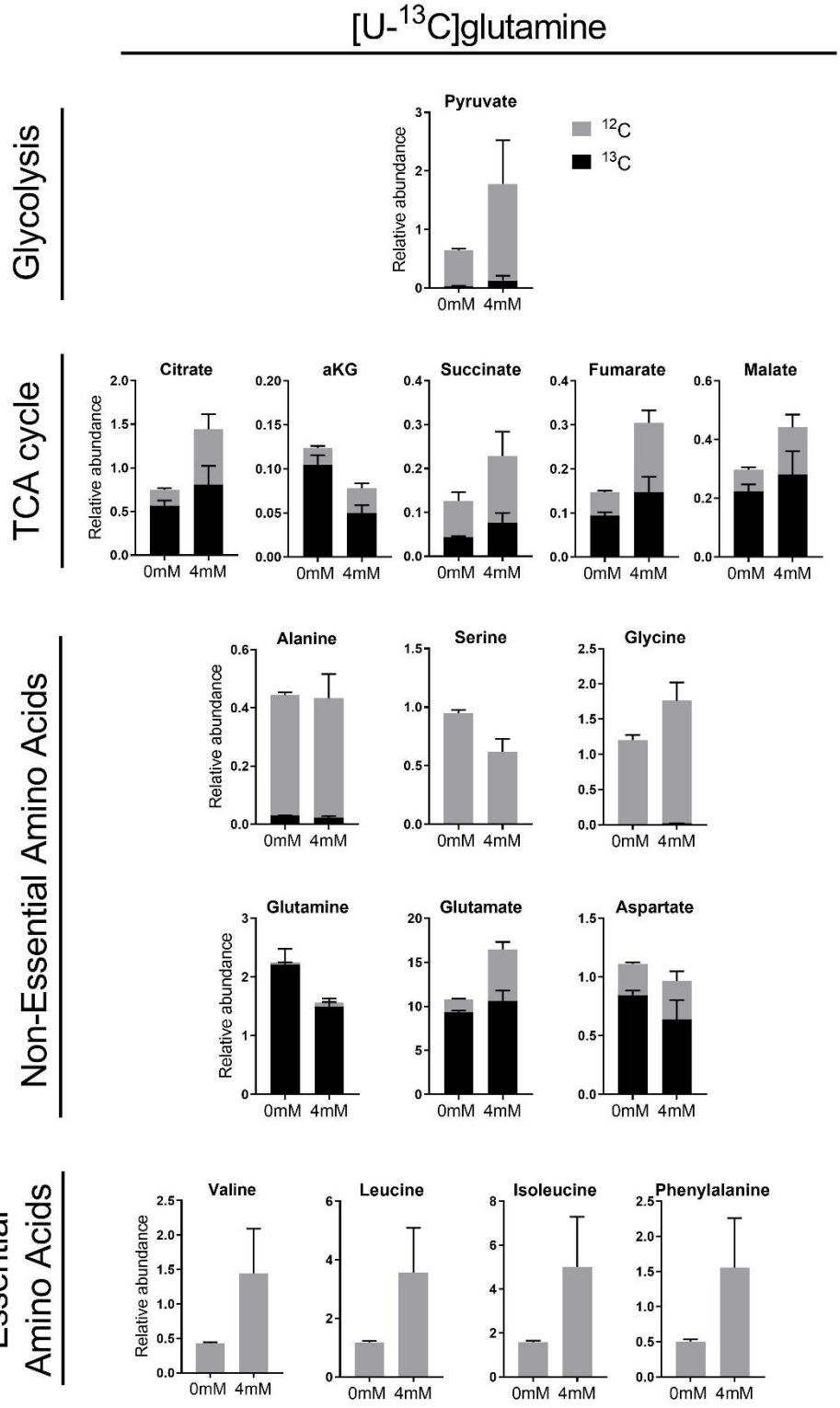

Figure 7.15 Abundance (relative to cell number) of ^{12}C and ^{13}C in metabolite pools after 8hrs incubation with [U-^{13}C]glutamine in long-term aspirin treated HCA7 cells

Long-term 4mM aspirin treatment compared to control. Error bars represent standard error (n=3).

7.6 Appendix 6

Metabolomics data of long-term (~52-week) aspirin treated SW620 cells treated with CB-839 for 24 hours.

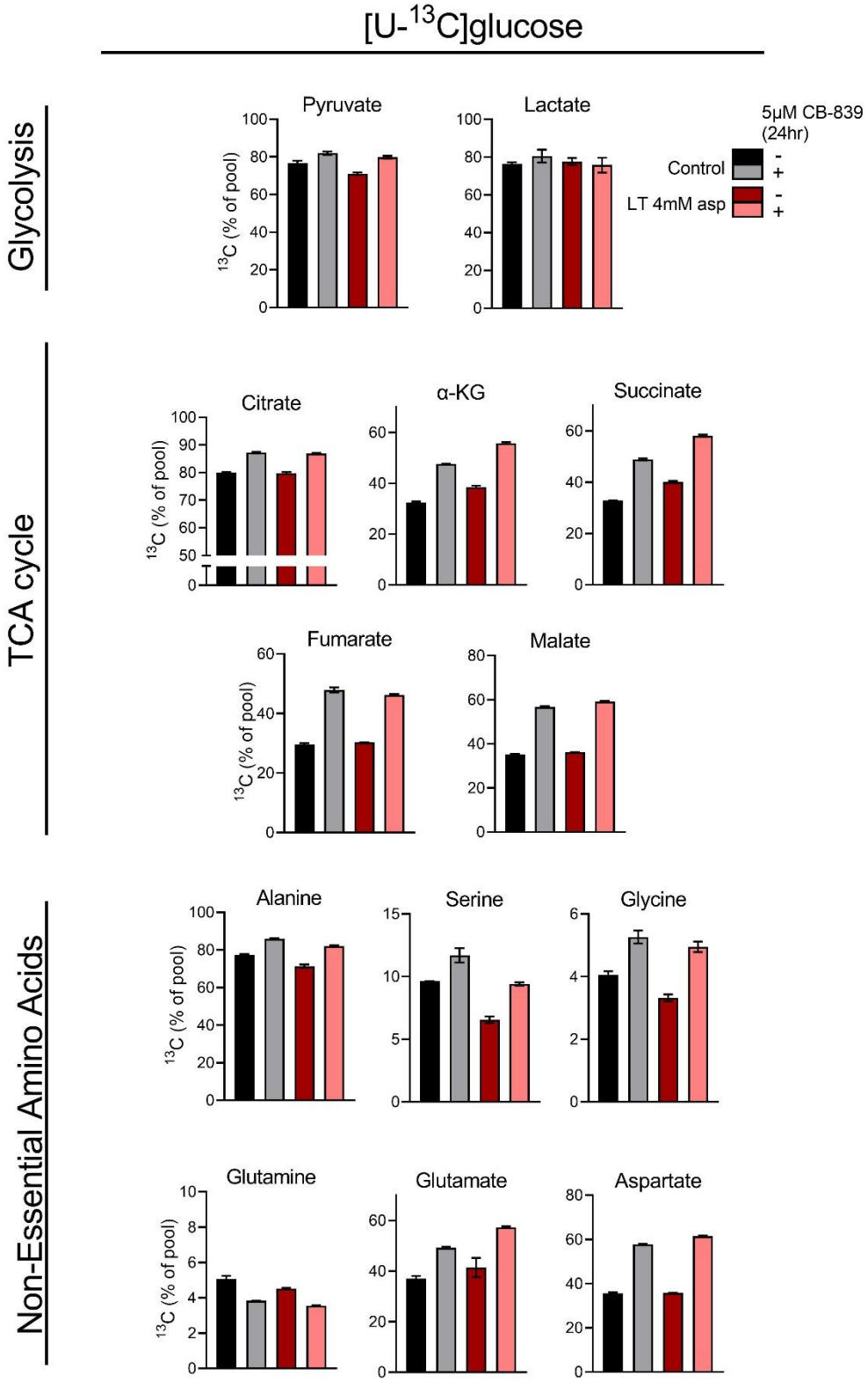

Figure 7.16 Incorporation of ^{13}C after 8 hours of incubation with [U-^{13}C]glucose in long-term aspirin treated SW620 cells treated with CB-839 for 24 hours

Error bars represent standard error (n=3).

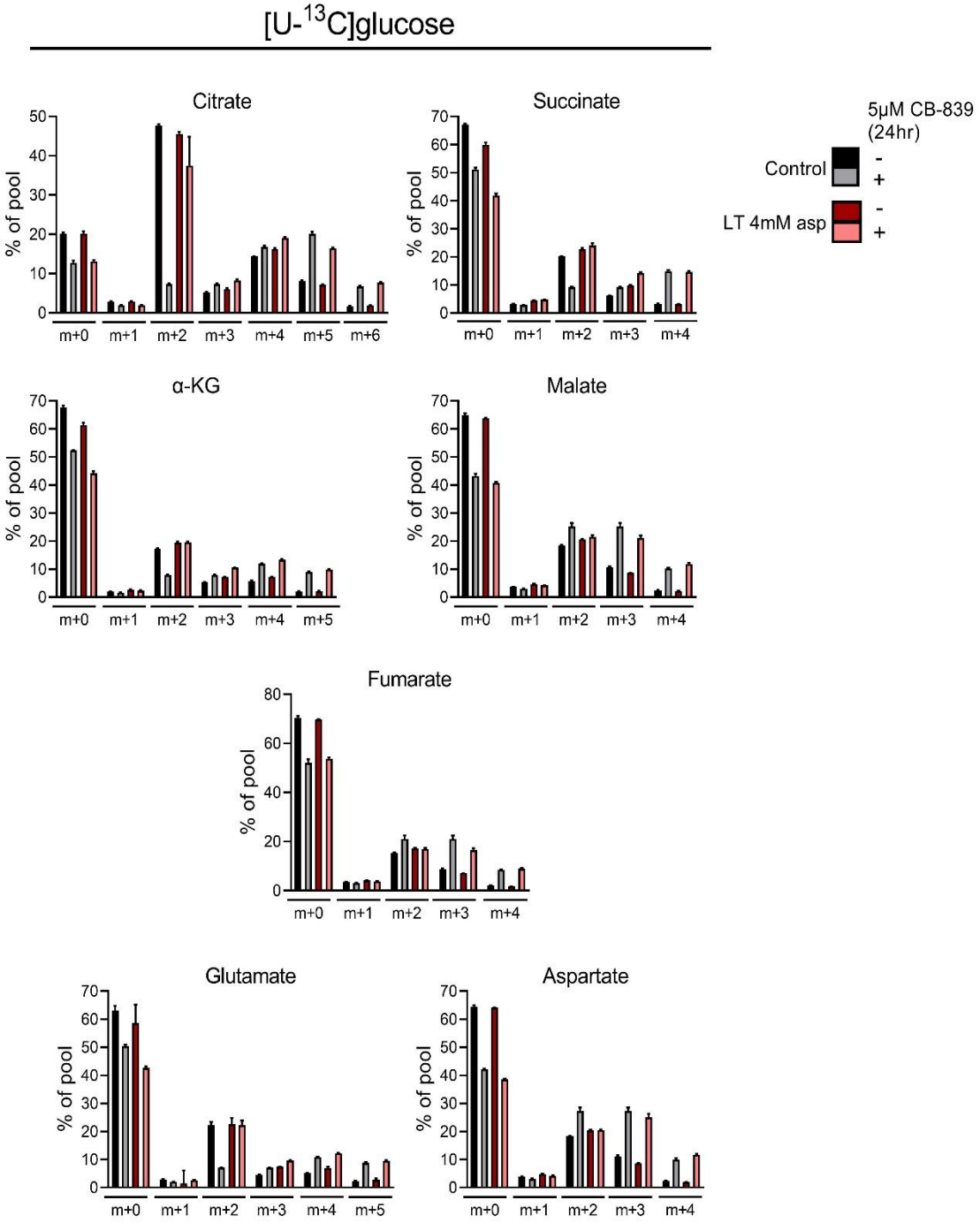

Figure 7.17 Mass isotopomer distribution (MID) data after 8hrs incubation with [U-^{13}C]glucose in long-term aspirin treated SW620 cells treated with CB-839 for 24 hours

Error bars represent standard error (n=3).

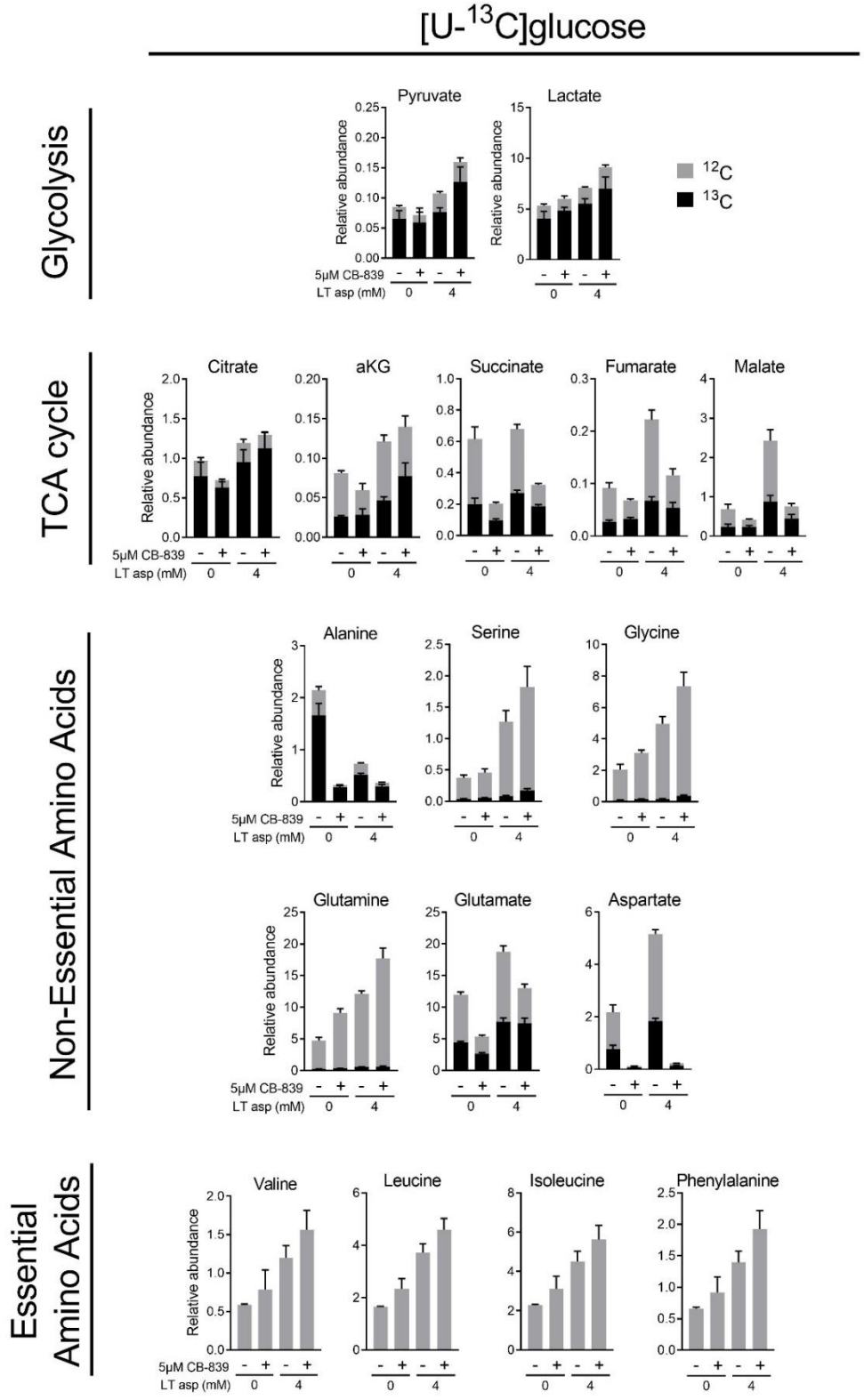

Figure 7.18 Abundance (relative to cell number) of ^{12}C and ^{13}C in metabolite pools after 8hrs incubation with [U-^{13}C]glucose in long-term aspirin treated SW620 cells treated with CB-839 for 24 hours

Error bars represent standard error (n=3).

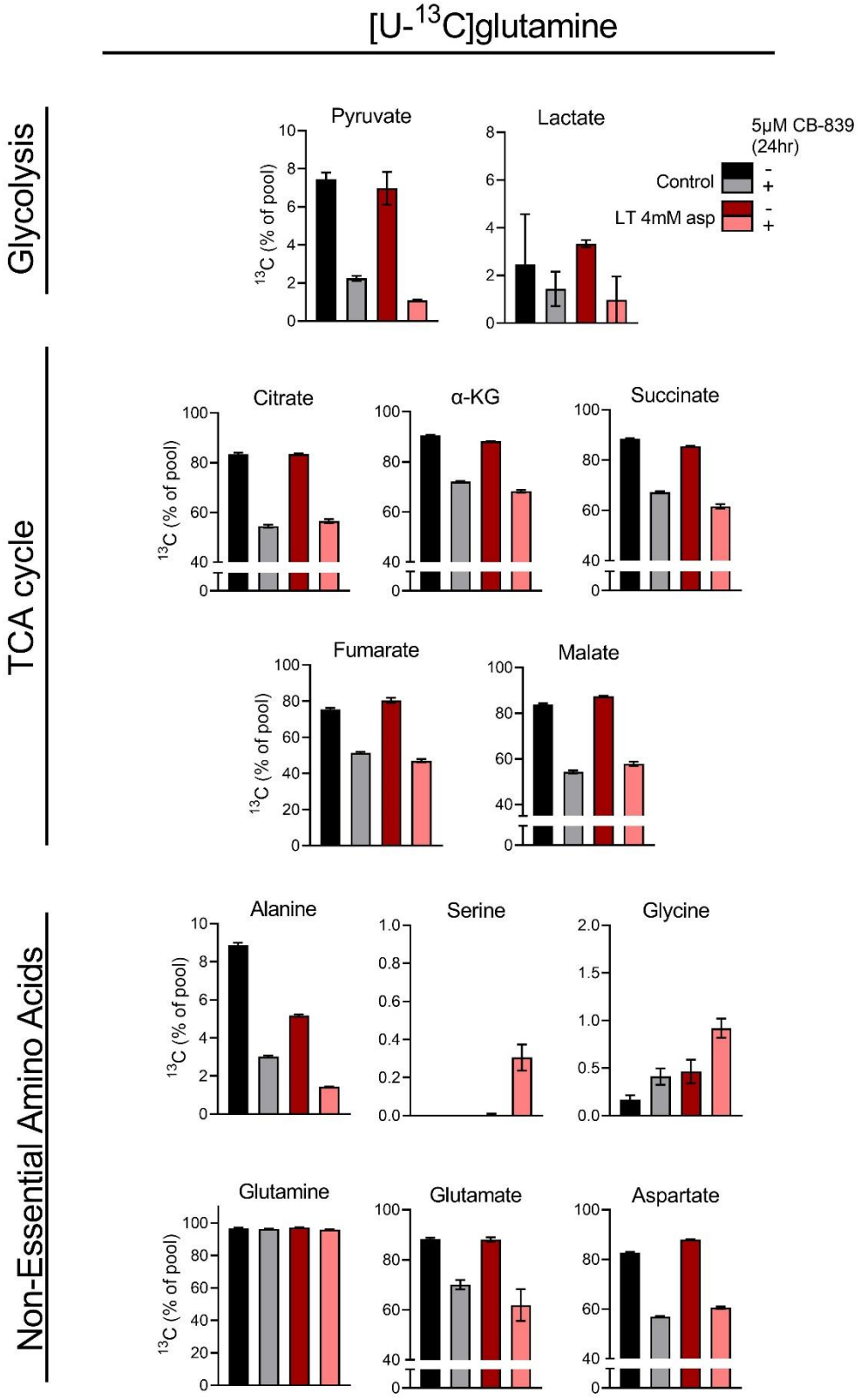

Figure 7.19 Incorporation of ^{13}C after 8 hours of incubation with [U-^{13}C]glucose in long-term aspirin treated SW620 cells treated with CB-839 for 24 hours

Error bars represent standard error (n=3).

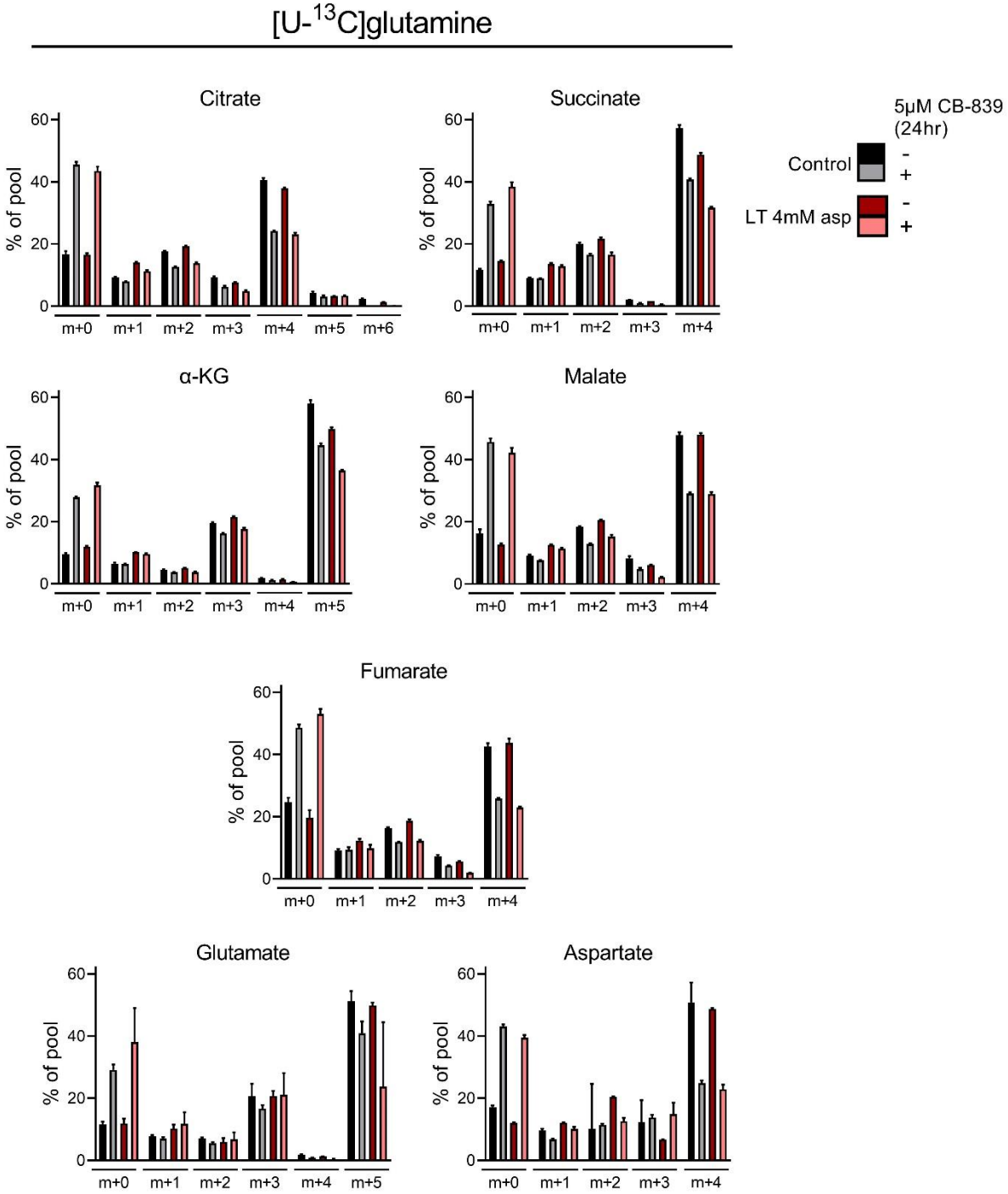

Figure 7.20 Mass isotopomer distribution (MID) data after 8hrs incubation with [U-^{13}C]glutamine in long-term aspirin treated SW620 cells treated with CB-839 for 24 hours

Error bars represent standard error (n=3).

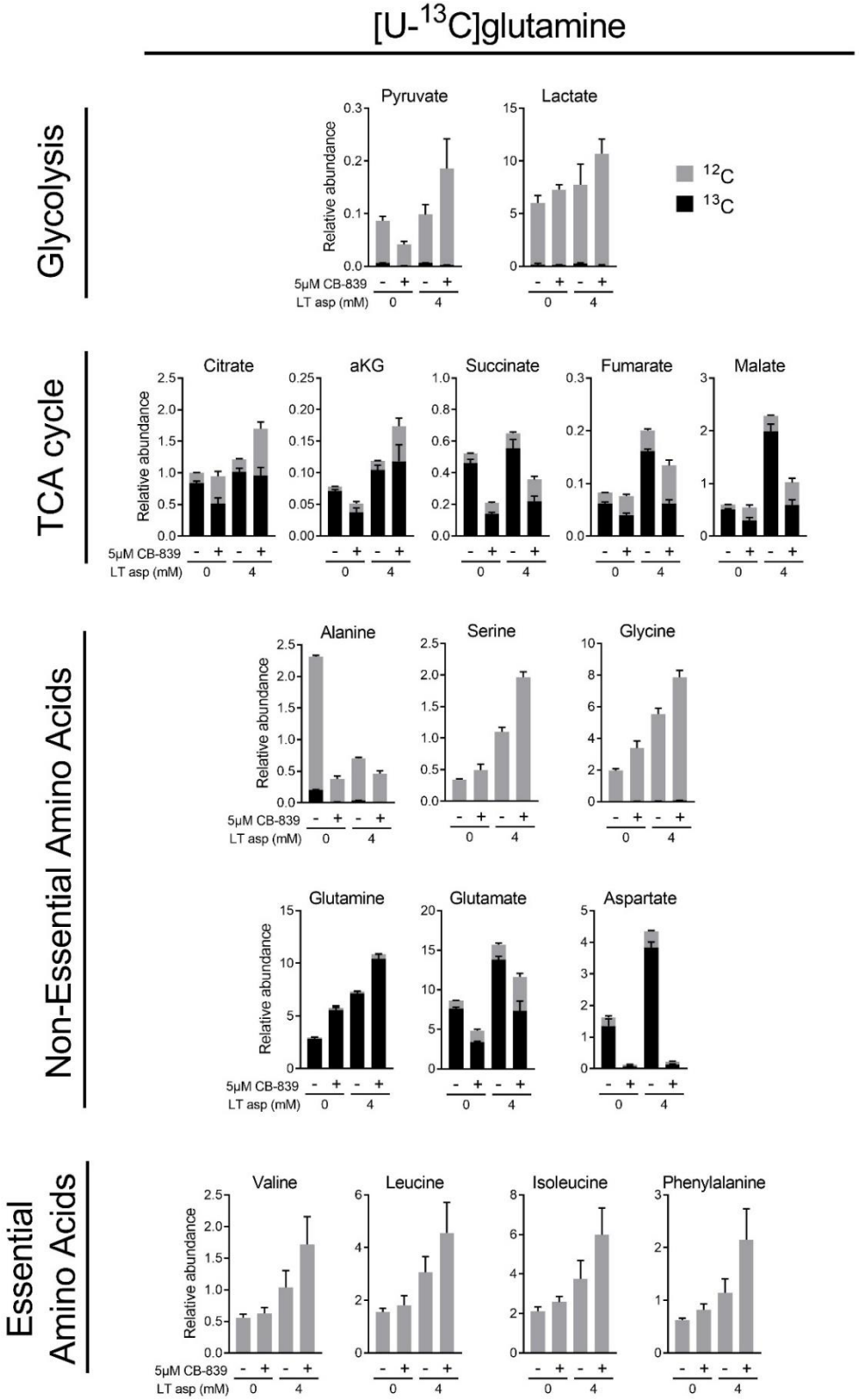

Figure 7.21 Abundance (relative to cell number) of ^{12}C and ^{13}C in metabolite pools after 8hrs incubation with [U-^{13}C]glucose in long-term aspirin treated SW620 cells treated with CB-839 for 24 hours

Error bars represent standard error (n=3).

References

1. Cancer Research UK. Bowel cancer statistics 2018 [Available from: https://www.cancerresearchuk.org/health-professional/cancer-statistics/statistics-by-cancer-type/bowel-cancer.

2. Siegel RL, Fedewa SA, Anderson WF, Miller KD, Ma JM, Rosenberg PS, et al. Colorectal Cancer Incidence Patterns in the United States, 1974-2013. JNCI-J Natl Cancer Inst. 2017;109(8):6.

3. Chambers AC, Dixon SW, White P, Williams AC, Thomas MG, Messenger DE. Demographic trends in the incidence of young-onset colorectal cancer: a population-based study. Br J Surg. 2020;107(5):595-605.

4. Yamagishi H, Kuroda H, Imai Y, Hiraishi H. Molecular pathogenesis of sporadic colorectal cancers. Chinese journal of cancer. 2016;35:4-.

5. Chenga HC, Changb TK, Sub WC, Tsaib HL, Wang JY. Narrative review of the influence of diabetes mellitus and hyperglycemia on colorectal cancer risk and oncological outcomes. Translational Oncology. 2021;14(7).

6. Weinberg RA. The Biology of Cancer. 2nd ed. USA: Garland Science; 2014.

7. Lynch HT, Lynch PM, Lanspa SJ, Snyder CL, Lynch JF, Boland CR. Review of the Lynch syndrome: history, molecular genetics, screening, differential diagnosis, and medicolegal ramifications. Clinical Genetics. 2009;76(1):1-18.

8. Dalerba P, Dylla SJ, Park IK, Liu R, Wang XH, Cho RW, et al. Phenotypic characterization of human colorectal cancer stem cells. Proceedings of the National Academy of Sciences of the United States of America. 2007;104(24):10158-63.

9. Ziskin JL, Dunlap D, Yaylaoglu M, Fodor IK, Forrest WF, Patel R, et al. In situ validation of an intestinal stem cell signature in colorectal cancer. Gut. 2013;62(7):1012-23.

10. Medema JP, Vermeulen L. Microenvironmental regulation of stem cells in intestinal homeostasis and cancer. Nature. 2011;474(7351):318-26.

11. Merlos-Suarez A, Barriga FM, Jung P, Iglesias M, Cespedes MV, Rossell D, et al. The Intestinal Stem Cell Signature Identifies Colorectal Cancer Stem Cells and Predicts Disease Relapse. Cell Stem Cell. 2011;8(5):511-24.

12. Fearon ER, Vogelstein B. A Genetic Model for Colorectal Tumorigenesis. Cell. 1990;61(5):759-67.

13. Walther A, Johnstone E, Swanton C, Midgley R, Tomlinson I, Kerr D. Genetic prognostic and predictive markers in colorectal cancer. Nature Reviews Cancer. 2009;9(7):489-99.

14. Bugter JM, Fenderico N, Maurice MM. Mutations and mechanisms of WNT pathway tumour suppressors in cancer. Nature Reviews Cancer. 2021;21(1):5-21.

15. Nandan MO, Yang VW. An Update on the Biology of RAS/RAF Mutations in Colorectal Cancer. Current colorectal cancer reports. 2011;7(2):113-20.

16. De Roock W, De Vriendt V, Normanno N, Ciardiello F, Tejpar S. KRAS, BRAF, PIK3CA, and PTEN mutations: implications for targeted therapies in metastatic colorectal cancer. Lancet Oncology. 2011;12(6):594-603.

17. Barault L, Veyrie N, Jooste V, Lecorre D, Chapusot C, Ferraz JM, et al. Mutations in the RAS-MAPK, PI(3)K (phosphatidylinositol-3-OH kinase) signaling network correlate with poor survival in a population-based series of colon cancers. Int J Cancer. 2008;122(10):2255-9.

18. Goel A, Arnold CN, Niedzwiecki D, Carethers JM, Dowell JM, Wasserman L, et al. Frequent inactivation of PTEN by promoter hypermethylation in microsatellite instability-high sporadic colorectal cancers. Cancer Research. 2004;64(9):3014-21.

19. Ciardiello F, Tortora G. EGFR antagonists in cancer treatment. The New England journal of medicine. 2008;358(11):1160-74.

20. Nazemalhosseini Mojarad E, Kuppen PJ, Aghdaei HA, Zali MR. The CpG island methylator phenotype (CIMP) in colorectal cancer. Gastroenterol Hepatol Bed Bench. 2013;6(3):120-8.

21. Dienstmann R, Vermeulen L, Guinney J, Kopetz S, Tejpar S, Tabernero J. Consensus molecular subtypes and the evolution of precision medicine in colorectal cancer. Nature Reviews Cancer. 2017;17(4).

22. Guinney J, Dienstmann R, Wang X, de Reynies A, Schlicker A, Soneson C, et al. The consensus molecular subtypes of colorectal cancer. Nature Medicine. 2015;21(11):1350-6.

23. DeBerardinis RJ, Thompson CB. Cellular Metabolism and Disease: What Do Metabolic Outliers Teach Us? Cell. 2012;148(6):1132-44.

24. Hanahan D, Weinberg RA. Hallmarks of Cancer: The Next Generation. Cell. 2011;144(5):646-74.

25. Ceder S, Eriksson SE, Liang YY, Cheteh EH, Zhang SM, Fujihara KM, et al. Mutant p53-reactivating compound APR-246 synergizes with asparaginase in inducing growth suppression in acute lymphoblastic leukemia cells. Cell Death Dis. 2021;12(7):10.

26. DeBerardinis RJ, Chandel NS. Fundamentals of cancer metabolism. Science Advances. 2016;2(5).

27. Mentch SJ, Locasale JW, New York Acad S. One-carbon metabolism and epigenetics: understanding the specificity. Diet, Sulfur Amino Acids, and Health Span. 2016;1363:91-8.

28. Martinez-Reyes I, Chandel NS. Mitochondrial TCA cycle metabolites control physiology and disease. Nat Commun. 2020;11(1).

29. Brown RE, Short SP, Williams CS. Colorectal Cancer and Metabolism. Current Colorectal Cancer Reports. 2018;14(6):226-41.

30. Pate KT, Stringari C, Sprowl-Tanio S, Wang KH, TeSlaa T, Hoverter NP, et al. Wnt signaling directs a metabolic program of glycolysis and angiogenesis in colon cancer. Embo Journal. 2014;33(13):1454-73.

31. Neitzel C, Demuth P, Wittmann S, Fahrer J. Targeting Altered Energy Metabolism in Colorectal Cancer: Oncogenic Reprogramming, the Central Role of the TCA Cycle and Therapeutic Opportunities. Cancers (Basel). 2020;12(7).

32. Hao YJ, Samuels Y, Li QL, Krokowski D, Guan BJ, Wang C, et al. Oncogenic PIK3CA mutations reprogram glutamine metabolism in colorectal cancer. Nat Commun. 2016;7:13.

33. Dang CV. MYC, Metabolism, Cell Growth, and Tumorigenesis. Cold Spring Harbor Perspectives in Medicine. 2013;3(8).

34. Satoh K, Yachida S, Sugimoto M, Oshima M, Nakagawa T, Akamoto S, et al. Global metabolic reprogramming of colorectal cancer occurs at adenoma stage and is induced by MYC. Proceedings of the National Academy of Sciences of the United States of America. 2017;114(37):E7697-E706.

35. Gao P, Tchernyshyov I, Chang TC, Lee YS, Kita K, Ochi T, et al. c-Myc suppression of miR-23a/b enhances mitochondrial glutaminase expression and glutamine metabolism. Nature. 2009;458(7239):762-U100.

36. Duvel K, Yecies JL, Menon S, Raman P, Lipovsky AI, Souza AL, et al. Activation of a Metabolic Gene Regulatory Network Downstream of mTOR Complex 1. Molecular Cell. 2010;39(2):171-83.

37. Meng DL, Yang QM, Wang HY, Melick CH, Navlani R, Frank AR, et al. Glutamine and asparagine activate mTORC1 independently of Rag GTPases. Journal of Biological Chemistry. 2020;295(10):2890-9.

38. Kreuzaler P, Panina Y, Segal J, Yuneva M. Adapt and conquer: Metabolic flexibility in cancer growth, invasion and evasion. Molecular Metabolism. 2020;33:83-101.

39. Kruiswijk F, Labuschagne CF, Vousden KH. p53 in survival, death and metabolic health: a lifeguard with a licence to kill. Nat Rev Mol Cell Biol. 2015;16(7):393-405.

40. Hutton JE, Wang XJ, Zimmerman LJ, Slebos RJC, Trenary IA, Young JD, et al. Oncogenic KRAS and BRAF Drive Metabolic Reprogramming in Colorectal Cancer. Molecular & Cellular Proteomics. 2016;15(9):2924-38.

41. Najumudeen AK, Ceteci F, Fey SK, Hamm G, Steven RT, Hall H, et al. The amino acid transporter SLC7A5 is required for efficient growth of KRAS-mutant colorectal cancer. Nature Genetics. 2021;53(1).

42. Yukimoto R, Nishida N, Hata T, Fujino S, Ogino T, Miyoshi N, et al. Specific activation of glycolytic enzyme enolase 2 in BRAF V600E-mutated colorectal cancer. Cancer Science. 2021;112(7):2884-94.

43. Sciacovelli M, Frezza C. Oncometabolites: Unconventional triggers of oncogenic signalling cascades. Free Radical Biology and Medicine. 2016;100:175-81.

44. Tran TQ, Hanse EA, Habowski AN, Li H, Ishak Gabra MB, Yang Y, et al. α-Ketoglutarate attenuates Wnt signaling and drives differentiation in colorectal cancer. Nature Cancer. 2020;1(3):345-58.

45. Baksh SC, Todorova PK, Gur-Cohen S, Hurwitz B, Ge YJ, Novak JSS, et al. Extracellular serine controls epidermal stem cell fate and tumour initiation. Nature Cell Biology. 2020;22(7):779-+.

46. Zhang D, Tang ZY, Huang H, Zhou GL, Cui C, Weng YJ, et al. Metabolic regulation of gene expression by histone lactylation. Nature. 2019;574(7779):575-+.

47. Warburg O, Wind F, Negelein E. THE METABOLISM OF TUMORS IN THE BODY. The Journal of general physiology. 1927;8(6):519-30.

48. Levine AJ, Puzio-Kuter AM. The Control of the Metabolic Switch in Cancers by Oncogenes and Tumor Suppressor Genes. Science. 2010;330(6009):1340-4.

49. Wang G, Wang JJ, Yin PH, Xu K, Wang YZ, Shi F, et al. New strategies for targeting glucose metabolism-mediated acidosis for colorectal cancer therapy. J Cell Physiol. 2019;234(1):348-68.

50. Li X, Wenes M, Romero P, Huang SC-C, Fendt S-M, Ho P-C. Navigating metabolic pathways to enhance antitumour immunity and immunotherapy. Nature Reviews Clinical Oncology. 2019.

51. Hui S, Ghergurovich JM, Morscher RJ, Jang C, Teng X, Lu WY, et al. Glucose feeds the TCA cycle via circulating lactate. Nature. 2017;551(7678):115-+.

52. Cha PH, Hwang JH, Kwak DK, Koh E, Kim KS, Choi KA-O. APC loss induces Warburg effect via increased PKM2 transcription in colorectal cancer. (1532-1827 (Electronic)).

53. Zhang C, Liu J, Liang YJ, Wu R, Zhao YH, Hong XH, et al. Tumour-associated mutant p53 drives the Warburg effect. Nat Commun. 2013;4.

54. Feng WM, Cui G, Tang CW, Zhang XL, Dai C, Xu YQ, et al. Role of glucose metabolism related gene GLUT1 in the occurrence and prognosis of colorectal cancer. Oncotarget. 2017;8(34):56850-7.

55. Yun JY, Rago C, Cheong I, Pagliarini R, Angenendt P, Rajagopalan H, et al. Glucose Deprivation Contributes to the Development of KRAS Pathway Mutations in Tumor Cells. Science. 2009;325(5947):1555-9.

56. Heikkinen S, Suppola S, Malkki M, Deeb SS, Janne J, Laakso M. Mouse hexokinase II gene: structure, cDNA, promoter analysis, and expression pattern. Mammalian Genome. 2000;11(2):91-6.

57. Sato-Tadano A, Suzuki T, Amari M, Takagi K, Miki Y, Tamaki K, et al. Hexokinase II in breast carcinoma: A potent prognostic factor associated with hypoxia-inducible factor-1 alpha and Ki-67. Cancer Science. 2013;104(10):1380-8.

58. Qiu MZ, Han B, Luo HY, Zhou ZW, Wang ZQ, Wang FH, et al. Expressions of hypoxia-inducible factor-1 alpha and hexokinase-II in gastric adenocarcinoma: the impact on prognosis and correlation to clinicopathologic features. Tumor Biol. 2011;32(1):159-66.

59. Hamabe A, Yamamoto H, Konno M, Uemura M, Nishimura J, Hata T, et al. Combined evaluation of hexokinase 2 and phosphorylated pyruvate dehydrogenase-E1 alpha in invasive front lesions of colorectal tumors predicts cancer metabolism and patient prognosis. Cancer Science. 2014;105(9):1100-8.

60. Ho N, Coomber BL. Hexokinase II expression is correlated with colorectal cancer prognosis. Cancer Treatment Communications. 2016;6:11-6.

61. Pavlides S, Whitaker-Menezes D, Castello-Cros R, Flomenberg N, Witkiewicz AK, Frank PG, et al. The reverse Warburg effect Aerobic glycolysis in cancer associated fibroblasts and the tumor stroma. Cell Cycle. 2009;8(23):3984-4001.

62. Mesker WE, Junggeburt JMC, Szuhai K, de Heer P, Morreau H, Tanke HJ, et al. The carcinoma-stromal ratio of colon carcinoma is an independent

factor for survival compared to lymph node status and tumor stage. Cell Oncol. 2007;29(5):387-98.

63. Chen M, David CJ, Manley JL. Concentration-dependent control of pyruvate kinase M mutually exclusive splicing by hnRNP proteins. Nature Structural & Molecular Biology. 2012;19(3):346-U110.

64. Takenaka M, Noguchi T, Sadahiro S, Hirai H, Yamada K, Matsuda T, et al. ISOLATION AND CHARACTERIZATION OF THE HUMAN PYRUVATE-KINASE M-GENE. European Journal of Biochemistry. 1991;198(1):101-6.

65. Israelsen WJ, Vander Heiden MG. Pyruvate kinase: Function, regulation and role in cancer. Seminars in Cell & Developmental Biology. 2015;43:43-51.

66. Clower CV, Chatterjee D, Wang ZX, Cantley LC, Heiden MGV, Krainer AR. The alternative splicing repressors hnRNP A1/A2 and PTB influence pyruvate kinase isoform expression and cell metabolism. Proceedings of the National Academy of Sciences of the United States of America. 2010;107(5):1894-9.

67. Wang ZX, Chatterjee D, Jeon HY, Akerman M, Vander Heiden MG, Cantley LC, et al. Exon-centric regulation of pyruvate kinase M alternative splicing via mutually exclusive exons. J Mol Cell Biol. 2012;4(2):79-87.

68. Christofk HR, Vander Heiden MG, Harris MH, Ramanathan A, Gerszten RE, Wei R, et al. The M2 splice isoform of pyruvate kinase is important for cancer metabolism and tumour growth. Nature. 2008;452(7184):230-U74.

69. Lunt SY, Muralidhar V, Hosios AM, Israelsen WJ, Gui DY, Newhouse L, et al. Pyruvate Kinase Isoform Expression Alters Nucleotide Synthesis to Impact Cell Proliferation. Molecular Cell. 2015;57(1):95-107.

70. Cui R, Shi XY. Expression of pyruvate kinase M2 in human colorectal cancer and its prognostic value. International Journal of Clinical and Experimental Pathology. 2015;8(9):11393-9.

71. Graziano F, Ruzzo A, Giacomini E, Ricciardi T, Aprile G, Loupakis F, et al. Glycolysis gene expression analysis and selective metabolic advantage in the clinical progression of colorectal cancer. Pharmacogenomics Journal. 2017;17(3):258-64.

72. Kuranaga Y, Sugito N, Shinohara H, Tsujino T, Taniguchi K, Komura K, et al. SRSF3, a Splicer of the PKM Gene, Regulates Cell Growth and Maintenance of Cancer-Specific Energy Metabolism in Colon Cancer Cells. Int J Mol Sci. 2018;19(10):16.

73. Lan ZX, Yao X, Sun KY, Li AM, Liu SD, Wang XK. The Interaction Between lncRNA SNHG6 and hnRNPA1 Contributes to the Growth of Colorectal Cancer by Enhancing Aerobic Glycolysis Through the Regulation of Alternative Splicing of PKM. Frontiers in Oncology. 2020;10.

74. Kim JW, Tchernyshyov I, Semenza GL, Dang CV. HIF-1-mediated expression of pyruvate dehydrogenase kinase: A metabolic switch required for cellular adaptation to hypoxia. Cell Metabolism. 2006;3(3):177-85.

75. Madhok BM, Yeluri S, Perry SL, Hughes TA, Jayne DG. Dichloroacetate induces apoptosis and cell-cycle arrest in colorectal cancer cells. Br J Cancer. 2010;102(12):1746-52.

76. Vander Heiden MG, Cantley LC, Thompson CB. Understanding the Warburg Effect: The Metabolic Requirements of Cell Proliferation. Science. 2009;324(5930):1029-33.

77. Wang J, Wang H, Liu AF, Fang CG, Hao JG, Wang ZH. Lactate dehydrogenase A negatively regulated by miRNAs promotes aerobic glycolysis and is increased in colorectal cancer. Oncotarget. 2015;6(23):19456-68.

78. Raghunand N, Gatenby RA, Gillies RJ. Microenvironmental and cellular consequences of altered blood flow in tumours. British Journal of Radiology. 2003;76:S11-S22.

79. Robey IF, Lien AD, Welsh SJ, Baggett BK, Gillies RJ. Hypoxia-inducible factor-1alpha and the glycolytic phenotype in tumors. Neoplasia (New York, NY). 2005;7(4):324-30.

80. Luo WB, Hu HX, Chang R, Zhong J, Knabel M, O'Meally R, et al. Pyruvate Kinase M2 Is a PHD3-Stimulated Coactivator for Hypoxia-Inducible Factor 1. Cell. 2011;145(5):732-44.

81. Baba Y, Nosho K, Shima K, Irahara N, Chan AT, Meyerhardt JA, et al. HIF1A Overexpression Is Associated with Poor Prognosis in a Cohort of 731 Colorectal Cancers. American Journal of Pathology. 2010;176(5):2292-301.

82. Warburg O. ORIGIN OF CANCER CELLS. Science. 1956;123(3191):309-14.

83. Montal ED, Bhalla K, Dewi RE, Ruiz CF, Haley JA, Ropell AE, et al. Inhibition of phosphoenolpyruvate carboxykinase blocks lactate utilization and impairs tumor growth in colorectal cancer. Cancer & Metabolism. 2019;7.

84. Vasan K, Werner M, Chandel NS. Mitochondrial Metabolism as a Target for Cancer Therapy. Cell Metabolism. 2020;32(3):341-52.

85. Martinez-Reyes I, Cardona LR, Kong H, Vasan K, McElroy GS, Werner M, et al. Mitochondrial ubiquinol oxidation is necessary for tumour growth. Nature. 2020;585(7824):288-+.

86. Sullivan LB, Luengo A, Danai LV, Bush LN, Diehl FF, Hosios AM, et al. Aspartate is an endogenous metabolic limitation for tumour growth. Nature Cell Biology. 2018;20(7):782-+.

87. Krall AS, Mullen PJ, Surjono F, Momcilovic M, Schmid EW, Halbrook CJ, et al. Asparagine couples mitochondrial respiration to ATF4 activity and tumor growth. Cell Metabolism. 2021;33(5):1013-+.

88. Ryan DG, Yang M, Prag HA, Blanco GR, Nikitopoulou E, Segarra-Mondejar M, et al. Disruption of the TCA cycle reveals an ATF4-dependent integration of redox and amino acid metabolism. bioRxiv. 2021:2021.07.27.453996.

89. Sullivan LB, Gui DY, Hosios AM, Bush LN, Freinkman E, Vander Heiden MG. Supporting Aspartate Biosynthesis Is an Essential Function of Respiration in Proliferating Cells. Cell. 2015;162(3):552-63.

90. Birsoy K, Wang T, Chen WW, Freinkman E, Abu-Remaileh M, Sabatini DM. An Essential Role of the Mitochondrial Electron Transport Chain in Cell Proliferation Is to Enable Aspartate Synthesis. Cell. 2015;162(3):540-51.

91. Garcia-Bermudez J, Baudrier L, La K, Zhu XG, Fidelin J, Sviderskiy VO, et al. Aspartate is a limiting metabolite for cancer cell proliferation under hypoxia and in tumours. Nature Cell Biology. 2018;20(7):775-+.

92. Momcilovic M, Jones A, Bailey ST, Waldmann CM, Li R, Lee JT, et al. In vivo imaging of mitochondrial membrane potential in non-small-cell lung cancer. Nature. 2019.

93. Chekulayev V, Mado K, Shevchuk I, Koit A, Kaldma A, Klepinin A, et al. Metabolic remodeling in human colorectal cancer and surrounding tissues: alterations in regulation of mitochondrial respiration and metabolic fluxes. (2405-5808 (Electronic)).

94. Denise C, Paoli P, Calvani M, Taddei ML, Giannoni E, Kopetz S, et al. 5-Fluorouracil resistant colon cancer cells are addicted to OXPHOS to survive and enhance stem-like traits. Oncotarget. 2015;6(39):41706-21.

95. Hirpara J, Eu JQ, Tan JKM, Wong AL, Clement MV, Kong LR, et al. Metabolic reprogramming of oncogene-addicted cancer cells to OXPHOS as a mechanism of drug resistance. Redox Biology. 2019;25.

96. Rai NK, Mathur S, Singh SK, Tiwari M, Singh VK, Haque R, et al. Differential regulation of mitochondrial complex I and oxidative stress based on metastatic potential of colorectal cancer cells. Oncology Letters. 2020;20(6).

97. Sun XC, Zhan L, Chen YB, Wang G, He LJ, Wang Q, et al. Increased mtDNA copy number promotes cancer progression by enhancing mitochondrial oxidative phosphorylation in microsatellite-stable colorectal cancer. Signal Transduction and Targeted Therapy. 2018;3.

98. Feng S, Xiong LL, Ji ZN, Cheng W, Yang HJ. Correlation between increased copy number of mitochondrial DNA and clinicopathological stage in colorectal cancer. Oncology Letters. 2011;2(5):899-903.

99. Smith ALM, Whitehall JC, Bradshaw C, Gay D, Robertson F, Blain AP, et al. Age-associated mitochondrial DNA mutations cause metabolic remodeling that contributes to accelerated intestinal tumorigenesis. Nature Cancer. 2020;1(10):976-+.

100. Ryall JG, Cliff T, Dalton S, Sartorelli V. Metabolic Reprogramming of Stem Cell Epigenetics. Cell Stem Cell. 2015;17(6):651-62.

101. Snyder V, Reed-Newman TC, Arnold L, Thomas SM, Anant S. Cancer Stem Cell Metabolism and Potential Therapeutic Targets. Frontiers in Oncology. 2018;8:9.

102. Song IS, Jeong YJ, Jeong SH, Heo HJ, Kim HK, Bae KB, et al. FOXM1-Induced PRX3 Regulates Stemness and Survival of Colon Cancer Cells via Maintenance of Mitochondrial Function. Gastroenterology. 2015;149(4):1006-U736.

103. Altman BJ, Stine ZE, Dang CV. From Krebs to clinic: glutamine metabolism to cancer therapy. Nature Reviews Cancer. 2016;16(10):619-34.

104. Wise DR, Thompson CB. Glutamine addiction: a new therapeutic target in cancer. Trends in Biochemical Sciences. 2010;35(8):427-33.

105. Bhutia YD, Babu E, Ramachandran S, Ganapathy V. Amino Acid Transporters in Cancer and Their Relevance to "Glutamine Addiction": Novel

Targets for the Design of a New Class of Anticancer Drugs. Cancer Research. 2015;75(9):1782-8.

106. Bhutia YD, Ganapathy V. Glutamine transporters in mammalian cells and their functions in physiology and cancer. Biochim Biophys Acta-Mol Cell Res. 2016;1863(10):2531-9.

107. Huang F, Zhao YC, Zhao JZ, Wu S, Jiang Y, Ma H, et al. Upregulated SLC1A5 promotes cell growth and survival in colorectal cancer. International Journal of Clinical and Experimental Pathology. 2014;7(9):6006-14.

108. Zhang J, Pavlova NN, Thompson CB. Cancer cell metabolism: the essential role of the nonessential amino acid, glutamine. Embo Journal. 2017;36(10):1302-15.

109. Moreadith RW, Lehninger AL. THE PATHWAYS OF GLUTAMATE AND GLUTAMINE OXIDATION BY TUMOR-CELL MITOCHONDRIA - ROLE OF MITOCHONDRIAL NAD(P)+-DEPENDENT MALIC ENZYME. Journal of Biological Chemistry. 1984;259(10):6215-21.

110. Le A, Lane AN, Hamaker M, Bose S, Gouw A, Barbi J, et al. Glucose-Independent Glutamine Metabolism via TCA Cycling for Proliferation and Survival in B Cells. Cell Metabolism. 2012;15(1):110-21.

111. DeBerardinis RJ, Mancuso A, Daikhin E, Nissim I, Yudkoff M, Wehrli S, et al. Beyond aerobic glycolysis: Transformed cells can engage in glutamine metabolism that exceeds the requirement for protein and nucleotide synthesis. Proceedings of the National Academy of Sciences of the United States of America. 2007;104(49):19345-50.

112. Wellen KE, Lu C, Mancuso A, Lemons JMS, Ryczko M, Dennis JW, et al. The hexosamine biosynthetic pathway couples growth factor-induced glutamine uptake to glucose metabolism. Genes & Development. 2010;24(24):2784-99.

113. Mathur D, Stratikopoulos E, Ozturk S, Steinbach N, Pegno S, Schoenfeld S, et al. PTEN Regulates Glutamine Flux to Pyrimidine Synthesis and Sensitivity to Dihydroorotate Dehydrogenase Inhibition. Cancer Discovery. 2017;7(4):380-90.

114. Kodama M, Oshikawa K, Shimizu H, Yoshioka S, Takahashi M, Izumi Y, et al. A shift in glutamine nitrogen metabolism contributes to the malignant progression of cancer. Nat Commun. 2020;11(1).

115. Xiao Y, Meierhofer D. Glutathione Metabolism in Renal Cell Carcinoma Progression and Implications for Therapies. Int J Mol Sci. 2019;20(15).

116. Nicklin P, Bergman P, Zhang BL, Triantafellow E, Wang H, Nyfeler B, et al. Bidirectional Transport of Amino Acids Regulates mTOR and Autophagy. Cell. 2009;136(3):521-34.

117. Cormerais Y, Massard PA, Vucetic M, Giuliano S, Tambutte E, Durivault J, et al. The glutamine transporter ASCT2 (SLC1A5) promotes tumor growth independently of the amino acid transporter LAT1 (SLC7A5). Journal of Biological Chemistry. 2018;293(8):2877-87.

118. Kandasamy P, Zlobec I, Nydegger DT, Pujol-Gimenez J, Bhardwaj R, Shirasawa S, et al. Oncogenic KRAS mutations enhance amino acid uptake by colorectal cancer cells via the hippo signaling effector YAP1. Mol Oncol. 2021:19.

119. Cantor JR, Abu-Remaileh M, Kanarek N, Freinkman E, Gao X, Louissaint A, et al. Physiologic Medium Rewires Cellular Metabolism and Reveals Uric Acid as an Endogenous Inhibitor of UMP Synthase. Cell. 2017;169(2):258-72.

120. Muir A, Danai LV, Gui DY, Waingarten CY, Lewis CA, Heidan MGV. Environmental cystine drives glutamine anaplerosis and sensitizes cancer cells to glutaminase inhibition. Elife. 2017;6.

121. Zhao YQ, Zhao X, Chen V, Feng Y, Wang L, Croniger C, et al. Colorectal cancers utilize glutamine as an anaplerotic substrate of the TCA cycle in vivo. Scientific Reports. 2019;9.

122. Kim MH, Kim H. The Roles of Glutamine in the Intestine and Its Implication in Intestinal Diseases. Int J Mol Sci. 2017;18(5).

123. Song Z, Wei B, Lu CR, Li PY, Chen L. Glutaminase sustains cell survival via the regulation of glycolysis and glutaminolysis in colorectal cancer. Oncology Letters. 2017;14(3):3117-23.

124. Huang F, Zhang QY, Ma H, Lv Q, Zhang T. Expression of glutaminase is upregulated in colorectal cancer and of clinical significance. International Journal of Clinical and Experimental Pathology. 2014;7(3):1093-100.

125. Xiang LS, Mou J, Shao B, Wei YQ, Liang HJ, Takano N, et al. Glutaminase 1 expression in colorectal cancer cells is induced by hypoxia and required for tumor growth, invasion, and metastatic colonization. Cell Death Dis. 2019;10:15.

126. Liu GJ, Zhu J, Yu ML, Cai CF, Zhou Y, Yu M, et al. Glutamate dehydrogenase is a novel prognostic marker and predicts metastases in colorectal cancer patients. Journal of Translational Medicine. 2015;13.

127. Wang RJ, Xiang WQ, Xu Y, Han LY, Li QG, Dai WX, et al. Enhanced glutamine utilization mediated by SLC1A5 and GPT2 is an essential metabolic feature of colorectal signet ring cell carcinoma with therapeutic potential. Annals of Translational Medicine. 2020;8(6).

128. Toda K, Nishikawa G, Iwamoto M, Itatani Y, Takahashi R, Sakai Y, et al. Clinical Role of ASCT2 (SLC1A5) in KRAS-Mutated Colorectal Cancer. Int J Mol Sci. 2017;18(8):13.

129. Elgadi KM, Meguid RA, Qian M, Souba WW, Abcouwer SF. Cloning and analysis of unique human glutaminase isoforms generated by tissue-specific alternative splicing. Physiological Genomics. 1999;1(2):51-62.

130. Wang ZF, Liu FY, Fan NB, Zhou CH, Li D, Macvicar T, et al. Targeting Glutaminolysis: New Perspectives to Understand Cancer Development and Novel Strategies for Potential Target Therapies. Frontiers in Oncology. 2020;10.

131. Masamha CP, LaFontaine P. Molecular targeting of glutaminase sensitizes ovarian cancer cells to chemotherapy. Journal of Cellular Biochemistry. 2018;119(7):6136-45.

132. Cassago A, Ferreira APS, Ferreira IM, Fornezari C, Gomes ERM, Greene KS, et al. Mitochondrial localization and structure-based phosphate activation mechanism of Glutaminase C with implications for cancer metabolism. Proceedings of the National Academy of Sciences of the United States of America. 2012;109(4):1092-7.

133. Pieter A, van den Heuvel J, Jing JP, Wooster RF, Bachman KE. Analysis of glutamine dependency in non-small cell lung cancer GLS1 splice variant GAC is essential for cancer cell growth. Cancer Biol Ther. 2012;13(12):1185-94.

134. Redis RS, Vela LE, Lu WQ, de Oliveira JF, Ivan C, Rodriguez-Aguayo C, et al. Allele-Specific Reprogramming of Cancer Metabolism by the Long Non-coding RNA CCAT2. Molecular Cell. 2016;61(4):520-34.

135. Csibi A, Lee G, Yoon SO, Tong HX, Iiter D, Elia I, et al. The mTORC1/S6K1 Pathway Regulates Glutamine Metabolism through the eIF4B-Dependent Control of c-Myc Translation. Curr Biol. 2014;24(19):2274-80.

136. Han TY, Zhan WH, Gan MX, Liu FR, Yu BT, Chin YE, et al. Phosphorylation of glutaminase by PKC epsilon is essential for its enzymatic activity and critically contributes to tumorigenesis. Cell Research. 2018;28(6):655-69.

137. Wilson KF, Erickson JW, Antonyak MA, Cerione RA. Rho GTPases and their roles in cancer metabolism. Trends in Molecular Medicine. 2013;19(2):74-82.

138. Thangavelu K, Pan CQ, Karlberg T, Balaji G, Uttamchandani M, Suresh V, et al. Structural basis for the allosteric inhibitory mechanism of human kidney-type glutaminase (KGA) and its regulation by Raf-Mek-Erk signaling in cancer cell metabolism. Proceedings of the National Academy of Sciences of the United States of America. 2012;109(20):7705-10.

139. Wang JB, Erickson JW, Fuji R, Ramachandran S, Gao P, Dinavahi R, et al. Targeting Mitochondrial Glutaminase Activity Inhibits Oncogenic Transformation. Cancer Cell. 2010;18(3):207-19.

140. Greene KS, Lukey MJ, Wang XY, Blank B, Druso JE, Lin MCJ, et al. SIRT5 stabilizes mitochondrial glutaminase and supports breast cancer tumorigenesis. Proceedings of the National Academy of Sciences of the United States of America. 2019;116(52):26625-32.

141. Tong YY, Guo D, Lin SH, Liang JZ, Yang DQ, Ma CM, et al. SUCLA2-coupled regulation of GLS succinylation and activity counteracts oxidative stress in tumor cells. Molecular Cell. 2021;81(11):2303-+.

142. Hu WW, Zhang C, Wu R, Sun Y, Levine A, Feng ZH. Glutaminase 2, a novel p53 target gene regulating energy metabolism and antioxidant function. Proceedings of the National Academy of Sciences of the United States of America. 2010;107(16):7455-60.

143. Suzuki S, Tanaka T, Poyurovsky MV, Nagano H, Mayama T, Ohkubo S, et al. Phosphate-activated glutaminase (GLS2), a p53-inducible regulator of glutamine metabolism and reactive oxygen species. Proceedings of the National Academy of Sciences of the United States of America. 2010;107(16):7461-6.

144. Xiang Y, Stine ZE, Xia JS, Lu YQ, O'Connor RS, Altman BJ, et al. Targeted inhibition of tumor-specific glutaminase diminishes cell-autonomous tumorigenesis. Journal of Clinical Investigation. 2015;125(6):2293-306.

145. Jin L, Alesi GN, Kang S. Glutaminolysis as a target for cancer therapy. Oncogene. 2016;35(28):3619-25.

146. Needs CJ, Brooks PM. CLINICAL PHARMACOKINETICS OF THE SALICYLATES. Clinical Pharmacokinetics. 1985;10(2):164-77.

147. Dovizio M, Tacconelli S, Sostres C, Ricciotti E, Patrignani P. Mechanistic and pharmacological issues of aspirin as an anticancer agent. Pharmaceuticals (Basel). 2012;5(12):1346-71.

148. Sankaranarayanan R, Kumar DR, Altinoz MA, Bhat GJ. Mechanisms of Colorectal Cancer Prevention by Aspirin-A Literature Review and Perspective on the Role of COX-Dependent and -Independent Pathways. Int J Mol Sci. 2020;21(23).

149. Cox D, Maree AO, Dooley M, Conroy R, Byrne MF, Fitzgerald DJ. Effect of enteric coating on antiplatelet activity of low-dose aspirin in healthy volunteers. Stroke. 2006;37(8):2153-8.

150. Frantz B, Oneill EA. THE EFFECT OF SODIUM-SALICYLATE AND ASPIRIN ON NF-KAPPA-B. Science. 1995;270(5244):2017-8.

151. Borthwick GM, Johnson AS, Partington M, Burn J, Wilson R, Arthur HM. Therapeutic levels of aspirin and salicylate directly inhibit a model of angiogenesis through a Cox-independent mechanism. Faseb Journal. 2006;20(12):2009-16.

152. Kune GA, Kune S, Watson LF. COLORECTAL-CANCER RISK, CHRONIC ILLNESSES, OPERATIONS, AND MEDICATIONS - CASE CONTROL RESULTS FROM THE MELBOURNE COLORECTAL-CANCER STUDY. Cancer Research. 1988;48(15):4399-404.

153. Drew DA, Cao Y, Chan AT. Aspirin and colorectal cancer: the promise of precision chemoprevention. Nature Reviews Cancer. 2016;16(3):173-86.

154. Flossmann E, Rothwell PM, British Doctors Aspirin T, Trial U-TA. Effect of aspirin on long-term risk of colorectal cancer: consistent evidence from randomised and observational studies. Lancet. 2007;369(9573):1603-13.

155. Rothwell PM, Wilson M, Elwin CE, Norrving B, Algra A, Warlow CP, et al. Long-term effect of aspirin on colorectal cancer incidence and mortality: 20-year follow-up of five randomised trials. Lancet. 2010;376(9754):1741-50.

156. Bibbins-Domingo K, Force USPST. Aspirin Use for the Primary Prevention of Cardiovascular Disease and Colorectal Cancer: US Preventive Services Task Force Recommendation Statement. Annals of Internal Medicine. 2016;164(12):836-U103.

157. Bosetti C, Santucci C, Gallus S, Martinetti M, La Vecchia C. Aspirin and the risk of colorectal and other digestive tract cancers: an updated meta-analysis through 2019. Annals of Oncology. 2020;31(5):558-68.

158. Drew DA, Chin SM, Gilpin KK, Parziale M, Pond E, Schuck MM, et al. ASPirin Intervention for the REDuction of colorectal cancer risk (ASPIRED): a study protocol for a randomized controlled trial. Trials. 2017;18.

159. Rothwell PM, Wilson M, Price JF, Belch JFF, Meade TW, Mehta Z. Effect of daily aspirin on risk of cancer metastasis: a study of incident cancers during randomised controlled trials. Lancet. 2012;379(9826):1591-601.

160. Li PW, Wu H, Zhang HH, Shi Y, Xu JM, Ye Y, et al. Aspirin use after diagnosis but not prediagnosis improves established colorectal cancer survival: a meta-analysis. Gut. 2015;64(9):1419-25.

161. Chan AT, Ogino S, Fuchs CS. Aspirin use and survival after diagnosis of colorectal cancer. Jama. 2009;302(6):649-58.

162. Coyle C, Cafferty FH, Rowley S, MacKenzie M, Berkman L, Gupta S, et al. ADD-ASPIRIN: A phase III, double-blind, placebo controlled, randomised trial assessing the effects of aspirin on disease recurrence and survival after primary therapy in common non-metastatic solid tumours. Contemp Clin Trials. 2016;51:56-64.

163. Joharatnam-Hogan N, Cafferty F, Hubner R, Swinson D, Sothi S, Gupta K, et al. Aspirin as an adjuvant treatment for cancer: feasibility results from the Add-Aspirin randomised trial. Lancet Gastroenterology & Hepatology. 2019;4(11):854-62.

164. Chan AT, Ogino S, Fuchs CS. Aspirin and the risk of colorectal cancer in relation to the expression of COX-2. New England Journal of Medicine. 2007;356(21):2131-42.

165. Liao XY, Lochhead P, Nishihara R, Morikawa T, Kuchiba A, Yamauchi M, et al. Aspirin Use, Tumor PIK3CA Mutation, and Colorectal-Cancer Survival. New England Journal of Medicine. 2012;367(17):1596-606.

166. Henry WS, Laszewski T, Tsang T, Beca F, Beck AH, McAllister SS, et al. Aspirin Suppresses Growth in PI3K-Mutant Breast Cancer by Activating AMPK and Inhibiting mTORC1 Signaling. Cancer Research. 2017;77(3):790-801.

167. McCarthy AM, Kumar NP, He W, Regan S, Welch M, Moy B, et al. Different associations of tumor PIK3CA mutations and clinical outcomes according to aspirin use among women with metastatic hormone receptor positive breast cancer. BMC Cancer. 2020;20(1):10.

168. Bains SJ, Mahic M, Myklebust TA, Smastuen MC, Yaqub S, Dorum LM, et al. Aspirin As Secondary Prevention in Patients With Colorectal Cancer: An Unselected Population-Based Study. J Clin Oncol. 2016;34(21):2501-+.

169. Marimuthu S, Chivukula RSV, Alfonso LF, Moridani M, Hagen FK, Bhat GJ. Aspirin acetylates multiple cellular proteins in HCT-116 colon cancer cells: Identification of novel targets. International Journal of Oncology. 2011;39(5):1273-83.

170. Gay LJ, Felding-Habermann B. Contribution of platelets to tumour metastasis. Nature Reviews Cancer. 2011;11(2):123-34.

171. Sostres C, Gargallo CJ, Lanas A. Aspirin, cyclooxygenase inhibition and colorectal cancer. World journal of gastrointestinal pharmacology and therapeutics. 2014;5(1):40-9.

172. Kaidi A, Qualtrough D, Williams AC, Paraskeva C. Direct transcriptional up-regulation of cyclooxygenase-2 by hypoxia-inducible factor (HIF)-1 promotes colorectal tumor cell survival and enhances HIF-1 transcriptional activity during hypoxia. Cancer Research. 2006;66(13):6683-91.

173. Eberhart CE, Coffey RJ, Radhika A, Giardiello FM, Ferrenbach S, Dubois RN. UP-REGULATION OF CYCLOOXYGENASE-2 GENE-EXPRESSION IN HUMAN COLORECTAL ADENOMAS AND ADENOCARCINOMAS. Gastroenterology. 1994;107(4):1183-8.

174. Greenhough A, Smartt HJM, Moore AE, Roberts HR, Williams AC, Paraskeva C, et al. The COX-2/PGE(2) pathway: key roles in the hallmarks of cancer and adaptation to the tumour microenvironment. Carcinogenesis. 2009;30(3):377-86.

175. Hanahan D, Weinberg RA. The Hallmarks of Cancer. Cell. 2000;100(1):57-70.

176. Castellone MD, Teramoto H, Williams BO, Druey KM, Gutkind JS. Prostaglandin E-2 promotes colon cancer cell growth through a G(s)-axin-beta-catenin signaling axis. Science. 2005;310(5753):1504-10.

177. Koundouros N, Karali E, Tripp A, Valle A, Inglese P, Perry NJS, et al. Metabolic Fingerprinting Links Oncogenic PIK3CA with Enhanced Arachidonic Acid-Derived Eicosanoids. Cell. 2020;181(7):1596-+.

178. Lai MY, Huang JA, Liang ZH, Jiang HX, Tang GD. Mechanisms underlying aspirin-mediated growth inhibition and apoptosis induction of cyclooxygenase-2 negative colon cancer cell line SW480. World Journal of Gastroenterology. 2008;14(26):4227-33.

179. Hanif R, Pittas A, Feng Y, Koutsos MI, Qiao L, StaianoCoico L, et al. Effects of nonsteroidal anti-inflammatory drugs on proliferation and on induction of apoptosis in colon cancer cells by a prostaglandin-independent pathway. Biochemical Pharmacology. 1996;52(2):237-45.

180. Gurpinar E, Grizzle WE, Piazza GA. COX-Independent Mechanisms of Cancer Chemoprevention by Anti-Inflammatory Drugs. Front Oncol. 2013;3:181.

181. Bak AW, McKnight W, Li P, Del Soldato P, Calignano A, Cirino G, et al. Cyclooxygenase-independent chemoprevention with an aspirin derivative in a rat model of colonic adenocarcinoma. Life Sciences. 1998;62(23):PL367-PL73.

182. Chen JY, Stark LA. Aspirin Prevention of Colorectal Cancer: Focus on NF-kappa B Signalling and the Nucleolus. Biomedicines. 2017;5(3).

183. Gilmore TD. Introduction to NF-kappa B: players, pathways, perspectives. Oncogene. 2006;25(51):6680-4.

184. Naugler WE, Karin M. NF-kappa B and cancer - identifying targets and mechanisms. Current Opinion in Genetics & Development. 2008;18(1):19-26.

185. Kaltschmidt B, Kaltschmidt C, Hofmann TG, Hehner SP, Droge W, Schmitz ML. The pro- or anti-apoptotic function of NF-kappa B is determined by the nature of the apoptotic stimulus. European Journal of Biochemistry. 2000;267(12):3828-35.

186. Yin MJ, Yamamoto Y, Gaynor RB. The anti-inflammatory agents aspirin and salicylate inhibit the activity of I kappa B kinase-beta. Nature. 1998;396(6706):77-80.

187. Kopp E, Ghosh S. INHIBITION OF NF-KAPPA-B BY SODIUM-SALICYLATE AND ASPIRIN. Science. 1994;265(5174):956-9.

188. Stark LA, Din FVN, Zwacka RM, Dunlop MG. Aspirin-induced activation of the NF-kappa B signaling pathway: a novel mechanism for aspirin-mediated apoptosis in colon cancer cells. Faseb Journal. 2001;15(7):1273-5.

189. Stark LA, Reid K, Sansom OJ, Din FV, Guichard S, Mayer I, et al. Aspirin activates the NF-kappa B signalling pathway and induces apoptosis in intestinal neoplasia in two in vivo models of human colorectal cancer. Carcinogenesis. 2007;28(5):968-76.

190. Chen JY, Lobb IT, Morin P, Novo SM, Simpson J, Kennerknecht K, et al. Identification of a novel TIF-IA-NF-kappa B nucleolar stress response pathway. Nucleic Acids Res. 2018;46(12):6188-205.

191. Chen JY, Stark LA. Crosstalk between NF-kappa B and Nucleoli in the Regulation of Cellular Homeostasis. Cells. 2018;7(10).

192. Fu JB, Xu YM, Yang YS, Liu Y, Ma LL, Zhang YY. Aspirin suppresses chemoresistance and enhances antitumor activity of 5-Fu in 5-Fu-resistant colorectal cancer by abolishing 5-Fu-induced NF-kappa B activation. Scientific Reports. 2019;9.

193. Colak S, ten Dijke P. Targeting TGF-beta Signaling in Cancer. Trends in Cancer. 2017;3(1):56-71.

194. Jin SH, Wu XG. Aspirin inhibits colon cancer cell line migration through regulating epithelial-mesenchymal transition via Wnt signaling. Oncology Letters. 2019;17(5):4675-82.

195. Wang YY, Du C, Zhang N, Li M, Liu YY, Zhao MY, et al. TGF-beta 1 mediates the effects of aspirin on colonic tumor cell proliferation and apoptosis. Oncology Letters. 2018;15(4):5903-9.

196. Dunbar K, Valanciute A, Lima ACS, Vinuela PF, Jamieson T, Rajasekaran V, et al. Aspirin Rescues Wnt-Driven Stem-like Phenotype in Human Intestinal Organoids and Increases the Wnt Antagonist Dickkopf-1. Cell Mol Gastroenterol Hepatol. 2021;11(2):465-89.

197. Guo Y, Liu Y, Zhang CY, Su ZY, Li WJ, Huang MT, et al. The epigenetic effects of aspirin: the modification of histone H3 lysine 27 acetylation in the prevention of colon carcinogenesis in azoxymethane- and dextran sulfate sodium-treated CF-1 mice. Carcinogenesis. 2016;37(6):616-24.

198. Passacquale G, Phinikaridou A, Warboys C, Cooper M, Lavin B, Alfieri A, et al. Aspirin-induced histone acetylation in endothelial cells enhances synthesis of the secreted isoform of netrin-1 thus inhibiting monocyte vascular infiltration. British Journal of Pharmacology. 2015;172(14):3548-64.

199. Zhang XY, Du RL, Luo N, Xiang R, Shen WZ. Aspirin mediates histone methylation that inhibits inflammation-related stemness gene expression to diminish cancer stemness via COX-independent manner. Stem Cell Research & Therapy. 2020;11(1).

200. Sankaranarayanan R, Valiveti CK, Dachineni R, Kumar DR, Lick T, Bhat GJ. Aspirin metabolites 2,3-DHBA and 2,5-DHBA inhibit cancer cell growth: Implications in colorectal cancer prevention. Molecular Medicine Reports. 2020;21(1):20-34.

201. Zhang X, Feng YK, Liu X, Ma JH, Li YF, Wang TZ, et al. Beyond a chemopreventive reagent, aspirin is a master regulator of the hallmarks of cancer. Journal of Cancer Research and Clinical Oncology. 2019;145(6):1387-403.

202. Doery JCG, Hirsh J, Degruchy GC. ASPIRIN - ITS EFFECT ON PLATELET GLYCOLYSIS AND RELEASE OF ADENOSINE DIPHOSPHATE. Science. 1969;165(3888):65-&.

203. Peng F, Wang JH, Fan WJ, Meng YT, Li MM, Li TT, et al. Glycolysis gatekeeper PDK1 reprograms breast cancer stem cells under hypoxia. Oncogene. 2018;37(8):1062-74.

204. Chiyoda T, Hart PC, Eckert MA, McGregor SM, Lastra RR, Hamamoto R, et al. Loss of BRCA1 in the Cells of Origin of Ovarian Cancer Induces Glycolysis: A Window of Opportunity for Ovarian Cancer Chemoprevention. Cancer Prevention Research. 2017;10(4):255-66.

205. Spitz GA, Furtado CM, Sola-Penna M, Zancan P. Acetylsalicylic acid and salicylic acid decrease tumor cell viability and glucose metabolism modulating 6-phosphofructo-1-kinase structure and activity. Biochemical Pharmacology. 2009;77(1):46-53.

206. Li SN, Dai WQ, Mo WH, Li JJ, Feng J, Wu LW, et al. By inhibiting PFKFB3, aspirin overcomes sorafenib resistance in hepatocellular carcinoma. Int J Cancer. 2017;141(12):2571-84.

207. Ai GQ, Dachineni R, Kumar DR, Alfonso LF, Marimuthu S, Bhat GJ. Aspirin inhibits glucose-6-phosphate dehydrogenase activity in HCT 116 cells through acetylation: Identification of aspirin-acetylated sites. Molecular Medicine Reports. 2016;14(2):1726-32.

208. Furuta E, Okuda H, Kobayashi A, Watabe K. Metabolic genes in cancer: Their roles in tumor progression and clinical implications. Biochimica Et Biophysica Acta-Reviews on Cancer. 2010;1805(2):141-52.

209. Ju HQ, Lu YX, Wu QN, Liu J, Zeng ZL, Mo HY, et al. Disrupting G6PD-mediated Redox homeostasis enhances chemosensitivity in colorectal cancer. Oncogene. 2017;36(45):6282-92.

210. Liu YX, Feng JY, Sun MM, Liu BW, Yang G, Bu YN, et al. Aspirin inhibits the proliferation of hepatoma cells through controlling GLUT1-mediated glucose metabolism. Acta Pharmacol Sin. 2019;40(1):122-32.

211. Hu YB, Lou XH, Wang RR, Sun CJ, Liu XM, Liu SC, et al. Aspirin, a potential GLUT1 inhibitor in a vascular endothelial cell line. Open Med. 2019;14(1):9.

212. Boku S, Watanabe M, Sukeno M, Yaoi T, Hirota K, Iizuka-Ohashi M, et al. Deactivation of Glutaminolysis Sensitizes PIK3CA-Mutated Colorectal Cancer Cells to Aspirin-Induced Growth Inhibition. Cancers. 2020;12(5).

213. Liu HC, Xiong C, Liu JW, Sun T, Ren ZZ, Li YQ, et al. Aspirin exerts anti-tumor effect through inhibiting Blimp1 and activating ATF4/CHOP pathway in multiple myeloma. Biomed Pharmacother. 2020;125.

214. Schworer S, Berisa M, Violante S, Qin WG, Zhu JJ, Hendrickson RC, et al. Proline biosynthesis is a vent for TGF beta-induced mitochondrial redox stress. Embo Journal. 2020;39(8).

215. Wang JD, Chen WY, Li JR, Lin SY, Wang YY, Wu CC, et al. Aspirin Mitigated Tumor Growth in Obese Mice Involving Metabolic Inhibition. Cells. 2020;9(3).

216. Beloribi-Djefaflia S, Vasseur S, Guillaumond F. Lipid metabolic reprogramming in cancer cells. Oncogenesis. 2016;5.

217. Yang G, Wang Y, Feng JY, Liu YX, Wang TJ, Zhao M, et al. Aspirin suppresses the abnormal lipid metabolism in liver cancer cells via disrupting an

NF kappa B-ACSL1 signaling. Biochem Biophys Res Commun. 2017;486(3):827-32.

218. Vargas T, Moreno-Rubio J, Herranz J, Cejas P, Molina S, Gonzalez-Vallinas M, et al. ColoLipidGene: signature of lipid metabolism-related genes to predict prognosis in stage-II colon cancer patients. Oncotarget. 2015;6(9):7348-63.

219. Uppala R, Dudiak B, Beck ME, Bharathi SS, Zhang YX, Stolz DB, et al. Aspirin increases mitochondrial fatty acid oxidation. Biochem Biophys Res Commun. 2017;482(2):346-51.

220. Barry EL, Fedirko V, Uppal K, Ma CY, Liu K, Mott LA, et al. Metabolomics Analysis of Aspirin's Effects in Human Colon Tissue and Associations with Adenoma Risk. Cancer Prevention Research. 2020;13(10):863-75.

221. Casero RA, Stewart TM, Pegg AE. Polyamine metabolism and cancer: treatments, challenges and opportunities. Nature Reviews Cancer. 2018;18(11):681-95.

222. Martinez ME, O'Brien TG, Fultz KE, Babbar N, Yerushalmi H, Qu N, et al. Pronounced reduction in adenoma recurrence associated with aspirin use and a polymorphism in the ornithine decarboxylase gene. Proceedings of the National Academy of Sciences of the United States of America. 2003;100(13):7859-64.

223. Hubner RA, Muir KR, Liu JF, Logan FA, Grainge M, Houlston RS, et al. Ornithine decarboxylase G316A genotype is prognostic for colorectal adenoma recurrence and predicts efficacy of aspirin chemoprevention. Clinical Cancer Research. 2008;14(8):2303-9.

224. Barry ELR, Baron JA, Bhat S, Grau MV, Burke CA, Sandler RS, et al. Ornithine decarboxylase polymorphism modification of response to aspirin treatment for colorectal adenoma prevention. J Natl Cancer Inst. 2006;98(20):1494-500.

225. Meyskens FL, McLaren CE, Pelot D, Fujikawa-Brooks S, Carpenter PM, Hawk E, et al. Difluoromethylornithine Plus Sulindac for the Prevention of Sporadic Colorectal Adenomas: A Randomized Placebo-Controlled, Double-Blind Trial. Cancer Prevention Research. 2008;1(1):32-8.

226. US National Library of Medicine. Acetylsalicylic Acid and Eflornithine in Treating Patients at High Risk of Colorectal Cancer 2018 [Available from: https://clinicaltrials.gov/ct2/show/study/NCT00983580.

227. Din FVN, Valanciute A, Houde VP, Zibrova D, Green KA, Sakamoto K, et al. Aspirin Inhibits mTOR Signaling, Activates AMP-Activated Protein Kinase, and Induces Autophagy in Colorectal Cancer Cells. Gastroenterology. 2012;142(7):1504-+.

228. Liesenfeld DB, Botma A, Habermann N, Toth R, Weigel C, Popanda O, et al. Aspirin Reduces Plasma Concentrations of the Oncometabolite 2-Hydroxyglutarate: Results of a Randomized, Double-Blind, Crossover Trial. Cancer Epidemiology Biomarkers & Prevention. 2016;25(1):180-7.

229. Kamble P, Selvarajan K, Narasimhulu CA, Nandave M, Parthasarathy S. Aspirin may promote mitochondrial biogenesis via the production of hydrogen peroxide and the induction of Sirtuin1/PGC-1 alpha genes. European Journal of Pharmacology. 2013;699(1-3):55-61.

230. Kamble P, Litvinov D, Narasimhulu CA, Jiang XT, Parthasarathy S. Aspirin may influence cellular energy status. European Journal of Pharmacology. 2015;749:12-9.

231. Zimmermann KC, Waterhouse NJ, Goldstein JC, Schuler M, Green DR. Aspirin induces apoptosis through release of cytochrome c from mitochondria. Neoplasia. 2000;2(6):505-13.

232. Tewari D, Majumdar D, Vallabhaneni S, Bera AK. Aspirin induces cell death by directly modulating mitochondrial voltage-dependent anion channel (VDAC). Scientific Reports. 2017;7.

233. Raza H, John A, Benedict S. Acetylsalicylic acid-induced oxidative stress, cell cycle arrest, apoptosis and mitochondrial dysfunction in human hepatoma HepG2 cells. European Journal of Pharmacology. 2011;668(1-2):15-24.

234. Raza H, John A. Implications of Altered Glutathione Metabolism in Aspirin-Induced Oxidative Stress and Mitochondrial Dysfunction in HepG2 Cells. Plos One. 2012;7(4).

235. Farrugia G, Bannister WH, Vassallo N, Balzan R. Aspirin-induced apoptosis of yeast cells is associated with mitochondrial superoxide radical accumulation and NAD(P)H oxidation. Fems Yeast Research. 2013;13(8):755-68.

236. Farrugia G, Azzopardi M, Saliba C, Grech G, Gross AS, Pistolic J, et al. Aspirin impairs acetyl-coenzyme A metabolism in redox-compromised yeast cells. Scientific Reports. 2019;9.

237. Ilyas M, Tomlinson IPM, Rowan A, Pignatelli M, Bodmer WF. beta-Catenin mutations in cell lines established from human colorectal cancers. Proceedings of the National Academy of Sciences of the United States of America. 1997;94(19):10330-4.

238. Rodrigues NR, Rowan A, Smith MEF, Kerr IB, Bodmer WF, Gannon JV, et al. P53 MUTATIONS IN COLORECTAL-CANCER. Proceedings of the National Academy of Sciences of the United States of America. 1990;87(19):7555-9.

239. Dunn EF, Iida M, Myers RA, Campbell DA, Hintz KA, Armstrong EA, et al. Dasatinib sensitizes KRAS mutant colorectal tumors to cetuximab. Oncogene. 2011;30(5):561-74.

240. Mouradov D, Sloggett C, Jorissen RN, Love CG, Li S, Burgess AW, et al. Colorectal Cancer Cell Lines Are Representative Models of the Main Molecular Subtypes of Primary Cancer. Cancer Research. 2014;74(12):3238-47.

241. Rowan AJ, Lamlum H, Ilyas M, Wheeler J, Straub J, Papadopoulou A, et al. APC mutations in sporadic colorectal tumors: A mutational "hotspot" and interdependence of the "two hits". Proceedings of the National Academy of Sciences of the United States of America. 2000;97(7):3352-7.

242. Aoki Y, Lee JC, Pillai S, Isselbacher KJ, Rustgi AK. RADIOLABELED POLYMERASE CHAIN-REACTION ASSAY FOR DETECTION OF RAS ONCOGENE POINT MUTATIONS IN TUMORS. Clinical Chemistry. 1994;40(5):705-9.

243. Arita D, Kambe M, Ishioka C, Kanamaru R. Induction of p53-independent apoptosis associated with G2M arrest following DNA damage in human colon cancer cell lines. Japanese Journal of Cancer Research. 1997;88(1):39-43.

244. Liu Y, Bodmer WF. Analysis of P53 mutations and their expression in 56 colorectal cancer cell lines. Proceedings of the National Academy of Sciences of the United States of America. 2006;103(4):976-81.

245. Wheeler JMD, Beck NE, Kim HC, Tomlinson IPM, Mortensen NJM, Bodmer WF. Mechanisms of inactivation of mismatch repair genes in human colorectal cancer cell lines: The predominant role of hMLH1. Proceedings of the National Academy of Sciences of the United States of America. 1999;96(18):10296-301.

246. Baker SJ, Preisinger AC, Jessup JM, Paraskeva C, Markowitz S, Willson JKV, et al. P53 GENE-MUTATIONS OCCUR IN COMBINATION WITH 17P ALLELIC DELETIONS AS LATE EVENTS IN COLORECTAL TUMORIGENESIS. Cancer Research. 1990;50(23):7717-22.

247. Browne SJ, Williams AC, Hague A, Butt AJ, Paraskeva C. LOSS OF APC PROTEIN EXPRESSED BY HUMAN COLONIC EPITHELIAL-CELLS AND THE APPEARANCE OF A SPECIFIC LOW-MOLECULAR-WEIGHT FORM IS ASSOCIATED WITH APOPTOSIS IN-VITRO. Int J Cancer. 1994;59(1):56-64.

248. Greenhough A, Wallam CA, Hicks DJ, Moorghen M, Williams AC, Paraskeva C. The proapoptotic BH3-only protein Bim is downregulated in a subset of colorectal cancers and is repressed by antiapoptotic COX-2/PGE(2) signalling in colorectal adenoma cells. Oncogene. 2010;29(23):3398-410.

249. Davarinejad H. Quantifications of Western Blots with ImageJ. http://www.yorku.ca/yisheng/Internal/Protocols/ImageJ.pdf.

250. Faubert B, Boily G, Izreig S, Griss T, Samborska B, Dong ZF, et al. AMPK Is a Negative Regulator of the Warburg Effect and Suppresses Tumor Growth In Vivo. Cell Metabolism. 2013;17(1):113-24.

251. Vincent EE, Sergushichev A, Griss T, Gingras MC, Samborska B, Ntimbane T, et al. Mitochondrial Phosphoenolpyruvate Carboxykinase Regulates Metabolic Adaptation and Enables Glucose-Independent Tumor Growth. Molecular Cell. 2015;60(2):195-207.

252. Ma EH, Verway MJ, Johnson RM, Roy DG, Steadman M, Hayes S, et al. Metabolic Profiling Using Stable Isotope Tracing Reveals Distinct Patterns of Glucose Utilization by Physiologically Activated CD8(+) T Cells. Immunity. 2019;51(5):856-+.

253. Mookerjee SA, Gerencser AA, Nicholls DG, Brand MD. Quantifying intracellular rates of glycolytic and oxidative ATP production and consumption using extracellular flux measurements. Journal of Biological Chemistry. 2017;292(17):7189-207.

254. Méndez-Lucas A, Lin W, Driscoll PC, Legrave N, Novellasdemunt L, Xie C, et al. Identifying strategies to target the metabolic flexibility of tumours. Nature Metabolism. 2020;2(4):335-50.

255. Harding HP, Zhang YH, Zeng HQ, Novoa I, Lu PD, Calfon M, et al. An integrated stress response regulates amino acid metabolism and resistance to oxidative stress. Molecular Cell. 2003;11(3):619-33.

256. Wortel IMN, van der Meer LT, Kilberg MS, van Leeuwen FN. Surviving Stress: Modulation of ATF4-Mediated Stress Responses in Normal and Malignant Cells. Trends in Endocrinology and Metabolism. 2017;28(11):794-806.

257. Elder DJE, Hague A, Hicks DJ, Paraskeva C. Differential growth inhibition by the aspirin metabolite salicylate in human colorectal tumor cell lines: Enhanced apoptosis in carcinoma and in vitro-transformed adenoma relative to adenoma cell lines. Cancer Research. 1996;56(10):2273-6.

258. Kim M, Gwak J, Hwang S, Yang S, Jeong SM. Mitochondrial GPT2 plays a pivotal role in metabolic adaptation to the perturbation of mitochondrial glutamine metabolism. Oncogene. 2019;38(24):4729-38.

259. Singleton DC, Harris AL. Targeting the ATF4 pathway in cancer therapy. Expert Opinion on Therapeutic Targets. 2012;16(12):1189-202.

260. Agilent Tecnologies Inc. Agilent Seahorse XF Cell

Mito Stress Test Kit2019. Available from: https://www.agilent.com/cs/library/usermanuals/public/XF_Cell_Mito_Stress_Test_Kit_User_Guide.pdf.

261. Mookerjee SA, Nicholls DG, Brand MD. Determining Maximum Glycolytic Capacity Using Extracellular Flux Measurements. Plos One. 2016;11(3).

262. Buescher JM, Antoniewicz MR, Boros LG, Burgess SC, Brunengraber H, Clish CB, et al. A roadmap for interpreting C-13 metabolite labeling patterns from cells. Current Opinion in Biotechnology. 2015;34:189-201.

263. Agilent Technologies Inc. Cell Characterization: XFp Analyzer and the Cell Energy Phenotype Test,2017. Available from: https://www.agilent.com/cs/library/usermanuals/public/New_Cell_Line_Characterization.pdf.

264. Chen PH, Cai L, Huffman K, Yang CD, Kim J, Faubert B, et al. Metabolic Diversity in Human Non-Small Cell Lung Cancer Cells. Molecular Cell. 2019;76(5):838-+.

265. Cheng TL, Sudderth J, Yang CD, Mullen AR, Jin ES, Mates JM, et al. Pyruvate carboxylase is required for glutamine-independent growth of tumor cells. Proceedings of the National Academy of Sciences of the United States of America. 2011;108(21):8674-9.

266. Cuzick J, Thorat MA, Bosetti C, Brown PH, Burn J, Cook NR, et al. Estimates of benefits and harms of prophylactic use of aspirin in the general population. Annals of Oncology. 2015;26(1):47-57.

267. Rossiter NJ, Huggler KS, Adelmann CH, Keys HR, Soens RW, Sabatini DM, et al. CRISPR screens in physiologic medium reveal conditionally essential genes in human cells. Cell Metabolism. 2021;33(6):1248-+.

268. Yin CX, Lu WH, Ma MZ, Yang Q, He WZ, Hu YM, et al. Efficacy and mechanism of combination of oxaliplatin with PKM2 knockdown in colorectal cancer. Oncology Letters. 2020;20(6).

269. Zhao YQ, Feng XJ, Chen YC, Selfridge JE, Gorityala S, Du ZW, et al. 5-Fluorouracil Enhances the Antitumor Activity of the Glutaminase Inhibitor CB-839 against PIK3CA-Mutant Colorectal Cancers. Cancer Research. 2020;80(21):4815-27.

270. Cao Y, Lin Y, Wang DX, Pan D, Zhang Y, Jin Y, et al. Enhancing 5-fluorouracil efficacy through suppression of PKM2 in colorectal cancer cells. Cancer Chemother Pharmacol. 2018;82(6):1081-6.

271. Li XY, Wenes M, Romero P, Huang SCC, Fendt SM, Ho PC. Navigating metabolic pathways to enhance antitumour immunity and immunotherapy. Nature Reviews Clinical Oncology. 2019;16(7):425-41.

272. Tajan M, Hennequart M, Cheung EC, Zani F, Hock AK, Legrave N, et al. Serine synthesis pathway inhibition cooperates with dietary serine and glycine limitation for cancer therapy. Nat Commun. 2021;12(1).

273. Tran Q, Lee H, Park J, Kim SH. Targeting Cancer Metabolism - Revisiting the Warburg Effects. Toxicological Research. 2016;32(3):177-93.

274. Raez LE, Papadopoulos K, Ricart AD, Chiorean EG, DiPaola RS, Stein MN, et al. A phase I dose-escalation trial of 2-deoxy-D-glucose alone or combined with docetaxel in patients with advanced solid tumors. Cancer Chemother Pharmacol. 2013;71(2):523-30.

275. Dunbar EM, Coats BS, Shroads AL, Langaee T, Lew A, Forder JR, et al. Phase 1 trial of dichloroacetate (DCA) in adults with recurrent malignant brain tumors. Invest New Drugs. 2014;32(3):452-64.

276. Ho N, Coomber BL. Pyruvate dehydrogenase kinase expression and metabolic changes following dichloroacetate exposure in anoxic human colorectal cancer cells. Experimental Cell Research. 2015;331(1):73-81.

277. Shiratori R, Furuichi K, Yamaguchi M, Miyazaki N, Aoki H, Chibana H, et al. Glycolytic suppression dramatically changes the intracellular metabolic profile of multiple cancer cell lines in a mitochondrial metabolism-dependent manner. Scientific Reports. 2019;9.

278. Meijer TWH, Kaanders J, Span PN, Bussink J. Targeting Hypoxia, HIF-1, and Tumor Glucose Metabolism to Improve Radiotherapy Efficacy. Clinical Cancer Research. 2012;18(20):5585-94.

279. Leung E, Cairns RA, Chaudary N, Vellanki RN, Kalliomaki T, Moriyama EH, et al. Metabolic targeting of HIF-dependent glycolysis reduces lactate, increases oxygen consumption and enhances response to high-dose single-fraction radiotherapy in hypoxic solid tumors. BMC Cancer. 2017;17.

280. Leone RD, Zhao L, Englert JM, Sun IM, Oh MH, Sun IH, et al. Glutamine blockade induces divergent metabolic programs to overcome tumor immune evasion. Science. 2019;366(6468):1013-+.

281. Gross MI, Demo SD, Dennison JB, Chen L, Chernov-Rogan T, Goyal B, et al. Antitumor Activity of the Glutaminase Inhibitor CB-839 in Triple-Negative Breast Cancer. Mol Cancer Ther. 2014;13(4):890-901.

282. Jacque N, Ronchetti AM, Larrue C, Meunier G, Birsen R, Willems L, et al. Targeting glutaminolysis has antileukemic activity in acute myeloid leukemia and synergizes with BCL-2 inhibition. Blood. 2015;126(11):1346-56.

283. Eads JR, Krishnamurthi SS, Saltzman JN, Bajor DL, Vinayak S, Barnholtz-Sloan J. Phase I clinical trial of the glutaminase inhibitor CB-839 plus capecitabine in patients with advanced solid tumors. J Clin Oncol. 2018;36(15):1.

284. Xiao DB, Ren P, Su HX, Yue M, Xiu RJ, Hu YF, et al. Myc promotes glutaminolysis in human neuroblastoma through direct activation of glutaminase 2. Oncotarget. 2015;6(38):40655-66.

285. Biancur DE, Paulo JA, Malachowska B, Del Rey MQ, Sousa CM, Wang XX, et al. Compensatory metabolic networks in pancreatic cancers upon perturbation of glutamine metabolism. Nat Commun. 2017;8.

286. Mates JM, Di Paola FJ, Campos-Sandoval JA, Mazurek S, Marquez J. Therapeutic targeting of glutaminolysis as an essential strategy to combat cancer. Seminars in Cell & Developmental Biology. 2020;98:34-43.

287. Mendez-Lucas A, Lin W, Driscoll PC, Legrave N, Novellasdemunt L, Xie CC, et al. Identifying strategies to target the metabolic flexibility of tumours. Nature Metabolism. 2020;2(4):335-+.

288. Lampa M, Arlt H, He T, Ospina B, Reeves J, Zhang BL, et al. Glutaminase is essential for the growth of triple-negative breast cancer cells with a deregulated glutamine metabolism pathway and its suppression synergizes with mTOR inhibition. Plos One. 2017;12(9).

289. Tanaka K, Sasayama T, Irino Y, Takata K, Nagashima H, Satoh N, et al. Compensatory glutamine metabolism promotes glioblastoma resistance to mTOR inhibitor treatment. Journal of Clinical Investigation. 2015;125(4):1591-602.

290. Li J, Song P, Zhu L, Aziz N, Zhou Q, Zhang Y, et al. Synthetic lethality of glutaminolysis inhibition, autophagy inactivation and asparagine depletion in colon cancer. Oncotarget. 2017;8(26):42664-72.

291. Han ST, Zhu LY, Zhu YR, Meng Y, Li JQ, Song P, et al. Targeting ATF4-dependent pro-survival autophagy to synergize glutaminolysis inhibition. Theranostics. 2021;11(17):8464-79.

292. Jin HJ, Wang SY, Zaal EA, Wang C, Wu HQ, Bosma A, et al. A powerful drug combination strategy targeting glutamine addiction for the treatment of human liver cancer. Elife. 2020;9.

293. dos Reis LM, Adamoski D, Souza ROO, Ascencao CFR, de Oliveira KRS, Correa-da-Silva F, et al. Dual inhibition of glutaminase and carnitine palmitoyltransferase decreases growth and migration of glutaminase inhibition-resistant triple-negative breast cancer cells. Journal of Biological Chemistry. 2019;294(24):9342-57.

294. Cantor JR. The Rise of Physiologic Media. Trends in Cell Biology. 2019;29(11):854-61.

295. Voorde JV, Ackermann T, Pfetzer N, Sumpton D, Mackay G, Kalna G, et al. Improving the metabolic fidelity of cancer models with a physiological cell culture medium. Science Advances. 2019;5(1).

296. Sullivan MR, Danai LV, Lewis CA, Chan SH, Gui DY, Kunchok T, et al. Quantification of microenvironmental metabolites in murine cancers reveals determinants of tumor nutrient availability. Elife. 2019;8.

297. Bell JA, Bull CJ, Gunter MJ, Carslake D, Mahajan A, Smith GD, et al. Early Metabolic Features of Genetic Liability to Type 2 Diabetes: Cohort Study With Repeated Metabolomics Across Early Life. Diabetes Care. 2020;43(7):1537-45.

298. Gao X, Sanderson SM, Dai ZW, Reid MA, Cooper DE, Lu M, et al. Dietary methionine influences therapy in mouse cancer models and alters human metabolism. Nature. 2019;572(7769):397-+.

299. Hildyard JCW, Ammala C, Dukes ID, Thomson SA, Halestrap AP. Identification and characterisation of a new class of highly specific and potent inhibitors of the mitochondrial pyruvate carrier. Biochimica Et Biophysica Acta-Bioenergetics. 2005;1707(2-3):221-30.

300. Zhong YL, Li XR, Yu DD, Li XL, Li YQ, Long Y, et al. Application of mitochondrial pyruvate carrier blocker UK5099 creates metabolic reprogram and greater stem-like properties in LnCap prostate cancer cells in vitro. Oncotarget. 2015;6(35):37758-69.

301. Vettore L, Westbrook RL, Tennant DA. New aspects of amino acid metabolism in cancer. Br J Cancer. 2020;122(2):150-6.

302. Jaune-Pons E, Vasseur S. Role of amino acids in regulation of ROS balance in cancer. Archives of Biochemistry and Biophysics. 2020;689.

303. Wang YW, Qi H, Liu Y, Duan C, Liu XL, Xia T, et al. The double-edged roles of ROS in cancer prevention and therapy. Theranostics. 2021;11(10):4839-57.

304. Patel D, Menon D, Bernfeld E, Mroz V, Kalan S, Loayza D, et al. Aspartate Rescues S-phase Arrest Caused by Suppression of Glutamine Utilization in KRas-driven Cancer Cells. Journal of Biological Chemistry. 2016;291(17):9322-9.

305. Giampieri R, Restivo A, Pusceddu V, Del Prete M, Maccaroni E, Bittoni A, et al. The Role of Aspirin as Antitumoral Agent for Heavily Pretreated Patients With Metastatic Colorectal Cancer Receiving Capecitabine Monotherapy. Clinical Colorectal Cancer. 2017;16(1):38-43.

306. Zhang W, Tan YS, Ma HP. Combined aspirin and apatinib treatment suppresses gastric cancer cell proliferation. Oncology Letters. 2017;14(5):5409-17.

307. Meric-Bernstam F, Tannir NM, Iliopoulos O, Lee RJ, Telli ML, Fan AC, et al. Telaglenastat Plus Cabozantinib or Everolimus For Advanced or Metastatic Renal Cell Carcinoma: an Open-Label Phase 1 Trial. Clinical Cancer Research. 2022:clincanres.2972.021.

308. Dixon SW, Collard TJ, Mortensson EMH, Legge DN, Chambers AC, Greenhough A, et al. 5-Aminosalicylic acid inhibits stem cell function in human adenoma-derived cells: implications for chemoprophylaxis in colorectal tumorigenesis. Br J Cancer. 2021;124(12):1959-69.

309. Annese V, Beaugerie L, Egan L, Biancone L, Bolling C, Brandts C, et al. European Evidence-based Consensus: Inflammatory Bowel Disease and Malignancies. Journal of Crohns & Colitis. 2015;9(11):945-65.

310. Qiu XY, Ma JJ, Wang K, Zhang HJ. Chemopreventive effects of 5-aminosalicylic acid on inflammatory bowel disease-associated colorectal cancer and dysplasia: a systematic review with meta-analysis. Oncotarget. 2017;8(1):1031-45.

311. Bonovas S, Fiorino G, Lytras T, Nikolopoulos G, Peyrin-Biroulet L, Danese S. Systematic review with meta-analysis: use of 5-aminosalicylates and risk of colorectal neoplasia in patients with inflammatory bowel disease. Alimentary Pharmacology & Therapeutics. 2017;45(9):1179-92.